The Colonization Strategies of Nontypeable Haemophilus influenzae - Bacterial Colonization Factors and Vaccine Development

Jalalvand, Farshid

2015

The Colonization Strategies of Nontypeable *Haemophilus influenzae*

Bacterial Colonization Factors and Vaccine Development

Farshid Jalalvand

LUNDS
UNIVERSITET

DOCTORAL DISSERTATION
by due permission of the Faculty of Medicine, Lund University, Sweden.

To be defended at the main lecture hall of the Pathology building,
Jan Waldenströms gata 59, Malmö, on Friday 30th of January 2015 at 13:00.

Faculty opponent

Professor Joachim Reidl, University of Graz

Organization	Document name
LUND UNIVERSITY	DOCTORAL DISSERTATION
	Date of issue January 30th 2015
Author(s) Farshid Jalalvand	Sponsoring organization

Title and subtitle: The Colonization Strategies of Nontypeable *Haemophilus influenzae* – Bacterial Colonization Factors and Vaccine Development

Abstract

Nontypeable *Haemophilus influenzae* (NTHi) is a remarkably proficient colonizer of the human respiratory tract. The aim of this thesis has been to characterize currently known, and identify novel, bacterial factors involved in the key processes of colonization and pathogenesis, namely adherence to host tissue and evasion of the host innate immunity.

We have shown that the NTHi virulence factor Protein E mediates innate immune evasion by interacting with the C-terminus of host complement down-regulatory protein vitronectin. This interaction delayed the formation of the membrane attack complex on the bacterial surface and increased the bacterial serum-resistance. Furthermore, we identified a novel surface-exposed virulence factor designated *Haemophilus* Protein F that also sequesters vitronectin on the surface of the bacteria, thus rendering the pathogen more serum-resistant. Moreover, we have revealed that Protein F mediates bacterial adherence to primary human bronchial cells and to the extracellular matrix protein laminin. Isogenic mutants devoid of Protein F were observed to adhere significantly less to vitronectin, epithelial cells and laminin. These interactions were characterized at the molecular level, and the N-terminus of Protein F was shown to contain the host-interacting region. Finally, we showed that immunization with Protein F conferred increased pulmonary clearance of NTHi *in vivo*.

In summary, we have identified, and at the molecular level characterized, novel virulence factors that may be suitable for future vaccine development.

Key words: ABC-transporter, bacterial colonization, *Haemophilus influenzae, Haemophilus* Protein F, laminin, NTHi, pathogenesis, vaccine, virulence, vitronectin.

Classification system and/or index terms (if any)

Supplementary bibliographical information	Language English
ISSN and key title 1652-8220	ISBN: 978-91-7619-093-7
Recipient's notes	Number of pages / Price / Security classification

Signature 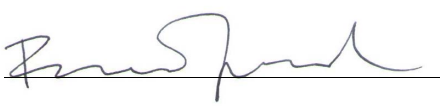 Date 2014/12/15

The Colonization Strategies of Nontypeable *Haemophilus influenzae*

Bacterial Colonization Factors and Vaccine Development

Farshid Jalalvand

LUNDS
UNIVERSITET

Faculty of Medicine, Department of Translational Medicine
ISBN 978-91-7619-093-7
ISSN 1652-8220

Printed in Sweden by Media-Tryck, Lund University
Lund 2015


To all my teachers
in and outside of the home.

Table of Content

List of Papers

I. Birendra Singh, **Farshid Jalalvand**, Matthias Mörgelin, Peter Zipfel, Anna M. Blom and Kristian Riesbeck. (2011) *Haemophilus influenzae* Protein E recognizes the C-terminal domain of vitronectin and modulates the membrane attack complex.
Molecular Microbiology, Jul;81(1):80-98.

II. Yu-Ching Su, **Farshid Jalalvand**, Matthias Mörgelin, Anna M. Blom, Birendra Singh and Kristian Riesbeck. (2013) *Haemophilus influenzae* acquires vitronectin via the ubiquitous Protein F to subvert host innate immunity.
Molecular Microbiology, Mar;87(6):1245-66

III. **Farshid Jalalvand,** Yu-Ching Su, Matthias Mörgelin, Marta Brant, Oskar Hallgren, Gunilla Westergren-Thorsson, Birendra Singh and Kristian Riesbeck. (2013) *Haemophilus influenzae* Protein F mediates binding to laminin and human pulmonary epithelial cells.
Journal of Infectious Diseases, Mar;207(5):803-13.

IV. **Farshid Jalalvand**, Nils Littorin, Yu-Ching Su and Kristian Riesbeck. (2014) Impact of immunization with Protein F on pulmonary clearance of nontypeable *Haemophilus influenzae.*
Vaccine, Apr 25;32(20):2261-4.

Abbreviations

ABC-transporter	Adenosine triphosphate (ATP)-binding cassette transporter
AOM	Acute otitis media
COPD	Chronic obstructive pulmonary disease
ECM	Extracellular matrix
Fur	Ferric uptake regulator protein
Hib	*Haemophilus influenzae* serotype b
Ln	Laminin
LOS	Lipooligosaccharide
LPS	Lipopolysaccharide
MAC	Membrane attack complex
MMP-9	Metalloproteinase-9
NAD	Nicotinamide adenine dinucleotide
NLR	Nucleotide-binding oligomerization domain (NOD)-like receptor
NTHi	Nontypeable *Haemophilus influenzae*
OM	Otitis media
OMV	Outer membrane vesicle
ORF	Open reading frame
PAMP	Pathogen-associated molecular pattern
PF	*Haemophilus* Protein F
PRR	Pathogen pattern recognition receptor
TIMP-1	Tissue inhibitor of metalloproteinase-1
TLR	Toll-like receptor

Populärvetenskaplig sammanfattning

Bakterier är små encelliga organismer som lever i nästan varje tänkbar miljö på jorden, inklusive i och på människor. Vi är kontinuerligt koloniserade av bakterier i bland annat våra luftvägar, munhålor och mag-tarmkanaler. Denna samexistens är oftast ömsesidigt fördelaktig, eller åtminstone ofarlig för oss människor, och det är känt att bakterier hjälper oss bryta ner dietära ämnen samt förser oss med vitaminer. Men mikrober som tillhör normalfloran kan under vissa omständigheter orsaka infektioner av varierande allvarlighetsgrad.

Att kolonisera människans övre luftvägar, d.v.s. näsa, svalg och de övre delarna av broncherna, är ingen lätt uppgift för bakterier. Vi har flera skyddsmekanismer på plats för att försvara oss mot invaderande mikrober. Luftvägarna är klädda med ett slemproducerande cellhinna som kallas det *mukosala epitelet*. Epitelet i luftvägarna har dessutom ett ytterligare vapen till sitt förfogande; mikroborstar eller så kallade *cilier*. När partiklar eller mikrober andas in i luftvägarna fastnar de oftast i epitelets slemhinna och transporteras bort av cilierna till svalget för att sväljas ner till magsäcken för destruktion eller spottas ut. Utöver detta mekaniska skydd, finns människans medfödda immunförsvar på plats för att bekämpa bakteriella inkräktare. Fördelen med det medfödda immunförsvaret är att den till skillnad från det adaptiva antikroppsgenererande immunförsvaret inte behöver en uppstartstid utan är ständigt igång. Avhandlingens mål har varit att kartlägga hur den övre luftvägskoloniserande bakterien *Haemophilus influenzae* kringgår dessa antimikrobiella mekanismer för att orsaka infektioner såsom öroninflammation och perioder av försämring i KOL-patienter.

Vi har här kunnat visa att två molekyler som finns på bakteriens yta, kallade *Haemophilus* Protein F och Protein E, kamouflerar *H. influenzae* genom att binda det mänskliga proteinet vitronektin. Vitronektin är vanligtvis involverat i skyddet av kroppens egna celler från det medfödda immunförsvaret, d.v.s. den skyddar oss mot autoimmunitet. Genom att klä sig i detta protein, lurar bakterier vårt immunförsvar att de är kroppsegna celler och undgår dödande av det medfödda immunförsvaret.

Utöver det har vi visat hur Protein F fungerar som ett slags kardborre i luftvägarna. Den vidhäftar till både epitelceller samt epitelets underliggande vävnad, det så kallade *basalmembranet*. Genom att klistra sig på dessa vävnader undgår bakterien att transporteras bort av cilierna. Dessa två mekanismer, vidhäftning till epitelet och

resistens mot det medfödda immunförsvaret, understödjer därmed *H. influenzaes* kolonisering av människans luftvägar.

Slutligen undersökte vi ifall Protein F kan användas som ett vaccin mot *H. influenzae*. Vi kunde visa att möss som immuniserades med Protein F rensade ut bakterierna mycket mer effektivt än möss som immuniserades med ett negativ kontrollprotein. Vår slutsats är att Protein F är en möjlig vaccinkandidat mot *H. influenzae* och bör utredas närmare.

Sammanfattningsvis har vi identifierat nya bakteriella koloniseringsfaktorer som hjälper *H. influenzae* överleva i människans luftvägar, samt visat att ett av dessa proteiner kan potentiellt utnyttjas i ett vaccin mot patogenen.

Introduction

Bacterial and Human Coexistence

Bacteria are remarkable life forms. Their presence is almost ubiquitous on Earth as they inhabit enormously diverse ecosystems ranging from oceanic and terrestrial subsurfaces devoid of sunlight, the mesosphere at altitudes exceeding 70 km above sea level, geothermally hot sulphur springs, to subglacial lakes and barren deserts (1-4). The majority, of course, live in the soil, shallow aquatic habitats and on other life forms such as animals and plants (1). Prokaryotes constitute a significant amount of the total biomass on the planet (5), "occupying" almost as much carbon as plants and an order of magnitude higher amounts of nitrogen and phosphorous according to some estimates, making them the largest living reservoir for essential nutrients (1). Simply put, their abundance and presence in every *milieu* on Earth is unquestionable. And since we humans are coinhabitants of the same planet, we too are ecological niches for bacterial life as they live in and on us (6).

Considering the ubiquity, abundance and remarkable adaptation of microbes to various environments, it does not come as a surprise that we, like all other multicellular life forms, become covered from head to toe (and inside out for that matter) in bacteria from the moment that we are born until we die, after which microbes help decompose our bodies in the proverbial "circle of life" (6, 7). Prokaryotic life traces back at least 3.4 billion years (8), and is considered to be the first cellular life form to exist on the planet (9, 10). Our own species, *Homo sapiens*, has existed for about 200 000 years (11). If we scale the duration of the bacterial inhabitation of Earth to 24 hours, humans have existed for approximately 5 seconds. With this in mind, one could argue that we are merely newly arrived visitors to an ancient microbial world.

Still, while here, the bacterial and human interplay is of huge importance for us. There are evidences of an intricate co-evolution of humans and our corresponding microbiota during our coexistence (12, 13). We humans each have a whopping 100 trillion bacterial cells living in our guts, oral cavity, upper airways, skin and, in the case of women, the vagina (6, 14). Many of these species are human-specific and cannot survive for exceedingly long periods outside of our bodies (15-21). Most commonly, our coexistence is mutually beneficial (12). We need them for, among

other things, the harvest of inaccessible nutrients from our diet and for vitamin synthesis (22). In return, we provide a predictable living-environment and act as a reliable nutrient source for them. The human genome encodes approximately 20 000 genes, but the bacterial species that live in symbiosis with us collectively provide an additional 530 000 unique genes to our biological system, many of which are believed to aid us in metabolism as mentioned (23). Indeed, some philosophically-minded scientists argue that we are multispecies "supra-organisms": part human, part microbial (22). New evidence indicating that the gut microbiota can alter human behaviour lends further merit to this notion (24, 25).

The life cycle of host-living bacteria consists of (i) reaching a host, (ii) establishing colonization and (iii) spreading to a new host. Colonization, that is adherence to host tissue and on site proliferation, all while withstanding the external stresses of that particular niche, is thus an absolutely central theme in host-microbe interactions. This interplay can be mutualistic, commensalistic, or parasitic, and depending on the bacterial species involved, may fall under multiple categories at various time points during its sojourn with us.

To colonize a healthy human host is not an easy feat for microbes. Truly, most bacteria cannot. There are nutrient limitations, potential pH-fluctuations, intramicrobial competition and the host's structural barriers. Prokaryotes that manage to colonize the host despite these factors, without inflicting substantial injury or eliciting an inflammatory response, are components of the normal flora. However, it is a well-known fact that coexistence with our microbial selves is not always friction-free. Bacteria that disrupt the human homeostasis and cause disease during colonization, proliferation or transmission, *e.g.* are pathogenic, are the subjects of study for medical microbiologists. If colonization of the host is hard to begin with, causing disease is an order of magnitude harder as a major additional factor kicks in: the host immunity. Any bacterium that colonizes humans to subsequently cause disease has to be able to cope with all these factors. And they do.

The topic of this thesis is how one outstanding bacterial species, *Haemophilus influenzae*, overcomes the structural barriers of the host by adhering to tissue it "shouldn't" be able to adhere to, and then circumvents the host innate immunity to survive, colonize, proliferate and finally transmit to a new host before the old host has eradicated it. By identifying the molecular factors involved in this scenic drama, we could show that it is possible to "turn the table" on the pathogen, using its own colonization factors against it and stopping it in its tracks before it can establish disease.

The Human Upper Airway

The human respiratory tract is directly subjected to the unsterile and particulate external environment. We breathe 6-12 litres of air/minute, and with inhalation follow chemicals, allergens, microparticles and, naturally, microbes (26). The upper airways fulfil the function of cleaning, moistening and warming up the air before it enters the (mostly) sterile lower airways (pulmonary system) distally of the bronchi, where gas exchange and respiration occurs. Figure 1 shows a schematic representation of the upper airways that is anatomically divided in the nasal cavity, pharynx, larynx, trachea and initial bronchia (26, 27).

The upper airways are lined with a ciliated mucosal epithelium (27). This respiratory epithelium is normally colonized by a specialized microbiota constituted primarily of bacteria from the phyla *Firmicutes*, *Actinobacteria*, *Bacteroidetes* and *Proteobacteria* (28, 29). The nasopharynx, which is the primary site of colonization of *H. influenzae*, is a subcompartment of the upper airways situated dorsally of the nasal cavity and superiorly to the oropharynx. Adjacent to the nasopharynx is the entrance to the auditory tube (also known as the Eustachian tube). The route of pathogen ascension to the middle ear starts in the nasopharynx and goes via the Eustachian tube (30).

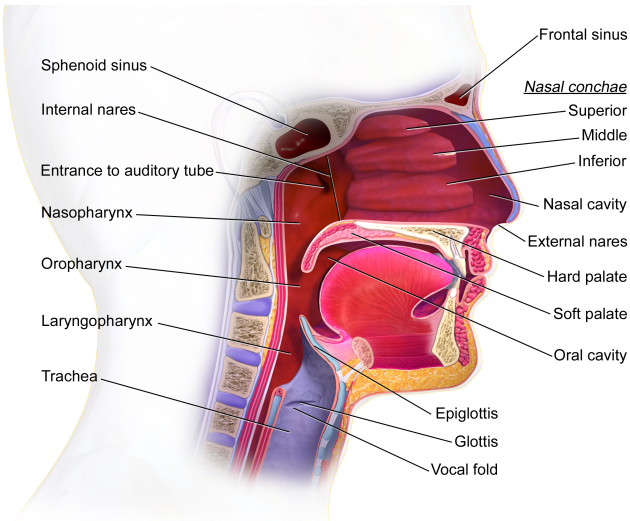

Figure 1. Schematic representation of the upper airways. The gross anatomical division of the upper airways can be observed above; air enters through the nasal cavity, continues through the naso- and oro- and laryngopharynx further down to the trachea and finally down to the lower airways. *H. influenzae* colonizes the nasopharynx, from which it can enter the autitory tube to cause otitis media, or descend down to the lower respiratory tract to produce other mucosal infections. Image used with permission (31).

The Mucociliary Elevator

The respiratory epithelium is constituted by three major cell types that jointly contribute to the physiological function of the tissue; ciliated, goblet (or mucus), and basal cells (Figure 2). The basal cells are progenitor stem cells that can differentiate into the other cell types present in the epithelium (26). They also regulate the inflammatory response and mediate attachment and communication with the underlying basement membrane. Goblet cells produce electron-lucent granules containing the acidic glycoproteins mucins that are secreted into the lumen to generate the protective mucus layer. This layer has multiple functions, including physically separating the epithelium from toxic compounds or invading microbes as well as trapping microparticles (such as infectious agents) in its mucoid consistency (26). Finally, the function of the ciliated cells is the constant removal of "dirty" mucus to the pharynx by coordinated beating of the cilia. Once the particulate-containing mucus arrives in the pharynx, it is discarded by deglutition to the gastric tract or expulsion from the mouth (26). Collectively, this system is called the mucociliary elevator and is our first-line of defence against invading microbes in the respiratory tract.

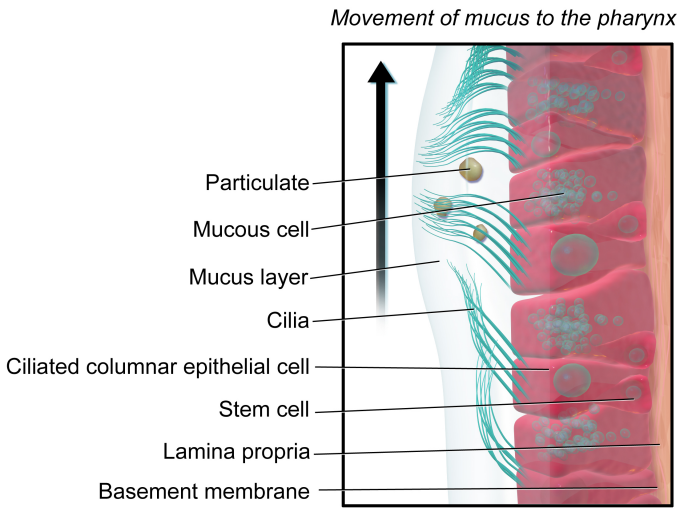

Figure 2. Schematic representation of the mucosal epithelium. The beating cilia move particulate mucus towards the pharynx for removal to the gastric tract or oral discardation. Image cropped and used with permission (31).

The Basement Membrane and Extracellular Matrix Proteins

The respiratory epithelium rests on a rigid structure designated as the basement membrane (Figure 2). This acellular tissue is comprised of extracellular protein matrices. The two major extracellular matrix (ECM) protein components of the basement membrane are laminins (Ln) and collagens that form separate polymer sheets interconnected via molecules such as nidogen, perlecan and agrin (32-34).

The basement membrane does not merely provide a structural scaffold for epithelial and endothelial cells, but is involved in many dynamic homeostatic processes including embryonic development, cell migration, differentiation, wound healing and cell signalling (33). It is directly connected to epithelial cells via hemodesmosomes as well as an array of dynamic protein-protein connections involving, for instance, basal cell membrane integrins (26). The ECM is therefore *de facto* connected to the cytoskeletons of epithelial cells and can alter their phenotype via complex signalling pathways (32). Patients suffering from deleterious mutations in genes encoding ECM-proteins can develop disorders such as muscular dystrophies, epidermolysis bullosa and glomerular disease (35-37).

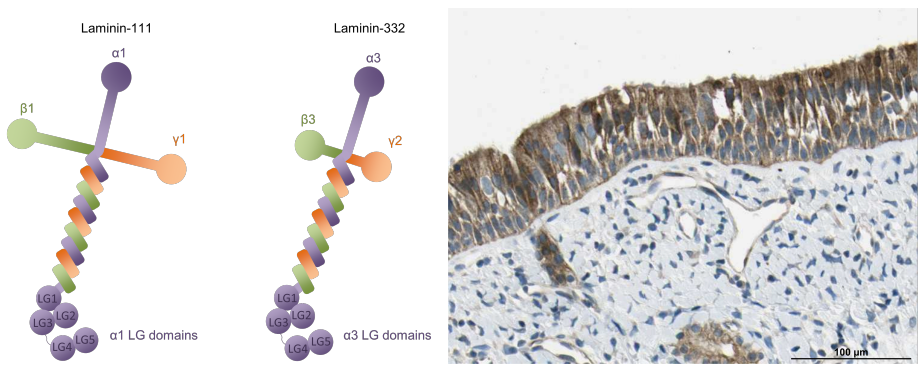

Figure 3. Schematic image of the Ln-heterotrimer (left) and histological section detecting Ln in the nasopharyngeal epithelium (right). Left: the isoforms Ln-111 and Ln-332 are shown. The different α, β and γ chains are of various lenghts but come together in a long coiled-coil region in all isoforms. At one end of the molecule, the α-chain C-terminus forms the globular domains known as LG1-5 that are important for interactions with cells. On the right: a histological section showing the distinct association of Ln α3 (serologically dyed brown) with the healthy adult respiratory epithelium. Image cropped and used with the permission of The Human Protein Atlas (38).

As Ln forms the connective scaffold for all epithelial cells (including the skin), one can picture the human body as perpetually coated in an underlying sheet of Ln from top to bottom. Laminins are large, heterotrimeric glycoproteins that once secreted autopolymerize extracellularly to form large matrices on the basal side of the cell-

linings (32). Comprising three separate chains designated as the α-, β- and γ-chain, the Ln monomer forms a large cruciform molecule with specific biological activities assigned to specific domains (Figure 3) (32). Moreover, there are five α-, four β- and three γ-chain variants encoded by separate genes in humans. These are combined in diverse constellations that form 16 different heterotrimeric isoforms. The nomenclature for Ln is based on the chain composition; the isoform consisting of α3, β3 and γ2 thus becomes Ln-332 (39). The different isoforms have distinct tropisms and plausibly functions; Ln-332 is the primary isoform in the basement membranes whereas Ln-211 is the primary isoform in muscle tissue, for instance. Recently, the Human Protein Atlas (http://www.proteinatlas.org/) has serologically and transcriptionally showed the specific presence of the majority of Ln chains in a large variety of organ systems. Judging by the detection of singular chains in the upper airways, the prevalent isoforms in this niche appear to be Ln-111, Ln-332 and Ln-411. These findings allow the future use of anatomically relevant isoforms in the field of Ln research.

If the epithelial integrity is compromised, the basement membrane becomes exposed to the lumen. In this occurrence, ECM-proteins are attractive targets for adherence by pathogens as a mean to circumvent the mucociliary elevator. Moreover, any microbes that disseminates past the epithelium need to cross this structure. As a testament to the importance of the basement membrane in host-pathogen interactions, microbes from every biological kingdom have been shown to bind to, and in some instances degrade, ECM-proteins (34, 40). This topic will be further discussed in the following chapters.

The Innate Immunity in The Airways

The second line of human defence against invading microbes is the innate immunity. The airway epithelial cells have a range of pathogen pattern recognition receptors (PRRs) that detect conserved microbial motifs known as pathogen-associated molecular patterns (PAMPs) including lipopolysaccharides (LPS), peptidoglycan, viral/bacterial nucleic acids and lipoproteins (41). When PRRs, such as the membrane bound Toll-like receptors (TLRs) or the intracellular nucleotide-binding oligomerization domain (NOD)-like receptors (NLRs), are activated by pathogen components, innate immune responses are induced. The result is the secretion of antimicrobial agents such as lysozymes, antimicrobial peptides (AMPs), interferons, lactoferrin and nitric oxide. Another consequence is the release of cytokines, which mediate inflammation and recruitment of phagocytes to the site of pathogen detection (41, 42). Moreover, inflammation causes augmented plasma exudation to the mucosa due to increased airway epithelial permeability, resulting in the

heightened presence of complement factors (43). Together, these innate immune responses exert a potent antimicrobial activity (44).

As one of the focuses of this thesis is the *H. influenzae* interaction with the complement system, this feature of the innate immunity will be discussed in greater detail.

The Function and Regulation of the Complement System

The complement system is an organized network comprising more than 30 (mainly serum) proteins whose chief function is to prevent microbial invasion (45, 46). This arm of the innate immunity exerts its effect in three steps: recognition of microbial non-self, opsonisation of the microbe, and in the case of Gram-negatives, osmolytic destruction of the bacterial cell via insertion of the pore-forming membrane attack complex (MAC) in the bacterial outer membrane (45, 46).

In many aspects, the central component of the complement is the C3 protein. Once cleaved, it yields the chemoattractant C3a and highly potent opsonin C3b (47). The function of C3b is two-fold; opsonize bacteria for neutrophil and macrophage phagocytosis and launch the terminal pathway of the complement system.

The mechanisms of C3 cleavage are well understood. Three separate and distinct pathways can lead to activation of the terminal pathway (47). The classical pathway is dependant on bactericidal IgG and IgM antibody-recognition of microbes. C1q recognition of two proximally close Fc-regions (indicating antibody opsonisation of a particle) activates a cascade that results in the formation of the C3-convertase C4b2a. The second route, called the lectin pathway, is activated by the recognition of mannose or N-acetylglucosamine on bacterial surfaces by mannose-binding lectin. Mannose-binding lectin-associated serine proteases are consequently activated and cleave C4 and C2 to yield the C3-convertase C4b2a. Finally, the alternative pathway is induced by the spontaneous hydrolysis of C3 and the subsequent attachment of C3b to the surface of cells (45).

Once C3 undergoes hydrolyzation, and the subcomponent C3b attaches to the nearby surfaces, the terminal pathway is induced (47, 48). In sequential interactions of the components C3b, C5, C6, C7 and C8, the pore-forming polymerization of C9 will finally result in MAC-formation that lyses the bacterial cells. Bacterial species that colonize the mucosal airway epithelium, where constant plasma exudation occurs, have to address the complement system proficiently in order to resist rapid clearance.

From the host's point of view, it is absolutely imperative to prevent complement-mediated autoimmunity (48). Therefore, the system is stringently regulated on almost every level. Complement down-regulatory proteins include C1-inhibitor, C4b-binding protein, clusterin, Factor H, Factor H-like protein 1, Factor I, properdin and

vitronectin (47). It has long been reported that bacterial pathogens sequester these soluble complement inhibitors on their surface as a mean of evading the innate immunity (49).

Vitronectin.

Vitronectin is a multifunctional glycoprotein present as a monomer in serum and as polymers in the ECM. Comprising 478 amino acids, it has domains with homology to the proteins somatomedin-B and haemopexin as well as reported binding sites for heparin, urokinase plasminogen activator-urokinase plasminogen activator receptor complex and integrins (50). Equipped with this vast set of tools, vitronectin is involved in a series of homeostatic processes that include cell migration, wound-healing, angiogenesis and complement regulation (51, 52). So far, vitronectin deficiency has not been reported in humans, but genetically engineered vitronectin-null (Vn(-/-)) mice have been shown to suffer from fibrinolytic imbalances and decreased microvascular angiogenesis (53, 54).

As an ECM-component, vitronectin safeguards the surrounding tissue against autoimmune complement activation. The glycoprotein inhibits the terminal pathway at two distinct steps; C5b-C7 formation and C9 polymerization, thus effectively preventing MAC-formation (52). Importantly, vitronectin is present in the airway lumen of healthy individuals, and at elevated levels in patients suffering from respiratory illnesses, as detected by bronchoalveolar lavage (55, 56). These two facts make soluble vitronectin an attractive ligand for bacteria. Indeed, respiratory tract pathogens such as *H. influenzae*, *Moraxella catarrhalis*, *Pseudomonas aeruginosa*, *Streptococcus pneumoniae*, *S. pyogenes* and *Staphylococcus aureus* have been reported to interact with vitronectin (50). Many of these species also use vitronectin as a mean of adherence to the host. Vitronectin is thus an important molecule in the host-microbe interactions in the upper airways.

Haemophilus influenzae – Expert Colonizer of the Human Upper Airways

A Commensal and An Opportunist

Haemophilus influenzae is a Gram-negative, facultative anaerobic small coccobacillus belonging to the *Pasteurellaceae* family of the Gammaproteobacteria class (57). The organism is well-known to microbiologists as it has been involved in several important scientific breakthroughs: it was the source of discovery of restriction enzymes (58), it was the first free-living organism to have its genome fully sequenced (59), and the first licensed glycoconjugate vaccine for use in humans was developed against the polysaccharide capsule of the serotype b (Hib) strains of the species (60).

The organism was first discovered in 1892 by Pfeiffer and mistakenly identified as the causative agent of influenza-disease, hence the species name (originally designated as *Bacillus influenzae*, or "Pfeiffer's bacillus") (61). The pathogen did not hold up to Koch's postulate as the aetiology of influenza and was eventually disproved as such (61). It is now known that *H. influenzae* is a cause of secondary bacterial infections after prior influenza virus-mediated disease (62), explaining the initial misidentification considering that viruses were not well-known at the time. In the 1930's, the bacteriologist Margaret Pittman conducted many pioneering studies on the organism, including the identification of encapsulated (divided into serotypes a-f depending on the biochemical features of the polyribosylribitol phosphate capsule that affects agglutination with antiserum) and non-capsulated strains, the latter designated nontypeable *H. influenzae* (NTHi) (63, 64).

H. influenzae is a fastidious and highly adapted human-specific commensal (20). So much so, that it has lost the ability to biosynthesize the essential co-factor molecules heme and nicotinamide adenine dinucleotide (NAD) (65-67), relying strictly on scavenging them from the environment in our bodies. This heme- and NAD-deficient phenotype is so rare that it has historically been used for clinical diagnostics of the species (65, 67). Clinical samples would be plated out together with a known "feeder" species that could provide these co-factors, and growth of "satellite colonies" in the immediate vicinity of the streak of "feeder" strain was an indication of *H. influenzae* (68).

H. influenzae colonization of humans, especially toddlers, is transient with a turnover rate of approximately three months (69). As the host clears the predominant residing strain, a successor strain replaces it in the available niche. The intermittent carriage rate of NTHi has been observed to be 32-77% in healthy children at any given time point (70-73). The earliest documented cases of carriage are from four Medieval German adult skeletons dated to 950-1200 A.D. (74). The dental plaque of these

individuals, when analysed with ancient-DNA technology, revealed concomitant carriage of capsulated and non-capsulated strains in the same individuals (74). Historically, the human nasopharynx has been regarded as the primary site of initial colonization, but recent reports show a prevalent presence of the species in the buccal mucosa of the oral cavity as well, lending additional merit to the dental plaque findings (6).

While residing in the upper airways and oral cavity, *H. influenzae* can proceed to cause mucosal infections including otitis media (OM), conjunctivitis, bronchitis and sinusitis if the host's stringent structural barriers and/or immune system is compromised by a preceding viral infection or prolonged episodes of inflammation (75, 76). Occasionally, further dissemination resulting in invasive disease such as meningitis and sepsis is manifested primarily (but not exclusively) by strains belonging to the capsulated serotype b clade (77-80).

Since the introduction of a capsular polysaccharide glycoconjugated vaccine against Hib, which practically eradicated Hib-mediated disease in the places vaccine-programs were employed, researchers have redirected their efforts to NTHi that is currently the most clinically relevant subgroup (77). The rest of this work, including the present investigation, will thus focus on the non-capsulated NTHi.

Genetic Heterogeneity

Margaret Pittman wrote this catching paragraph about *H. influenzae* as early as 1931:

> "*The bacteria of this group do not form a well characterized bacterial species, and it has long been recognized that individual strains differ from one another in morphology and virulence, in the appearance of the colonies which they form, in their ability to form indole, in power to ferment sugar and to induce hemolysis, in their immunological reactions, and even in their requirements for growth inartificial cultures.*"(63)

One hallmark of *H. influenzae* is its genetic (and subsequently phenotypic) diversity. This fact is mirrored by the difference in the number of annotated genes in whole genome sequenced strains, ranging from 1688-2355 open reading frames (ORFs) per strain. In parallel with this, the genome sizes vary between 1.79-2.01 mega base pairs (http://www.ncbi.nlm.nih.gov/genome/genomes/165). Recently, the "supragenome" of the species has been estimated to contain up to 4500 unique ORFs, while the core set of genes existing in all strains amounts to only 1485 of said ORFs (81). This means that 2/3 of the "supragenome" of *H. influenzae* is perpetually distributed among countless strains. According to the "Distributed Genome Hypothesis", naturally competent *H. influenzae* strains undergo continuous and dynamic genetic recombination processes during simultaneous colonization of the same host (82, 83). As the organism exclusively takes up intraspecies DNA (under normal circumstance),

naturally competent strains would "have access" to a wide variety of genes throughout time, allowing them to evolve with an altering environment without the burden of maintaining a large genome, thus gaining a fitness advantage (82, 83).

As a parenthesis, it can be noted that the introduction of the capsule biosynthesis loci has seemingly occurred twice throughout evolution in the NTHi background (plausibly via a rare horizontal gene transfer from other Gram-negative bacterial species including *Actinobacillus* spp., *Neisseria meningitides* and *Mannheimia haemolytica* (84)), as capsulated types can be grouped in two distinct lineages (85). Because the capsulated strains are thus largely clonal, the greatest genetic diversity is observed in the NTHi (85).

Due to this high intraspecies variation, researchers have invested substantial efforts on identifying genes and/or strains that are exclusively associated with commensalism and pathogenicity. Recent studies have managed to identify such genetic elements via genome array analysis of a wide range of clinical isolates and avirulent commensal strains from a broad geographical collection (81). A curious finding of this investigation was that the 28 genes identified as primarily pathogen-associated were not any of the already known and well-studied virulence factors such as adhesins or immune evasion factors, but comprised mostly uncharacterized proteins. It remains highly interesting to study the functions of these disease-associated genes.

Finally, it also has to be noted that the genetic heterogeneity of the species has implications for vaccine development, a subject that will receive more attention in a subsequent chapter.

Bacterial Factors Involved in Colonization and Virulence

As previously stated, colonization of the host is a central aspect of any host-dependant bacterial life. In medical microbiology, colonization is commonly equated to pathogenesis. As this may be true in some cases, and while conceding that colonization is a prerequisite for any following episodes of illness, it is certainly not true for all. Respiratory tract illnesses, for instance, originate in the vast majority of cases from bacteria belonging to the normal flora. These opportunistic pathogens that most often only cause asymptomatic colonization include *H. influenzae*, *S. pneumoniae*, *M. catarrhalis*, *S. aureus* and *S. pyogenes* (86-88). However, immature immune systems, defective structural barriers, primary or acquired immune deficiencies, prior viral infections and chronic inflammation may alter the conditions in this microecology, allowing otherwise commensal bacteria to take over and go rogue (89-93). But in order to do so, opportunistic pathogens need to be able to address several obstacles in the process. The *H. influenzae* factors involved in colonization and virulence are briefly reviewed here.

Adherence to Host Tissue

The first step of colonization when arriving in a new host is avoiding mechanical clearance by the mucociliary elevator. At this crucial stage, NTHi induces a decrease in (or arrest of) the ciliary beating, adheres to host cells or the surrounding tissue and forms microcolonies on the epithelium (20, 94, 95).

The importance of the ciliated cells for clearance of *H. influenzae* can be appreciated by reports regarding patients suffering from primary ciliary dyskinesia; *H. influenzae* is the predominant pathogen found in the sputum of these patients (94, 96). *Haemophilus* Protein D is a glycerol-3-phosphodiester phosphodiesterase surface-exposed lipoprotein (97). It has previously been shown to induce both a decreased ciliary beating frequency as well as detachment of ciliated cells in primary polarized epithelial cells (98), displaying one mechanism by which NTHi compromises the mucociliary epithelium. Other investigations have implicated NTHi-mediated activation of host protein kinase C epsilon in the process of decreased ciliary beating (99).

The Gram-negative endotoxin, also known as LPS or lipooligosaccharide (LOS) in some species including *H. influenzae*, is a well-characterized virulence factor and potent inducer of TLR-4-dependant inflammation (100, 101). A lipid-A-tethered outer membrane structure, it consists of a triheptose-3-deoxy-D-manno-octulosonic acid backbone that branches off with highly varied subsets of oligosaccharides (101). The LOS has been alternately implicated and refuted in the involvement of *H. influenzae*-mediated decrease of ciliary beating frequency (102-105). However, as the LOS structure has been shown to be highly variable in NTHi (101, 106), these results need not to be mutually exclusive. NTHi LOS has also been observed to directly bind to epithelial cells, thus potentiating bacterial adherence to host tissue (107, 108). Interestingly, in an experimental human nasopharyngeal colonization model, significant changes were only observed in two out of 16 investigated phase-variable genes (109). One encoded the IgA1-protease and the other was *licA*, whose gene product incorporates exogenously acquired phosphorylcholine into the LOS to increase the adherence to epithelial cells. The *in vivo* selection for LicA-producing subpopulations indicates that this mechanism is very important for host colonization.

Type IV pilus, a multicomponent, long filamentous surface structure commonly associated with bacterial conjugation, has also been shown to contribute to NTHi adherence to epithelial cells (110-112). Moreover, there is a number of proteinous adhesins imperative for the direct mucin- or host cell-binding of NTHi, including the autotransporters Hap (113, 114) and Hia (115), lipoproteins *Haemophilus* Protein D (97) and *Haemophilus* Protein E (116), P2 porin (117), outer membrane protein P5 (117-119) and the high molecular weight (HMW) adhesins (120). These proteins belong to vastly different protein families with little, if any, structural resemblance, indicating a highly multifactorial mechanism for the NTHi adherence to the

respiratory tract epithelium. Importantly, it has been frequently observed that the pathogen adheres to sites of epithelial damage, forming microcolonies in places where the cell confluency has been compromised (94, 98, 121). As the basement membrane on the basal side of the epithelium becomes exposed to the lumen during damage, it is highly plausible that bacterial interaction with the host ECM-proteins is imperative for pathogenesis. Several of the adhesins mentioned, including Hap and PE, have been shown to interact with ECM proteins such as Ln, collagen IV, fibronectin and vitronectin (122-125).

There are also conflicting reports about the occurrence of epithelial cell invasion. Some argue it is a pathogen-beneficial mechanism, others claim it to be host-beneficial (resulting in bacterial death) and yet a third group states it is not occurring at all (126-129). This particular mechanism needs further evaluation before consensus can be reached.

Biofilm-formation

Once adherence to the host tissue is established, many NTHi strains have the capacity to produce biofilms in particular anatomical locations (130). This colonization mechanism is also observed in other otopathogens including *M. catarrhalis* and *S. pneumoniae* (131). Biofilms are highly structured microbial communities consisting of bacterial cells embedded in extracellular protein-, DNA- and polysaccharide-matrices (132). "Fortified" biofilm-associated bacteria display much increased resistance to biological, chemical and physical environmental stresses (including antibiotics and the host immune system) as compared to planktonic microbes, and are believed to be the cause of persistent NTHi infections (132, 133). Indeed, it has been proposed that the majority of prokaryotic life on earth exists in biofilms rather than as dispersed singular cells (134).

Many bacterial factors have been implicated in NTHi biofilm-formation, including double stranded DNA and the previously discussed type IV pili and LOS (111, 135-137). Recently, the entire proteinous content of the extracellular material of the NTHi biofilm was mapped (138). Eighteen proteins, including P2 and P5, were shown to comprise the biofilm-specific extracellular proteome. Bacterial DNA as well as proteins from the cytoplasm, periplasm and the outer membrane were all reported to be present in the biofilm, a fact the authors accredit to bacterial cell lysis being integral to the origination of the community (138). Finally, it should also be noted that several quorum signalling pathways involved in the induction of NTHi biofilm-formation have been elucidated (139, 140).

From a clinical perspective, NTHi biofilms have primarily been implicated in (recurrent) OM with effusion and exacerbations of chronic obstructive pulmonary disease (COPD) (130). It is very plausible that biofilm-associated NTHi can cause chronic infections, as these communities are difficult to eradicate with conventional

antibiotics. Interestingly, one study showed that targeting key factors of the extracellular components of the NTHi biofilm for destruction would collapse the entire biofilm organization and increase clearance of the pathogen from the middle ear of chinchillas (141). Continued research of this persistent mode of bacterial colonization will be highly interesting to follow.

Host Immune Evasion

It is vital for bacteria living in the human body to either avoid, or circumvent, the host immune system during colonization. Investigators have shown how NTHi effectively addresses innate immune effectors such as AMPs, transferrin and nitric oxide (142-145). Moreover, the highly substrate-specific IgA1-protease of NTHi has epidemiologically been implicated in virulence (146). As secretory IgA1 is the main immunoglobulin present in the human airway mucosa, the IgA1-protease may facilitate NTHi persistence in the niche by hydrolysing the main effector of the acquired immunity in the respiratory tract (147). This mechanism has been shown *in vivo* for its upper airways coinhabitant *S. pneumoniae* (148).

Protection against phagocytosis is mediated by the capsule in serotypable strains (149), but recently it was shown that NTHi can produce a "pseudo-capsule" via extensive branching of the LOS that blocks IgM from binding to bacterial surface epitopes (150). Subsequently, neutrophil-mediated killing of NTHi was significantly impaired, providing one mechanistic explanation as to why the excessive presence of neutrophils in the inflamed middle ear does not clear NTHi infections.

The host humoral response has also been shown to be unspecifically activated via a yet unknown factor in NTHi outer membrane vesicles (OMVs) in a "super antigen"-like manner (151). The proliferating lymphocytes would produce antibodies that did not recognize NTHi, resulting in the diversion of the human adaptive immunity.

Evasion of complement-mediated killing is also of utter importance for NTHi colonization and virulence. The evidence shows that NTHi employs two distinct strategies for complement-resistance: i) blocking antibodies and complement components from reaching the surface via LOS-branching and ii) surface sequestration of complement down-regulatory host proteins.

It has been shown that NTHi incorporates host-derived molecules such as sialic acid and phosphorylcholine into its LOS as a mean of camouflage (100, 152). Moreover, alterations of surface glycans have shown to be important in preventing bactericidal antibodies from opsonizing NTHi, thereby preventing complement activation via the classical pathway (150, 153-155). In addition to these, LgtC-mediated modification of the LOS has been shown to delay C4b deposition on the bacterial surface via an unclear mechanism (156, 157). As a testament to their importance, several of these processes have been shown to be activated during exposure to normal human serum

(153-155), a scenario that is likely to occur *in vivo* during inflammation-mediated plasma exudation in the airway epithelium.

Nontypeable *H. influenzae* has also been shown to acquire host-derived complement inhibitors, such as C4BP, Factor H and vitronectin, to its surface (158-162). The outer membrane proteins P5 and Protein E have been shown to be important for Factor H- and vitronectin-binding, respectively, whereas the C4BP-binding factor of NTHi has remained elusive. In all instances, it has been shown that NTHi evades complement-mediated killing by these sequestration events, thus increasing its serum-resistance.

Despite the struggle that the bacteria put forth, each specific NTHi strain is normally cleared from the human host within three months after initial colonization (69). The eventual clearance is likely attributed to an overpowering pressure mounted over time by the host acquired immunity.

Niche Adaptability and Nutrient Acquisition

The nasopharyngeal tract is a nutrient-poor *milieu* for bacteria (163). Microbes that colonize this surface rely on sensing and responding to nutrient-scarcity and external environmental changes by activation of an array of scavenging and adaptation systems. It has even been hypothesized that the DNA transformation machinery in *H. influenzae* was primarily evolved as a nutrient uptake system in this barren niche rather than for genetic recombination purposes (164).

As previously stated, *H. influenzae* has lost the genes for *de novo* biosynthesis of heme and NAD. Exogenous NAD uptake is mediated by the outer membrane lipoprotein P4 and the P2 porin (165-167) before the molecule is further metabolized for utilization downstream in the peri- and cytoplasm (168, 169). Porin P2 is the most abundant protein in the outer membrane of NTHi (170), plausibly contributing significantly to maintaining a steady uptake of exogenous NAD. As no specific regulation element has been reported for either P4 or P2, the NAD uptake system is likely perpetually switched on.

This is in stark contrast to transport systems involved in the uptake and metabolism of heme and iron, which are tightly regulated. It was early reported that *H. influenzae* can scavenge human transferrin via an uptake system that is only active in the absence of heme, a scenario that would correlate with the mucosal epithelial environment (171). More recently, the ferric uptake regulator (Fur) regulon of NTHi was shown to contain 73 genes (172), meaning that approximately 4% of the genome was directly regulated by the intracellular Fe^{2+}-sensing of Fur. Many of these genes were expectedly involved in iron-utilization but, interestingly, it was shown that iron/heme-independent virulence factors such as the IgA1-protease were also under the regulatory control of Fur. This again suggests that NTHi re-wired several

virulence factors to be automatically switched on in iron/heme-depleted environments, *i.e.* in the human nasopharynx.

But the response to iron/heme-deficiency is not exclusively regulated by Fur. The core (identical in a five capsulated and non-capsulated strains) and non-core modulon response to low levels of iron/heme has been mapped *in vitro* and *in vivo* (173). Investigators identified 55 core and 200 non-core ORFs that are up- or down-regulated in the absence of iron/heme, exhibiting how NTHi saves energy by tightly regulating the expression of iron/heme-utilization genes. One factor that has been implicated in sensing heme-availability is the multifunctional Sap-transporter that also recognizes host-derived molecules in the microenvironment and alters the bacterial response accordingly (128, 174).

The urease operon has been shown to be one of the most upregulated genetic elements of NTHi *in vivo* (175, 176). The importance of urease for onset of disease has been demonstrated in several studies, establishing the role of the enzyme in raising the pH in the human respiratory tract microenvironment to facilitate bacterial growth (177, 178). This is in analogy with several other human pathogens in unrelated niches including *Helicobacter pylori* and *Proteus mirabilis*. As human mucins are highly acidic, NTHi is likely dependant on proficient pH-buffering during inflammation and mucus-hypersecretion.

The conditions NTHi encounters in the human nasopharynx and Eustachian tube differ considerably from those in the lower respiratory tract of COPD-patients. The latter environment is characterized by chronic inflammation, excessive presence of phagocytic cells, epithelial damage, failure of the mucociliary elevator, mucus hypersecretion (causing local hypoxia), elevated cytokine levels and oxidant/antioxidant dysregulation (92). NTHi adapts ably to both these settings, and the genetic elements that allow descension into the bronchia of COPD-patients have been studied (92, 176, 179). Urease, IgA1-protease, anti-oxidants and HMW-adhesins are among the factors reported to be upregulated during exposure to this *milieu*. Moreover, it has been observed that COPD-patient-derived alveolar macrophages are defective in phagocytosis of NTHi but not of *M. catarrhalis* or *S. pneumoniae* (90). These data collectively cast light on the bacterial adaptation and survival in various niches of the human body.

Polymicrobial Interactions

Although NTHi is a proficient colonizer of the human respiratory epithelium, onset of disease most commonly requires prior priming of the host by viral agents (76). For this reason, the polymicrobial interactions that underlie NTHi-virulence are important but somewhat overlooked aspects of pathogenesis.

Clinical evidence shows a prevalent manifestation of viral-NTHi co-infections, with the viruses involved being primarily influenza A, rhinovirus, adenovirus and human

respiratory syncytical virus (180-186). More than 20 years ago, researchers showed how the mucociliary elevator of the middle ear was severely compromised by adenoviral infections for up to 35 days (187). This would surely diminish the host defence against intruding secondary bacterial microbes such as NTHi. Several more molecular mechanisms behind viral facilitation of secondary NTHi-infections have recently been unfolded. Respiratory syncytial virus has been reported to induce down-regulation of the host antimicrobial peptide beta-defensin-1, an attenuation of the host immunity that markedly promoted over-growth of NTHi in the nasopharynx (188). Other investigators have shown that rhinovirus attenuated the host TLR-2-mediated immune response to NTHi via the adaptor protein IRAK-1 signalling (189). In a third study, researchers reported that if the host was subjected to a primary influenza A virus infection, NTHi could survive in the pulmonary system of mice without many of the genes normally required for stress responses *in vivo* (190). They also showed that NTHi needed to address excessive oxidative stress brought on by the influenza A virus during co-infection, a condition that the pathogen adapted to by activating the oxidative stress response modulator *iscR*. These studies exemplify molecular mechanisms by which viral infections render the host highly susceptible to secondary NTHi infections and how the bacteria can exploit and adapt to various microenvironments *in situ*.

But intermicrobial cooperation is not restricted to interkingdom partners. Indeed, NTHi is often isolated with other bacterial otopathogens, including *M. catarrhalis* and *S. pneumoniae,* in clinical settings (180, 191-195). Mixed species experiments have shown that NTHi quorum signalling can induce the biofilm-formation of *M. catarrhalis* and *S. pneumoniae* (140, 196, 197). Other reports suggest that mixed NTHi-*S. pneumoniae* OM are unique clinical entities, separate from single pathogen infections with regard to pneumococcal serotype distribution, suggesting that specific interspecies strain-strain interactions facilitate virulence (198). The mechanisms behind these synergistic infections remains to be more fully elucidated.

Finally, the highly interesting outer membrane vesiculation systems have been shown to play important roles for interspecies cooperation, conferring antibiotic resistance and serum resistance to bacterial coinhabitants in the same niche (199-201). The dispersion of OMVs in the environment may mediate many more polymicrobial interactions, including long-range signalling and nutrient allocation.

Transmission

The molecular mechanisms of bacterial transmission between hosts are the least studied aspect of the cycle of colonization and spread. Indeed, doing a literature search revealed that there are no such investigations published regarding NTHi. However, one recent publication revealed the mechanistic potentiation of *S. pneumoniae* spread by a concomitant influenza A superinfection (202). Authors showed that influenza A virus-mediated mucus-hypersecretion facilitated shedding of

the bacterial pathogen in an infant mouse model. Moreover, they showed that TLR-2 activation decreases this effect, as transmission of *S. pneumoniae* was much increased in *tlr2-/-* mice. Interestingly, a strong bottleneck effect was observed during transmission: colonization was established by a very small number of bacterial cells that transmitted to the new host. As. *S. pneumoniae* and NTHi colonize the same niche and have very similar clinical manifestations, it is plausible that respiratory tract viruses may facilitate the shedding of NTHi in the same manner. However, this remains to be experimentally addressed.

It is known that *H. influenzae* can survive for several days on inanimate surfaces (203). This fact, taken together with the extensive presence of the species in saliva and nasal mucus (204, 205), could potentially explain one route of transmission in, for instance, children's day care centres.

It will be interesting to follow the research in this field to see if additional bacterial factors involved in ensuring shedding from biofilm and transmission to a new host can be identified at the molecular level.

H. influenzae-Mediated Disease

As mentioned, NTHi can cause a range of mucosal infections when given the opportunity. These include OM, conjunctivitis, sinusitis, bronchitis and exacerbations of COPD (75). Moreover, NTHi is observed to occasionally disseminate and cause invasive infections (78, 79). This work will focus on the two most prevalent NTHi-mediated diseases; OM and COPD exacerbations.

Otitis Media

Otitis media, or middle ear inflammation, is a common childhood disease. In large cohort studies, it has been shown that up to 49%-80% of children experience one or several episodes of OM before the age of 3 years (206, 207). The incidence rate has been estimated to an astonishing 709 million cases/year globally (208). In Sweden alone, the incidence of acute OM (AOM) is 200 000 cases per year (209). Otitis media is one the most common reasons, if not the single most common cause, of children seeking medical attention, experiencing hearing loss, receiving antibiotic treatment, and undergoing surgery (41). The socio-economic burden of OM is therefore of considerable significance.

Aetiological agents of OM can be viral, bacterial, or both simultaneously (42). The most common viral agents are respiratory syncytial virus and adenovirus, whereas the most common bacterial agents are *S. pneumoniae*, NTHi and *M. catarrhalis*. It has been repeatedly shown that viral upper respiratory tract infections precede episodes of OM, highlighting the microbial interplay and complexity of disease onset (210), and the molecular mechanisms behind these phenomena are beginning to unravel as previously discussed.

The reason for OM being principally a childhood disease is partly anatomical (Figure 4). The Eustachian tube (also called auditory tube) is shorter and the angle is horizontal in the small, round skull of toddlers, potentiating microbe ascension from the nasopharynx to the middle ear (211). Moreover, the muscles that control the entry to the Eustachian tube are not well-developed in infants. As children reach 4-5 years of age, their skulls elongate, the entry tightens and the Eustachian tube takes on the conformation of later life. Consequently, a marked drop in OM incidence rate is observed between the age groups 1-3 years and 4-6 years (212).

Once pathogens reach the middle ear and proliferate, inflammatory responses will be induced via the host's PRRs such the TLRs and NLRs (41). At this point, inflowing fluids and mucus that clog hearing and prompt otalgia (due to the sheer pressure) will fill and be trapped in the normally gaseous tympanic cavity. In rare instances, the tympanic membrane might succumb to the internal pressure and burst. The clinical symptoms of AOM include fever, otalgia, malaise and occasionally otorrhea (213).

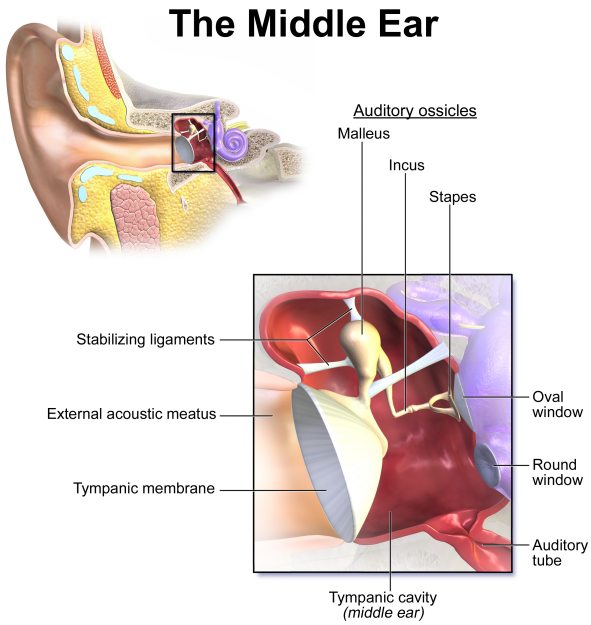

Figure 4. The anatomy of the middle ear. The Eustachian tube (also called autitory tube) seals of the tympanic cavity from the nasopharynx. However, should microbes be able to invade the middle ear from the nasopharyngeal tract, they cause a strong inflammatory reponse resulting in OM. Image used with permission (31).

Most patients can clear the acute infection without treatment, but many require medical attention including antibiotic therapy (209). In some cases, OM can become chronic, resulting in recurrent episodes of middle ear inflammation after the completion of each antibiotic treatment, often caused by the same pathogen. Biofilm-associated NTHi have been implicated in this disease, as NTHi is the primary aetiology for recurrent OM (130, 213, 214). Nontypeable *H. influenzae* is also the reported cause of 55-95% of bacterial AOM in children (75). Considering the extremely high global incidence rate of OM, NTHi is quite plausibly one of the most common bacterial pathogens of man.

Exacerbation of COPD

Chronic obstructive pulmonary disease occurs with a high incidence rate in the world, affecting 5-10% of the population (215). It is estimated that 400 000-700 000 patients suffer from COPD in Sweden (216) and 15.9% of all hospital admissions in the UK are reported to be COPD-related (217). This chronic condition is also associated with a high degree of morbidity and mortality, being the third leading cause of death in USA (218). Collectively, the socio-economical burden of COPD is, in analogy with OM, of striking scope.

Patients suffering from COPD are diagnosed with an irreversible chronic inflammation of the lower airways. The clinical symptoms of COPD include obstruction of breathing, excessive coughing, fatigue, chest tightness and susceptibility to respiratory infections (219). The number one risk factor of developing COPD is cigarette smoking, albeit subjection to air pollution, occupational exposure to dust, gases and fumes as well as genetic factors (such as α1-antitrypsin deficiency) have been implicated in disease onset (215).

As the pathophysiology of the disease includes the displacement of the mucociliary elevator, the airways of COPD-patients are intermittently colonized by opportunistic pathogens such as NTHi, *S. pneumoniae*, *M. catarrhalis* and *P. aeruginosa* (220). These bacterial species, as well as a series of viruses such as rhinovirus, parainfluenza virus, influenza virus and respiratory syncytical virus, cause acute exacerbations of COPD (218). Exacerbation is associated with abnormal and sudden worsening of respiratory symptoms, including increased dyspnea, cough, sputum purulence and general symptoms of common cold (221). Pathogen-mediated exacerbations are induced by the activation of the host's PRRs after the acquisition of a new strain and the severity of single episodes varies from mild to life threatening (222, 223). NTHi is the primary aetiology of COPD exacerbation, causing approximately 20-30% of the cases (217, 218). Frequent exacerbations have been shown to strongly affect disease progression (including the decline of lung functionality as well as the mortality rate) and often require antibiotic treatment (221).

Investigators studying the pulmonary physiology of COPD-patients colonized by NTHi have made some highly interesting observations. One study showed that in addition to NTHi-specific IgA being significantly lower in NTHi-colonized patients compared to non-colonized patients, a fact that can plausibly be attributed to the NTHi IgA1-protease, the presence of host metalloproteinase-9 (MMP-9) was in average approximately three times higher in the sputum of individuals colonized by the microbe (224). This was true for both the pro- and active form of the enzyme. Moreover, the ratio of the tissue inhibitor of metalloproteinase-1 (TIMP-1) to MMP-9 was 10 times lower in patients colonized by NTHi, suggesting a high activity of MMP-9 *in situ*. As MMP-9 is involved in ECM-rearrangement, the researchers hypothesized that "bronchial colonization by *H. influenzae* may cause structural

changes in the ECM". These findings again suggest that pathogen interaction with the ECM-proteins may be highly important for bacterial pathogenesis.

Other studies have discovered that alveolar macrophages derived from COPD-patients are defective in NTHi phagocytosis. The mechanism behind this dysfunction is currently unclear (90).

Finally, investigators have reported that the presence of AMPs are significantly lower in COPD patients colonized by, or experiencing exacerbations mediated by, NTHi (220). These observations collectively cast light on selected aspects of NTHi-mediated exacerbations of COPD and open the door for evaluation, and potentially inhibition, of the molecular mechanisms behind pathogenesis.

Vaccine Development Against Nontypeable *H. influenzae*

The first commercial *H. influenzae* vaccines were not the glycoconjugate Hib-vaccines, but a series of vaccines launched in the US during the Spanish flu pandemic of 1918-1919 when *H. influenzae* was still believed to be the aetiological agent of influenza (61, 225). As pressure was mounting on authorities to provide a treatment for the disease, various medical institutions launched at least five different vaccines based on isolated strains of "*Bacillus influenzae*" from the airways of influenza patients. This took place more than a decade before Pittman's discovery of capsulated and non-capsulated strains in 1931, so there are no details on what serotypes/NTHi strains were used. However, based on current understanding of epidemiology, they were most probably Hib and perhaps a number of NTHi strains. In any event, most of the vaccines were merely heat-inactivated bacterial preparations that were injected into patients. Several hundreds of thousands of adults were immunized with these heat-denatured *H. influenzae* lysates. Curiously enough, high efficacies in influenza-disease prevention were unanimously reported for them (61). This could indicate that i) heat-inactivated and adjuvant supplemented bacterial preparations induced a potent immune response in adults (to perhaps the Hib-capsule antigen) and ii) secondary *H. influenzae* infection following the influenzae A virus infection played a large role in the high mortality observed during the 1918-1919 pandemic.

With the repudiation of *H. influenzae* as the causative agent of influenza, the use of these vaccines were soon discontinued and forgotten (61). However, in the 1990s, with a rise in interest in the medical community to address prevention of bacterial meningitis in children, the protein-conjugated capsular-polysaccharide vaccine against Hib was licenced as the first glycoconjugate vaccine for use in humans (60). This vaccine provided a T-cell-dependant memory cell-inducing protection in toddlers, something that could not be achieved with a capsular polysaccharide-antigen alone.

A highly efficient vaccine, Hib-mediated infections were practically eliminated in the wake of its introduction in national immunization programs (226). In should be noted, however, that Hib-disease is currently still a major problem in areas that have not yet employed the vaccine on a large population scale (227).

Since the achievement of developing a Hib-vaccine, the focus in *H. influenzae* vaccinology has shifted to NTHi. The non-capsulated strains provide a vastly different scientific challenge than Hib due the absence of a singular main surface antigen, which in the case of Hib was the capsule. Moreover, as previously discussed, NTHi strains are highly heterogeneous, making the identification of suitable antigens a partly epidemiological task. In addition to ubiquity, promising antigens need to display conservedness, cell surface-exposure and antigenicity. Currently, there are no licensed NTHi vaccines.

Table 1. List of NTHi antigens tested experimentally *in vivo* for potential as vaccines.

Antigen(s)	Animal Model	Outcome of Immunization	Reference
Hap	Mouse nasopharyngeal colonization	Significantly reduced colonization	(228, 229)
Integration Host Factor (DNABII protein)	Chinchilla middle ear biofilm clearance	Significantly enhanced clearance	(230)
LOS	Chinchilla middle ear and nasopharyngeal clearance	Significantly reduced colonization	(231)
Omp26	Rat pulmonary clearance	Significantly enhanced clearance	(232)
Outer membran vesicles	Mouse nasopharyngeal colonization clearance	Significantly reduced colonization	(233)
P4	Mouse nasopharyngeal clearance Mouse nasal colonization	Significantly enhanced clearance Significantly reduced colonization	(234) (235)
P5 + PilA	Chinchilla middle ear and nasopharyngeal clearance	Significantly earlier clearance and significant reduction of middle ear biofilm	(236, 237)
P6	Mouse nasopharyngeal clearance	Significantly enhanced clearance	(238, 239)
Protein D	Chinchilla middle ear clearance Rat middle ear clearance Rat pulmonary clearance	Mixed results	(240, 241)
Protein E	Mouse pulmonary clearance	Significantly enhanced clearance	(116)

The potential of a series of NTHi antigens for vaccine development has been experimentally investigated (116, 228-241). The bacterial components that have been studied in *in vivo* models are compiled in Table 1. The majority of the tested antigens elicit the desired immune protection, but, with one exception, these findings remain to be verified in translational clinical trials in humans. Moreover, whereas protection against heterologous strains have been addressed in a number of the studies, generally larger strain collections need to be assessed for evaluation of potential prophylaxis in humans.

There is currently one NTHi-component-based vaccine licenced for use in humans, but not against NTHi-mediated disease. *Haemophilus* Protein D has been used as the antigenic protein-carrier for pneumococcal capsular polysaccharides (242). Whereas the efficacy of the vaccine in prevention of invasive pneumococcal disease has been confirmed (243), ambivalent results have been reported regarding its prophylactic capacity with regard to NTHi-mediated infections. One cohort study reported a 33% decrease in NTHi-mediated OM in vaccinated children as compared to an unvaccinated control group (244), but these findings have not been observed in any additional published investigations. On the contrary, other studies have reported that no significant decrease in nasopharyngeal carriage of NTHi has been observed in vaccinated contra unvaccinated children (245-247). This is in stark contrast to the Hib-vaccines, where an abolishment in Hib carriage is observed. As NTHi is an opportunistic pathogen, it is likely that the rate of carriage and incidence of infections correlate. In any regard, the hunt for a more potent NTHi vaccine is currently on going.

Finally, one particularly interesting study merits additional attention. As previously mentioned, bacterial biofilms contain a large amount of extracellular DNA. Goodman and co-workers could show that this DNA is structured in a highly organized three-dimensional grid where bacterial DNA-binding proteins, designated DNABII, appear with regular spatial intervals as the “cornerstones” of every “grid-monomer” (230). Targeting these structural components for immune destruction, researchers could show that immunization with a DNABII-protein known as Integration Host Factor would collapse the entire NTHi biofilm *in vitro* and *in vivo*. This resulted in significantly enhanced clearance of biofilms in a chinchilla middle ear model. Moreover, they could show that biofilm-associated bacteria that were subjected to this treatment displayed a significantly increased susceptibility to antibiotics (141, 230). These findings show that targeting biofilm-components as immunization antigens may yield highly efficient vaccines that could be used in patients already chronically colonized by biofilms.

The Present Investigation

Aims

The aim of this thesis was to at the molecular level study NTHi factors involved in host colonization processes, namely complement-resistance and adherence to the ECM. Newly identified bacterial colonization factors were to be evaluated for potential vaccine development. The specified aims were:

- To in detail characterize the previously reported interaction between *Haemophilus* Protein E and vitronectin.

- To identify novel ECM-binding proteins in NTHi.

- To characterize the interactions between newly identified ECM-binding bacterial proteins and their host ligands.

- To conduct epitope-mapping on newly identified potential antigens.

- To evaluate the effect of immunization with novel bacterial colonization factors in a mouse pulmonary clearance model.

Results and Discussion

Paper I & II: *Haemophilus* Protein E and Protein F delay C9 deposition on the surface of NTHi by interacting with the C-terminal domain of vitronectin.

Nontypeable *H. influenzae* has previously been shown to interact with the complement inhibitory protein vitronectin as a mean to evade the host innate immunity (160). However, the details of this interaction were not elucidated. Moreover, the actual bacterial components that are responsible for vitronectin-binding remain presently unidentified in a series of pathogens (50), suggesting a lack of knowledge of the molecular mechanisms that underlie this virulence trait. By characterizing the protein-protein interaction between Protein E and vitronectin, we aimed to provide new insight into this aspect of bacterial pathogenesis.

In Paper I, we employed site-directed mutagenesis of recombinant Protein E to show that the two positively charged amino acid residues lysine 85 and arginine 86 are responsible for the electrostatic interaction with vitronectin. Moreover, by producing full-length and truncated recombinant human vitronectin in mammalian expression systems, we could identify that Protein E binds to a C-terminal region of vitronectin between amino acid residues 353-363. Importantly, a delayed C9 deposition and MAC-formation was observed in the NTHi wild type strain as compared to the isogenic Δ*pe* deletion mutant. In conclusion, we showed the molecular function of Protein E in the direct vitronectin-mediated inhibition of complement-induced osmolytic killing of NTHi.

It has since been reported that Protein E also interact with Ln and plasminogen, rendering it a highly multifunctional virulence factor (122, 248). Moreover, the crystal structure of Protein E has also been solved (249). The three-dimensional arrangement of the protein revealed that it dimerizes on the bacterial surface, and observations of the concomitant vitronectin- and Ln-binding could be strengthened by the spatially separated binding-sites for the host components (Figure 5).

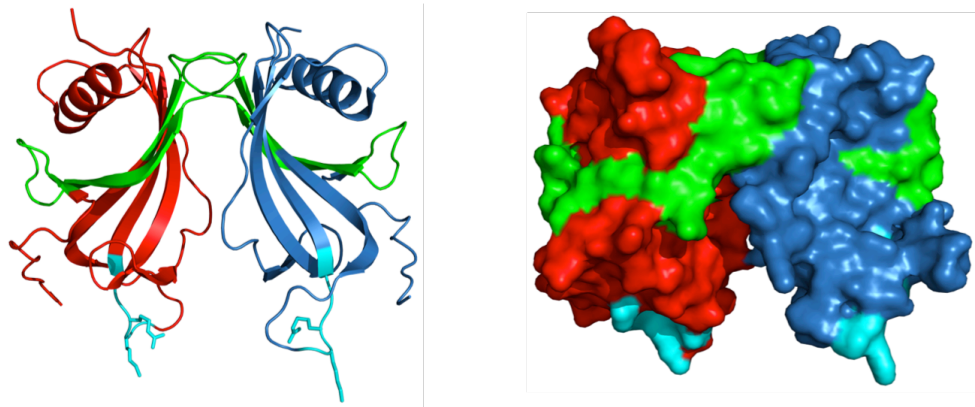

Figure 5. The crystal stucture of the Protein E dimer. The cartoon and surface-structure representation on the left and right, respectively, show two monomers colored red and blue that dimerize to complete the quaternary stucture of the complex. The vitronectin- and Ln-binding regions are colored in cyan and green, respectively. Image used courtesy of Dr. Birendra Singh.

As important as the Protein E interaction with vitronectin is for NTHi, the isogenic Δ*pe* deletion mutant strain did not display a completely abolished vitronectin-binding, suggesting the presence of additional bacterial components involved in the interplay with the complement inhibitor. The aim of Paper II was to identify these factors.

We ran the NTHi outer membrane vesicle proteome on a 2D-gel and conducted Far-western blotting with vitronectin to pull down novel vitronectin-binding proteins. This yielded a particularly strong hit to an approximately 30-kDa component. We identified the spot using mass spectrometry and designated the previously uncharacterized protein as *Haemophilus* Protein F (PF), in keeping with tradition of Protein D and E.

Protein F is annotated as a 32 kDa substrate-binding component of an adenosine triphosphate (ATP)-binding cassette (ABC)-transporter and a homolog of the manganese-utilizing YfeA protein of *Yersinia pestis* (250). It has no primary sequence homology to Protein E, ruling out a conserved vitronectin-binding motif in NTHi. However, in analogy with Protein E, we could show that PF sequesters vitronectin on the bacterial surface, inhibits C9 deposition and polymerization, thus down-regulating the MAC-mediated killing and increasing the serum-resistance of NTHi. The simultaneous deletion of Protein E and PF was shown to have a cumulative negative effect on the vitronectin-binding capacity of NTHi. Interestingly, it was observed that PF interacts with the same vitronectin region as Protein E, possibly suggesting a conserved pathogen-binding region on the host molecule as has been reported for Factor H (251). These studies shed light on the multifactorial interactions of NTHi with complement down-regulatory proteins.

Paper III: *Haemophilus* Protein F mediates bacterial adherence to host tissue by interacting with laminin and epithelial cells.

When conducting structural 3D-modeling of PF, we noticed a strong resemblance to streptococcal Ln-binding proteins Lmb and Lbp. This was striking, as the primary sequence homology was very low. We hypothesized that due to the structural properties of PF it could potentially interact with Ln in analogy to Lmb and Lbp.

In Paper III, we could show that PF is a Ln-binding protein that promotes bacterial adherence to immobilized Ln. Isogenic Δ*hpf* knock out mutants (in six different clinical strains) displayed consistently decreased Ln-binding capability as compared to parental wild type strains. Moreover, a cumulative decreased effect in Ln-binding was observed in an isogenic Δ*pe*/*hpf* double mutant.

We could also show that the N-terminus of PF, the same region that interacts with vitronectin, was mediating the binding to Ln. Electronmicrographs of gold-labelled PF indicated that the protein was binding to the LG-domains on the C-terminus of the Ln α-chain. This was highly interesting, as the same binding-region had previously been shown for Protein E (122) as well as for *Mycobacterium leprae* (252), indicating a potentially conserved pathogen-associated motif. This hypothesis is currently under investigation in our lab.

Finally, as many bacterial Ln-binding proteins have been observed to also interact with epithelial cells, we evaluated the PF-mediated bacterial adherence to human epithelial cells. We could show, at both the protein-cell level as well as the cell-cell level, that PF promoted direct bacterial binding to primary human bronchial epithelial cells. We concluded that PF is a novel multifunctional NTHi adhesin that potentiates bacterial colonization of the host by interacting with vitronectin, Ln and epithelial cells.

As ECM reconstruction and NTHi accumulation in sites of disintegrated epithelium have been observed during NTHi infections, the interaction with Ln is indicatively highly important for the pathogenesis of this species (94, 98, 121, 224). This merits further efforts to identify additional Ln-binding proteins, which is currently undergoing in our lab.

One very curious aspect of PF is its presence at the cell surface. As previously mentioned, PF is annotated as a periplasmic substrate-binding component of the ABC-transporter superfamily. Judging by its structure and homology, it is plausibly involved in divalent metal ion transport (Figure 6). It lacks lipidation sites and transmembrane domains but is still consistently detected with highly specific affinity-purified antibodies on the surface of wild type NTHi, and is absent from the surface of the isogenic deletion mutant. Indeed, introducing the *hpf* ORF in a heterologous *Escherichia coli* host results in ascent of PF to the surface of *E. coli*. The mechanism

behind this surface relocation is presently unknown, and we are currently conducting investigations of the phenomenon. It can be mentioned that there are an abundance of reports that show the surface-association of cytoplasmic bacterial enzymes, many of which have been implicated in host-pathogen interactions (253). The term coined to describe these multifunctional factors is "moonlighting proteins". Our data indicated that PF is a moonlighting NTHi protein that exerts diverse functions in the periplasm and on the outer membrane.

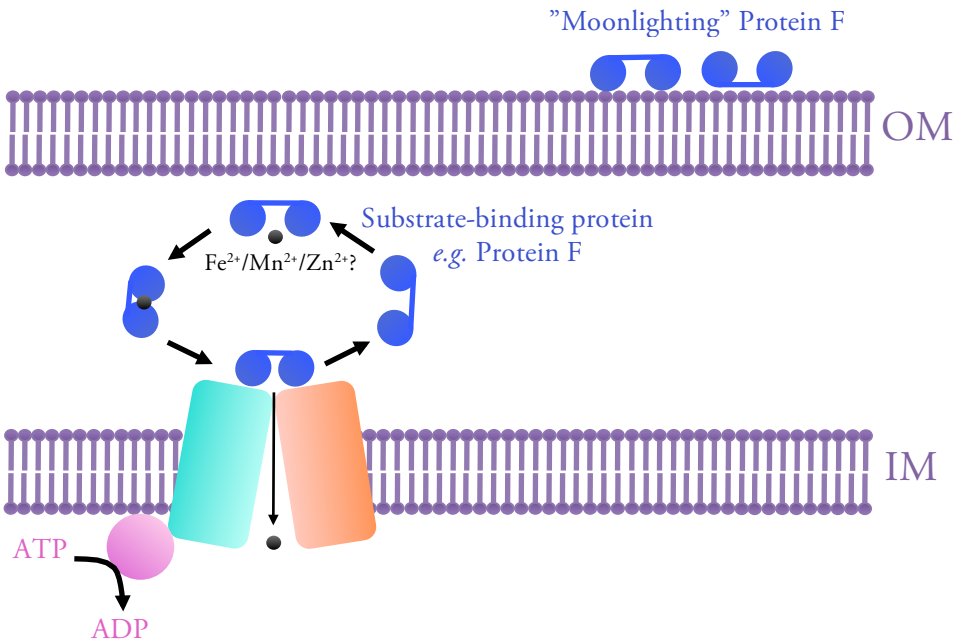

Figure 6. Schematic representation of a Gram-negative ABC-transporter. The substrate-binding component (blue), such as Protein F, moves freely in the periplasm. Once it binds its substrate, the protein undergoes a conformational change and gains affinity for the two inner membrane bound permeases (orange and green). It will deliver its cargo to these pores, and the cytoplasmic ATPase component (pink) will help pump the substrate into the cytoplasm by hydrolysing ATP to ADP. Once the substrate-binding protein has delivered its cargo, its conformation opens again, the protein loses affinity for the permeases and is released back into the periplasm (254). Protein F, however, is also consistently detected "moonlighting" on the bacterial cell surface. The mechanism behind the surface-association is currently unclear.

In a recent study, the extracellular biofilm-specific proteins of *S. aureus* were mapped (255). Researchers showed an excessive cell surface-association of cytoplasmic proteins in the early stages of biofilm-formation. They could also show that this mechanism was pH-dependant and suggested that the cytoplasmic proteins adhering to the surface of bacterial cells were crucial for biofilm-formation. The mechanism of release

of cytoplasmic proteins in the environment were not elucidated, but the authors hypothesize that lysis of subpopulations within the bacterial microcommunity is important for the generation of biofilms. As PF has been shown to be a part of the extracellular protein network in NTHi biofilms (138), it is not impossible that a similar mechanism can explain the moonlighting activity of PF. This question remains to be answered.

For being, until recently, uncharacterized, PF is very well-studied protein. As a testament to its importance in NTHi physiology, PF has regularly been detected in several "-omics" studies (Table 2). The protein has been shown to be significantly upregulated during iron/heme deficient growth conditions as well as during bacterial growth in pooled human sputum from COPD patients (173, 176). Moreover, it has been detected as a part the NTHi OMV- and extracellular biofilm-specific proteome (138, 256). Finally, in a seminal study, the PF-operon was shown to be one of 85 non-essential gene elements that are indispensable for bacterial virulence *in vivo* (190). Collectively, these findings show that PF is a highly important host colonization factor and a potential target for antimicrobial therapy.

Table 2. Detection/role of PF in various NTHi "–omics" studies.

Investigated Element	Type of Study	Protein F Annotation	Result	Reference
Growth in Fe/Heme restricted media	Transcriptomic	HI0362/*yfeA*	PF upregulated 1.17-11.74x	(173)
Growth in COPD sputum	Proteomic	NP_438524.1/YfeA	PF present in 3.932x greater abundance	(176)
NTHi OMV proteome	Proteomic	NTHi0481	PF present (142 proteins in total)	(256)
NTHi biofilm-specific extracellular proteome	Proteomic	HI0362/Q57449	PF present (18 proteins in total)	(138)
Single and IAV co-infection in murine lung	High-throughput sequencing of transposon insertion sites	*yfeABCD*	PF essential for single and co-infection alike	(190)

Paper IV: Immunization with *Haemophilus* Protein F confers increased mouse pulmonary clearance of NTHi.

As previously stated, a promising antigen to be used as a component in a NTHi vaccine needs to be surface-exposed, antigenic, conserved and ubiquitous in the heterogenic strains. As PF excellently fulfils these criteria, we characterized its antigenicity and investigated the effect of PF-immunization on the pulmonary clearance of NTHi in mice.

In Paper IV, we could show that antibodies raised against the host-interacting N-terminus of the protein were functional in opsonizing our model NTHi strain as well as a heterologous clinical isolate and promote phagocyte-mediated killing of the bacteria in an opsonophagocytic assay.

If PF is ever to be used in a human vaccine, caution has to be observed in order not to induce autoimmunity by forcing an immune response to epitopes that might resemble self-structures. In order to get an indication of the human response to PF without experimental immunization, we assumed that majority of adults have experienced previous bouts of NTHi infections during childhood. Hence, we tested the sera of 60 healthy adult blood donors for presence of anti-PF IgG. In our experimental set up, we could detect circulating anti-PF IgG in the sera of approximately 26% of the individuals, suggesting that PF does not resemble a host-like epitope and is probably immunogenic in humans. Conducting epitope mapping of PF, we recognized that the human humoral response to PF differed considerably from that obtained in the anti-PF antiserum raised in rabbits using recombinant PF. Human IgG primarily reacted with the host-interacting PF N-terminus, whereas this region was immunoprivileged in rabbits. As NTHi is a human-specific pathogen, it is plausible that the human response confers better protection. To force a humoral response to the N-terminus, mice were immunized four times with KLH-conjugated PF^{23-48} or a negative control peptide. Once the immunization schedule was completed, animals were challenged intranasally with NTHi and the pulmonary clearance of bacteria was examined. Our results showed that immunization with PF^{23-48} caused a significantly increased clearance of NTHi at both tested time points.

These results should be seen in the light of the human-specificity of NTHi. In nature, NTHi is never observed to infect any other species than man. Pfeiffer himself never managed to find an animal model for *H. influenzae* despite inoculating mice, rats, guinea pigs, rabbits, pigs, cats, dogs and monkeys (61). The effect observed in our study can thus conceivably be amplified when translated to human biology. This remains, however, to be experimentally addressed.

In conclusion, immunization with PF will have a three-fold effect. Firstly, blocking a NTHi colonization factor to decrease its adherence to the upper airways. Secondly, opsonizing NTHi with bactericidal antibodies to promote a more rapid clearance in

the case of pathogenesis. And lastly, as PF has been reported to be an integral part of the NTHi biofilm-specific proteome, immunization with PF could potentially help eradicate biofilms as demonstrated for DNABII. We therefore suggest that PF can be a promising candidate as one of the antigens in a multicomponent NTHi vaccine.

Future Perspectives

With new knowledge arise new questions. Without presenting detailed proposals, I would like to highlight some aspects of *H. influenzae* colonization in particular, and bacteriological research in general, that in my opinion need further attention in the future.

Firstly, all available evidence points to a sophisticated bacterial detection of, adaptation to, and selection in, various microenvironments during colonization and pathogenesis. At the same time, the majority of *in vitro* studies are conducted using highly nutrient-rich media developed more than 100 years ago. This is counter-intuitive. Moreover, in the immensely multifactorial *in vivo* studies, it is almost impossible to analyse singular mechanisms at a reductionist molecular level. While conceding that these methods have evidently been effective in uncovering a vast array of bacterial physiological processes, there are plausibly many aspects that have been unnoticed due to the use of irrelevant stress-free culture conditions that may induce down-regulations of important factors. Therefore, I think we will see the field move toward the employment of more sophisticated culture conditions in the future, relevant to the particular biological aspect investigated.

Another interesting issue, in my opinion, is the mechanisms behind moonlighting proteins. The highly common observation of surface-associated cyto- and periplasmic proteins across the entire bacterial kingdom needs to be more systematically investigated. How do proteins relocate? Is the mechanism active or passive? Is it selective or random? And, most importantly, what are the biological roles of these dual locations? As previously mentioned, researchers are gaining new insight into the biological features of moonlighting and this field will hopefully continue to expand.

When NTHi arrives to the site of initial colonization, it has to interact with the other residing prokaryotes. It is plausible that intense and dynamic interspecies exchanges occur. The impact of NTHi colonization on the rest of the normal flora is currently not well studied. It would be of utmost interest to investigate potential changes in the transcriptome and secretome of NTHi and the interacting neighbouring bacteria upon direct cell-cell contact. Does NTHi induce deleterious alterations in the surrounding species in order to prevail in the niche? Or do synergistic interactions occur with regard to the metabolism of, for instance, NAD and heme? Can the normal flora manipulate the gene expression, or the phenotype, of the invading

NTHi strain? Simply put, do synergistic, mutualistic or antagonistic interactions occur between NTHi and avirulent members of the human upper airway microbiota? These questions remain largely unknown at the moment but may very well be vital for colonization.

Recently, a large variety of recombinant human Ln isoforms have been commercialized, allowing the study of bacterial interactions with particular Ln variants. In our studies, we could observe that NTHi still interacted with Ln in the absence of Protein E and PF. Using niche-specific Lns, it would be exciting to pull down the additional factors involved in NTHi interaction with the ECM-protein.

The role of PF in NTHi biofilm remains highly interesting to investigate. As the extracellular matrices of bacterial biofilms have consistently been proven to be decidedly coordinated structures rather than gelatinous soups of proteins and DNA, the question that naturally arises is how PF fits into this architecture. And if targeting PF for chemo- or immunotherapy will result in the collapse of already established NTHi biofilm? It would be fascinating to find out.

Lastly, the role of PF in divalent metal ion utilization should be investigated. It is still unclear which function of the multicompetent protein renders it essential for NTHi virulence. By elucidating its role in metal ion utilization, or any other potential role in metabolism, it will be easier to appreciate the importance of its various functions.

In conclusion, many intriguing enigmas of the biology of the humans-specific bacterium *H. influenzae* and its multifunctional colonization factor PF remain to be deciphered. This bodes well for the curious microbiologist.

Acknowledgements

I would like to first and foremost thank my supervisor **Kristian Riesbeck** for your excellent guidance and support during my doctoral studies. I remember when we met the first time in the old office in 2009, when I was still an undergrad. I was extremely nervous when I arrived, and extremely happy when I left an hour later with a preliminary promise about a PhD-position. Thank you for trusting me, accepting me to your group, encouraging me at all times, teaching me the ways of science and maintaining that initial feeling of happiness through-out this period. I have the greatest admiration for your work, never-give-up attitude and generosity with your time and help. I have had the best job in the world these past years.

Marta Brant, you are the cornerstone of the lab. Thank you for magically fixing broken equipment on the spot, helping out with experiments that silly PhD-students screw up and for making key contributions to my projects at several critical time points, including the animal studies for the Vaccine paper. Most of all, thank you for your never-ending patience, support and coolness. And for all the chats. I count myself lucky to have had a colleague like you.

Therése Nordström. Thank you for always going out of your way to try to make things better for everyone in the lab and for always having time to guide us juniors through the labyrinth quicksand that is academia. I have great appreciation for your knowledge and wise words. Thank you for always being genuinely supportive, sympathetic and kind. I hold your opinion in the highest esteem.

Yu-Ching Su and **Birendra Singh**, my main collaborators during my doctoral studies. Thank you for teaching me experimental protocols, how to approach scientific problems in a scientific manner and how to structure projects. This thesis would not be possible if not for you. I hope some of your creativity and excellent scientific mannerism has rubbed off on me after all these years. Mainly, thank you for being outstanding friends and supporting along the way.

To my former colleagues **Can Ünal** and **Christophe Fleury**, thank you for keeping in touch and continuing to help me out even though you left the lab a long time ago. My admiration for your scientific knowledge is immense. I want to especially express my deep gratitude to Can. You always took time from your busy schedule to discuss and help out with anything that might have come up during my first years in the lab when I needed supervision the most. You are a true gentleman.

Corinna Richter, my deepest thanks for reading this work and giving invaluable comments. Also, for putting up with my singing and other antics in the office. :)

My most heartfelt thanks to past and present colleagues at the division of Medical Microbiology (and adjacent labs) that put up with me and made the lab a dynamic and fun environment. In no particular order: **Tamim al Jubair, Emma Mattsson, Micke Ristovski, Viveka Schaar, Burcu Bayrak, Ida Uddbäck, Magnus Paulsson, Fredrik Resman, Roni Allaoui, Chrystelle Derache, Florence Deknuydt, Oindrilla Mukherjee, Tamara Ringwood, Kerstin Norrman, Kalpana Singh, Nils Littorin, Sharon Oosterhuis, Alfonso Felipe-Lopez, Ben Duell, Petra Halang** and anyone else that might have slipped my mind. You, if anyone, should know that I possess a certain absent-mindedness, so forgive me if I forgot to list you above.

My warmest thanks to **Nasida, Anki** and **Margareta** at the substrate department. You ladies are an integral part of our research group. Thank you for going out of your way to help me.

To my inquisitive and hard-working MSc students **Jasmina Suljanovic** and **Charlotte Anesten:** thank you for the great contributions to my current projects. It's been my pleasure to supervise two such outstanding undergrads.

To, so far, uncredited teachers, past and present, formal and informal: thank you. My sincerest appreciation to **Tina Wehtje**, **Margareta Lindbom**, **Lars Hederstedt, Anna Blom**, **Gunnar Lindahl, Einar Everitt** and everybody at the old Department of Cell and Organism Biology for instilling, or helping to maintain, my interest in microbiology and encouraging me to pursue this path.

To the funding bodies that supported this work, including **Kungliga Fysiografen** and **VR**: I hope we will continue to have a fruitful relationship. :D

To my parents **Fakhri Payami** and **Jamshid Jalalvand**, I owe everything to you. Thank you for your never-ending love, support and help, from the cradle until now. The most valuable lessons I always learned at home. Thank you for instilling the value of education in us.

To my siblings **Farhad Jalalvand** and **Farnaz Jalalvand**, you are lucky to have a brother like me. Seriously, the best big brother in the world. ;) Thank you for your support and love. I couldn't imagine any two better people to grow up to experience the world with. You mean the world to me.

To my friends **Fabio Nasr** and **Dino Klopic**: I don't have many close friends, and I don't need to, as long as I have the two of you. Thank you for serving up the correct ratio of humble-pie and ego-boost at the exact right time points. You are the men.

And most importantly, to my wife **Frida** and my son **Lev**. You make everything worthwhile. Thank you for your unrelenting support, love and every moment of happiness. You are the loves of my life.

References

1. **Whitman WB, Coleman DC, Wiebe WJ.** 1998. Prokaryotes: the unseen majority. Proc Natl Acad Sci U S A **95:**6578-6583.
2. **Pikuta EV, Hoover RB, Tang J.** 2007. Microbial extremophiles at the limits of life. Crit Rev Microbiol **33:**183-209.
3. **Imshenetsky AA, Lysenko SV, Kazakov GA.** 1978. Upper boundary of the biosphere. Appl Environ Microbiol **35:**1-5.
4. **Shtarkman YM, Kocer ZA, Edgar R, Veerapaneni RS, D'Elia T, Morris PF, Rogers SO.** 2013. Subglacial Lake Vostok (Antarctica) accretion ice contains a diverse set of sequences from aquatic, marine and sediment-inhabiting bacteria and eukarya. PLoS One **8:**e67221.
5. **Kallmeyer J, Pockalny R, Adhikari RR, Smith DC, D'Hondt S.** 2012. Global distribution of microbial abundance and biomass in subseafloor sediment. Proc Natl Acad Sci U S A **109:**16213-16216.
6. **Human Microbiome Project C.** 2012. Structure, function and diversity of the healthy human microbiome. Nature **486:**207-214.
7. **Hyde ER, Haarmann DP, Lynne AM, Bucheli SR, Petrosino JF.** 2013. The living dead: bacterial community structure of a cadaver at the onset and end of the bloat stage of decomposition. PLoS One **8:**e77733.
8. **Wacey D, Kilburn MR, Saunders M, Cliff J, Brasier MD.** 2011. Microfossils of sulphur-metabolizing cells in 3.4-billion-year-old rocks of Western Australia. Nature Geoscience **4:**698-702.
9. **Trevors JT.** 2011. Origin of microbial life: Nano- and molecular events, thermodynamics/entropy, quantum mechanisms and genetic instructions. J Microbiol Methods **84:**492-495.
10. **Brochier C, Philippe H.** 2002. Phylogeny: a non-hyperthermophilic ancestor for bacteria. Nature **417:**244.
11. **Wood B, Lonergan N.** 2008. The hominin fossil record: taxa, grades and clades. J Anat **212:**354-376.
12. **Dethlefsen L, McFall-Ngai M, Relman DA.** 2007. An ecological and evolutionary perspective on human-microbe mutualism and disease. Nature **449:**811-818.
13. **Quercia S, Candela M, Giuliani C, Turroni S, Luiselli D, Rampelli S, Brigidi P, Franceschi C, Bacalini MG, Garagnani P, Pirazzini C.** 2014. From lifetime to evolution: timescales of human gut microbiota adaptation. Front Microbiol **5:**587.
14. **Hill DA, Artis D.** 2010. Intestinal bacteria and the regulation of immune cell homeostasis. Annu Rev Immunol **28:**623-667.
15. **Spaan AN, Surewaard BG, Nijland R, van Strijp JA.** 2013. Neutrophils versus *Staphylococcus aureus*: a biological tug of war. Annu Rev Microbiol **67:**629-650.

16. **Taube C, Muller A.** 2012. The role of *Helicobacter pylori* infection in the development of allergic asthma. Expert Rev Respir Med **6:**441-449.
17. **Borkowski J, Li L, Steinmann U, Quednau N, Stump-Guthier C, Weiss C, Findeisen P, Gretz N, Ishikawa H, Tenenbaum T, Schroten H, Schwerk C.** 2014. *Neisseria meningitidis* elicits a pro-inflammatory response involving IkappaBzeta in a human blood-cerebrospinal fluid barrier model. J Neuroinflammation **11:**163.
18. **Kapoor V, Pitkanen T, Ryu H, Elk M, Wendell D, Santo Domingo JW.** 2014. Distribution of human-specific *Bacteroidales* and fecal indicators in an urban watershed impacted by sewage pollution using RNA and DNA based quantitative PCR assays. Appl Environ Microbiol doi:10.1128/AEM.02446-14.
19. **Spinler JK, Sontakke A, Hollister EB, Venable SF, Oh PL, Balderas MA, Saulnier DM, Mistretta TA, Devaraj S, Walter J, Versalovic J, Highlander SK.** 2014. From prediction to function using evolutionary genomics: human-specific ecotypes of *Lactobacillus reuteri* have diverse probiotic functions. Genome Biol Evol **6:**1772-1789.
20. **Jalalvand F, Riesbeck K.** 2014. *Haemophilus influenzae*: recent advances in the understanding of molecular pathogenesis and polymicrobial infections. Curr Opin Infect Dis **27:**268-274.
21. **Kasper KJ, Zeppa JJ, Wakabayashi AT, Xu SX, Mazzuca DM, Welch I, Baroja ML, Kotb M, Cairns E, Cleary PP, Haeryfar SM, McCormick JK.** 2014. Bacterial superantigens promote acute nasopharyngeal infection by *Streptococcus pyogenes* in a human MHC Class II-dependent manner. PLoS Pathog **10:**e1004155.
22. **Turnbaugh PJ, Ley RE, Hamady M, Fraser-Liggett CM, Knight R, Gordon JI.** 2007. The Human Microbiome Project. Nature **449:**804-810.
23. **Qin J, Li R, Raes J, Arumugam M, Burgdorf KS, Manichanh C, Nielsen T, Pons N, Levenez F, Yamada T, Mende DR, Li J, Xu J, Li S, Li D, Cao J, Wang B, Liang H, Zheng H, Xie Y, Tap J, Lepage P, Bertalan M, Batto JM, Hansen T, Le Paslier D, Linneberg A, Nielsen HB, Pelletier E, Renault P, Sicheritz-Ponten T, Turner K, Zhu H, Yu C, Li S, Jian M, Zhou Y, Li Y, Zhang X, Li S, Qin N, Yang H, Wang J, Brunak S, Dore J, Guarner F, Kristiansen K, Pedersen O, Parkhill J, Weissenbach J, et al.** 2010. A human gut microbial gene catalogue established by metagenomic sequencing. Nature **464:**59-65.
24. **Alcock J, Maley CC, Aktipis CA.** 2014. Is eating behavior manipulated by the gastrointestinal microbiota? Evolutionary pressures and potential mechanisms. Bioessays **36:**940-949.
25. **Williams BB, Van Benschoten AH, Cimermancic P, Donia MS, Zimmermann M, Taketani M, Ishihara A, Kashyap PC, Fraser JS, Fischbach MA.** 2014. Discovery and characterization of gut microbiota decarboxylases that can produce the neurotransmitter tryptamine. Cell Host Microbe **16:**495-503.
26. **Ganesan S, Comstock AT, Sajjan US.** 2013. Barrier function of airway tract epithelium. Tissue Barriers **1:**e24997.
27. **Harkema JR.** 1991. Comparative aspects of nasal airway anatomy: relevance to inhalation toxicology. Toxicol Pathol **19:**321-336.

28. **Allen EK, Koeppel AF, Hendley JO, Turner SD, Winther B, Sale MM.** 2014. Characterization of the nasopharyngeal microbiota in health and during rhinovirus challenge. Microbiome **2:**22.
29. **Park H, Shin JW, Park SG, Kim W.** 2014. Microbial communities in the upper respiratory tract of patients with asthma and chronic obstructive pulmonary disease. PLoS One **9:**e109710.
30. **Miyamoto N, Bakaletz LO.** 1997. Kinetics of the ascension of NTHi from the nasopharynx to the middle ear coincident with adenovirus-induced compromise in the chinchilla. Microb Pathog **23:**119-126.
31. **Blausen.com-staff.** 2013. Blausen gallery 2014 doi:10.15347/wjm/2014.010. Wikiversity Journal of Medicine.
32. **Domogatskaya A, Rodin S, Tryggvason K.** 2012. Functional diversity of laminins. Annu Rev Cell Dev Biol **28:**523-553.
33. **Hynes RO.** 2009. The extracellular matrix: not just pretty fibrils. Science **326:**1216-1219.
34. **Singh B, Fleury C, Jalalvand F, Riesbeck K.** 2012. Human pathogens utilize host extracellular matrix proteins laminin and collagen for adhesion and invasion of the host. FEMS Microbiol Rev **36:**1122-1180.
35. **Holmberg J, Durbeej M.** 2013. Laminin-211 in skeletal muscle function. Cell Adh Migr **7:**111-121.
36. **Bruckner-Tuderman L, Has C.** 2014. Disorders of the cutaneous basement membrane zone--the paradigm of epidermolysis bullosa. Matrix Biol **33:**29-34.
37. **Miner JH.** 2011. Glomerular basement membrane composition and the filtration barrier. Pediatr Nephrol **26:**1413-1417.
38. **The-Human-Protein-Atlas.** 2014. http://www.proteinatlas.com. http://www.proteinatlas.org/ENSG00000053747-LAMA3/tissue/nasopharynx. Accessed 2014/12/03.
39. **Aumailley M, Bruckner-Tuderman L, Carter WG, Deutzmann R, Edgar D, Ekblom P, Engel J, Engvall E, Hohenester E, Jones JC, Kleinman HK, Marinkovich MP, Martin GR, Mayer U, Meneguzzi G, Miner JH, Miyazaki K, Patarroyo M, Paulsson M, Quaranta V, Sanes JR, Sasaki T, Sekiguchi K, Sorokin LM, Talts JF, Tryggvason K, Uitto J, Virtanen I, von der Mark K, Wewer UM, Yamada Y, Yurchenco PD.** 2005. A simplified laminin nomenclature. Matrix Biol **24:**326-332.
40. **Henderson B, Nair S, Pallas J, Williams MA.** 2011. Fibronectin: a multidomain host adhesin targeted by bacterial fibronectin-binding proteins. FEMS Microbiol Rev **35:**147-200.
41. **Mittal R, Kodiyan J, Gerring R, Mathee K, Li JD, Grati M, Liu XZ.** 2014. Role of innate immunity in the pathogenesis of otitis media. Int J Infect Dis **29C:**259-267.
42. **Murphy TF, Chonmaitree T, Barenkamp S, Kyd J, Nokso-Koivisto J, Patel JA, Heikkinen T, Yamanaka N, Ogra P, Swords WE, Sih T, Pettigrew MM.** 2013. Panel 5: Microbiology and immunology panel. Otolaryngol Head Neck Surg **148:**E64-89.
43. **Persson CG.** 1991. Plasma exudation in the airways: mechanisms and function. Eur Respir J **4:**1268-1274.

44. **Zhang P, Summer WR, Bagby GJ, Nelson S.** 2000. Innate immunity and pulmonary host defense. Immunol Rev **173:**39-51.
45. **Sjoberg AP, Trouw LA, Blom AM.** 2009. Complement activation and inhibition: a delicate balance. Trends Immunol **30:**83-90.
46. **Carroll MC.** 2004. The complement system in regulation of adaptive immunity. Nat Immunol **5:**981-986.
47. **Noris M, Remuzzi G.** 2013. Overview of complement activation and regulation. Semin Nephrol **33:**479-492.
48. **Holers VM.** 2014. Complement and its receptors: new insights into human disease. Annu Rev Immunol **32:**433-459.
49. **Blom AM, Hallstrom T, Riesbeck K.** 2009. Complement evasion strategies of pathogens-acquisition of inhibitors and beyond. Mol Immunol **46:**2808-2817.
50. **Singh B, Su YC, Riesbeck K.** 2010. Vitronectin in bacterial pathogenesis: a host protein used in complement escape and cellular invasion. Mol Microbiol **78:**545-560.
51. **Preissner KT, Seiffert D.** 1998. Role of vitronectin and its receptors in haemostasis and vascular remodeling. Thromb Res **89:**1-21.
52. **Milis L, Morris CA, Sheehan MC, Charlesworth JA, Pussell BA.** 1993. Vitronectin-mediated inhibition of complement: evidence for different binding sites for C5b-7 and C9. Clin Exp Immunol **92:**114-119.
53. **Schvartz I, Seger D, Shaltiel S.** 1999. Vitronectin. Int J Biochem Cell Biol **31:**539-544.
54. **Jang YC, Tsou R, Gibran NS, Isik FF.** 2000. Vitronectin deficiency is associated with increased wound fibrinolysis and decreased microvascular angiogenesis in mice. Surgery **127:**696-704.
55. **Eklund AG, Sigurdardottir O, Ohrn M.** 1992. Vitronectin and its relationship to other extracellular matrix components in bronchoalveolar lavage fluid in sarcoidosis. Am Rev Respir Dis **145:**646-650.
56. **Teschler H, Pohl WR, Thompson AB, Konietzko N, Mosher DF, Costabel U, Rennard SI.** 1993. Elevated levels of bronchoalveolar lavage vitronectin in hypersensitivity pneumonitis. Am Rev Respir Dis **147:**332-337.
57. **Dewhirst FE, Paster BJ, Olsen I, Fraser GJ.** 1992. Phylogeny of 54 representative strains of species in the family *Pasteurellaceae* as determined by comparison of 16S rRNA sequences. J Bacteriol **174:**2002-2013.
58. **Smith HO, Wilcox KW.** 1970. A restriction enzyme from *Hemophilus influenzae*. I. Purification and general properties. J Mol Biol **51:**379-391.
59. **Fleischmann RD, Adams MD, White O, Clayton RA, Kirkness EF, Kerlavage AR, Bult CJ, Tomb JF, Dougherty BA, Merrick JM, et al.** 1995. Whole-genome random sequencing and assembly of *Haemophilus influenzae* Rd. Science **269:**496-512.
60. **Goldblatt D.** 2000. Conjugate vaccines. Clin Exp Immunol **119:**1-3.
61. **Eyler JM.** 2010. The state of science, microbiology, and vaccines circa 1918. Public Health Rep **125 Suppl 3:**27-36.

62. **Wang XY, Kilgore PE, Lim KA, Wang SM, Lee J, Deng W, Mo MQ, Nyambat B, Ma JC, Favorov MO, Clemens JD.** 2011. Influenza and bacterial pathogen coinfections in the 20th century. Interdiscip Perspect Infect Dis **2011:**146376.
63. **Pittman M.** 1931. Variation and Type Specificity in the Bacterial Species *Hemophilus Influenzae*. J Exp Med **53:**471-492.
64. **Crisel RM, Baker RS, Dorman DE.** 1975. Capsular polymer of *Haemophilus influenzae*, type b. I. Structural characterization of the capsular polymer of strain Eagan. J Biol Chem **250:**4926-4930.
65. **Poje G, Redfield RJ.** 2003. General methods for culturing *Haemophilus influenzae*. Methods Mol Med **71:**51-56.
66. **Holt LB.** 1962. The Growth-factor Requirements of *Haemophilus influenzae*. Journal of General Microbiology **27:**317-322.
67. **Evans NM, Smith DD.** 1972. The effect of the medium and source of growth factors on the satellitism test for *Haemophilus* species. J Med Microbiol **5:**509-514.
68. **Evans NM, Bell SM, Smith DD.** 1975. New satellitism test for isolation and identification of *Haemophilus influenzae* and *Haemophilus parainfluenzae* in sputum. J Clin Microbiol **1:**89-95.
69. **Kaur R, Chang A, Xu Q, Casey JR, Pichichero ME.** 2011. Phylogenetic relatedness and diversity of non-typable *Haemophilus influenzae* in the nasopharynx and middle ear fluid of children with acute otitis media. J Med Microbiol **60:**1841-1848.
70. **Puig C, Marti S, Fleites A, Trabazo R, Calatayud L, Linares J, Ardanuy C.** 2014. Oropharyngeal colonization by nontypeable *Haemophilus influenzae* among healthy children attending day care centers. Microb Drug Resist **20:**450-455.
71. **de Carvalho CX, Kipnis A, Thorn L, de Andrade JG, Pimenta F, Brandileone MC, Zanella RC, Flannery B, Sgambatti S, Andrade AL.** 2011. Carriage of *Haemophilus influenzae* among Brazilian children attending day care centers in the era of widespread Hib vaccination. Vaccine **29:**1438-1442.
72. **Tian GZ, Zhang LJ, Wang XL, Zhang L, Li SF, Gu CM, Sun J, Cui BY.** 2012. Rapid detection of *Haemophilus influenzae* and *Haemophilus parainfluenzae* in nasopharyngeal swabs by multiplex PCR. Biomed Environ Sci **25:**367-371.
73. **da Silva ME, Marin JM.** 2001. An epidemiological study of *Haemophilus influenzae* at a Brazilian day care center. Braz J Infect Dis **5:**260-268.
74. **Warinner C, Rodrigues JF, Vyas R, Trachsel C, Shved N, Grossmann J, Radini A, Hancock Y, Tito RY, Fiddyment S, Speller C, Hendy J, Charlton S, Luder HU, Salazar-Garcia DC, Eppler E, Seiler R, Hansen LH, Castruita JA, Barkow-Oesterreicher S, Teoh KY, Kelstrup CD, Olsen JV, Nanni P, Kawai T, Willerslev E, von Mering C, Lewis CM, Jr., Collins MJ, Gilbert MT, Ruhli F, Cappellini E.** 2014. Pathogens and host immunity in the ancient human oral cavity. Nat Genet **46:**336-344.
75. **Van Eldere J, Slack MP, Ladhani S, Cripps AW.** 2014. Non-typeable *Haemophilus influenzae*, an under-recognised pathogen. Lancet Infect Dis doi:10.1016/S1473-3099(14)70734-0.
76. **Bakaletz LO.** 2010. Immunopathogenesis of polymicrobial otitis media. J Leukoc Biol **87:**213-222.

77. **Agrawal A, Murphy TF.** 2011. *Haemophilus influenzae* infections in the *H. influenzae* type b conjugate vaccine era. J Clin Microbiol **49:**3728-3732.
78. **Livorsi DJ, Macneil JR, Cohn AC, Bareta J, Zansky S, Petit S, Gershman K, Harrison LH, Lynfield R, Reingold A, Schaffner W, Thomas A, Farley MM.** 2012. Invasive *Haemophilus influenzae* in the United States, 1999-2008: epidemiology and outcomes. J Infect **65:**496-504.
79. **Resman F, Ristovski M, Ahl J, Forsgren A, Gilsdorf JR, Jasir A, Kaijser B, Kronvall G, Riesbeck K.** 2011. Invasive disease caused by *Haemophilus influenzae* in Sweden 1997-2009; evidence of increasing incidence and clinical burden of non-type b strains. Clin Microbiol Infect **17:**1638-1645.
80. **Bijlmer HA.** 1991. World-wide epidemiology of *Haemophilus influenzae* meningitis; industrialized versus non-industrialized countries. Vaccine **9 Suppl:**S5-9; discussion S25.
81. **Eutsey RA, Hiller NL, Earl JP, Janto BA, Dahlgren ME, Ahmed A, Powell E, Schultz MP, Gilsdorf JR, Zhang L, Smith A, Murphy TF, Sethi S, Shen K, Post JC, Hu FZ, Ehrlich GD.** 2013. Design and validation of a supragenome array for determination of the genomic content of *Haemophilus influenzae* isolates. BMC Genomics **14:**484.
82. **Mell JC, Hall IM, Redfield RJ.** 2012. Defining the DNA uptake specificity of naturally competent *Haemophilus influenzae* cells. Nucleic Acids Res **40:**8536-8549.
83. **Hogg JS, Hu FZ, Janto B, Boissy R, Hayes J, Keefe R, Post JC, Ehrlich GD.** 2007. Characterization and modeling of the *Haemophilus influenzae* core and supragenomes based on the complete genomic sequences of Rd and 12 clinical nontypeable strains. Genome Biol **8:**R103.
84. **Lam TT, Claus H, Frosch M, Vogel U.** 2011. Sequence analysis of serotype-specific synthesis regions II of *Haemophilus influenzae* serotypes c and d: evidence for common ancestry of capsule synthesis in *Pasteurellaceae* and *Neisseria meningitidis*. Res Microbiol **162:**483-487.
85. **Power PM, Bentley SD, Parkhill J, Moxon ER, Hood DW.** 2012. Investigations into genome diversity of *Haemophilus influenzae* using whole genome sequencing of clinical isolates and laboratory transformants. BMC Microbiol **12:**273.
86. **Rogers GB, Shaw D, Marsh RL, Carroll MP, Serisier DJ, Bruce KD.** 2014. Respiratory microbiota: addressing clinical questions, informing clinical practice. Thorax doi:10.1136/thoraxjnl-2014-205826.
87. **Dickson RP, Martinez FJ, Huffnagle GB.** 2014. The role of the microbiome in exacerbations of chronic lung diseases. Lancet **384:**691-702.
88. **Davis CP.** 1996. Normal Flora. Chapter 6 in Medical Microbiology, 4th ed. The Texas Medical Branch at Galveston, Galveston, TX.
89. **McCullers JA.** 2014. The co-pathogenesis of influenza viruses with bacteria in the lung. Nat Rev Microbiol **12:**252-262.
90. **Berenson CS, Kruzel RL, Eberhardt E, Sethi S.** 2013. Phagocytic dysfunction of human alveolar macrophages and severity of chronic obstructive pulmonary disease. J Infect Dis **208:**2036-2045.

91. **Taylor AE, Finney-Hayward TK, Quint JK, Thomas CM, Tudhope SJ, Wedzicha JA, Barnes PJ, Donnelly LE.** 2010. Defective macrophage phagocytosis of bacteria in COPD. Eur Respir J **35:**1039-1047.
92. **Doring G, Parameswaran IG, Murphy TF.** 2011. Differential adaptation of microbial pathogens to airways of patients with cystic fibrosis and chronic obstructive pulmonary disease. FEMS Microbiol Rev **35:**124-146.
93. **Ram S, Lewis LA, Rice PA.** 2010. Infections of people with complement deficiencies and patients who have undergone splenectomy. Clin Microbiol Rev **23:**740-780.
94. **Wilson R, Read R, Cole P.** 1992. Interaction of *Haemophilus influenzae* with mucus, cilia, and respiratory epithelium. J Infect Dis **165 Suppl 1:**S100-102.
95. **Hendrixson DR, St Geme JW, 3rd.** 1998. The *Haemophilus influenzae* Hap serine protease promotes adherence and microcolony formation, potentiated by a soluble host protein. Mol Cell **2:**841-850.
96. **Pedersen M, Stafanger G.** 1983. Bronchopulmonary symptoms in primary ciliary dyskinesia. A clinical study of 27 patients. Eur J Respir Dis Suppl **127:**118-128.
97. **Ahren IL, Janson H, Forsgren A, Riesbeck K.** 2001. Protein D expression promotes the adherence and internalization of non-typeable *Haemophilus influenzae* into human monocytic cells. Microb Pathog **31:**151-158.
98. **Janson H, Carl n B, Cervin A, Forsgren A, Magnusdottir AB, Lindberg S, Runer T.** 1999. Effects on the ciliated epithelium of protein D-producing and -nonproducing nontypeable *Haemophilus influenzae* in nasopharyngeal tissue cultures. J Infect Dis **180:**737-746.
99. **Bailey KL, LeVan TD, Yanov DA, Pavlik JA, DeVasure JM, Sisson JH, Wyatt TA.** 2012. Non-typeable *Haemophilus influenzae* decreases cilia beating via protein kinase Cepsilon. Respir Res **13:**49.
100. **Apicella MA.** 2012. Nontypeable *Haemophilus influenzae*: the role of N-acetyl-5-neuraminic acid in biology. Front Cell Infect Microbiol **2:**19.
101. **Swords WE, Jones PA, Apicella MA.** 2003. The lipo-oligosaccharides of *Haemophilus influenzae*: an interesting array of characters. J Endotoxin Res **9:**131-144.
102. **Raichvarg D, Siou G, Dubreuil A, Bonnaire Y, Brossard C, Boudene C.** 1982. *In vivo* and *in vitro* effect of the *Haemophilus influenzae* lipopolysaccharide on ciliated respiratory epithelium. J Hyg Epidemiol Microbiol Immunol **26:**112-116.
103. **Johnson AP, Inzana TJ.** 1986. Loss of ciliary activity in organ cultures of rat trachea treated with lipo-oligosaccharide from *Haemophilus influenzae*. J Med Microbiol **22:**265-268.
104. **Harada T, Saida S, Majima Y, Ukai K, Sakakura Y.** 1987. Effect of Lipopolysaccharide of *Haemophilus influenzae* on Ciliary Activity of the Human Nasal Mucosa and Bullfrog Palate Clearance. Acta Otolaryngol **103:**307-311.
105. **Mason PS, Adam E, Prior M, Warner JO, Randall CJ.** 2002. Effect of bacterial endotoxin and middle ear effusion on ciliary activity: implications for otitis media. Laryngoscope **112:**676-680.
106. **McCrea KW, Xie J, Daniel D, Ulrich-Lewis JT, Zhang L.** 2014. Predicted configurations of oligosaccharide extensions in the lipooligosaccharide of nontypeable *Haemophilus influenzae* isolates. J Clin Microbiol **52:**2659-2661.

107. **Gorter AD, Oostrik J, van der Ley P, Hiemstra PS, Dankert J, van Alphen L.** 2003. Involvement of lipooligosaccharides of *Haemophilus influenzae* and *Neisseria meningitidis* in defensin-enhanced bacterial adherence to epithelial cells. Microb Pathog **34:**121-130.
108. **Swords WE, Buscher BA, Ver Steeg Ii K, Preston A, Nichols WA, Weiser JN, Gibson BW, Apicella MA.** 2000. Non-typeable *Haemophilus influenzae* adhere to and invade human bronchial epithelial cells via an interaction of lipooligosaccharide with the PAF receptor. Mol Microbiol **37:**13-27.
109. **Poole J, Foster E, Chaloner K, Hunt J, Jennings MP, Bair T, Knudtson K, Christensen E, Munson RS, Jr., Winokur PL, Apicella MA.** 2013. Analysis of nontypeable *Haemophilus influenzae* phase-variable genes during experimental human nasopharyngeal colonization. J Infect Dis **208:**720-727.
110. **Carruthers MD, Tracy EN, Dickson AC, Ganser KB, Munson RS, Jr., Bakaletz LO.** 2012. Biological roles of nontypeable *Haemophilus influenzae* type IV pilus proteins encoded by the pil and com operons. J Bacteriol **194:**1927-1933.
111. **Jurcisek JA, Bookwalter JE, Baker BD, Fernandez S, Novotny LA, Munson RS, Jr., Bakaletz LO.** 2007. The PilA protein of non-typeable *Haemophilus influenzae* plays a role in biofilm formation, adherence to epithelial cells and colonization of the mammalian upper respiratory tract. Mol Microbiol **65:**1288-1299.
112. **Bakaletz LO, Baker BD, Jurcisek JA, Harrison A, Novotny LA, Bookwalter JE, Mungur R, Munson RS, Jr.** 2005. Demonstration of Type IV pilus expression and a twitching phenotype by *Haemophilus influenzae*. Infect Immun **73:**1635-1643.
113. **St Geme JW, 3rd, de la Morena ML, Falkow S.** 1994. A *Haemophilus influenzae* IgA protease-like protein promotes intimate interaction with human epithelial cells. Mol Microbiol **14:**217-233.
114. **Fink DL, Cope LD, Hansen EJ, Geme JW, 3rd.** 2001. The *Hemophilus influenzae* Hap autotransporter is a chymotrypsin clan serine protease and undergoes autoproteolysis via an intermolecular mechanism. J Biol Chem **276:**39492-39500.
115. **St Geme JW, 3rd, Cutter D.** 2000. The *Haemophilus influenzae* Hia adhesin is an autotransporter protein that remains uncleaved at the C terminus and fully cell associated. J Bacteriol **182:**6005-6013.
116. **Ronander E, Brant M, Eriksson E, Morgelin M, Hallgren O, Westergren-Thorsson G, Forsgren A, Riesbeck K.** 2009. Nontypeable *Haemophilus influenzae* adhesin protein E: characterization and biological activity. J Infect Dis **199:**522-531.
117. **Reddy MS, Bernstein JM, Murphy TF, Faden HS.** 1996. Binding between outer membrane proteins of nontypeable *Haemophilus influenzae* and human nasopharyngeal mucin. Infect Immun **64:**1477-1479.
118. **Avadhanula V, Rodriguez CA, Ulett GC, Bakaletz LO, Adderson EE.** 2006. Nontypeable *Haemophilus influenzae* adheres to intercellular adhesion molecule 1 (ICAM-1) on respiratory epithelial cells and upregulates ICAM-1 expression. Infect Immun **74:**830-838.
119. **Miyamoto N, Bakaletz LO.** 1996. Selective adherence of non-typeable *Haemophilus influenzae* (NTHi) to mucus or epithelial cells in the chinchilla eustachian tube and middle ear. Microb Pathog **21:**343-356.

120. **St Geme JW, 3rd, Falkow S, Barenkamp SJ.** 1993. High-molecular-weight proteins of nontypable *Haemophilus influenzae* mediate attachment to human epithelial cells. Proc Natl Acad Sci U S A **90:**2875-2879.
121. **Read RC, Wilson R, Rutman A, Lund V, Todd HC, Brain AP, Jeffery PK, Cole PJ.** 1991. Interaction of nontypable *Haemophilus influenzae* with human respiratory mucosa in vitro. J Infect Dis **163:**549-558.
122. **Hallstrom T, Singh B, Resman F, Blom AM, Morgelin M, Riesbeck K.** 2011. *Haemophilus influenzae* protein E binds to the extracellular matrix by concurrently interacting with laminin and vitronectin. J Infect Dis **204:**1065-1074.
123. **Fink DL, Green BA, St Geme JW, 3rd.** 2002. The *Haemophilus* influenzae Hap autotransporter binds to fibronectin, laminin, and collagen IV. Infect Immun **70:**4902-4907.
124. **Bresser P, Virkola R, Jonsson-Vihanne M, Jansen HM, Korhonen TK, van Alphen L.** 2000. Interaction of clinical isolates of nonencapsulated *Haemophilus influenzae* with mammalian extracellular matrix proteins. FEMS Immunol Med Microbiol **28:**129-132.
125. **Virkola R, Lahteenmaki K, Eberhard T, Kuusela P, van Alphen L, Ullberg M, Korhonen TK.** 1996. Interaction of *Haemophilus influenzae* with the mammalian extracellular matrix. J Infect Dis **173:**1137-1147.
126. **Ren D, Nelson KL, Uchakin PN, Smith AL, Gu XX, Daines DA.** 2012. Characterization of extended co-culture of non-typeable *Haemophilus influenzae* with primary human respiratory tissues. Exp Biol Med (Maywood) **237:**540-547.
127. **Clementi CF, Hakansson AP, Murphy TF.** 2014. Internalization and Trafficking of Nontypeable *Haemophilus influenzae* in Human Respiratory Epithelial Cells and Roles of IgA1 Proteases for Optimal Invasion and Persistence. Infect Immun **82:**433-444.
128. **Raffel FK, Szelestey BR, Beatty WL, Mason KM.** 2013. The *Haemophilus influenzae* Sap transporter mediates bacterium-epithelial cell homeostasis. Infect Immun **81:**43-54.
129. **Clementi CF, Murphy TF.** 2011. Non-typeable *Haemophilus influenzae* invasion and persistence in the human respiratory tract. Front Cell Infect Microbiol **1:**1.
130. **Swords WE.** 2012. Nontypeable *Haemophilus influenzae* biofilms: role in chronic airway infections. Front Cell Infect Microbiol **2:**97.
131. **Hoa M, Tomovic S, Nistico L, Hall-Stoodley L, Stoodley P, Sachdeva L, Berk R, Coticchia JM.** 2009. Identification of adenoid biofilms with middle ear pathogens in otitis-prone children utilizing SEM and FISH. Int J Pediatr Otorhinolaryngol **73:**1242-1248.
132. **Hall-Stoodley L, Costerton JW, Stoodley P.** 2004. Bacterial biofilms: from the natural environment to infectious diseases. Nat Rev Microbiol **2:**95-108.
133. **Swords WE.** 2012. Quorum signaling and sensing by nontypeable *Haemophilus influenzae*. Front Cell Infect Microbiol **2:**100.
134. **Stoodley P, Sauer K, Davies DG, Costerton JW.** 2002. Biofilms as complex differentiated communities. Annu Rev Microbiol **56:**187-209.

135. **Jurcisek JA, Bakaletz LO.** 2007. Biofilms formed by nontypeable *Haemophilus influenzae in vivo* contain both double-stranded DNA and type IV pilin protein. J Bacteriol **189:**3868-3875.
136. **Jurcisek J, Greiner L, Watanabe H, Zaleski A, Apicella MA, Bakaletz LO.** 2005. Role of sialic acid and complex carbohydrate biosynthesis in biofilm formation by nontypeable *Haemophilus influenzae* in the chinchilla middle ear. Infect Immun **73:**3210-3218.
137. **Swords WE, Moore ML, Godzicki L, Bukofzer G, Mitten MJ, VonCannon J.** 2004. Sialylation of lipooligosaccharides promotes biofilm formation by nontypeable *Haemophilus influenzae*. Infect Immun **72:**106-113.
138. **Wu S, Baum MM, Kerwin J, Guerrero D, Webster S, Schaudinn C, VanderVelde D, Webster P.** 2014. Biofilm-specific extracellular matrix proteins of nontypeable *Haemophilus influenzae*. Pathog Dis doi:10.1111/2049-632X.12195.
139. **Armbruster CE, Hong W, Pang B, Dew KE, Juneau RA, Byrd MS, Love CF, Kock ND, Swords WE.** 2009. LuxS promotes biofilm maturation and persistence of nontypeable *Haemophilus influenzae in vivo* via modulation of lipooligosaccharides on the bacterial surface. Infect Immun **77:**4081-4091.
140. **Armbruster CE, Pang B, Murrah K, Juneau RA, Perez AC, Weimer KE, Swords WE.** 2011. RbsB (NTHI_0632) mediates quorum signal uptake in nontypeable *Haemophilus influenzae* strain 86-028NP. Mol Microbiol **82:**836-850.
141. **Brockson ME, Novotny LA, Mokrzan EM, Malhotra S, Jurcisek JA, Akbar R, Devaraj A, Goodman SD, Bakaletz LO.** 2014. Evaluation of the kinetics and mechanism of action of anti-integration host factor-mediated disruption of bacterial biofilms. Mol Microbiol **93:**1246-1258.
142. **Shelton CL, Raffel FK, Beatty WL, Johnson SM, Mason KM.** 2011. Sap transporter mediated import and subsequent degradation of antimicrobial peptides in *Haemophilus*. PLoS Pathog **7:**e1002360.
143. **Khan AG, Shouldice SR, Kirby SD, Yu RH, Tari LW, Schryvers AB.** 2007. High-affinity binding by the periplasmic iron-binding protein from *Haemophilus influenzae* is required for acquiring iron from transferrin. Biochem J **404:**217-225.
144. **Harrington JC, Wong SM, Rosadini CV, Garifulin O, Boyartchuk V, Akerley BJ.** 2009. Resistance of *Haemophilus influenzae* to reactive nitrogen donors and gamma interferon-stimulated macrophages requires the formate-dependent nitrite reductase regulator-activated ytfE gene. Infect Immun **77:**1945-1958.
145. **Morey P, Viadas C, Euba B, Hood DW, Barberan M, Gil C, Grillo MJ, Bengoechea JA, Garmendia J.** 2013. Relative contributions of lipooligosaccharide inner and outer core modifications to nontypeable *Haemophilus influenzae* pathogenesis. Infect Immun **81:**4100-4111.
146. **Murphy TF, Lesse AJ, Kirkham C, Zhong H, Sethi S, Munson RS, Jr.** 2011. A clonal group of nontypeable *Haemophilus influenza*e with two IgA proteases is adapted to infection in chronic obstructive pulmonary disease. PLoS One **6:**e25923.
147. **Kilian M, Reinholdt J, Lomholt H, Poulsen K, Frandsen EV.** 1996. Biological significance of IgA1 proteases in bacterial colonization and pathogenesis: critical evaluation of experimental evidence. APMIS **104:**321-338.

148. **Janoff EN, Rubins JB, Fasching C, Charboneau D, Rahkola JT, Plaut AG, Weiser JN.** 2014. Pneumococcal IgA1 protease subverts specific protection by human IgA1. Mucosal Immunol **7:**249-256.
149. **Noel GJ, Hoiseth SK, Edelson PJ.** 1992. Type b capsule inhibits ingestion of *Haemophilus influenzae* by murine macrophages: studies with isogenic encapsulated and unencapsulated strains. J Infect Dis **166:**178-182.
150. **Langereis JD, Weiser JN.** 2014. Shielding of a lipooligosaccharide IgM epitope allows evasion of neutrophil-mediated killing of an invasive strain of nontypeable *Haemophilus influenzae*. MBio **5:**e01478-01414.
151. **Deknuydt F, Nordstrom T, Riesbeck K.** 2014. Diversion of the host humoral response: a novel virulence mechanism of *Haemophilus influenzae* mediated via outer membrane vesicles. J Leukoc Biol **95:**983-991.
152. **Clark SE, Snow J, Li J, Zola TA, Weiser JN.** 2012. Phosphorylcholine allows for evasion of bactericidal antibody by *Haemophilus influenzae*. PLoS Pathog **8:**e1002521.
153. **Clark SE, Eichelberger KR, Weiser JN.** 2013. Evasion of killing by human antibody and complement through multiple variations in the surface oligosaccharide of *Haemophilus influenzae*. Mol Microbiol **88:**603-618.
154. **Langereis JD, Stol K, Schweda EK, Twelkmeyer B, Bootsma HJ, de Vries SP, Burghout P, Diavatopoulos DA, Hermans PW.** 2012. Modified lipooligosaccharide structure protects nontypeable *Haemophilus influenzae* from IgM-mediated complement killing in experimental otitis media. MBio **3:**e00079-00012.
155. **Nakamura S, Shchepetov M, Dalia AB, Clark SE, Murphy TF, Sethi S, Gilsdorf JR, Smith AL, Weiser JN.** 2011. Molecular basis of increased serum resistance among pulmonary isolates of non-typeable *Haemophilus influenzae*. PLoS Pathog **7:**e1001247.
156. **Ho DK, Ram S, Nelson KL, Bonthuis PJ, Smith AL.** 2007. *lgtC* expression modulates resistance to C4b deposition on an invasive nontypeable *Haemophilus influenzae*. J Immunol **178:**1002-1012.
157. **Erwin AL, Allen S, Ho DK, Bonthuis PJ, Jarisch J, Nelson KL, Tsao DL, Unrath WC, Watson ME, Jr., Gibson BW, Apicella MA, Smith AL.** 2006. Role of *lgtC* in resistance of nontypeable *Haemophilus influenzae* strain R2866 to human serum. Infect Immun **74:**6226-6235.
158. **Hallstrom T, Jarva H, Riesbeck K, Blom AM.** 2007. Interaction with C4b-binding protein contributes to nontypeable *Haemophilus influenzae* serum resistance. J Immunol **178:**6359-6366.
159. **Hallstrom T, Zipfel PF, Blom AM, Lauer N, Forsgren A, Riesbeck K.** 2008. *Haemophilus influenzae* interacts with the human complement inhibitor factor H. J Immunol **181:**537-545.
160. **Hallstrom T, Blom AM, Zipfel PF, Riesbeck K.** 2009. Nontypeable *Haemophilus influenzae* protein E binds vitronectin and is important for serum resistance. J Immunol **183:**2593-2601.
161. **Langereis JD, de Jonge MI, Weiser JN.** 2014. Binding of human factor H to outer membrane protein P5 of non-typeable *Haemophilus influenzae* contributes to complement resistance. Mol Microbiol **94:**89-106.

162. **Rosadini CV, Ram S, Akerley BJ.** 2014. Outer membrane protein P5 is required for resistance of nontypeable *Haemophilus influenzae* to both the classical and alternative complement pathways. Infect Immun **82:**640-649.
163. **Krismer B, Liebeke M, Janek D, Nega M, Rautenberg M, Hornig G, Unger C, Weidenmaier C, Lalk M, Peschel A.** 2014. Nutrient Limitation Governs *Staphylococcus aureus* Metabolism and Niche Adaptation in the Human Nose. PLoS Pathog **10:**e1003862.
164. **Redfield RJ.** 1993. Genes for breakfast: the have-your-cake-and-eat-it-too of bacterial transformation. J Hered **84:**400-404.
165. **Reidl J, Schlor S, Kraiss A, Schmidt-Brauns J, Kemmer G, Soleva E.** 2000. NADP and NAD utilization in *Haemophilus influenzae*. Mol Microbiol **35:**1573-1581.
166. **Kemmer G, Reilly TJ, Schmidt-Brauns J, Zlotnik GW, Green BA, Fiske MJ, Herbert M, Kraiss A, Schlor S, Smith A, Reidl J.** 2001. NadN and e (P4) are essential for utilization of NAD and nicotinamide mononucleotide but not nicotinamide riboside in *Haemophilus influenzae*. J Bacteriol **183:**3974-3981.
167. **Andersen C, Maier E, Kemmer G, Blass J, Hilpert AK, Benz R, Reidl J.** 2003. Porin OmpP2 of *Haemophilus influenzae* shows specificity for nicotinamide-derived nucleotide substrates. J Biol Chem **278:**24269-24276.
168. **Garavaglia S, Bruzzone S, Cassani C, Canella L, Allegrone G, Sturla L, Mannino E, Millo E, De Flora A, Rizzi M.** 2012. The high-resolution crystal structure of periplasmic *Haemophilus influenzae* NAD nucleotidase reveals a novel enzymatic function of human CD73 related to NAD metabolism. Biochem J **441:**131-141.
169. **Singh SK, Kurnasov OV, Chen B, Robinson H, Grishin NV, Osterman AL, Zhang H.** 2002. Crystal structure of *Haemophilus influenzae* NadR protein. A bifunctional enzyme endowed with NMN adenyltransferase and ribosylnicotinimide kinase activities. J Biol Chem **277:**33291-33299.
170. **Murphy TF, Bartos LC.** 1988. Human bactericidal antibody response to outer membrane protein P2 of nontypeable *Haemophilus influenzae*. Infect Immun **56:**2673-2679.
171. **Morton DJ, Musser JM, Stull TL.** 1993. Expression of the *Haemophilus influenzae* transferrin receptor is repressible by hemin but not elemental iron alone. Infect Immun **61:**4033-4037.
172. **Harrison A, Santana EA, Szelestey BR, Newsom DE, White P, Mason KM.** 2013. Ferric uptake regulator and its role in the pathogenesis of nontypeable *Haemophilus influenzae*. Infect Immun **81:**1221-1233.
173. **Whitby PW, Vanwagoner TM, Seale TW, Morton DJ, Stull TL.** 2013. Comparison of transcription of the *Haemophilus influenzae* iron/heme modulon genes *in vitro* and *in vivo* in the chinchilla middle ear. BMC Genomics **14:**925.
174. **Vogel AR, Szelestey BR, Raffel FK, Sharpe SW, Gearinger RL, Justice SS, Mason KM.** 2012. SapF-mediated heme-iron utilization enhances persistence and coordinates biofilm architecture of *Haemophilus*. Front Cell Infect Microbiol **2:**42.
175. **Mason KM, Munson RS, Jr., Bakaletz LO.** 2003. Nontypeable *Haemophilus influenzae* gene expression induced *in vivo* in a chinchilla model of otitis media. Infect Immun **71:**3454-3462.

176. **Qu J, Lesse AJ, Brauer AL, Cao J, Gill SR, Murphy TF.** 2010. Proteomic expression profiling of *Haemophilus influenzae* grown in pooled human sputum from adults with chronic obstructive pulmonary disease reveal antioxidant and stress responses. BMC Microbiol **10:**162.
177. **Murphy TF, Brauer AL.** 2011. Expression of urease by *Haemophilus influenzae* during human respiratory tract infection and role in survival in an acid environment. BMC Microbiol **11:**183.
178. **Zhang L, Patel M, Xie J, Davis GS, Marrs CF, Gilsdorf JR.** 2013. Urease operon and urease activity in commensal and disease-causing nontypeable *Haemophilus influenzae*. J Clin Microbiol **51:**653-655.
179. **Zhang L, Xie J, Patel M, Bakhtyar A, Ehrlich GD, Ahmed A, Earl J, Marrs CF, Clemans D, Murphy TF, Gilsdorf JR.** 2012. Nontypeable *Haemophilus influenzae* genetic islands associated with chronic pulmonary infection. PLoS One **7:**e44730.
180. **van den Bergh MR, Biesbroek G, Rossen JW, de Steenhuijsen Piters WA, Bosch AA, van Gils EJ, Wang X, Boonacker CW, Veenhoven RH, Bruin JP, Bogaert D, Sanders EA.** 2012. Associations between pathogens in the upper respiratory tract of young children: interplay between viruses and bacteria. PLoS One **7:**e47711.
181. **Molyneaux PL, Mallia P, Cox MJ, Footitt J, Willis-Owen SA, Homola D, Trujillo-Torralbo MB, Elkin S, Kon OM, Cookson WO, Moffatt MF, Johnston SL.** 2013. Outgrowth of the bacterial airway microbiome after rhinovirus exacerbation of chronic obstructive pulmonary disease. Am J Respir Crit Care Med **188:**1224-1231.
182. **Blyth CC, Webb SA, Kok J, Dwyer DE, van Hal SJ, Foo H, Ginn AN, Kesson AM, Seppelt I, Iredell JR.** 2013. The impact of bacterial and viral co-infection in severe influenza. Influenza Other Respir Viruses **7:**168-176.
183. **Hishiki H, Ishiwada N, Fukasawa C, Abe K, Hoshino T, Aizawa J, Ishikawa N, Kohno Y.** 2011. Incidence of bacterial coinfection with respiratory syncytial virus bronchopulmonary infection in pediatric inpatients. J Infect Chemother **17:**87-90.
184. **Arrevillaga G, Gaona J, Sanchez C, Rosales V, Gomez B.** 2012. Respiratory syncytial virus persistence in macrophages downregulates intercellular adhesion molecule-1 expression and reduces adhesion of non-typeable *Haemophilus influenzae*. Intervirology **55:**442-450.
185. **Pettigrew MM, Gent JF, Pyles RB, Miller AL, Nokso-Koivisto J, Chonmaitree T.** 2011. Viral-bacterial interactions and risk of acute otitis media complicating upper respiratory tract infection. J Clin Microbiol **49:**3750-3755.
186. **Henderson FW, Collier AM, Sanyal MA, Watkins JM, Fairclough DL, Clyde WA, Jr., Denny FW.** 1982. A longitudinal study of respiratory viruses and bacteria in the etiology of acute otitis media with effusion. N Engl J Med **306:**1377-1383.
187. **Bakaletz LO, Daniels RL, Lim DJ.** 1993. Modeling adenovirus type 1-induced otitis media in the chinchilla: effect on ciliary activity and fluid transport function of eustachian tube mucosal epithelium. J Infect Dis **168:**865-872.
188. **McGillivary G, Mason KM, Jurcisek JA, Peeples ME, Bakaletz LO.** 2009. Respiratory syncytial virus-induced dysregulation of expression of a mucosal beta-defensin augments colonization of the upper airway by non-typeable *Haemophilus influenzae*. Cell Microbiol **11:**1399-1408.

189. **Unger BL, Faris AN, Ganesan S, Comstock AT, Hershenson MB, Sajjan US.** 2012. Rhinovirus attenuates non-typeable *Hemophilus influenzae*-stimulated IL-8 responses via TLR2-dependent degradation of IRAK-1. PLoS Pathog **8:**e1002969.
190. **Wong SM, Bernui M, Shen H, Akerley BJ.** 2013. Genome-wide fitness profiling reveals adaptations required by *Haemophilus* in coinfection with influenza A virus in the murine lung. Proc Natl Acad Sci U S A **110:**15413-15418.
191. **Shiri T, Nunes MC, Adrian PV, Van Niekerk N, Klugman KP, Madhi SA.** 2013. Interrelationship of *Streptococcus pneumoniae*, *Haemophilus influenzae* and *Staphylococcus aureus* colonization within and between pneumococcal-vaccine naive mother-child dyads. BMC Infect Dis **13:**483.
192. **Hong W, Khampang P, Erbe C, Kumar S, Taylor SR, Kerschner JE.** 2013. Nontypeable *Haemophilus influenzae* inhibits autolysis and fratricide of *Streptococcus pneumoniae in vitro*. Microbes Infect doi:10.1016/j.micinf.2013.11.006.
193. **Ruohola A, Pettigrew MM, Lindholm L, Jalava J, Raisanen KS, Vainionpaa R, Waris M, Tahtinen PA, Laine MK, Lahti E, Ruuskanen O, Huovinen P.** 2013. Bacterial and viral interactions within the nasopharynx contribute to the risk of acute otitis media. J Infect **66:**247-254.
194. **Tikhomirova A, Kidd SP.** 2013. *Haemophilus influenzae* and *Streptococcus pneumoniae*: living together in a biofilm. Pathog Dis **69:**114-126.
195. **Verhaegh SJ, Snippe ML, Levy F, Verbrugh HA, Jaddoe VW, Hofman A, Moll HA, van Belkum A, Hays JP.** 2011. Colonization of healthy children by *Moraxella catarrhalis* is characterized by genotype heterogeneity, virulence gene diversity and co-colonization with *Haemophilus influenzae*. Microbiology **157:**169-178.
196. **Armbruster CE, Hong W, Pang B, Weimer KE, Juneau RA, Turner J, Swords WE.** 2010. Indirect pathogenicity of *Haemophilus influenzae* and *Moraxella catarrhalis* in polymicrobial otitis media occurs via interspecies quorum signaling. MBio **1**.
197. **Weimer KE, Armbruster CE, Juneau RA, Hong W, Pang B, Swords WE.** 2010. Coinfection with *Haemophilus influenzae* promotes pneumococcal biofilm formation during experimental otitis media and impedes the progression of pneumococcal disease. J Infect Dis **202:**1068-1075.
198. **Dagan R, Leibovitz E, Greenberg D, Bakaletz L, Givon-Lavi N.** 2013. Mixed pneumococcal-nontypeable *Haemophilus influenzae* otitis media is a distinct clinical entity with unique epidemiologic characteristics and pneumococcal serotype distribution. J Infect Dis **208:**1152-1160.
199. **Schaar V, Nordstrom T, Morgelin M, Riesbeck K.** 2011. *Moraxella catarrhalis* outer membrane vesicles carry beta-lactamase and promote survival of *Streptococcus pneumoniae* and *Haemophilus influenzae* by inactivating amoxicillin. Antimicrob Agents Chemother **55:**3845-3853.
200. **Schaar V, Uddback I, Nordstrom T, Riesbeck K.** 2014. Group A streptococci are protected from amoxicillin-mediated killing by vesicles containing beta-lactamase derived from *Haemophilus influenzae*. J Antimicrob Chemother **69:**117-120.
201. **Tan TT, Morgelin M, Forsgren A, Riesbeck K.** 2007. *Haemophilus influenzae* survival during complement-mediated attacks is promoted by *Moraxella catarrhalis* outer membrane vesicles. J Infect Dis **195:**1661-1670.

202. **Richard AL, Siegel SJ, Erikson J, Weiser JN.** 2014. TLR2 signaling decreases transmission of *Streptococcus pneumoniae* by limiting bacterial shedding in an infant mouse Influenza A co-infection model. PLoS Pathog **10:**e1004339.
203. **Kramer A, Schwebke I, Kampf G.** 2006. How long do nosocomial pathogens persist on inanimate surfaces? A systematic review. BMC Infect Dis **6:**130.
204. **Hasan NA, Young BA, Minard-Smith AT, Saeed K, Li H, Heizer EM, McMillan NJ, Isom R, Abdullah AS, Bornman DM, Faith SA, Choi SY, Dickens ML, Cebula TA, Colwell RR.** 2014. Microbial community profiling of human saliva using shotgun metagenomic sequencing. PLoS One **9:**e97699.
205. **Murphy TV, Clements JF, Petroni M, Coury S, Stetler L.** 1989. *Haemophilus influenzae* type b in respiratory secretions. Pediatr Infect Dis J **8:**148-151.
206. **Macintyre EA, Karr CJ, Koehoorn M, Demers P, Tamburic L, Lencar C, Brauer M.** 2010. Otitis media incidence and risk factors in a population-based birth cohort. Paediatr Child Health **15:**437-442.
207. **Grindler DJ, Blank SJ, Schulz KA, Witsell DL, Lieu JE.** 2014. Impact of Otitis Media Severity on Children's Quality of Life. Otolaryngol Head Neck Surg **151:**333-340.
208. **Monasta L, Ronfani L, Marchetti F, Montico M, Vecchi Brumatti L, Bavcar A, Grasso D, Barbiero C, Tamburlini G.** 2012. Burden of disease caused by otitis media: systematic review and global estimates. PLoS One **7:**e36226.
209. **Läkemedelsverket.** 2010-12-01. Diagnostik, behandling och uppföljning av akut öroninflammation. http://www.lakemedelsverket.se/malgrupp/Allmanhet/Att-anvanda-lakemedel/Sjukdom-och-behandling/Behandlingsrekommendationer---listan/Otit-akut-oroninflammation/. Accessed 2014-12-03.
210. **Patel JA, Nair S, Revai K, Grady J, Chonmaitree T.** 2009. Nasopharyngeal acute phase cytokines in viral upper respiratory infection: impact on acute otitis media in children. Pediatr Infect Dis J **28:**1002-1007.
211. **Swarts JD, Alper CM, Luntz M, Bluestone CD, Doyle WJ, Ghadiali SN, Poe DS, Takahashi H, Tideholm B.** 2013. Panel 2: Eustachian tube, middle ear, and mastoid--anatomy, physiology, pathophysiology, and pathogenesis. Otolaryngol Head Neck Surg **148:**E26-36.
212. **Hatakka K, Piirainen L, Pohjavuori S, Poussa T, Savilahti E, Korpela R.** 2010. Factors associated with acute respiratory illness in day care children. Scand J Infect Dis **42:**704-711.
213. **Stol K, Verhaegh SJ, Graamans K, Engel JA, Sturm PD, Melchers WJ, Meis JF, Warris A, Hays JP, Hermans PW.** 2013. Microbial profiling does not differentiate between childhood recurrent acute otitis media and chronic otitis media with effusion. Int J Pediatr Otorhinolaryngol **77:**488-493.
214. **Pumarola F, Mares J, Losada I, Minguella I, Moraga F, Tarrago D, Aguilera U, Casanovas JM, Gadea G, Trias E, Cenoz S, Sistiaga A, Garcia-Corbeira P, Pircon JY, Marano C, Hausdorff WP.** 2013. Microbiology of bacteria causing recurrent acute otitis media (AOM) and AOM treatment failure in young children in Spain: shifting pathogens in the post-pneumococcal conjugate vaccination era. Int J Pediatr Otorhinolaryngol **77:**1231-1236.

215. **Eisner MD, Anthonisen N, Coultas D, Kuenzli N, Perez-Padilla R, Postma D, Romieu I, Silverman EK, Balmes JR, Committee on Nonsmoking Copd E, Occupational Health A.** 2010. An official American Thoracic Society public policy statement: Novel risk factors and the global burden of chronic obstructive pulmonary disease. Am J Respir Crit Care Med **182:**693-718.
216. **Svensk-Lungmedicinsk-Förening.** 2014. Allmänt om KOL. http://slmf.se/kol/niva-1/allmant-om-kol-niva-1/. Accessed 2014/12/03.
217. **Wedzicha JA, Seemungal TA.** 2007. COPD exacerbations: defining their cause and prevention. Lancet **370:**786-796.
218. **Qureshi H, Sharafkhaneh A, Hanania NA.** 2014. Chronic obstructive pulmonary disease exacerbations: latest evidence and clinical implications. Ther Adv Chronic Dis **5:**212-227.
219. **Vestbo J, Hurd SS, Agusti AG, Jones PW, Vogelmeier C, Anzueto A, Barnes PJ, Fabbri LM, Martinez FJ, Nishimura M, Stockley RA, Sin DD, Rodriguez-Roisin R.** 2013. Global strategy for the diagnosis, management, and prevention of chronic obstructive pulmonary disease: GOLD executive summary. Am J Respir Crit Care Med **187:**347-365.
220. **Parameswaran GI, Sethi S, Murphy TF.** 2011. Effects of bacterial infection on airway antimicrobial peptides and proteins in COPD. Chest **140:**611-617.
221. **Wedzicha JA, Singh R, Mackay AJ.** 2014. Acute COPD exacerbations. Clin Chest Med **35:**157-163.
222. **Veeramachaneni SB, Sethi S.** 2006. Pathogenesis of bacterial exacerbations of COPD. COPD **3:**109-115.
223. **Burge S, Wedzicha JA.** 2003. COPD exacerbations: definitions and classifications. Eur Respir J Suppl **41:**46s-53s.
224. **Millares L, Marin A, Garcia-Aymerich J, Sauleda J, Belda J, Monso E.** 2012. Specific IgA and metalloproteinase activity in bronchial secretions from stable chronic obstructive pulmonary disease patients colonized by *Haemophilus influenzae*. Respir Res **13:**113.
225. **Leary T.** 1918. The Use of Influenza Vaccine in the Present Epidemic. Am J Public Health (N Y) **8:**754-768.
226. **Morris SK, Moss WJ, Halsey N.** 2008. *Haemophilus influenzae* type b conjugate vaccine use and effectiveness. Lancet Infect Dis **8:**435-443.
227. **Levine OS, Knoll MD, Jones A, Walker DG, Risko N, Gilani Z.** 2010. Global status of *Haemophilus influenzae* type b and pneumococcal conjugate vaccines: evidence, policies, and introductions. Curr Opin Infect Dis **23:**236-241.
228. **Liu DF, Mason KW, Mastri M, Pazirandeh M, Cutter D, Fink DL, St Geme JW, 3rd, Zhu D, Green BA.** 2004. The C-terminal fragment of the internal 110-kilodalton passenger domain of the Hap protein of nontypeable *Haemophilus influenzae* is a potential vaccine candidate. Infect Immun **72:**6961-6968.
229. **Cutter D, Mason KW, Howell AP, Fink DL, Green BA, St Geme JW, 3rd.** 2002. Immunization with *Haemophilus influenzae* Hap adhesin protects against nasopharyngeal colonization in experimental mice. J Infect Dis **186:**1115-1121.
230. **Goodman SD, Obergfell KP, Jurcisek JA, Novotny LA, Downey JS, Ayala EA, Tjokro N, Li B, Justice SS, Bakaletz LO.** 2011. Biofilms can be dispersed by

focusing the immune system on a common family of bacterial nucleoid-associated proteins. Mucosal Immunol **4:**625-637.

231. **Hong W, Peng D, Rivera M, Gu XX.** 2010. Protection against nontypeable *Haemophilus influenzae* challenges by mucosal vaccination with a detoxified lipooligosaccharide conjugate in two chinchilla models. Microbes Infect **12:**11-18.

232. **Riedmann EM, Lubitz W, McGrath J, Kyd JM, Cripps AW.** 2011. Effectiveness of engineering the nontypeable *Haemophilus influenzae* antigen Omp26 as an S-layer fusion in bacterial ghosts as a mucosal vaccine delivery. Hum Vaccin 7 **Suppl:**99-107.

233. **Roier S, Leitner DR, Iwashkiw J, Schild-Prufert K, Feldman MF, Krohne G, Reidl J, Schild S.** 2012. Intranasal immunization with nontypeable *Haemophilus influenzae* outer membrane vesicles induces cross-protective immunity in mice. PLoS One **7:**e42664.

234. **Hotomi M, Ikeda Y, Suzumoto M, Yamauchi K, Green BA, Zlotnick G, Billal DS, Shimada J, Fujihara K, Yamanaka N.** 2005. A recombinant P4 protein of *Haemophilus influenzae* induces specific immune responses biologically active against nasopharyngeal colonization in mice after intranasal immunization. Vaccine **23:**1294-1300.

235. **Mason KW, Zhu D, Scheuer CA, McMichael JC, Zlotnick GW, Green BA.** 2004. Reduction of nasal colonization of nontypeable *Haemophilus influenzae* following intranasal immunization with rLP4/rLP6/UspA2 proteins combined with aqueous formulation of RC529. Vaccine **22:**3449-3456.

236. **Novotny LA, Clements JD, Bakaletz LO.** 2011. Transcutaneous immunization as preventative and therapeutic regimens to protect against experimental otitis media due to nontypeable *Haemophilus influenzae*. Mucosal Immunol **4:**456-467.

237. **Novotny LA, Clements JD, Bakaletz LO.** 2013. Kinetic analysis and evaluation of the mechanisms involved in the resolution of experimental nontypeable *Haemophilus influenzae*-induced otitis media after transcutaneous immunization. Vaccine **31:**3417-3426.

238. **Noda K, Kodama S, Umemoto S, Abe N, Hirano T, Suzuki M.** 2010. Nasal vaccination with P6 outer membrane protein and alpha-galactosylceramide induces nontypeable *Haemophilus influenzae*-specific protective immunity associated with NKT cell activation and dendritic cell expansion in nasopharynx. Vaccine **28:**5068-5074.

239. **Noda K, Kodama S, Umemoto S, Nomi N, Hirano T, Suzuki M.** 2011. Th17 cells contribute to nontypeable *Haemophilus influenzae*-specific protective immunity induced by nasal vaccination with P6 outer membrane protein and alpha-galactosylceramide. Microbiol Immunol **55:**574-581.

240. **Poolman JT, Bakaletz L, Cripps A, Denoel PA, Forsgren A, Kyd J, Lobet Y.** 2000. Developing a nontypeable *Haemophilus influenzae* (NTHi) vaccine. Vaccine **19 Suppl 1:**S108-115.

241. **Bakaletz LO, Kennedy BJ, Novotny LA, Duquesne G, Cohen J, Lobet Y.** 1999. Protection against development of otitis media induced by nontypeable *Haemophilus influenzae* by both active and passive immunization in a chinchilla model of virus-bacterium superinfection. Infect Immun **67:**2746-2762.

242. **Forsgren A, Riesbeck K, Janson H.** 2008. Protein D of *Haemophilus influenzae*: a protective nontypeable *H. influenzae* antigen and a carrier for pneumococcal conjugate vaccines. Clin Infect Dis **46:**726-731.
243. **Gladstone RA, Jefferies JM, Faust SN, Clarke SC.** 2011. Continued control of pneumococcal disease in the UK - the impact of vaccination. J Med Microbiol **60:**1-8.
244. **Prymula R, Peeters P, Chrobok V, Kriz P, Novakova E, Kaliskova E, Kohl I, Lommel P, Poolman J, Prieels JP, Schuerman L.** 2006. Pneumococcal capsular polysaccharides conjugated to protein D for prevention of acute otitis media caused by both *Streptococcus pneumoniae* and non-typable *Haemophilus influenzae*: a randomised double-blind efficacy study. Lancet **367:**740-748.
245. **Prymula R, Kriz P, Kaliskova E, Pascal T, Poolman J, Schuerman L.** 2009. Effect of vaccination with pneumococcal capsular polysaccharides conjugated to *Haemophilus influenzae*-derived protein D on nasopharyngeal carriage of *Streptococcus pneumoniae* and *H. influenzae* in children under 2 years of age. Vaccine **28:**71-78.
246. **Prymula R, Hanovcova I, Splino M, Kriz P, Motlova J, Lebedova V, Lommel P, Kaliskova E, Pascal T, Borys D, Schuerman L.** 2011. Impact of the 10-valent pneumococcal non-typeable *Haemophilus influenzae* Protein D conjugate vaccine (PHiD-CV) on bacterial nasopharyngeal carriage. Vaccine **29:**1959-1967.
247. **van den Bergh MR, Spijkerman J, Swinnen KM, Francois NA, Pascal TG, Borys D, Schuerman L, Ijzerman EP, Bruin JP, van der Ende A, Veenhoven RH, Sanders EA.** 2013. Effects of the 10-valent pneumococcal nontypeable *Haemophilus influenzae* protein D-conjugate vaccine on nasopharyngeal bacterial colonization in young children: a randomized controlled trial. Clin Infect Dis **56:**e30-39.
248. **Barthel D, Singh B, Riesbeck K, Zipfel PF.** 2012. *Haemophilus influenzae* uses the surface protein E to acquire human plasminogen and to evade innate immunity. J Immunol **188:**379-385.
249. **Singh B, Al-Jubair T, Morgelin M, Thunnissen MM, Riesbeck K.** 2013. The unique structure of *Haemophilus influenzae* protein E reveals multiple binding sites for host factors. Infect Immun **81:**801-814.
250. **Perry RD, Craig SK, Abney J, Bobrov AG, Kirillina O, Mier I, Truszczynska H, Fetherston JD.** 2012. Manganese transporters Yfe and MntH are Fur-regulated and important for the virulence of *Yersinia pestis*. Microbiology **158:**804-815.
251. **Meri T, Amdahl H, Lehtinen MJ, Hyvarinen S, McDowell JV, Bhattacharjee A, Meri S, Marconi R, Goldman A, Jokiranta TS.** 2013. Microbes bind complement inhibitor factor H via a common site. PLoS Pathog **9:**e1003308.
252. **Soares de Lima C, Zulianello L, Marques MA, Kim H, Portugal MI, Antunes SL, Menozzi FD, Ottenhoff TH, Brennan PJ, Pessolani MC.** 2005. Mapping the laminin-binding and adhesive domain of the cell surface-associated Hlp/LBP protein from *Mycobacterium leprae*. Microbes Infect **7:**1097-1109.
253. **Henderson B, Martin A.** 2011. Bacterial virulence in the moonlight: multitasking bacterial moonlighting proteins are virulence determinants in infectious disease. Infect Immun **79:**3476-3491.
254. **Koster W.** 2001. ABC transporter-mediated uptake of iron, siderophores, heme and vitamin B12. Res Microbiol **152:**291-301.

255. **Foulston L, Elsholz AK, DeFrancesco AS, Losick R.** 2014. The extracellular matrix of *Staphylococcus aureus* biofilms comprises cytoplasmic proteins that associate with the cell surface in response to decreasing pH. MBio **5:**e01667-01614.
256. **Sharpe SW, Kuehn MJ, Mason KM.** 2011. Elicitation of epithelial cell-derived immune effectors by outer membrane vesicles of nontypeable *Haemophilus influenzae*. Infect Immun **79:**4361-4369.

Molecular Microbiology (2011) 81(1), 80–98

doi:10.1111/j.1365-2958.2011.07678.x
First published online 12 May 2011

Haemophilus influenzae protein E recognizes the C-terminal domain of vitronectin and modulates the membrane attack complex

Birendra Singh,[1] Farshid Jalalvand,[1] Matthias Mörgelin,[3] Peter Zipfel,[4] Anna M. Blom[2] and Kristian Riesbeck[1]*

[1]*Medical Microbiology and* [2]*Medical Protein Chemistry, Department of Laboratory Medicine Malmö, Lund University, Skåne University Hospital, SE-205 02 Malmö, Sweden.*

[3]*Section of Clinical and Experimental Infectious Medicine, Department of Clinical Sciences, Lund University, SE-221 84 Lund, Sweden.*

[4]*Leibniz Institute for Natural Product Research and Infectious Biology, Hans Knoell Institute, Friedrich Schiller University, Beutenbergstr. 11a, D 07745 Jena, Germany.*

Summary

Haemophilus influenzae **protein E (PE) is a 16 kDa adhesin that induces a pro-inflammatory immune response in lung epithelial cells. The active epithelial binding region comprising amino acids PE 84–108 also interferes with complement-mediated bacterial killing by capturing vitronectin (Vn) that prevents complement deposition and formation of the membrane attack complex (MAC). Here, the interaction between PE and Vn was characterized using site-directed mutagenesis. Protein E variants were produced both in soluble forms and in surface-expressed molecules on *Escherichia coli*. Mutations within $PE^{84–108}$ in the full-length molecule revealed that K85 and R86 residues were important for the Vn binding. Bactericidal activity against *H. influenzae* was higher in human serum pre-treated with full-length PE as compared with serum incubated with $PE^{K85E, R86D}$, suggesting that PE quenched Vn. A series of truncated Vn molecules revealed that the C-terminal domain comprising $Vn^{353–363}$ harboured the major binding region for PE. Interestingly, MAC deposition was significantly higher on mutants devoid of PE due to a decreased Vn-binding capacity when compared with wild-type *H. influenzae*. Our results define a fine-tuned interaction between *H. influenzae* and the innate immune system, and identify the mode of control of the MAC that is important for pathogen complement evasion.**

Accepted 19 April, 2011. *For correspondence. E-mail kristian.riesbeck@med.lu.se; Tel. (+46) 40 338494; Fax (+46) 40 336234.

Introduction

Haemophilus influenzae is a Gram-negative, human respiratory tract pathogen and is categorized as typeable (encapsulated) and non-typeable (unencapsulated) strains. Typeable strains are further classified into serotypes a to f (Meats *et al.*, 2003). Among the typeable strains, *H. influenzae* type b (Hib) is considered to be most virulent causing bacteraemia, pneumonia and acute bacterial meningitis or occasionally, osteomyelitis, epiglottitis and joint infections (Watt *et al.*, 2009). Non-typeable *H. influenzae* (NTHi) is most commonly associated with otitis media, sinusitis and chronic obstructive pulmonary disease (COPD) (Murphy, 2003; Sethi *et al.*, 2004, Look *et al.*, 2006). A crucial factor in the *H. influenzae* pathogenesis involves the initial adherence to the respiratory mucosa. When *H. influenzae* overcomes the mucociliary escalator and attaches to the epithelium, it may colonize and also damage epithelial cells. This consequently leads to inflammation and deep tissue penetration. *H. influenzae* usually adheres to and interacts with epithelial cells by many surface exposed proteins including the adhesins high-molecular-weight protein (HMW-1 and HMW-2) (Dawid *et al.*, 1999; Giufre *et al.*, 2008; Gross *et al.*, 2008), *Haemophilus* surface fibrils (Hsf) (Hallström *et al.*, 2006), *H. influenzae* adhesin (Hia) (Winter and Barenkamp, 2009), *Haemophilus* adhesion penetration protein (Hap) (Fink and St Geme, 2003), cryptic *Haemophilus* adhesin protein (Cha) (Sheets *et al.*, 2008), haemagglutinating (HA) pili (Gilsdorf *et al.*, 1992), Pil A (Jurcisek *et al.*, 2007), protein D (Forsgren *et al.*, 2008) and protein E (PE) (Ronander *et al.*, 2008). Several autotransporters are also *H. influenzae* virulence determinants and function as adhesins (Poolman *et al.*, 2000). In recent years, characterization of NTHi adhesins has gained much attention since a future vaccine against NTHi is required (Murphy, 2009).

Gram-negative pathogens are usually recognized by the innate immune system comprising complement components, and are finally killed by the membrane attack complex (MAC). However, many respiratory tract pathogens including *H. influenzae* can overcome the activation of the complement system as well as inhibit the deposition of MAC on the outer membrane (Blom *et al*., 2009; Hallström and Riesbeck, 2010). *H. influenzae* inhibits complement activation by interacting with complement C4b-binding protein (C4 BP) that is an inhibitor of the classical and lectin complement pathways (Hallström *et al*., 2007). Similarly, *Haemophilus* also binds factor H, which inhibits the alternative complement pathway resulting in marked serum resistance (Hallström *et al*., 2008). In addition, *H. influenzae* interacts with several extracellular matrix proteins (ECM) such as vitronectin (Vn), laminin, fibronectin and different types of collagens (Bresser *et al*., 2000; Fink *et al*., 2002), which help in adhesion and colonization in the respiratory tract. Among these ECM, Vn is a multifunctional serum glycoprotein that binds to complement complex C5b-6 and complement 9 (C9). Recruitment of Vn to the bacterial surface thus leads to inhibition of the MAC (Singh *et al*., 2010a). The precise mechanisms and protein–protein interactions involved between bacteria and Vn are largely unknown.

We have isolated and characterized the *H. influenzae* adhesin PE (Ronander *et al*., 2008; 2009). A *pe*-deficient isogenic *H. influenzae* mutant showed a significantly reduced adherence to epithelial cell as compared with wild-type bacteria, and recombinant soluble PE as well as PE-expressing *Escherichia coli* efficiently bound to epithelial cells. Moreover, PE induces a pro-inflammatory response leading to IL-8 secretion in addition to an increased upregulation of ICAM-1 (CD54) in both cell lines and primary epithelial cells originating from patients with COPD (Ronander *et al*., 2009). The central core domain of PE (amino acids 84–108) is the active epithelial cell-binding region. Importantly, mice immunized with $PE^{84–108}$ demonstrated a significantly increased pulmonary clearance of NTHi as compared with controls immunized with a non-related peptide (Ronander *et al*., 2009). Protein E is a highly conserved ubiquitous adhesin among all *Haemophilus* spp. and homologues of PE also exists in other members of the *Pasteurellaceae* family (Singh *et al*., 2010b). Intriguingly, the region PE 84–106 is completely conserved at the amino acid level suggesting an important role in bacterial pathogenesis. These reports indicate that PE may be a valuable vaccine candidate. We also recently reported that PE binds to Vn and contributes to serum resistance (Hallström *et al*., 2009). The isogenic *pe*-mutant was unable to bind Vn and was also significantly more serum sensitive. When the PE–Vn interaction was analysed, $PE^{84–108}$ was identified as the active Vn-binding region. Most interestingly, it was shown that the PE–Vn complex was functionally active and inhibited the MAC assembly *in vitro*.

In the present study, we examined in detail the $PE^{84–108}$ active binding region at the amino acid level in order to understand the mode of Vn binding. In addition, the Vn regions bearing the PE-binding properties were characterized. Several variants of recombinant $PE^{84–108}$ were generated by using site-directed mutagenesis and the K85 and R86 residues of PE were found to be involved in the interaction with Vn. In agreement with the observation that heparin blocks the binding of PE to Vn (Hallström *et al*., 2009), we found that the C-terminal heparin-binding domain (HBD-3) of Vn corresponding to residues 353–363 is mainly involved in this interaction. It is known that PE-dependent binding of Vn to the NTHi surface plays a role in acquiring serum resistance (Hallström *et al*., 2009; Singh *et al*., 2010a). Therefore, we directly measured the MAC deposition at the bacterial surface, and a several-fold higher deposition of MAC on the NTHi Δ*pe* mutant was observed in comparison with the NTHi wild type. In conclusion, this study shows that the PE–Vn interaction at the molecular level plays a highly important role in *H. influenzae* serum resistance.

Results

Lysine 85 and arginine 86 of PE are involved in vitronectin binding

To identify amino acid residues responsible for binding to Vn, the Vn binding region of PE ($PE^{84–108}$) was targeted. According to the internet-based tool GOR4 (http://npsa-pbil.ibcp.fr) PE had 33.8% α-helices, 25.6% extended strand and 40.6% random coils in its secondary structure (Fig. 1A). This estimation was further confirmed using circular dichroism (CD) spectroscopy (Fig. 1E) and small-angle X-ray scattering (SAX). The Vn-binding region $PE^{84–108}$, which contains a helical region and loops was expected to be surface-exposed, at least partially, in order to interact with its ligand Vn (Fig. 1A black background). Thus, based on our previous findings (Hallström *et al*., 2009; Ronander *et al*., 2009) and this secondary structure prediction, $PE^{84–108}$ was targeted by site-directed mutagenesis to identify the amino acid residues involved in the interaction with Vn. The charges of amino acid side-chains were altered to opposite charges, or the amino acids were changed to alanine (Fig. 1B).

The mutated PE variants were recombinantly expressed in *E. coli* and purified using Ni-NTA affinity chromatography. The binding of Vn to PE^{WT} (amino acids 22–160) or variants was analysed using ELISA and surface plasmon resonance. The change of the positively charged side-chain of Lys-85 to a negatively charged Glu reduced the binding by 50% (Fig. 1C). Another positively charged

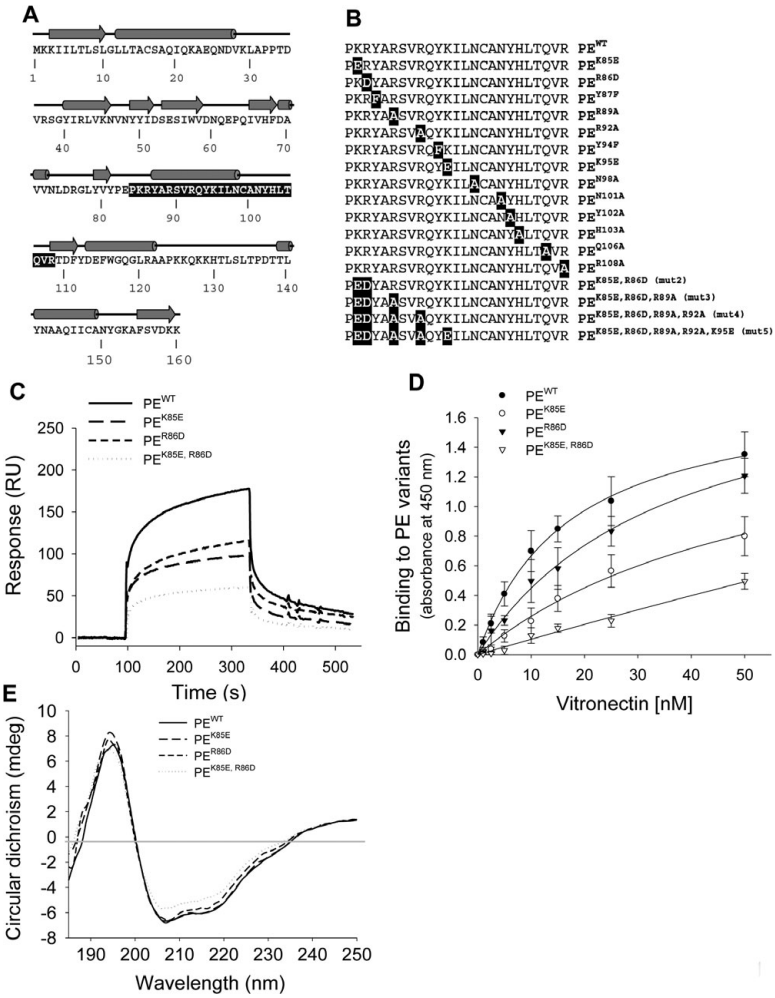

Fig. 1. Amino acids K85 and R86 of PE are involved in binding to Vn.
A. Prediction of the PE secondary structure by the internet-based tool GOR4 (http://npsa-pbil.ibcp.fr). Arrows represent extended strands while tubes represent α-helices. The Vn binding region 84–108 is indicated with a black background.
B. The plan of site-directed mutagenesis of the recombinant His-tagged PE molecules (amino acids 84–108). The side-chains of charged amino acids were either switched to opposite charged side-chains or mutated to alanine.
C. Binding of Vn (Sigma) to PE and variants as revealed by surface plasmon resonance (Biacore). Vn was immobilized on a chip and PE variants (200 μg ml^{-1}) were analysed for binding. The binding of Vn to PE^{WT} in addition to PE^{K85E}, PE^{R86D} and $PE^{K85E,\ R86D}$ are shown as sensorgrams.
D. ELISA showing binding of PE variants to Vn. Approximately 0.01 μM of each protein was coated on ELISA plates followed by addition of increasing amounts of Vn (Sigma). Bound Vn was detected by using sheep anti-Vn pAb. Mean values of triplicates from three independent experiments were plotted, error bars representing standard deviations and curves are hyperbolic fits. The binding at 5–50 nM Vn concentration was statistical significant when PE^{WT} was compared with mutants ($P \leq 0.001$) (ANOVA).
E. CD spectra of PE variants. Five spectra for each protein (5 μM) were recorded and mean values plotted.

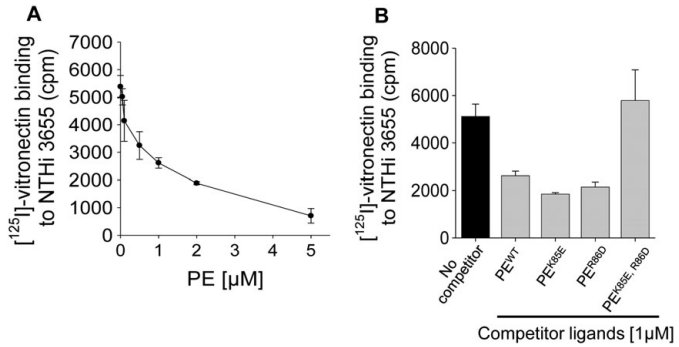

Fig. 2. PE blocks the Vn interaction with NTHi 3655.
A. Unlabelled PE^{WT} blocks binding of [^{125}I]-labelled Vn to NTHi 3655 in a direct binding assay as described in detail in *Experimental procedures*.
B. Binding of [^{125}I]–Vn to NTHi 3655 is blocked with PE^{WT}, PE^{K85E}, PE^{R86D}, whereas the double mutant $PE^{K85E,\ R86D}$ does not block. Mean values of triplicates from three independent experiments were plotted and standard deviations were shown as error bars. Differences between the control (without any competitor) and $PE^{K85E,\ R86D}$ were statistically significant with PE^{WT}, PE^{K85E}, PE^{R86D} ($P \leq 0.001$). When PE^{WT}, PE^{K85E} and PE^{R86D} were compared these were not significant (ANOVA).

side-chain containing amino acid residue Arg-86 was changed to Asp, and also showed a 48% reduction in binding to Vn. Alteration of the charged side-chains of K85 and R86 in the double mutant $PE^{K85E,\ R86D}$ (Fig. 1B: mut2) showed defective Vn binding (Fig. 1C). In addition, similar experiments were performed with all PE variants using ELISA, where PE variants were coated on microtitre plates and Vn binding was detected using anti-Vn pAb. Our results revealed that PE^{K85E} and PE^{R86D} decreased Vn binding by 30–50% and that the $PE^{K85E,\ R86D}$ double mutant of PE lost 70% Vn binding (Fig. 1D). PE^{WT}, PE^{K85E}, PE^{R86D} and $PE^{K85E,\ R86D}$ were analysed for folding pattern by using CD, and these analyses suggested that PE variants were folded (Fig. 1E). All the PE variants shown in Fig. 1B were tested for Vn binding by Biacore and ELISA. Other multiple mutations (Fig. 1B: mut3, mut4, mut5) in the PE molecule showed similar binding pattern to the Vn molecule as shown by $PE^{K85,\ R86}$ (data not shown).

Lysine 85 and arginine 86 residues of PE on NTHi surface recognize Vn

The specificity of the binding of Vn to non-typeable *H. influenzae* (NTHi) 3655 was also verified by a competition assay, where [^{125}I]–Vn binding was blocked with unlabelled PE variants. Vn binding to NTHi was inhibited by unlabelled PE^{WT} in a dose-dependent manner (Fig. 2A). Single mutants of the PE molecule, i.e. PE^{K85E} and PE^{R86D} competed with Vn (Fig. 2B), whereas the double mutant $PE^{K85E,\ R86D}$ did not inhibit Vn binding to NTHi 3655. These results suggested that K85 and R86 were crucial for Vn binding and were involved in the PE–Vn interaction at the bacterial surface. Moreover, since recombinant proteins with alterations of the K85 and R86 side-chains to acidic charged counterparts lost PE–Vn binding, indicating that the interaction may be electrostatic. However, these data solely cannot prove the nature of this interaction.

To analyse the effect of mutated K85 and R86 when expressed at the surface (similarly as expression in NTHi 3655), PE variants were expressed in *E. coli*. Expression of PE was monitored by flow cytometry (Fig. 3D) followed by binding of recombinant $Vn^{80–396}$ that was analysed by transmission electron microscopy (TEM) (Fig. 3A). *E. coli* (PE^{WT}) displayed a similar binding pattern as compared with the single mutants expressing PE^{K85E} and PE^{R86D} (857–945 gold particles μm^{-2}), whereas the double mutant ($PE^{K85E,\ R86D}$) had a five- to sixfold reduced binding (248 particles μm^{-2}) to recombinant Vn (Fig. 3A). The compilation of several fields of vision of $Vn^{80–396}$ binding to *E. coli* variants is shown in Fig. 3B.

In addition to experiments with recombinant $Vn^{80–396}$, the binding of native serum Vn to *E. coli* expressing PE wild type and variants at the surface was analysed by semi-quantitative Western blotting. Bacteria were treated with normal human serum (NHS) diluted 1:25 to 1:500 in PBS containing 2.5% BSA followed by analysis of Vn bound to the bacterial surface using anti-Vn pAb (Fig. 3C). These results demonstrated that *E. coli* expressing PE^{WT} at the surface acquired Vn binding capacity, whereas *E. coli* ($PE^{K85E,\ R86D}$) lost Vn binding and showed a similar Vn binding as the control *E. coli* devoid of PE (Fig. 3B). Thus, these two data sets indicated that K85 and R86 are both necessary for Vn binding when PE was present at the *E. coli* surface. This experimental model with *E. coli* also mimicked the functional role of PE as compared with expression in NTHi 3655.

The C-terminal of Vn (amino acids 353–363) is a major PE binding region

Vitronectin is a 65–75 kDa glycoprotein that contains a 43-amino-acid-long somatomedin-B (SMB) domain, which binds plasminogen activator inhibitor-1 (PAI-1) (Arroyo De Prada *et al.*, 2002; Schroeck *et al.*, 2002). In addition, Vn has four putative haemopexin-like regions and three heparin-binding domains (HBDs) (Singh *et al.*, 2010a), and in the case of PE, heparin is known to inhibit binding to Vn (Hallström *et al.*, 2009). To exclude that the

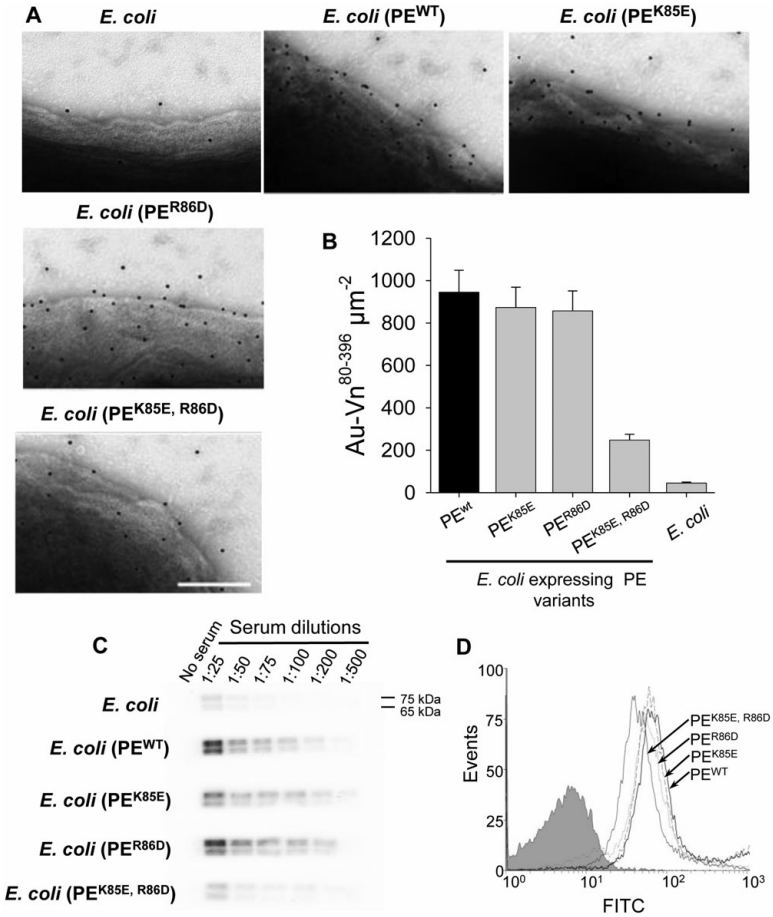

Fig. 3. PE at the bacterial surface binds to Vn by the residues K85 and R86.
A. Binding of gold-labelled $Vn^{80–396}$ to *E. coli* expressing PE variants at the surface as shown with TEM.
B. The results analysed from (A) were plotted as a bar diagram. Number of gold particles was determined in 60 independent bacterial profiles and number of particles μm^{-2} was calculated. Mean of triplicates from three experiments are shown and error bars represent SD. The difference between *E. coli* expressing PE^{WT} and $PE^{K85E, R86D}$ was statistically significant ($P \leq 0.001$). The bar represents 100 nm.
C. Serum Vn binds to *E. coli* expressing PE variants. Bacteria (10^8) were treated with different serum dilutions in PBS containing 2.5% BSA and washed three times in PBS. Total cellular proteins were separated on SDS-PAGE and blotted to a PVDF membrane followed by detection with anti-human Vn pAbs. Two bands with Vn (molecular weights 75 kDa and 65 kDa) were detected in Western blot. This experiment was repeated twice and one representative experiment is shown here.
D. Flow cytometry profile of *E. coli* expressing PE variants that were used in these experiments. Filled curve represents control *E. coli* with empty pET16b vector.

SMB domain was involved in the PE–Vn binding, we pre-incubated PE with PAI-1 followed by addition of Vn. Binding was analysed by ELISA and dot blot, but no inhibitory effect of PAI-1 was observed (data not shown). We have recently shown that *Moraxella catarrhalis* Ubiquitous surface protein (Usp) A2 binds to the C-terminus (HBD-3) of the Vn molecule (Singh *et al.*, 2010c). In addition to recombinant Vn molecules used in that particular study, we created a series of new truncated Vn fragments (Fig. 4A). The protein fragments were purified and their purity and nature was studied by using SDS-PAGE, native PAGE and CD (Fig. 4B–E). All Vn fragments showed monomeric and multimeric forms and folding patterns in non-reducing PAGE and CD respectively. However, the smallest fragment $Vn^{80–229}$ lacked a secondary structure in CD (Fig. 4E).

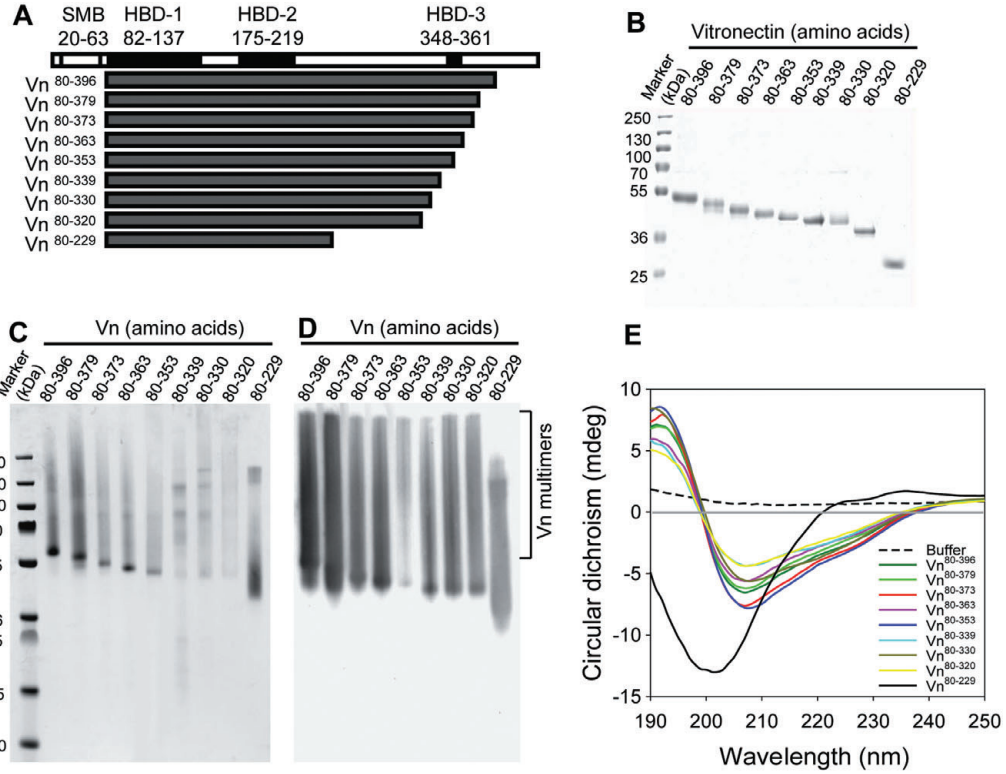

Fig. 4. Expression of recombinant Vn fragments and analyses for folding and multimerization.
A. Schematic representation of the different truncated Vn molecules that were expressed in a mammalian expression system.
B. Quality control of purified recombinant Vn molecules expressed in HEK293T cells. All protein fragments were purified by Ni-NTA chromatography and subjected to 15% SDS-PAGE (approximately 2 μg per lane) that was stained with Coomassie blue R250.
C. Non-reducing SDS-PAGE showing the Vn fragments monomers and multimers. Each fragment (5 μg) was loaded in a 4–12% gradient SDS polyacrylamide gel and stained with Coomassie blue R250.
D. A similar gel (as shown in C) was analysed by Western blotting by using anti-Vn antibodies.
E. CD spectra of Vn fragments at a concentration of 5 μM. Five spectra for each Vn fragment were recorded and mean values are shown here.

The purified recombinant Vn proteins (Fig. 4B) were used for binding to whole bacteria and different soluble PE variants. NTHi 3655 wild type (10^8 bacterial cells) were incubated with Vn fragments (0.5 μg) and Vn bound to the bacterial surface was analysed by whole-cell protein Western blotting (Fig. 5A). Only $Vn^{80–396}$, $Vn^{80–379}$, $Vn^{80–373}$ and $Vn^{80–363}$ bound to the NTHi surface, whereas $Vn^{80–353}$ and further shorter truncated fragments of Vn did not interact with NTHi. In the next series of experiments we analysed binding of Vn fragments to purified PE in ELISA. Microtitre plates were coated with PE^{WT} and Vn fragments (0–100 nM) were allowed to bind. Resulting bound Vn fragments were quantified by anti-Vn pAb. The results revealed that $Vn^{80–396}$ and $Vn^{80–379}$ displayed similar binding saturation kinetics, while $Vn^{80–373}$ and $Vn^{80–363}$ showed a 20–30% reduced PE binding in comparison with $Vn^{80–396}$ and $Vn^{80–379}$ (Fig. 5B). Further truncation of Vn reduced binding to the PE molecule, indicated that Vn 353–363 is a major PE binding region while a minor interaction may also be involved in Vn 363-373. A comparative binding analysis of PE variants to all Vn fragments was also performed (Fig. 5C). $Vn^{80–396}$, $Vn^{80–379}$ bound PE^{WT}, PE^{K85E} and PE^{R86D} stronger than $Vn^{80–373}$ and $Vn^{80–363}$. In contrast, the double mutant $PE^{K85E,\ R86D}$ significantly lost Vn binding with all Vn fragments (Fig. 5C). Our data thus confirmed that further truncation after amino acids $Vn^{80–363}$ resulted in lost binding to the PE molecule.

Binding of the $Vn^{80–396}$ fragments to the NTHi 3655 surface was also analysed for binding specificity and competition with other smaller fragments. NTHi 3655 was

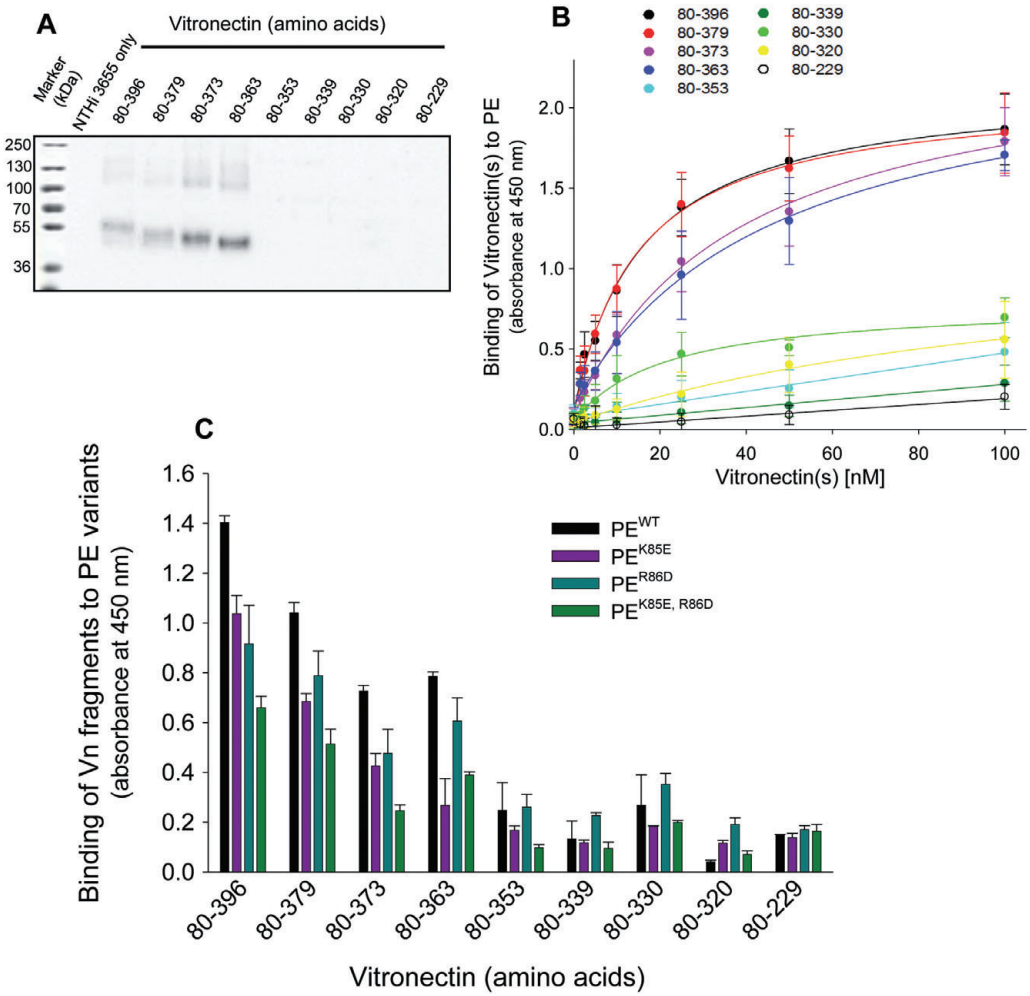

Fig. 5. Vn 353–363 binds to NTHi PE.

A. Binding of Vn fragments to PE-expressing NTHi 3655 wild type as revealed by Western blot. Bacteria (10^8) were incubated with 0.5 μg of each Vn fragment and washed twice with PBS. Thereafter, total cellular proteins were separated on an SDS-PAGE and blotted onto a PVDF membrane. This experiment was repeated three times, and one representative blot is shown here.

B. Binding of Vn fragments to wild-type PE. Recombinant PE (0.1 μM) was coated in microtitre plates and increasing amounts of all Vn fragments were added, followed by detection of bound Vn using anti-human Vn pAbs. Data shown are the means of triplicates from three independent experiments and curves shown are hyperbolic fits. The binding of Vn to PE^{WT} at 1.5–100 nM was statistically significant ($P \leq 0.001$) when $Vn^{80–396}$ or $Vn^{80–379}$ and other fragments were compared. Differences between $Vn^{80–396}$ and $Vn^{80–379}$, and between $Vn^{80–373}$ and $Vn^{80–363}$ were not significant (ANOVA).

C. Comparison of PE variants bound to different Vn fragments. Equimolar amounts (0.1 μM) of PE variants were coated on microtitre plates and 20 nM of each Vn fragment was allowed to bind. Data represent means of triplicates from three independent experiments and error bars indicate standard deviations. In the Vn groups $Vn^{80–396}$, $Vn^{80–379}$, $Vn^{80–373}$ and $Vn^{80–363}$ the binding differences between PE^{WT} and PE mutants were statistically significant ($P \leq 0.01$) (ANOVA).

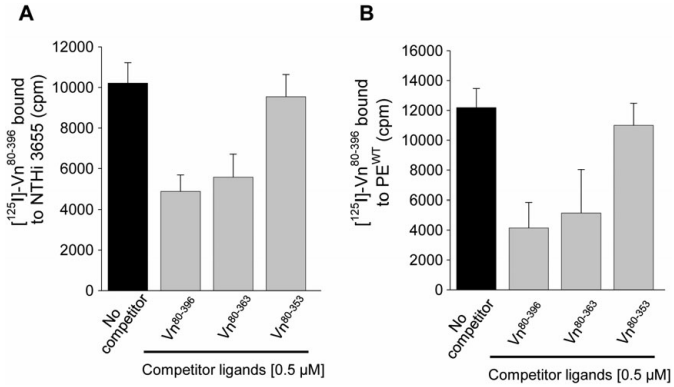

Fig. 6. Vn 353–363 amino acids interact to PE at the NTHi surface.
A. Binding of [^{125}I]–Vn$^{80–396}$ (approximately 300 000 kcpm) at the NTHi 3655 surface and inhibition by using cold Vn fragments. [^{125}I]–Vn$^{80–396}$ was added to 10^8 bacterial cells, after extensive washing bound fraction was counted in a gamma counter. In blocking experiments, bacteria were treated with Vn$^{80–396}$, Vn$^{80–363}$ and Vn$^{80–353}$ prior to addition of labelled Vn. [^{125}I]–Vn$^{80–396}$ binding without any competitor was compared with treated samples.
B. PE^{WT} protein was coated on MaxiSorp ELISA plates (strip plates), [^{125}I]–Vn$^{80–396}$ (approximately 300 000 kcpm) was added, the unbound fractions were washed and bound fractions were counted. In competitive experiments Vn$^{80–396}$, Vn$^{80–363}$ and Vn$^{80–353}$ were added to PE-coated wells prior to addition of the [^{125}I]–Vn$^{80–396}$.
In both experiments means of triplicates from three independent experiments (A and B) were plotted and standard deviations are shown as error bars. Differences between control (without any competitor) or Vn$^{80–353}$ were statistically significant with Vn$^{80–396}$ and Vn$^{80–363}$ treatment ($P \leq 0.01$). Differences between Vn$^{80–396}$ and Vn$^{80–363}$ were not significant (ANOVA).

allowed to bind [^{125}I]–Vn$^{80–396}$ and the other smaller unlabelled fragments (Vn$^{80–363}$ and Vn$^{80–353}$) were used for competition. Results showed that Vn$^{80–396}$ and Vn$^{80–363}$ blocked 40–50% binding of the [^{125}I]–Vn$^{80–396}$ molecule, whereas Vn$^{80–353}$ did not inhibit binding (Fig. 6A). Similar results were also observed when PE^{WT} was coated on a microtitre plate and [^{125}I]–Vn$^{80–396}$ binding to immobilized PE^{WT} was analysed. Here also Vn$^{80–396}$ and Vn$^{80–363}$ blocked 60–70% of the binding to the [^{125}I]–Vn$^{80–396}$ fragment, whereas Vn$^{80–353}$ did not significantly block (Fig. 6B). These both experiments directly indicated that the major PE binding region of Vn is located between amino acids 353 and 363.

In our next set of experiments, Vn fragments were labelled with gold particles and their interaction with whole NTHi 3655 and NTHi 3655Δ*pe* in addition to *E. coli* expressing PE at the surface was analysed by TEM. As exemplified in Fig. 7A, only the gold-labelled fragments Vn$^{80–396}$, Vn$^{80–379}$, Vn$^{80–373}$ and Vn$^{80–363}$ interacted with NTHi 3655, whereas the other fragments were unable to bind (all data not shown). As can be seen in the bar diagram (Fig. 7C), 636 gold-Vn$^{80–396}$ particles, 798 gold-Vn$^{80–363}$ particles μm^{-2} were bound to the surface of NTHi 3655, and this was in comparison with Vn$^{80–353}$ and Vn$^{80–320}$ that only bound 125 and 61 particles μm^{-2} respectively. NTHi 3655Δ*pe* mutants showed a sixfold reduced Vn$^{80–396}$ binding with 106 particles μm^{-2}. The observed minor Vn binding to the PE-deficient NTHi 3655Δ*pe* could be due to other weak Vn-binding surface proteins (Fig. 7A). Moreover, PE-expressing *E. coli* had a similar Vn-binding pattern as compared with NTHi 3655 (Fig. 7B). *E. coli* (PE^{WT}) bound 881 Vn$^{80–396}$ gold particles μm^{-2}, whereas the *E. coli* control without PE bound considerably less Vn$^{80–396}$ (45 particles μm^{-2}). Regarding the other Vn fragments, a similar pattern as with NTHi 3655 was observed with *E. coli* (PE^{WT}) (Fig. 7B and D). The TEM data were thus comparable and in agreement with results obtained *in vitro* (Fig. 5B), or *in vivo* at the bacterial surface (Figs 5A and 6*A*). These results clearly indicated that the C-terminal domain in Vn corresponding to residues Vn 353–363 is a major region for the interaction with PE.

Non-typeable H. influenzae *is more sensitive to human serum that is pre-treated with PE*

Vitronectin binds C9 and thus inhibits its insertion into the bacterial membrane during MAC assembly (Singh *et al.*, 2010a). When Vn is bound to the bacterial surface, the MAC is inhibited and bacteria have a prolonged survival when exposed to NHS. The PE-expressing wild-type NTHi 3655 was resistant to 10% NHS, and compared with the PE-deficient mutant NTHi 3655Δ*pe* that was significantly less serum resistant (Fig. 8A). We recently reported that Vn-depleted serum markedly increased *H. influenzae* killing, and that addition of Vn to depleted NHS restored the bacterial serum resistance (Hallström *et al.*, 2009).

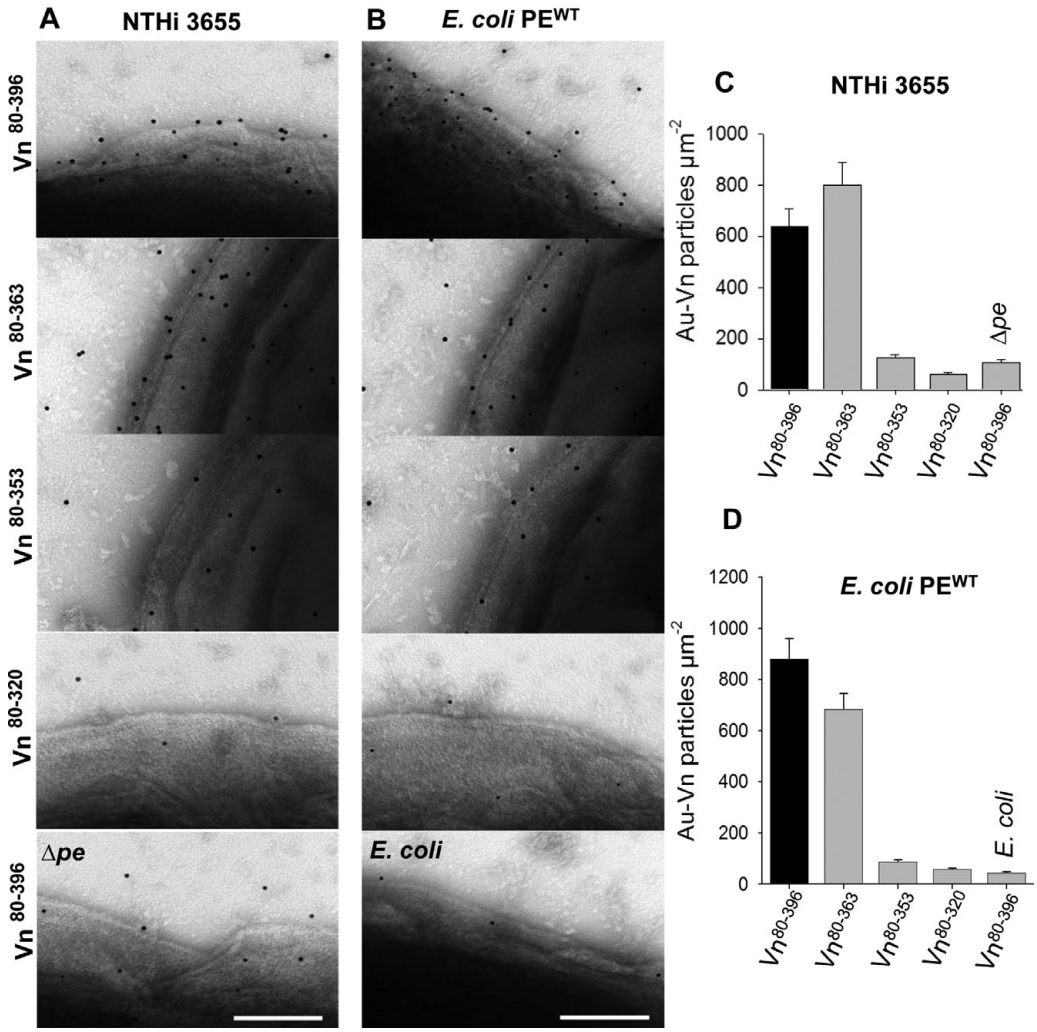

Fig. 7. Transmission electron microscopy of NTHi 3655 and *E. coli* expressing PE^{WT}.
A. Binding of gold-labelled recombinant $Vn^{80–396}$, $Vn^{80–363}$, $Vn^{80–353}$ and $Vn^{80–320}$ to the surface of NTHi 3655.
B. Binding of similar gold-labelled Vn fragments to *E. coli* expressing PE^{WT} at the surface.
C and D. Bar diagrams based upon the experiments delineated in (A) and (B). Vn molecules (gold particles μm^{-2}) that were bound to NTHi 3655 and *E. coli* expressing PE^{WT} were determined in 60 independent bacterial profiles and number of particles μm^{-2} was calculated. Mean of triplicates from three experiments are shown and error bars represent SD. Differences were statistically significant when PE binding to $Vn^{80–396}$ and $Vn^{80–363}$ were compared with the other truncated Vn fragments ($P \leq 0.001$).
Bars in (A) and (B) indicate 100 nm.

Hypothetically, if NHS is incubated with soluble PE, an increased C9 deposition at the bacterial surface may occur due to quenching of Vn, and will be followed by an accelerated MAC-mediated killing. Hence, the Vn-binding capacity of recombinant PE^{WT} or PE variants was analysed by pre-incubation of these recombinant proteins with NHS followed by exposure to NTHi 3655. When purified PE^{WT} was added to NHS, a dose-dependent decrease in bacterial survival was seen in comparison with the recombinant control protein $MID^{962–1200}$ (Fig. 8B). This effect of

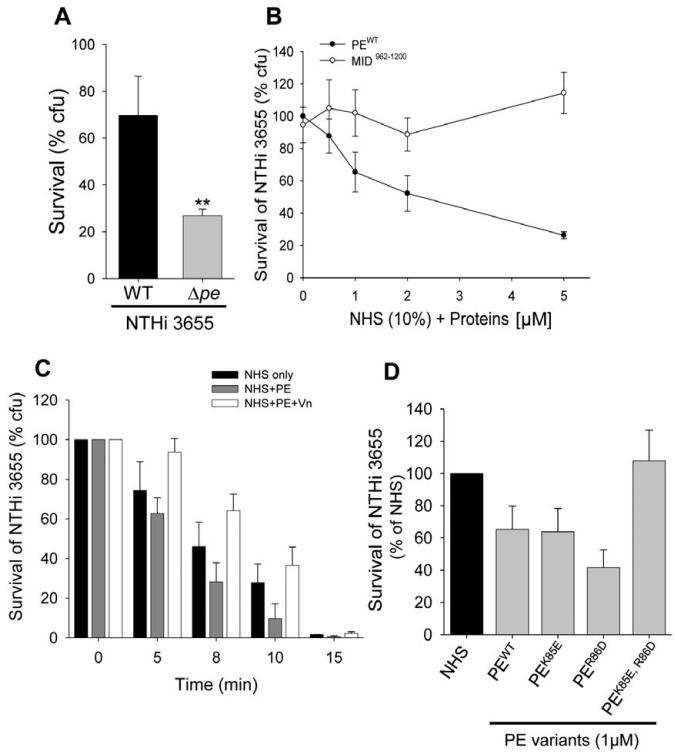

Fig. 8. *H. influenzae* is more sensitive to serum that has been pre-treated with PE.
A. Serum resistance of NTHi 3655 and NTHi 3655Δ*pe* when incubated with 10% NHS.
B. Pre-incubation of NHS with increasing concentrations (1–5 μM) of recombinant PE^{WT} quenches Vn and hence NTHi appears more serum sensitive. $MID^{962–1200}$ is a protein fragment from *Moraxella catarrhalis* IgD-binding protein (MID) that was used as a negative control (Nordström *et al.*, 2006).
C. NTHi 3655 was incubated with NHS, NHS treated with PE (2 μM) and PE-treated NHS was added to Vn (2 μM)-treated bacterial cells. Differences were statistically significant (5–10 min) when NHS only and NHS+PE or NHS+PE+Vn were compared ($P \leq 0.05$), as well as differences between NHS+PE and NHS+PE+Vn ($P \leq 0.001$) (ANOVA).
D. PE^{WT}, PE^{K85E}, PE^{R86D} showed decrease in serum resistance, whereas $PE^{K85E,\ R86D}$ did not show any decrease of resistance when added to NHS. PE^{WT}, PE^{K85E} and PE^{R86D} were significantly different ($P \leq 0.001$) when compared with control NHS or $PE^{K85E,\ R86D}$ (ANOVA). No significant difference was observed between control NHS and $PE^{K85E,\ R86D}$.
In (A)–(D) means of triplicates from three independent experiments are shown and standard deviations are indicated as error bars.

Vn neutralization could be replenished if NTHi 3655 was treated with Vn prior to addition of PE treated serum (Fig. 8C). We also tested whether it was possible to quench Vn by incubating NHS with the different mutated PE variants followed by incubation with whole bacteria. Interestingly, pre-incubation of NHS with PE^{K85E} and PE^{R86D} resulted in significantly higher bacterial killing, whereas experiments with $PE^{K85E,\ R86D}$ did not reveal any difference in bactericidal serum activity (Fig. 8D). Pre-treatment of NHS with recombinant PE^{WT} and mutated variants thus indicated that PE was able to bind Vn derived from serum, and that in particular residues K85 and R86 were responsible for the binding. These results were in parallel with findings obtained with the direct binding assays (Figs 2, 3 and 5).

Vitronectin bound to PE prevents MAC deposition at the surface of H. influenzae

It is well known that Vn inhibits the MAC complex and this property of Vn is successfully utilized by many pathogens to evade the host innate immune response (Singh *et al.*, 2010a). Recently we found that NTHi 3655Δ*pe* significantly lost Vn binding (as also shown in Fig. 7A and C), and that this PE-dependent Vn interaction is involved in serum resistance (Hallström *et al.*, 2009). To analyse the effect of the PE–Vn interaction on MAC formation, we performed a serum resistance assay and observed the concentrations of C9 polymerized, and measured C9 monomers consumed during MAC deposition. Western blotting using a specific anti-C9 pAb that recognizes both monomeric and polymeric C9, and subsequent densitometric analyses were performed. Under these experimental conditions, MAC deposition on bacteria occurred in a time-dependent manner (Fig. 9A and B). C9 is a 71 kDa monomer that may exist in a monomeric or oligomeric state, associated as a C5b-9 complex in NHS under normal physiological conditions (Podack and Tschopp, 1982). After complete polymerization of C9 (ring closure), a high-molecular-weight band of approximately 400–500 kDa (a C9 oligomer) appears (Podack and Tschopp, 1982; Deng *et al.*, 2007). The disappearance of the C9 monomer in the presence of NTHi 3655Δ*pe* (Fig. 9B) was more evident in comparison with the NTHi 3655 wild type, and an increased C9 oligomerization directly revealed that MAC formation was more efficient in reactions

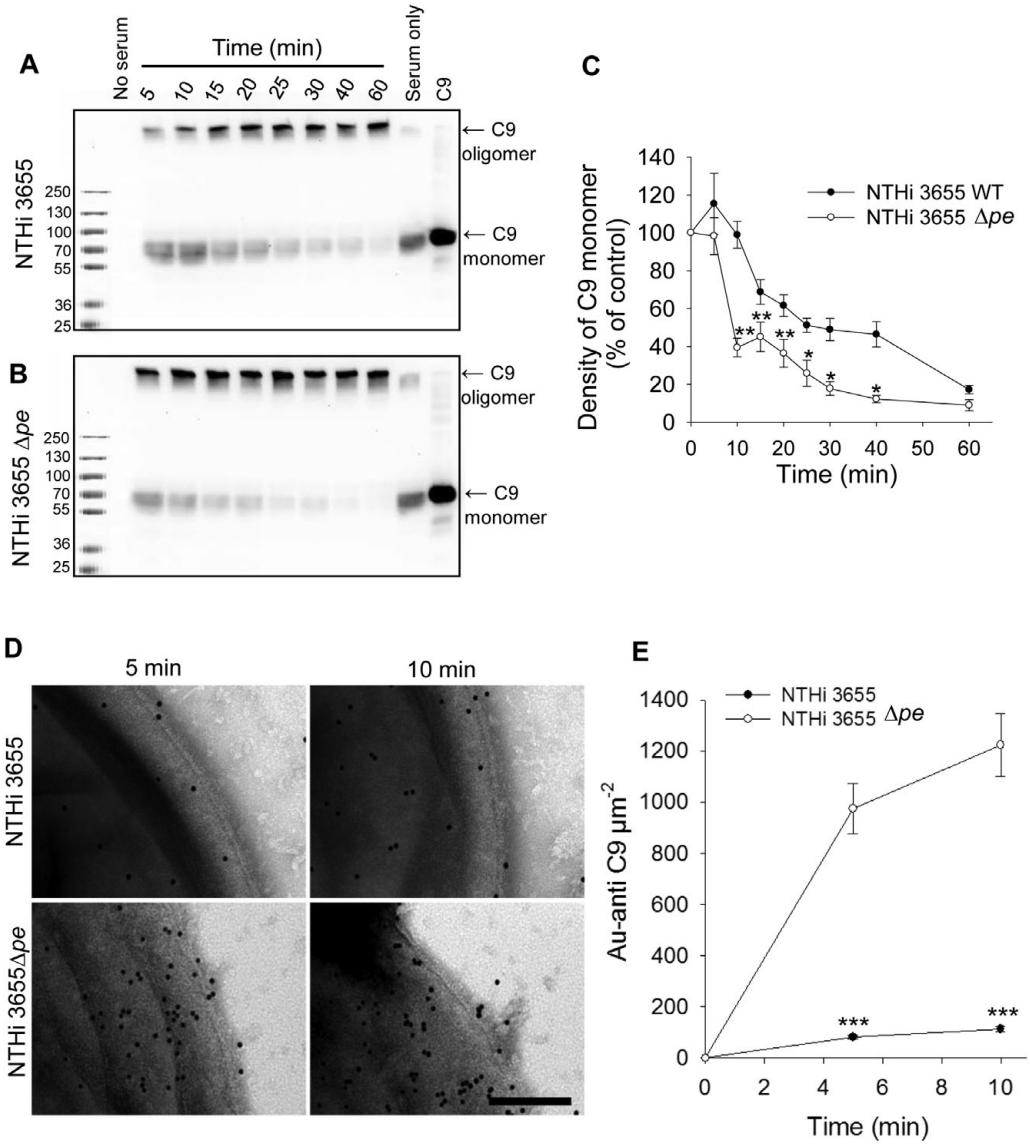

containing PE-deficient NTHi mutants (Fig. 9A and B). Densitometric measurements of C9 when incubated with the PE-expressing NTHi 3655 revealed that within 10–15 min of incubation 75–90% of C9 was a monomer (Fig. 9C). In contrast, only 40–45% of C9 was remaining as a monomer when exposed to NTHi 3655Δ*pe*.

We also performed TEM of these serum-treated samples. Samples at 5 and 10 min (as described in Fig. 9A and B) were chosen and analysed by gold-labelled anti-C9 pAbs. Data obtained by TEM also suggested a time-dependent deposition of C9. The number of gold particles reflecting C9 was counted from 60 independent bacterial profiles. At 5 min, 82 gold particles μm^{-2} were found on the NTHi 3655 wild type, whereas 974 gold particles μm^{-2} were detected on the NTHi 3655Δ*pe* mutant. Similarly, 114 particles μm^{-2} and 1224 particles

Fig. 9. MAC deposition at the *H. influenzae* surface is regulated by PE-dependent Vn binding.
A and B. NTHi 3655 and NTHi 3655Δ*pe* (10^8 cells) were resuspended in GVB^{++} buffer containing 10% NHS and incubated at 37°C. MAC deposition is seen as increase in C9 oligomer and disappearance of the C9 monomer. The complement reaction was terminated at different time points (5–60 min) by snap freezing of samples. Samples were subjected to 4–12% gradient SDS-PAGE, blotted onto PVDF membrane followed by detection using an anti-human C9 pAb. The experiment was repeated twice. One of the representative blots from triplicates of a single experiment is shown here.
C. The C9 monomer density was measured from triplicate blots of a single experiment. Error bars indicate standard deviations. Statistical significant differences were observed between 10 and 40 min (ANOVA). The experiment was repeated twice.
D. TEM analysis that demonstrates C9 deposition on the surface of NTHi 3655 and NTHi 3655Δ*pe*. Samples obtained at 5 and 10 min from (A) and (B) were probed with gold labelled anti-human C9 pAb.
E. Estimation of gold-labelled Vn bound to the wild type and PE-deficient NTHi mutant. The curve shows the number of particles μm^{-2} evaluated from 60 independent bacterial profiles. Mean of triplicates from three experiments are shown and error bars represent SD.
Bar represents 100 nm. $*P \leq 0.05$; $**P \leq 0.01$; $***P \leq 0.001$.

μm^{-2} were seen after 10 min on the NTHi wild type and the mutant surface, respectively (Fig. 9D and E). These results directly explained why NTHi 3655Δ*pe* mutants were more serum-sensitive as compared with the wild type, and also that the PE–Vn interaction was highly important for NTHi serum resistance.

In our next set of experiments we analysed the capacity of the PE^{WT} and $PE^{K85E,\ R86D}$ variant for Vn binding and subsequent effect in MAC formation at the NTHi 3655 surface. PE^{WT} and $PE^{K85E,\ R86D}$ were immobilized on CNBr agarose beads to simulate PE as a surface bound protein and checked on a Western blot (Fig. 10A). Control beads were treated similarly without any added protein. The pull-down capacity of these beads was measured by semi-quantitative Western blotting at different serum dilutions. PE^{WT} bound Vn more intensely in comparison with $PE^{K85E,\ R86D}$ (Fig. 10B). To bind Vn, beads coated with PE (equivalent to 2 μM protein) and control beads were

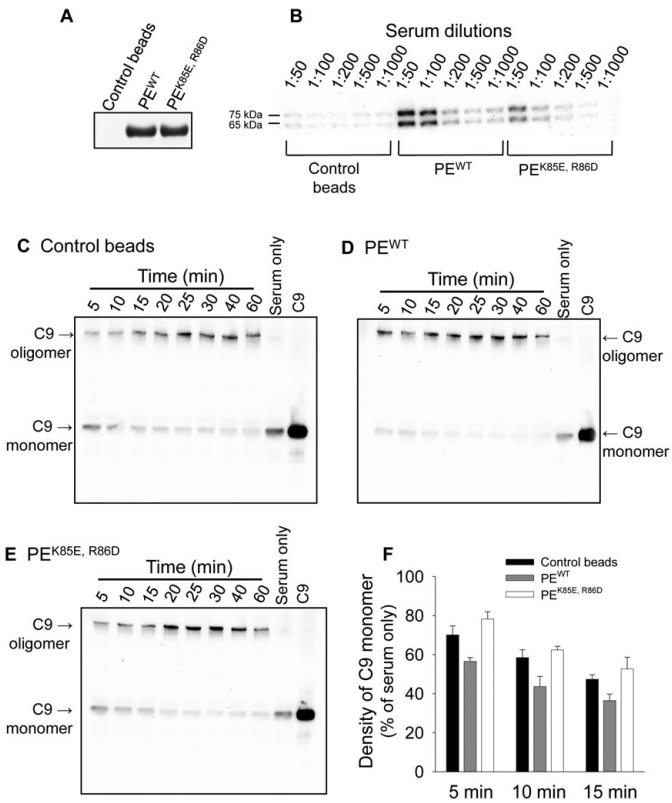

Fig. 10. PE-treated serum increases MAC deposition at the bacterial surface.
A. CNBr agarose beads were immobilized with PE^{WT} and $PE^{K85E,\ R86D}$ proteins (see *Experimental procedures*). One set of beads were treated similarly without protein to generate control beads. Agarose beads bound PE (5 μg) along with control were resolved in a 12% SDS-PAGE and stained with Coomassie blue R250.
B. Pull-down assay showing binding of Vn by PE-coated beads. PE-coated beads (1 μg) and control beads were added to 100 μl of different serum dilutions in PBS containing 2.5% BSA. Beads were washed extensively with PBS and proteins were separated in SDS-PAGE followed by Western blotting and detection of Vn by anti-Vn antibodies. This experiment was repeated twice; one representative blot is shown here.
C–E. Normal human serum was treated with control, PE^{WT}- and $PE^{K85E,\ R86D}$-coated beads (2 μM) prior to adding to bacteria. C9 deposition experiments were performed as described in Fig. 9. This experiment was repeated twice. From a single experiment samples, each blot was performed in triplicate; one representative blot out of triplicate is shown here.
F. The C9 monomer density was measured from triplicate blot of a single experiment. The data for 5–15 min are shown. The differences (5–15 min) between control beads and PE^{WT} were statistically significant ($P \leq 0.01$). A comparison between PE^{WT} and $PE^{K85E,\ R86D}$ beads revealed $P \leq 0.05$ (ANOVA). Any statistical significance was not observed between control beads and $PE^{K85E,\ R86D}$-coated beads.

added to serum and incubated for 1 h. This serum was subsequently tested for C9 deposition at the NTHi 3655 surface. The results shown in Fig. 10C–E represent C9 deposition on control, PE^{WT} and $PE^{K85E,\ R86D}$ beads when incubated with serum. Three blots from a typical experiment were scanned for C9 band intensity and are shown in the bar chart (Fig. 10F). The serum incubated with control beads showed a similar C9 disappearance as treatment with beads coated with $PE^{K85E,\ R86D}$, whereas serum incubated with PE^{WT}-containing beads had a comparatively faster disappearance of C9 (Fig. 10F). These results directly suggested the involvement of K85 and R86 during Vn interaction.

Discussion

Vitronectin plays a crucial role in many biological systems including cell migration, adhesion, repair angiogenesis (Singh *et al.,* 2010a) and microbial pathogenesis (Leroy-Dudal *et al*., 2004; Attia *et al*., 2006; Hallström *et al*., 2006; Bergmann *et al*., 2009; Hallström and Riesbeck, 2010; Singh *et al.,* 2010a). It has a multi-domain structural arrangement, where the N-terminal SMB domain is well characterized for its role in several biological processes. The C-terminal HBD-1 (amino acids 175–219), HBD-2 (amino acids 175–219) and HBD-3 (amino acids 348–361) are known to bind to bacterial pathogens (Singh *et al.,* 2010a). Being one of the major regulators of the complement system, Vn has a crucial impact on MAC deposition on the membrane of Gram-negative respiratory pathogens that successfully exploit the MAC-inhibitory role of Vn (Hallström *et al*., 2009; Singh *et al.,* 2010a). On the other hand, Gram-positive bacteria have been shown to use the Vn–integrin interaction for cellular invasion and internalization (Bergmann *et al*., 2009).

Recently we reported that the $PE^{84–108}$ domain is completely conserved in all *Haemophilus* spp. including 186 NTHi clinical isolates, Hib and other *Haemophilus* spp. The conserved property of PE among NTHi makes this protein valuable as a future vaccine candidate (Singh *et al*., 2010b). PE interacts with Vn at a $K_D = 4 \times 10^{-7}$ M and protects NTHi from serum-mediated lysis. Vn bound to PE at the NTHi surface has a functional capacity to inhibit the MAC assembly, and this observation supports the involvement of a PE–Vn interaction in NTHi-dependent serum resistance. Furthermore, a peptide mapping analysis indicated that $PE^{84–108}$ is the active Vn binding region (Hallström *et al*., 2009). In the present article, we focused on the properties of PE involved in binding to Vn. The $PE^{84–108}$ region was studied in detail by using a site-directed mutagenesis approach. Interestingly, the $PE^{84–108}$ region harbours K85 and R86, which are significantly involved in the function of PE. Mutation of K85 to the opposite charged side-chain E85, and R86 to D86 resulted in loss of PE binding to Vn. The mutated PE variants were also verified for any defective protein folding and tertiary structures by using CD spectroscopy, where PE^{WT}, PE^{K85E}, PE^{R86D} and $PE^{K85,\ R86D}$ showed similar helix and beta-sheet patterns (Fig. 1E).

Previously it has been demonstrated that Vn binds to *Streptococcus pneumoniae* and contributes to bacterial internalization. This interaction can be efficiently blocked in the presence of heparin, indicating that the HBD(s) of Vn are involved in this interaction. Moreover, addition of Vn to epithelial cells significantly increases the adhesion of *S. pneumoniae* (Bergmann *et al*., 2009). Another pathogenic organism, *Pseudomonas aeruginosa*, has a potential binding capacity with Vn and binding of Vn with αvβ5 plays a key role in *P. aeruginosa* internalization by A549 cells (Leroy-Dudal *et al*., 2004; Leduc *et al*., 2007). *H. influenzae* binds Vn by the two outer membrane proteins Hsf and PE, which both contribute serum resistance (Hallström *et al*., 2006; 2009). However, *Haemophilus ducreyi* binds Vn via the trimeric autotransporter DsrA and thus exhibits serum resistance (Leduc *et al*., 2009). Many other research reports suggest that Vn potentially plays important roles in the pathogenesis of *Yersinia pseudotuberculosis* (Gustavsson *et al*., 2002), *Neisseria meningitidis* (Duensing and Putten, 1998; Sa *et al*., 2010) and *Candida albicans* (Limper and Standing, 1994). In light of the important role of Vn in microbial pathogenesis, there is not much data published that in detail characterize the interaction between Vn and its microbial ligands. The lack of structural data on the HBD(s) of Vn also limits the clear views about the Vn–bacterial interactions. In this study, Vn 353–363 amino acids region was identified as the major PE binding region. We designed a peptide library for the sequence Vn 312–396 and analysed for PE binding, but were not successful in defining the binding site (data not shown). Thus, there might be a secondary structure within the Vn 353–363 region that is involved in the interaction with PE that could not be mimicked by short synthetic peptides. Previously, it has been reported by us that heparin binding region (HBD-3) comprising Vn amino acids 341–368 might have an interaction with the PE molecule (Hallström *et al*., 2009). These data are in agreement with our previous findings indicating that Vn 353–363 are involved in binding to PE. The detailed alignment of Vn 320–396 has been published by us (Singh *et al*., 2010c) and reveals that the 353–363 amino acid region of Vn is variable among different mammalian species. This variation might be responsible for selective binding of Vn to pathogens, as reported recently with *S. pneumoniae*. Interestingly, mouse Vn binds several-fold less efficiently in comparison with human Vn (Bergmann *et al*., 2009).

Recently we reported that Vn plays a significant role in the survival of NTHi. The Vn-depleted serum decreases

the survival, whereas, addition of Vn restores serum resistance capacity (Hallström *et al*., 2009). *M. catarrhalis* also showed similar Vn-dependent serum survival, whereas Vn-depleted serum kills bacteria faster than NHS and addition of Vn restores serum resistance. UspA2 was found as the major Vn-binding protein of *M. catarrhalis* and UspA2-deficient mutants were highly sensitive to NHS (Attia *et al*., 2005; 2006). Based upon those earlier findings, we recently examined the UspA2–Vn interaction in detail. Interestingly, UspA2-treated human serum more efficiently killed bacteria as compared with control serum, and this was directly linked to quenching of Vn (Singh *et al*., 2010c). In parallel to *Moraxella* UspA2, our results on *Haemophilus* PE in the present study suggested that the enhanced killing of *H. influenzae* when NHS was pre-incubated with PE^{WT} as well with the single mutated variants PE^{K85E} or PE^{R86D} was due to the interaction and consequently quenching of the biological activity of Vn.

Previously we have shown that NTHi 3655Δ*pe* is serum-sensitive and that the Vn-binding capacity significantly decreased in these PE-deficient mutants. The Vn depleted serum killed NTHi 3655 more efficiently in comparison with NHS and addition of Vn restored serum resistance of NTHi 3655 (Hallström *et al*., 2009). In support of that study we showed in the present study that MAC deposition is significantly higher in NTHi 3655Δ*pe* mutants in comparison with wild-type counterparts (Fig. 9A–E). Thus, the decrease in Vn binding to NTHi 3655Δ*pe* is responsible for a considerably higher deposition of MAC.

In conclusion, this study suggests that the role of *H. influenzae* PE is important for Vn binding and consequently serum resistance. Lysine 85 and arginine 86 are located within the active binding region $PE^{84–108}$ and are necessary for the Vn interaction. However, it is not completely evident that PE interacts with Vn by only K85 and R86. A future ultrastructure of the PE–Vn complex may prove details on the interaction. A detailed analysis of the Vn molecule and characterization of the precise amino acids that are responsible for the interaction with PE also remains to be done.

Experimental procedures

Bacterial strains, reagents and cell culture

The NTHi 3655 and an isogenic mutant (NTHi 3655Δ*pe*) were grown in brain heart infusion (BHI) liquid broth, supplemented with 10 μg ml^{-1} nicotinamide adenine dinucleotide (NAD) and haemin, or streaked on chocolate agar plates and incubated at 37°C in a humid atmosphere with 5% CO_2. The NTHi 3655Δ*pe* mutant was grown in the presence of 20 μg ml^{-1} kanamycin (Ronander *et al*., 2009). *E. coli* BL21 (DE3) and DH5α were cultured in Luria–Bertani (LB) broth or on LB agar plates at 37°C in a humid atmosphere containing 5% CO_2. The vectors pET26b*pe* and pET16b*pe* were as described (Hallström *et al*., 2009). pET26b*pe* and variants were supplemented with 50 μg ml^{-1} kanamycin and pET16b*pe* and variants were supplemented with 100 μg ml^{-1} ampicillin in LB medium. Human embryo kidney (HEK293T) cells were grown in advanced DMEM (Gibco; Invitrogen, Stockholm, Sweden) with 2 mM L-glutamine, 100 μg ml^{-1} streptomycin and 100 U ml^{-1} penicillin.

Recombinant DNA techniques and site-directed mutagenesis

The construct pET26b*pe* as described in Hallström *et al*. (2009) was used for expression and mutation of PE. The nucleotide region (250–324) of the *pe* gene (CGSHi3655_04936) encodes for $PE^{84–108}$ and was manipulated at several amino acids by using a site-directed mutagenesis approach. The QuikChange site-directed mutagenesis was performed using high fidelity *PfuTurbo*® DNA polymerase (Stratagene, La Jolla, CA). The primers used for mutagenesis are listed in Table 1. The mutagenesis procedure including PCR and DpnI digestion was performed as described previously (Singh and Röhm, 2008). Mutant vectors were sequenced and finally transformed into *E. coli* BL21 (DE3) cells. The *E. coli* cells containing pET26b*pe* and variants were used for expression and purification, while *E. coli* containing pET16b*pe* was used for surface expression of PE (Ronander *et al*., 2009). Truncated Moraxella IgD-binding protein ($MID^{962–1200}$) was prepared as described (Nordström *et al*., 2006).

Recombinant protein expression and purification

The *E. coli* BL21 (DE3) containing recombinant pET26b vectors were grown in 500 ml of LB medium with kanamycin at 37°C until OD_{600} to 0.8–1. Expression was induced by 1 mM IPTG and cultivation continued for another 3 h at 37°C. The cells were harvested at 5000 *g* for 15 min at 4°C. The periplasmic fraction was separated according to a protocol described in Singh and Röhm (2008). Purified proteins were dialysed by several exchanges of HNET buffer (50 mM HEPES, pH 7.5, 150 mM NaCl, 3 mM EDTA and 0.005% Tween-20) for Biacore assay and concentrated by using Centricon cartridge (3 kDa molecular weight cut-off; Millipore, Bedford, MA). Protein concentrations were measured by UV absorbance using a Nano-drop spectrophotometer (Thermo Scientific, Wilmington, DE) in addition to verification by a Bicinchoninic acid (BCA) assay (Pierce, Rockford, IL). The purity and concentrations of expressed proteins was verified on SDS-PAGE stained with Coomassie blue R250.

Expression of Vn fragments in HEK293 cell lines and purification

Vitronectin domains harbouring heparin binding sites have been expressed in HEK293T cells as Vn amino acids 80–396, 80–320 and 80–229 as described in Singh *et al*. (2010c). Furthermore, new constructs corresponding to amino acids 80–379, 80–373, 80–363, 80–353, 80–339 and

Table 1. Primers used in site-directed mutagenesis of PE amino acids 84-108.

Primer name	Sequence 5′–3′	PE variants
K85E _For	GTTTATCCTGAGCCTGAACGTTATGCACGTTC	K85E
R86D _For	GTTTATCCTGAGCCTAAAGATTATGCACGTTCTGTTCG	R86D
Y87F _For	CCTGAGCCTAAACGTTTTGCACGTTCTGTTCGTC	Y87F
R89A_For	GAGCCTAAACGTTATGCAGCTTCTGTTCGTCAGTATAAG	R89A
R92A_For	GCACGTTCTGTTGCTCAGTATAAGATTTTGAATTGTGC	R92A
Y94F_For	GCACGTTCTGTTCGTCAGTTTAAGATTTTGAATTGTGC	Y94F
K95E_For	GTTCTGTTCGTCAGTATGAGATTTTGAATTGTGC	K95E
N98A_For	TCTGTTCGTCAGTATAAGATTTTGGCTTGTGCAAATTATCATTTAACTC	N98A
N101A _For	GTATAAGATTTTGAATTGTGCAGCTTATCATTTAACTCAAATACGAACTG	N101A
Y102A_For	GTATAAGATTTTGAATTGTGCAAATGCTCATTTAACTCAAATACGAACTG	Y102A
H103A_For	ATAAGATTTTGAATTGTGCAAATTATGCTTTAACTCAAATACGAACTGAT	H103A
Q106A_For	GAATTGTGCAAATTATCATTTAACTGCAATACGAACTGATTTCTATGATG	Q106A
R108A_For	GCAAATTATCATTTAACTCAAATAGCAACTGATTTCTATGATGAATTTTG	R108A
Mut 2_For	GTTTATCCTGAGCCTGAAGATTATGCACGTTC	K85E, R86D (mut 2)
Mut 3_For	GAGCCTGAAGATTATGCAGCTTCTGTTCGTCAGTATAAG	K85E, R86D, R89A (mut 3)
Mut 4_For	GCAGATTCTGTTGCTCAGTATAAGATTTTGAATTGTGC	K85E, R86D, R89A, R92A (mut 4)
Mut 5_For	ATTCTGTTGATCAGTATGAGATTTTGAATTGTGC	K85E, R86D, R89A, R92A, K95E (mut 5)

The mutated bases are underlined in all primers. The forward primer for each mutation is shown here, while reverse primer of same sequence was also used.

80–330, all containing C-terminal 6x-His tags (Fig. 4A) were amplified by using Vn 80–396 as template. The forward primer was inserted with BshT1 (AgeI) and the reverse primer with Acc65I (KpnI) restriction enzyme sites. Amplified and digested inserts were ligated into the pHLsec vector (28). Protein expression and purification was performed as described elsewhere (Singh *et al.*, 2010c).

Circular dichroism (CD)

Purified PE variants and Vn fragments were dialysed against 20 mM phosphate buffer and the concentrations were measured by using Nano-drop at (280 nm) and BCA method (Pierce, Rockford, IL). Finally, 5.0 μM proteins were transferred to a cuvette and CD spectrum was recorded between the wavelengths of 190 nm to 250 nm by using a CD spectropolarimeter J815 (Jasco, Essex, UK).

SDS-PAGE and non-reducing PAGE

Routine SDS-PAGE was performed according to standard laboratory protocols. In gradient separations NuPAGE Gradient 4–12% Bis-tris readymade gels were used (Invitrogen, Carlsbad, CA) and separation was performed according to protocol suggested by the manual. In non-reducing conditions protein samples were loaded with SDS-PAGE loading dye without β-mercaptoethanol.

Flow cytometry (FACS)

E. coli cells were grown in LB medium containing appropriate antibiotics and induced by 1 mM IPTG for 1 h at 37°C. Bacteria (10^8) were resuspended in 100 μl of PBS containing 2.5% BSA and treated with affinity-purified rabbit polyclonal anti-PE antibodies for 1 h at room temperature. After one washing with PBS-BSA, FITC-conjugated anti-rabbit antibodies (Dakopatts) were added (diluted according to the manufacturer's instructions) and incubated for 1 h at room temperature. Additionally three washes performed with PBS containing 2.5% BSA and finally cells were resuspended in 100 μl of PBS containing 2.5% BSA. *E. coli* harbouring empty vector was used as a control and treated similarly. Samples were analysed in a flow cytometer (EPICS XL_MCL; Beckman Coulter).

Immobilization of PE on CNBr-activated agarose beads

Cyanogen bromide-activated Sepharose™ 4 Fast Flow (GE Healthcare Biosciences, Uppsala, Sweden) was used for immobilization of PE variants. Sepharose powder (330 mg ml^{-1}) was washed several times in 1 mM HCl and resuspended in coupling buffer (0.1 M $NaHCO_3$, pH 8.3 containing 0.5 M NaCl). Protein solutions were also dialysed against coupling buffer and added to the resin (5–10 mg protein ml^{-1} of resin) and incubated overnight at 4°C in a rolling shaker. Unbound ligands were washed with 5 gel volume of coupling buffer and free groups were blocked by blocking buffer (0.1 M Tris-HCl, pH 8.0) for 2 h at room temperature. Beads were then washed three times by alternating buffers, NaAc, pH 4.0 containing 500 mM NaCl and 0.1 M Tris-HCl, pH 8.0 containing 500 mM NaCl. Finally beads were washed with PBS and stored at 4°C. The protein ligands immobilized were measured by Nano-Drop and BCA methods.

ELISA

Purified PE variants were coated on PolySorp microtitre plates (Nunc-Immuno, Roskilde, Denmark). Coating of PE (0.1 μM) was performed in 100 mM Tris-HCl, pH 9.0 for 15 h at 4°C. Plates were washed three times with PBS to remove excess unbound protein and blocked with PBS-2.5% BSA for 1 h at 25°C. The Vn was added to the wells in PBS-2.5% BSA and incubated for 1 h at 25°C. In competitive ELISA, increasing concentration of competitor ligand was added to the binding reactions and allowed to bind for 1 h at room

temperature. The unbound Vn fraction was removed by washing with PBS containing 0.05% Tween-20, and bound Vn was detected by polyclonal sheep anti-human Vn antibodies (pAb) (AbD Serotec, Kidlington, Oxford, UK) and secondary horseradish peroxidase (HRP)-conjugated donkey anti-sheep pAb (AbD Serotec). After four additional washing steps, plates were developed and read at 450 nm in a microplate reader (Multiskan® plus, Labsystems, Helsinki, Finland).

Surface plasmon resonance (Biacore)

The interaction between PE variants and Vn was analysed using surface plasmon resonance (Biacore 2000, Uppsala, Sweden). Four flow cells of a CM5 sensor chip were activated, each with 20 μl of a mixture of 0.2 M 1-ethyl-3-(3-dimethylaminopropyl) carbodiimide and 0.05 M *N*-hydroxysulphosuccinimide at a flow rate of 10 μl min^{-1}, after which Vn (10 μl ml^{-1} in 10 mM sodium acetate buffer, pH 4.0) was injected over flow cell 2 to reach 4000 resonance units (RU). Unreacted groups were blocked with 20 μl of 1 M ethanolamine (pH 8.5). A negative control was prepared by activating and subsequently blocking the surface of flow cell 1. The comparative association kinetics were studied for various concentrations of the PE variants. The flow buffer (50 mM HEPES, pH 7.5 containing 150 mM NaCl, 3 mM EDTA and 0.005% Tween-20) was used for binding. Protein solutions were injected for 600 s during the association phase at a constant flow rate of 30 μl min^{-1}. The sample was first injected over the negative control surface and then over immobilized Vn. The signal from the control surface was subtracted. The dissociation was followed for 200 s at the same flow rate. In all experiments, 30 μl of 2 M NaCl was used to remove bound ligands during a regeneration step. BiaEvaluation 3.0 software (Biacore) was used for data analysis and SigmaPlot 8.0 to generate final figures.

[^{125}I] labelling of Vn fragments and binding assay

The labelling of Vn was performed by the Chloramine-T method (25). For labelling, 0.05 M [^{125}I] isotope (Amersham Biosciences, Buckinghamshire, UK) was used per mole of protein. The labelled proteins were purified from unincorporated [^{125}I] using PD10 columns (GE Healthcare Biosciences, Uppsala, Sweden).

NTHi and mutants were grown in BHI medium to OD_{A600} = 1.0 and washed with PBS-2.5% BSA. Approximately, 10^8 bacterial cells per well were added to microtitre plates and increasing concentrations of [^{125}I]–Vn were added. For competition experiments, cold ligands were added to the binding reactions. Bacteria were incubated for 30 min at 37°C and were pelleted at 4200 *g* for 10 min, followed by two washing steps of PBS-2.5% BSA. The unbound radiolabelled protein was removed by three washes with PBS, harvested in a 96-well plate harvester (Tomtec, Hamden, CT), and finally counted in a liquid scintillation counter (Trilux, Microbeta 1450, Perkin Elmer).

In the radioactive ligand direct binding assay, PE (0.1 μM) was coated on ELISA strip plate (MaxiSorp) and washed three times with PBS to remove excess unbound protein and blocked with PBS-2.5% BSA for 1 h at room temperature. [^{125}I]–Vn was added to the wells in PBS-2.5% BSA and incubated for 1 h at 25°C. In the competitive assay, competitor ligands were added to the binding reaction prior to addition of labelled Vn and allowed to bind for 1 h at room temperature. The unbound [^{125}I]–Vn fraction was removed by washing with PBS containing 0.005% Tween-20. Each single well was separated from strip by mechanical breaking and total radioactivity was counted in a scintillation counter.

Serum resistance assay

NTHi 3655 wild type was tested for impact of PE variants in NHS-mediated killing. Approximately, 10^5 cells were resuspended in 100 μl of dextrose-GVB ($DGVB^{++}$) buffer, pH 7.3, containing 140 mM glucose, 0.1% (w/v) gelatin, 1 mM $MgCl_2$, 0.15 mM $CaCl_2$ and finally 10% NHS. Bacteria were incubated at 37°C and samples (10 μl) were collected at different time intervals and plated on chocolate agar plates. The effect of PE variants on serum proteins was analysed by pre-incubating increasing concentrations of PE variants (0.5–5 μM) with 10% serum at room temperature for 1 h and subsequently used in the serum resistance assay. Similarly, the effect of Vn was evaluated by treating bacterial cells with Vn for 1 h at room temperature, prior to addition of NHS. The viable bacterial cells were determined by counting colony-forming units (cfu) after incubation overnight at 37°C.

Transmission electron microscopy (TEM)

Proteins were directly labelled with colloidal gold as described (Roth, 1996). The wild-type *H. influenzae* and mutants were grown in BHI for 3 h at 37°C. Bacterial solutions were incubated with gold-labelled Vn fragments (100 μg ml^{-1}), fixed in PBS containing 4% paraformaldehyde and 0.1% glutaraldehyde and prepared for electron microscopy as described (Carlemalm, 1990). TEM was thereafter performed as described (Bengtson *et al.*, 2008), and specimens were examined in a JEOL JEM 1230 transmission electron microscope (JEOL, Peabody, MA) at 60 kV accelerating voltage. Images were recorded with a Gatan Multiscan 791 CCD camera (Gatan, Pleasanton, CA). Only particles observed within a distance of 15 nm or less adjacent to the cell surface were counted. This corresponds to the established maximum distance between an IgG and its antigen, or between a protein labelled with gold of this size, and its target. Differences between groups concerning Vn–PE interaction, and complement activation were analysed by the one-tailed test for differences between means. The following *a priori* null hypotheses were tested: full-length Vn does not bind to PE (Fig. 3), or full-length Vn binds to PE double point mutation with the same affinity (Fig. 3), or different Vn constructs exhibit the same affinity to PE (Fig. 7), or NTHi 3655 and NTHi Δ*pe* show the same C9 deposition (Fig. 9). The null hypothesis was rejected and statistical significance was assumed when $P \leq 0.05$.

Western blotting and MAC deposition assay

After processing, bacterial cells were boiled with 1× SDS-PAGE (containing β-mercaptoethanol) loading buffer for

10 min at 95°C and centrifuged for 5 min at 20 000 *g*. Supernatants (10–15 μl) were loaded in 12% or 15% SDS-polyacrylamide gels, or 4–12% gradient SDS-polyacrylamide gels (Invitrogen, Carlsbad, CA). The gels were subjected to run at particular current as recommended in standard protocols. Gels were blotted to PVDF membranes. Membranes were blocked with PBS containing 5% milk for 1 h at room temperature. All reactions were performed in PBS containing 5% milk and washing was done with PBS containing 0.05% Tween-20. Vn detection was performed with anti-human Vn antibodies (pAb) (AbD Serotec, Kidlington, Oxford, UK) and HRP-conjugated donkey anti-sheep secondary pAb (AbD Serotec).

Membrane attack complex deposition at the bacterial surface was estimated by C9 polymerization. Usually C9 monomer is a 71 kDa and it polymerizes into 14–16 mer tubules to make a pore at bacterial surface. In NHS C9 exists as a monomer or is associated in an oligomeric form, but when the complement reaction is initiated C9 is polymerized to make the ring closure (cytolytic pore). This C9 oligomer is stable and not dissociated in SDS containing buffer and reducing conditions, thus can be easily detected by SDS-PAGE (Podack and Tschopp, 1982; Deng *et al*., 2007). Bacterial cells (10^8) were taken from chocolate agar plates and resuspended into GVB^{++} buffer followed by addition of 10% NHS and incubation at 37°C. The effect of PE^{WT} and $PE^{K85E,\ R86D}$ was evaluated by addition of 2 μM protein coated beads in 10% NHS and incubation at room temperature for 1 h. This treated serum was analysed for bactericidal activity and compared with non-coated control beads. The complement activity was stopped at indicated time points by cooling in an ice bath. Samples were boiled with SDS loading buffer (containing β-mercaptoethanol) for 10 min at 95°C and centrifuged for 5 min at 20 000 *g*. Supernatants were resolved in 4–12% gradient SDS-PAGE gels and blotted on to PVDF membranes. The detection of C9 was performed by using anti-human C9 pAbs (Complement Technology, Texas) and HRP-conjugated donkey anti-sheep secondary pAb as described above. Blots were finally developed with an ECL Western blotting kit (Pierce, Thermo Scientific, Rockford, IL).

Statistical analysis

Statistical analysis was performed by using Student's *t*-test for paired or unpaired data in SigmaPlot 8.0. ANOVA (one-way/two-way) analysis was performed by GraphPad Prism 5 (GraphPad Software, San Diego, CA). *P*-values ≤ 0.05 were considered statistically significant. *P*-values are presented as $^*P \leq 0.05$, $^{**}P \leq 0.01$, $^{***}P \leq 0.001$ and n.s., not significant.

Acknowledgements

This work was supported by grants from the Alfred Österlund, the Anna and Edwin Berger, the Marianne and Marcus Wallenberg, Knut and Alice Wallenberg, Inga-Britt and Arne Lundberg, the Söderberg, and the Greta and Johan Kock Foundations, the Swedish Medical Research Council, the Swedish Foundation for Strategic Research, the Cancer Foundation at the University Hospital in Malmö, and Skane county council's research and development foundation.

References

Arroyo De Prada, N., Schroeck, F., Sinner, E.K., Muehlenweg, B., Twellmeyer, J., Sperl, S., *et al*. (2002) Interaction of plasminogen activator inhibitor type-1 (PAI-1) with vitronectin. *Eur J Biochem* **269:** 184–192.

Attia, A.S., Lafontaine, E.R., Latimer, J.L., Aebi, C., Syrogiannopoulos, G.A., and Hansen, E.J. (2005) The UspA2 protein of *Moraxella catarrhalis* is directly involved in the expression of serum resistance. *Infect Immun* **73:** 2400–2410.

Attia, A.S., Ram, S., Rice, P.A., and Hansen, E.J. (2006) Binding of vitronectin by the *Moraxella catarrhalis* UspA2 protein interferes with late stages of the complement cascade. *Infect Immun* **74:** 1597–1611.

Bengtson, S.H., Eddleston, J., Morgelin, M., Zuraw, B.L., and Herwald, H. (2008) Regulation of kinin B(2) receptors by bradykinin in human lung cells. *Biol Chem* **389:** 1435–1440.

Bergmann, S., Lang, A., Rohde, M., Agarwal, V., Rennemeier, C., Grashoff, C., *et al*. (2009) Integrin-linked kinase is required for vitronectin-mediated internalization of *Streptococcus pneumoniae* by host cells. *J Cell Sci* **122:** 256–267.

Blom, A.M., Hallström, T., and Riesbeck, K. (2009) Complement evasion strategies of pathogens-acquisition of inhibitors and beyond. *Mol Immunol* **46:** 2808–2817.

Bresser, P., Virkola, R., Jonsson-Vihanne, M., Jansen, H.M., Korhonen, T.K., and van Alphen, L. (2000) Interaction of clinical isolates of nonencapsulated *Haemophilus influenzae* with mammalian extracellular matrix proteins. *FEMS Immunol Med Microbiol* **28:** 129–132.

Carlemalm, E. (1990) Lowicryl resins in microbiology. *J Struct Biol* **104:** 189–191.

Dawid, S., Barenkamp, S.J., and St Geme, J.W., 3rd (1999) Variation in expression of the *Haemophilus influenzae* HMW adhesins: a prokaryotic system reminiscent of eukaryotes. *Proc Natl Acad Sci USA* **96:** 1077–1082.

Deng, J., Gold, D., LoVerde, P.T., and Fishelson, Z. (2007) Mapping of the complement C9 binding domain in paramyosin of the blood fluke *Schistosoma mansoni*. *Int J Parasitol* **37:** 67–75.

Duensing, T.D., and Putten, J.P. (1998) Vitronectin binds to the gonococcal adhesin OpaA through a glycosaminoglycan molecular bridge. *Biochem J* **334** (Part 1)**:** 133–139.

Fink, D.L., and St Geme, J.W., 3rd (2003) Chromosomal expression of the *Haemophilus influenzae* Hap autotransporter allows fine-tuned regulation of adhesive potential via inhibition of intermolecular autoproteolysis. *J Bacteriol* **185:** 1608–1615.

Fink, D.L., Green, B.A., and St Geme, J.W., 3rd (2002) The *Haemophilus influenzae* Hap autotransporter binds to fibronectin, laminin, and collagen IV. *Infect Immun* **70:** 4902–4907.

Forsgren, A., Riesbeck, K., and Janson, H. (2008) Protein D of *Haemophilus influenzae*: a protective nontypeable *H. influenzae* antigen and a carrier for pneumococcal conjugate vaccines. *Clin Infect Dis* **46:** 726–731.

Gilsdorf, J.R., Chang, H.Y., McCrea, K.W., Forney, L.J., and Marrs, C.F. (1992) Comparison of hemagglutinating pili of type b and nontypeable *Haemophilus influenzae*. *J Infect Dis* **165** (Suppl. 1)**:** S105–S106.

Giufre, M., Carattoli, A., Cardines, R., Mastrantonio, P., and Cerquetti, M. (2008) Variation in expression of HMW1 and HMW2 adhesins in invasive nontypeable *Haemophilus influenzae* isolates. *BMC Microbiol* **8:** 83.

Gross, J., Grass, S., Davis, A.E., Gilmore-Erdmann, P., Townsend, R.R., and St Geme, J.W., 3rd (2008) The *Haemophilus influenzae* HMW1 adhesin is a glycoprotein with an unusual N-linked carbohydrate modification. *J Biol Chem* **283:** 26010–26015.

Gustavsson, A., Armulik, A., Brakebusch, C., Fassler, R., Johansson, S., and Fallman, M. (2002) Role of the beta1-integrin cytoplasmic tail in mediating invasin-promoted internalization of *Yersinia*. *J Cell Sci* **115:** 2669–2678.

Hallström, T., and Riesbeck, K. (2010) *Haemophilus influenzae* and the complement system. *Trends Microbiol* **18:** 258–265.

Hallström, T., Trajkovska, E., Forsgren, A., and Riesbeck, K. (2006) *Haemophilus influenzae* surface fibrils contribute to serum resistance by interacting with vitronectin. *J Immunol* **177:** 430–436.

Hallström, T., Jarva, H., Riesbeck, K., and Blom, A.M. (2007) Interaction with C4b-binding protein contributes to nontypeable *Haemophilus influenzae* serum resistance. *J Immunol* **178:** 6359–6366.

Hallström, T., Zipfel, P.F., Blom, A.M., Lauer, N., Forsgren, A., and Riesbeck, K. (2008) *Haemophilus influenzae* interacts with the human complement inhibitor factor H. *J Immunol* **181:** 537–545.

Hallström, T., Blom, A.M., Zipfel, P.F., and Riesbeck, K. (2009) Nontypeable *Haemophilus influenzae* protein E binds vitronectin and is important for serum resistance. *J Immunol* **183:** 2593–2601.

Jurcisek, J.A., Bookwalter, J.E., Baker, B.D., Fernandez, S., Novotny, L.A., Munson, R.S., Jr, and Bakaletz, L.O. (2007) The PilA protein of non-typeable *Haemophilus influenzae* plays a role in biofilm formation, adherence to epithelial cells and colonization of the mammalian upper respiratory tract. *Mol Microbiol* **65:** 1288–1299.

Leduc, D., Beaufort, N., de Bentzmann, S., Rousselle, J.C., Namane, A., Chignard, M., and Pidard, D. (2007) The *Pseudomonas aeruginosa* LasB metalloproteinase regulates the human urokinase-type plasminogen activator receptor through domain-specific endoproteolysis. *Infect Immun* **75:** 3848–3858.

Leduc, I., Olsen, B., and Elkins, C. (2009) Localization of the domains of the *Haemophilus ducreyi* trimeric autotransporter DsrA involved in serum resistance and binding to the extracellular matrix proteins fibronectin and vitronectin. *Infect Immun* **77:** 657–666.

Leroy-Dudal, J., Gagniere, H., Cossard, E., Carreiras, F., and Di Martino, P. (2004) Role of alphavbeta5 integrins and vitronectin in *Pseudomonas aeruginosa* PAK interaction with A549 respiratory cells. *Microbes Infect* **6:** 875–881.

Limper, A.H., and Standing, J.E. (1994) Vitronectin interacts with *Candida albicans* and augments organism attachment to the NR8383 macrophage cell line. *Immunol Lett* **42:** 139–144.

Look, D.C., Chin, C.L., Manzel, L.J., Lehman, E.E., Humlicek, A.L., Shi, L., *et al.* (2006) Modulation of airway inflammation by *Haemophilus influenzae* isolates associated with chronic obstructive pulmonary disease exacerbation. *Proc Am Thorac Soc* **3:** 482–483.

Meats, E., Feil, E.J., Stringer, S., Cody, A.J., Goldstein, R., Kroll, J.S., *et al.* (2003) Characterization of encapsulated and noncapsulated *Haemophilus influenzae* and determination of phylogenetic relationships by multilocus sequence typing. *J Clin Microbiol* **41:** 1623–1636.

Murphy, T.F. (2003) Respiratory infections caused by nontypeable *Haemophilus influenzae*. *Curr Opin Infect Dis* **16:** 129–134.

Murphy, T.F. (2009) Current and future prospects for a vaccine for nontypeable *Haemophilus influenzae*. *Curr Infect Dis Rep* **11:** 177–182.

Nordström, T., Jendholm, J., Samuelsson, M., Forsgren, A., and Riesbeck, K. (2006) The IgD-binding domain of the *Moraxella* IgD-binding protein MID (MID962–1200) activates human B cells in the presence of T cell cytokines. *J Leukoc Biol* **79:** 319–329.

Podack, E.R., and Tschopp, J. (1982) Circular polymerization of the ninth component of complement. Ring closure of the tubular complex confers resistance to detergent dissociation and to proteolytic degradation. *J Biol Chem* **257:** 15204–15212.

Poolman, J.T., Bakaletz, L., Cripps, A., Denoel, P.A., Forsgren, A., Kyd, J., and Lobet, Y. (2000) Developing a nontypeable *Haemophilus influenzae* (NTHi) vaccine. *Vaccine* **19** (Suppl. 1)**:** S108–S115.

Ronander, E., Brant, M., Janson, H., Sheldon, J., Forsgren, A., and Riesbeck, K. (2008) Identification of a novel *Haemophilus influenzae* protein important for adhesion to epithelial cells. *Microbes Infect* **10:** 87–96.

Ronander, E., Brant, M., Eriksson, E., Morgelin, M., Hallgren, O., Westergren-Thorsson, G., *et al.* (2009) Nontypeable *Haemophilus influenzae* adhesin protein E: characterization and biological activity. *J Infect Dis* **199:** 522–531.

Roth, J. (1996) The silver anniversary of gold: 25 years of the colloidal gold marker system for immunocytochemistry and histochemistry. *Histochem Cell Biol* **106:** 1–8.

Sa, E.C.C., Griffiths, N.J., and Virji, M. (2010) *Neisseria meningitidis* Opc invasin binds to the sulphated tyrosines of activated vitronectin to attach to and invade human brain endothelial cells. *PLoS Pathog* **6:** e1000911.

Schroeck, F., Arroyo de Prada, N., Sperl, S., Schmitt, M., and Viktor, M. (2002) Interaction of plasminogen activator inhibitor type-1 (PAI-1) with vitronectin (Vn): mapping the binding sites on PAI-1 and Vn. *Biol Chem* **383:** 1143–1149.

Sethi, S., Wrona, C., Grant, B.J., and Murphy, T.F. (2004) Strain-specific immune response to *Haemophilus influenzae* in chronic obstructive pulmonary disease. *Am J Respir Crit Care Med* **169:** 448–453.

Sheets, A.J., Grass, S.A., Miller, S.E., and St Geme, J.W., 3rd (2008) Identification of a novel trimeric autotransporter adhesin in the cryptic genospecies of *Haemophilus*. *J Bacteriol* **190:** 4313–4320.

Singh, B., and Röhm, K.H. (2008) A new subfamily of bacterial glutamate/aspartate receptors. *Biol Chem* **389:** 33–36.

Singh, B., Su, Y.C., and Riesbeck, K. (2010a) Vitronectin in bacterial pathogenesis: a host protein used in complement escape and cellular invasion. *Mol Microbiol* **78:** 545–560.

Singh, B., Brant, M., Kilian, M., Hallström, B., and Riesbeck, K. (2010b) Protein E of *Haemophilus influenzae* is a ubiquitous highly conserved adhesin. *J Infect Dis* **201:** 414–419.

Singh, B., Blom, A.M., Unal, C., Nilson, B., Morgelin, M., and Riesbeck, K. (2010c) Vitronectin binds to the head region of *Moraxella catarrhalis* ubiquitous surface protein A2 and confers complement-inhibitory activity. *Mol Microbiol* **75:** 1426–1444.

Watt, J.P., Wolfson, L.J., O'Brien, K.L., Henkle, E., Deloria-Knoll, M., McCall, N., *et al.* (2009) Burden of disease caused by *Haemophilus influenzae* type b in children younger than 5 years: global estimates. *Lancet* **374:** 903–911.

Winter, L.E., and Barenkamp, S.J. (2009) Antibodies specific for the Hia adhesion proteins of nontypeable *Haemophilus influenzae* mediate opsonophagocytic activity. *Clin Vaccine Immunol* **16:** 1040–1046.

II

Molecular Microbiology (2013) 87(6), 1245–1266 ■
doi:10.1111/mmi.12164
First published online 26 February 2013

Haemophilus influenzae acquires vitronectin via the ubiquitous Protein F to subvert host innate immunity

Yu-Ching Su,[1] Farshid Jalalvand,[1] Matthias Mörgelin,[2] Anna M. Blom,[3] Birendra Singh[1] and Kristian Riesbeck[1]*

[1]*Medical Microbiology, Department of Laboratory Medicine Malmö, Lund University, Skåne University Hospital, SE-205 02 Malmö, Sweden.*
[2]*Section of Clinical and Experimental Infectious Medicine, Department of Clinical Sciences, Lund University, SE-221 84 Lund, Sweden.*
[3]*Medical Protein Chemistry, The Wallenberg Laboratory, Department of Laboratory Medicine Malmö, Lund University, Skåne University Hospital, SE-205 02 Malmö, Sweden.*

Summary

Acquisition of the complement inhibitor vitronectin (Vn) is important for the respiratory tract pathogen nontypeable *Haemophilus influenzae* (NTHi) to escape complement-mediated killing. NTHi actively recruits Vn, and we previously showed that this interaction involves Protein E (PE). Here we describe a second Vn-binding protein, a 30 kDa *Yersinia* YfeA homologue designated as Protein F (PF). An isogenic NTHi 3655Δ*hpf* mutant devoid of PF displayed a reduced binding of Vn, and was consequently more sensitive to killing by human serum compared with the wild type. Surface expression of PF on *Escherichia coli* conferred binding of Vn that resulted in a serum resistant phenotype. Molecular analyses revealed that the N-terminal of PF (Lys23-Glu48) bound to the C-terminal of Vn (Phe352-Ser374) without disrupting the inhibitory role of Vn on the membrane attack complex. The PF–Vn complex actively delayed C9 deposition on PF-expressing bacteria. Comparative studies of binding affinity and multiple mutants demonstrated that both PE and PF contribute individually to NTHi serum survival. PF was highly conserved and ubiquitously expressed in a series of randomly selected NTHi clinical isolates ($n = 18$). In conclusion, the multifaceted binding of Vn is beneficial for NTHi survival in serum and may contribute to successful colonization and consequently infection.

Accepted 22 January, 2013. *For correspondence. E-mail kristian.riesbeck@med.lu.se; Tel. (+46) 40 338494; Fax (+46) 40 336234.

Introduction

Nontypeable *Haemophilus influenzae* (NTHi) is a Gram-negative human-specific bacterium that is predominantly found as an upper respiratory tract commensal in up to 80% of healthy children (Foxwell *et al.*, 1998). NTHi is occasionally pathogenic and causes conjunctivitis, acute otitis media, sinusitis, and pneumonia. The species is also the leading cause of exacerbations in patients that suffer from chronic obstructive pulmonary disease (COPD) (Thanavala and Lugade, 2011). Furthermore, an increased incidence of invasive disease caused by NTHi has lately been observed (Resman *et al.*, 2011).

Colonization of healthy individuals with NTHi is restricted by the host immune system including the complement system (Zwahlen *et al.*, 1983; Toews *et al.*, 1985). The complement cascade is part of the innate immunity and serves as the first line of defence. It consists of more than 30 distinct plasma and cell bound proteins that form three major pathways: the classical, alternative and lectin pathway (Ricklin *et al.*, 2010). Activation of any pathway results in the formation of the membrane attack complex (MAC) consisting of C5b, C6, C7, C8 and C9, which form a pore in the cell membrane leading to cell lysis. Complement activation also results in an inflammatory process including opsonization, increased phagocytosis and recruitment of leucocytes.

Complement is involved in the mucosal immunity of the nasopharynx, the primary site of NTHi colonization. Activation of complement in the nasal mucosa has been implicated in the inflammatory and immunological processes of several respiratory tract diseases including allergic rhinitis, asthma, nasal polyposis, otitis media and COPD (Stenfors and Raisanen, 1992; Narkio-Makela *et al.*, 1999; Mezei *et al.*, 2001; Marc *et al.*, 2004; Van Zele *et al.*, 2009). Airway inflammation may induce increased mucosal permeability and leads to increased plasma exudation of complement proteins and antibodies into the airway (Stenfors and Raisanen, 1992; Narkio-Makela *et al.*, 1999; Mezei *et al.*, 2001). The role of plasma exudation as the first line of defence against infection and injuries in the respiratory mucosa has been extensively reviewed (Persson *et al.*, 1998). Importantly, airway infection with NTHi has been shown to result in secretion of the pro-inflammatory cytokines interleukin (IL)-6, IL-8 and TNF-α

leading to inflammation (Clemans *et al.*, 2000; Sharpe *et al.*, 2011). Moreover, NTHi-specific IgG exudate in the nasal fluid of infected animals effectively limited bacterial load in the nasopharynx (Zola *et al.*, 2009).

The complement system is tightly regulated to prevent self-damage from excessive activation. It is governed by inhibitors including C4b-binding protein (C4BP) in the classical/lectin pathways (Blom *et al.*, 2004), and factor H (FH) in addition to factor H-like protein 1 in the alternative pathway (Ferreira *et al.*, 2010). Clusterin and vitronectin (Vn) inhibit the formation of MAC in the terminal pathway (Morgan, 1999). Importantly, some of these inhibitors are also involved in the prevention of complement-dependent self-lysis at mucosal sites (Narkio-Makela *et al.*, 2001).

NTHi is generally susceptible to complement-mediated killing, which predominantly involves the C-reactive protein- and antibody-dependent classical pathway, although a minor role for the alternative pathway has also been reported (Weiser *et al.*, 1998; Williams *et al.*, 2001; Figueira *et al.*, 2007). Several studies, however, show that most of the nasal mucosa and invasive NTHi isolates are capable of surviving in 5–40% normal human serum (NHS) (Williams *et al.*, 2001; Figueira *et al.*, 2007; Hallström *et al.*, 2010). Serum resistance of *H. influenzae* is multifactorial and orchestrated by phase variation in lipooligosaccharides (LOS) (Williams *et al.*, 2001; Figueira *et al.*, 2007; Ho *et al.*, 2007; Nakamura *et al.*, 2011; Clark *et al.*, 2012; Langereis *et al.*, 2012) as well as through polymicrobial interactions that delay deposition of the complement components C3 and C4 (Tan *et al.*, 2007). Acquisition of human complement inhibitors including plasminogen, C4BP, FH and Vn has recently also been reported for *H. influenzae* (Hallström *et al.*, 2006; 2007; 2008; 2009; Barthel *et al.*, 2012). NTHi surface adhesin Protein E (PE) and *Haemophilus* surface fibrils (Hsf) of serotype b (Hib) have been defined as Vn-binding proteins (Hallström *et al.*, 2006; 2009).

Vn is a multifunctional glycoprotein present in the extracellular matrix (ECM), human plasma and in complex with epithelial cell integrins (Schvartz *et al.*, 1999; Singh *et al.*, 2010a). In human plasma, Vn is in a native monomeric (folded) conformation and multimerizes to its active (unfolded) form in serum (Stockmann *et al.*, 1993). Vn inhibits the formation of cytolytic MAC by occupying the metastable membrane binding site of C5b-7 complex and hinders the insertion of the complex into the cell membrane, and thus prevents the completion of the lytic pore complex C5b-9. In addition, formation of soluble C5b-7 with Vn causes the complex to bind C8 and C9 and form soluble C5b-9, which is haemolytically inactive (Podack *et al.*, 1984; Milis *et al.*, 1993; Sheehan *et al.*, 1995). Furthermore, selective masking of C5b and C8 by Vn has been proposed to interfere with the polymerization of C9 (Su, 1996). Activated (unfolded) Vn inhibits MAC and does not bind to C5b-7 (Hogasen *et al.*, 1992). Intriguingly, the bacterial Vn binding usually does not interfere with the Vn domain involved in inhibition of the MAC (Hallström *et al.*, 2009; Sa *et al.*, 2010).

We previously observed that the reduced Vn-binding capacity of an NTHi mutant devoid of PE was gradually increased when bacteria were incubated with high concentrations of Vn. This observation suggested an additional NTHi Vn-binding factor (Hallström *et al.*, 2009). The goal of the present study was to define the total Vn-binding proteome using NTHi outer membrane vesicles (OMV). An additional outer membrane protein (OMP) was found to be important for NTHi-dependent Vn acquisition, and this newly identified Vn-binding protein we designated as *Haemophilus* Protein F (PF). In parallel with PE, PF promoted Vn-dependent bacterial adhesion and resistance against complement-mediated killing. The PF–Vn complex was active in delaying MAC formation on the bacterial surface. Importantly, PF was highly conserved and detected in all clinical NTHi isolates analysed.

Results

Nontypeable H. influenzae *expresses multiple vitronectin-binding proteins*

We have previously shown that NTHi binds Vn through PE (Hallström *et al.*, 2009; Singh *et al.*, 2011). The Vn-binding phenotype was not, however, completely abolished in the isogenic NTHi mutant devoid of PE. Therefore, we hypothesized that NTHi may express alternative Vn-binding OMPs. To identify these putative Vn-binding proteins, OMV fractions of NTHi 3655 were separated by two-dimensional gel electrophoresis (2D-SDS-PAGE) (Fig. 1A) and probed with human Vn in a Far western immunoblotting assay (Fig. 1C). In addition to LOS and DNA, the NTHi OMV contain periplasmic and OMPs (Sharpe *et al.*, 2011). Our OMV proteome profile showed approximately 112 protein spots including the two major OMP P2 and P5. This was in agreement with the established outer membrane proteome of *H. influenzae* (Link *et al.*, 1997). We found protein spots (~ 16 kDa to ~ 30 kDa) that bound Vn at different intensities (Fig. 1C) compared with the negative blot in the absence of Vn (data not shown). Due to the known difficulties of high molecular weight proteins to enter the IPG strips (Link *et al.*, 1997), we also analysed the immunoblots by one-dimensional SDS-PAGE. Only one Vn-reactive protein band was observed (Fig. 1B and D), and was most likely the ~ 30 kDa Vn-binding protein seen in Fig. 1C. Of note, the ~ 16 kDa Vn-binding spot on Fig. 1C was the previously defined Vn-binding PE (Fig. S1), confirming a successful strategy used in the present study. The recruitment of Vn by NTHi thus involves at least two different proteins.

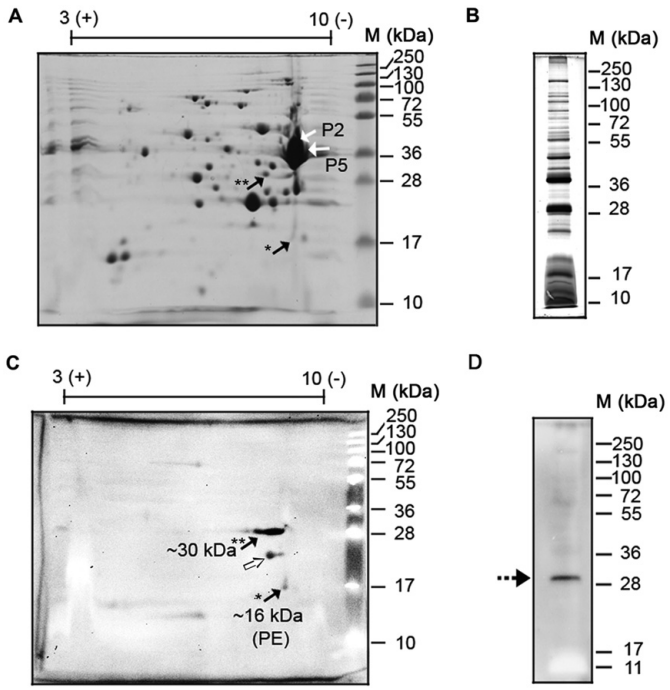

Fig. 1. Immunoblotting assay for identification of *Haemophilus* PF as a Vn-binding protein.
A. Separation of NTHi 3655 OMV (100 μg) on a 2D-SDS-PAGE (pH 3–10). Major OMP P2 and P5 are indicated with white arrows.
B. Separation of OMV (10 μg) in 1D-SDS-PAGE.
C. Far western blotting of the 2D gel with human Vn. Signals that represent Vn-binding PE (~ 16 kDa, tagged with *) and PF (~ 30 kDa, tagged with **) are indicated with black arrows in the Coomassie stained gel (A) and western blot (C). The open arrow indicates a background signal detected on a replica negative control blot (blot not shown). A negative control blot was incubated with only the primary and secondary antibodies without Vn. The background signal was attributed to the unspecific protein recognition by the antibodies.
D. Far western blotting of OMV separated on an 1D-SDS-PAGE. The arrow indicates the ~ 30 kDa protein that binds Vn. M, protein marker in kilo Dalton (kDa). A representative gel image and blot of two independent experiments are shown.

Identification of Haemophilus *Protein F as a novel vitronectin-binding protein of NTHi*

We further characterized the ~ 30 kDa NTHi Vn-binding protein using in-gel trypsin digestion and MALDI-TOF analysis. The protein spot was defined as an uncharacterized putative chelated iron-binding protein (GI: 145632610). The peptide ion covered 64% of the total protein sequence with Mascot score of 572, and no other statistically significant matches were identified. We designated this putative Vn-binding protein as *Haemophilus* Protein F (PF) (Fig. S2), which is a homologue of *Yersinia pestis* YfeA (74.9% of sequence identity; 86.7% of similarity). PF consists of 293 amino acid residues with a theoretical molecular weight of 32.4 kDa and a pI of 8.75. According to SignalP 3.0 (http://www.cbs.dtu.dk/services/SignalP/), PF has a predicted 22-amino acid long signal peptide yielding a 30.1 kDa mature protein with the pI of 7.92 as seen in Fig. 1A.

We also wanted to analyse whether the *Haemophilus* PF was surface exposed on intact *H. influenzae*. The wild-type strain NTHi 3655 was mutated by replacing the *Haemophilus* PF gene (*hpf*) with a chloramphenicol resistance open reading frame (ORF) without interfering with the expression of other NTHi OMPs (Fig. S3). Using flow cytometry analyses, we found that rabbit anti-PF polyclonal antibodies (pAb) detected PF on NTHi 3655, whereas the protein was absent in NTHi 3655Δ*hpf* (Fig. 2B). More importantly, complementing the *hpf* gene restored the PF expression at the bacterial surface to almost 70% of the wild type in NTHi 3655Δ*hpf* (pKR7.2) (Figs 2B and S3). In support of these observations, transmission electron microscopy (TEM) using gold-labelled anti-PF pAb showed that PF was abundantly expressed on the outer surface membrane of NTHi 3655 (Fig. 2C), whereas only background staining was detected with the isogenic NTHi 3655Δ*hpf* mutant (Fig. 2D). Taken together, our data corroborated that PF is a surface-exposed molecule.

NTHi devoid of PF displays a reduced binding to vitronectin

To ensure that the PF–Vn interaction identified in the Far western immunoblotting assay (Fig. 1C) was not an artifact due to non-native conformation of proteins presented in the 2D-gel electrophoresis, a direct binding assay was done with whole bacteria. At increasing concentrations of Vn (1–400 nM), flow cytometry analyses revealed that knocking out PF expression in the NTHi 3655 Δ*hpf* mutant

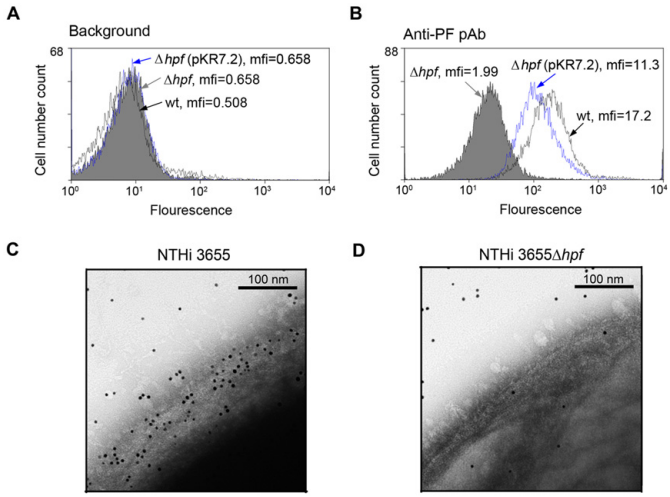

Fig. 2. Detection of *Haemophilus* PF as a surface-associated protein on NTHi.
A and B. The presence of PF at the NTHi surface as measured by flow cytometry. A representative histogram of three independent experiments is shown. Numbers represent the mfi. Left panel (A) illustrates the background binding of the FITC-conjugated goat anti-rabbit pAb, whereas the right panel (B) shows detection by rabbit anti-PF pAb followed by incubation with the FITC-conjugated goat anti-rabbit pAb. Based upon the relative mfi, PF expression in the trans-complemented NTHi 3655Δ*hpf* (pKR7.2) mutant was restored to almost 70% of the wild type level. wt, NTHi 3655 wild type; Δ*hpf*, PF-knockout mutant; Δ*hpf* (pKR7.2), *hpf*-complemented mutant.
C and D. Visualization of PF on NTHi 3655 and NTHi 3655 Δ*hpf* by TEM. PF was detected by the gold-labelled rabbit anti-PF pAb that is visualized as black dots at the NTHi surface (C). Scatter dots presented in (D) was due to background labelling by antibodies on the solid matrix. Representative images of two independent experiments are shown.

resulted in significant reduction of the Vn-binding population (Fig. 3A) and mean fluorescence intensity (mfi) (Fig. 3B) as compared with the PF-expressing NTHi 3655 wild type. Importantly, trans-complementation of *hpf* with pKR7.2 in the mutant restored the Vn-binding to similar levels as the wild type (Fig. 3C).

In addition to the soluble form, Vn is also localized at the surface of epithelial cells or tethered within the ECM together with several other host proteins (Schvartz *et al*., 1999). To evaluate the role of PF in adherence to immobilized Vn, we incubated both NTHi 3655 and the isogenic PF mutant on Vn-coated glass slides. NTHi 3655Δ*hpf* adhered less efficiently to the Vn-coated glass slides compared with the wild type NTHi 3655 (Fig. 3D). In conclusion, we proved that the surface expressed PF has the capability to interact with both soluble and immobilized Vn.

Protein F binds vitronectin at the bacterial surface when expressed in Escherichia coli

To demonstrate the direct role of PF in Vn-binding on intact bacteria in the absence of other NTHi Vn-binding proteins, PF was recombinantly expressed at the surface of *E. coli* BL21(DE3), an isolate that does not bind Vn (Hallström *et al*., 2009) (Fig. 4A). When the PF-expressing *E. coli* was incubated with increasing concentrations of Vn (5–1000 nM), a dose-dependent increase of the Vn-binding population was observed and bacteria were saturated at ≥ 350 nM (Fig. 4B). In contrast, control *E. coli* transformed with the empty vector pET-16b bound less Vn. We further validated the specificity of Vn binding to PF-expressing *E. coli* by the ability of anti-PF pAb to block the interaction. A significantly reduced binding was observed at a dilution of up to 1:50 compared with the control incubated in the absence of antibodies (Fig. 4C). In parallel, the adherence of PF-expressing *E. coli* to immobilized Vn was increased compared with the control *E. coli* (Fig. 4D). Taken together, we showed that PF confers a Vn-binding property to the heterologous host *E. coli* providing further evidence of PF being a significant Vn-binding NTHi OMP.

The vitronectin-binding region is located within Lys23-Glu48 at the N-terminus of Protein F

To pinpoint the Vn-binding domain of PF, a series of polyhistidine-tagged truncated fragments (Fig. 5A) spanning the entire polypeptide of PF (amino acids 12–293) were recombinantly produced in *E. coli* BL21(DE3). As quantified by ELISA, full-length $PF^{12–293}$ bound Vn in a dose-dependent manner when incubated with increasing concentrations of Vn (1–50 nM) (Fig. 5B). The dissociation constant (K_D) of the interaction was calculated to 12.82 nM. Thereafter, Vn at pre-saturated concentrations (5 nM and 10 nM) were used for incubation with immobilized full-length and truncated fragments of PF. We found that two fragments encompassing mainly the N-terminus of PF, i.e. $PF^{12–98}$ and $PF^{12–177}$, showed similar Vn binding to that observed with the full-length $PF^{12–293}$ (Fig. 5C). An uncharacterized NTHi protein, UHP_09011 (GI: 145632833), which does not bind Vn, was included as a

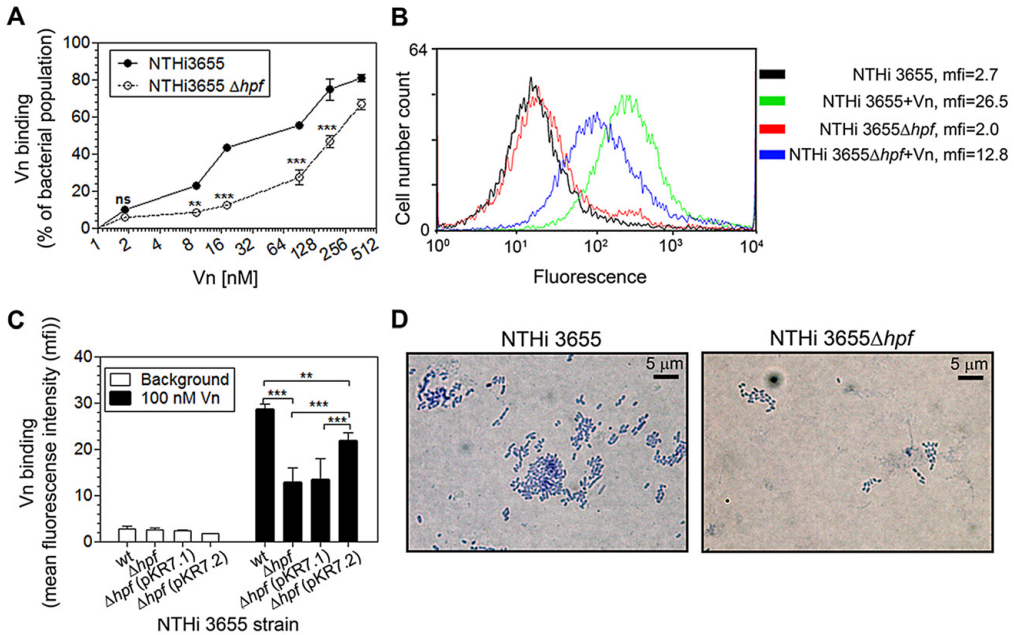

Fig. 3. The NTHi mutant devoid of PF has a reduced Vn-binding.
A. Analysis of the Vn-binding population (%) of NTHi 3655 wild type and Δ*hpf* mutant at increasing concentrations of Vn (1–400 nM) as measured by flow cytometry.
B. A representative flow cytometry histogram of NTHi-dependent binding of Vn at 100 nM. Numbers represent mfi of the corresponding experiment. A background control without Vn added is also included (black). Three independent experiments were done.
C. Restoration of the Vn-binding phenotype in an *hpf*-trans-complemented mutant. Binding was quantified as mfi by flow cytometry ($n = 3$). wt, NTHi 3655 wild type; Δ*hpf*, mutant devoid of PF; Δ*hpf* (pKR7.1), trans-complemented control mutant; Δ*hpf* (pKR7.2), *hpf* trans-complemented mutant. For (A) and (C), data represent the mean of three independent experiments and error bars represent standard deviations. Two-way ANOVA was used to calculate the differences in Vn binding between the NTHi 3655 strains. $^{**}P \leq 0.01$ and $^{***}P \leq 0.001$; n.s., not significant.
D. Adherence on Vn-coated glass slides of NTHi 3655 wild type and the PF-knockout mutant. Bacteria were visualized under light microscope after a standard Gram-staining. Representative images of two independent experiments are shown.

negative control. The specificity of the protein–protein interactions was further confirmed in a competition assay. Pre-incubation of Vn with increasing concentrations of $PF^{12–293}$ or $PF^{12–98}$ (0.05–5.0 μM) resulted in a significant decrease of Vn binding to the immobilized $PF^{12–293}$ (Fig. 5D). The fragment $PF^{81–293}$ that was devoid of the N-terminus, and the negative control UHP_09011 did not inhibit the interaction.

The exact Vn binding site on the PF molecule was further revealed with a series of synthetic peptides constituting of 23–26 amino acid residues, each with four amino acids overlap (Fig. 5E). Among the peptides, we found that only $PF^{23–48}$ reacted preferentially with Vn both at 5 and 20 nM (Fig. 5F). The K_D value for the interaction was estimated to 16.36 nM (Fig. 5G), which is comparable with the K_D value of $PF^{12–293}$. In a competition assay (Fig. 5H), pre-incubation of Vn with increasing concentrations of the $PF^{23–48}$ peptide significantly reduced Vn binding to immobilized $PF^{12–293}$. Neither the peptide $PF^{44–68}$ nor $PF^{225–255}$ competed, however, with the full-length recombinant PF. To summarize, our data indicated that the N-terminal (Lys23-Glu48) is the major Vn-binding region of PF and that the interaction is specific as revealed by competition assays.

Protein F interacts with the C-terminus of vitronectin

We also wanted to identify the putative PF binding site on the Vn molecule (Fig. 6A). Heparin and plasminogen activator inhibitor-1 (PAI-1) have multiple distinct binding sites throughout the Vn molecule (Lane *et al.*, 1987; Kost *et al.*, 1992; Liang *et al.*, 1997; Gibson *et al.*, 1999). PAI-1 has one primary binding site at the SMB domain of the N-terminus and a secondary binding site at the C-terminus of Vn (Schar *et al.*, 2008a,b) (Fig. 6A). Among the three heparin-binding domains (HBD-1 to 3), only

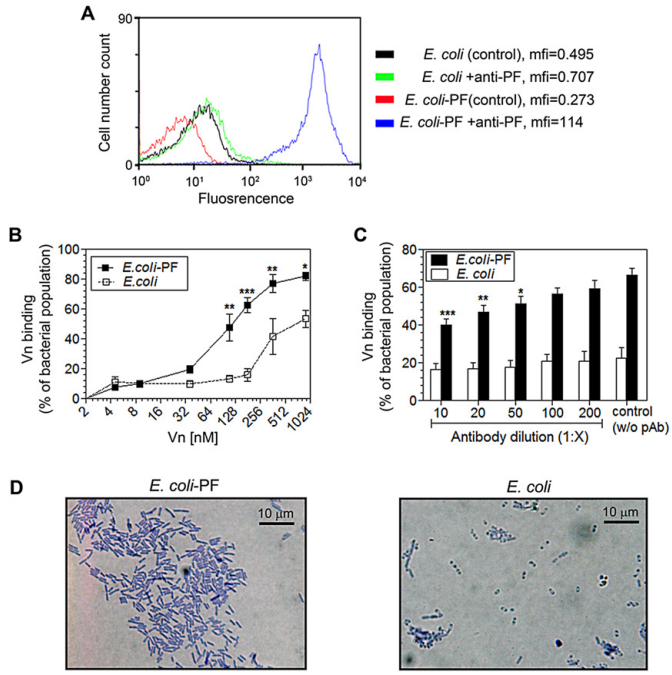

Fig. 4. *E. coli*-expressing *Haemophilus* PF at the surface acquires Vn binding.
A. Surface expression of *Haemophilus* PF by the heterologous host *E. coli* BL21(DE3) as measured by flow cytometry with anti-PF pAb. Histogram of a single representative experiment from three independent experiments is shown and numbers represent mfi. Background binding by the FITC-conjugated secondary pAb in the absence of vitronectin is included.
B. Percentage of the Vn-binding population in *E. coli* strains (*E. coli*-expressing PF and control *E. coli* containing the expression vector pET-16b only) at various concentrations of Vn (5–1 × 10^3 nM) as quantified by flow cytometry. Differences in the Vn-binding population observed between the PF-expressing *E. coli* and control *E. coli* were estimated by a two-way ANOVA.
C. Anti-PF pAb specifically block vitronectin-binding to PF. Data show percentages of the bacterial binding population to 120 nM Vn after pre-incubation with various dilutions of anti-PF pAb followed by flow cytometry analyses. Statistical significances regarding differences between antibody blocking for each strain compared with the conditions without antibody were determined by an one-way ANOVA. For (B) and (C), data represent the mean of three independent experiments and error bars show the standard deviations. $*P \leq 0.05$; $**P \leq 0.01$; $***P \leq 0.001$.
D. Bacterial attachment on a Vn-coated glass slide. Adherence was visualized under a light microscope after conventional Gram-staining. A representative image of two independent experiments is shown.

HBD-3 [amino acids (aa) 348–361] is known to overlap with the secondary PAI-1 binding site (aa 348–370) located at the C-terminus of Vn (Kost *et al.*, 1992; Schar *et al.*, 2008a,b). The majority of bacterial surface proteins known to date interact with the C-terminus of Vn (Singh *et al.*, 2010a,b; 2011). Therefore, we investigated the PF binding site on the Vn molecule by using heparin and PAI-1 as blocking agents. We determined that both

Fig. 5. N-terminal Lys23-Glu48 of PF is involved in the Vn binding.
A. Schematic representation of PF recombinant truncated fragments, and (E) synthetic peptides encompassing the entire PF polypeptide. SP, signal peptide.
B and G. Estimation of the K_D value of the (B) $PF^{12–293}$ fragment and (G) $PF^{23–48}$ peptide in interaction with Vn (1–50 nM) by ELISA. The K_D and B_{MAX} values are shown as average values with standard deviations from three independent experiments. Small inserts represent the Scatchard plots.
C and F. Binding of Vn to truncated PF fragments (C), and PF peptides (F).
D and H. Inhibition assays of the PF–Vn interaction by (D) PF fragments and (H) PF peptides. IC_{50}, the 50% inhibitory concentration of each fragment and peptide.
All data represent the mean of three independent experiments and error bars show standard deviations. The increased Vn binding observed for the PF fragments or peptides compared with the negative control (UHP_09011); or inhibition in Vn binding compared with the absence of inhibitor was statistically significant when calculated by the two-way ANOVA test. $*P \leq 0.05$; $**P \leq 0.01$ and $***P \leq 0.001$. n.a., not analysed.

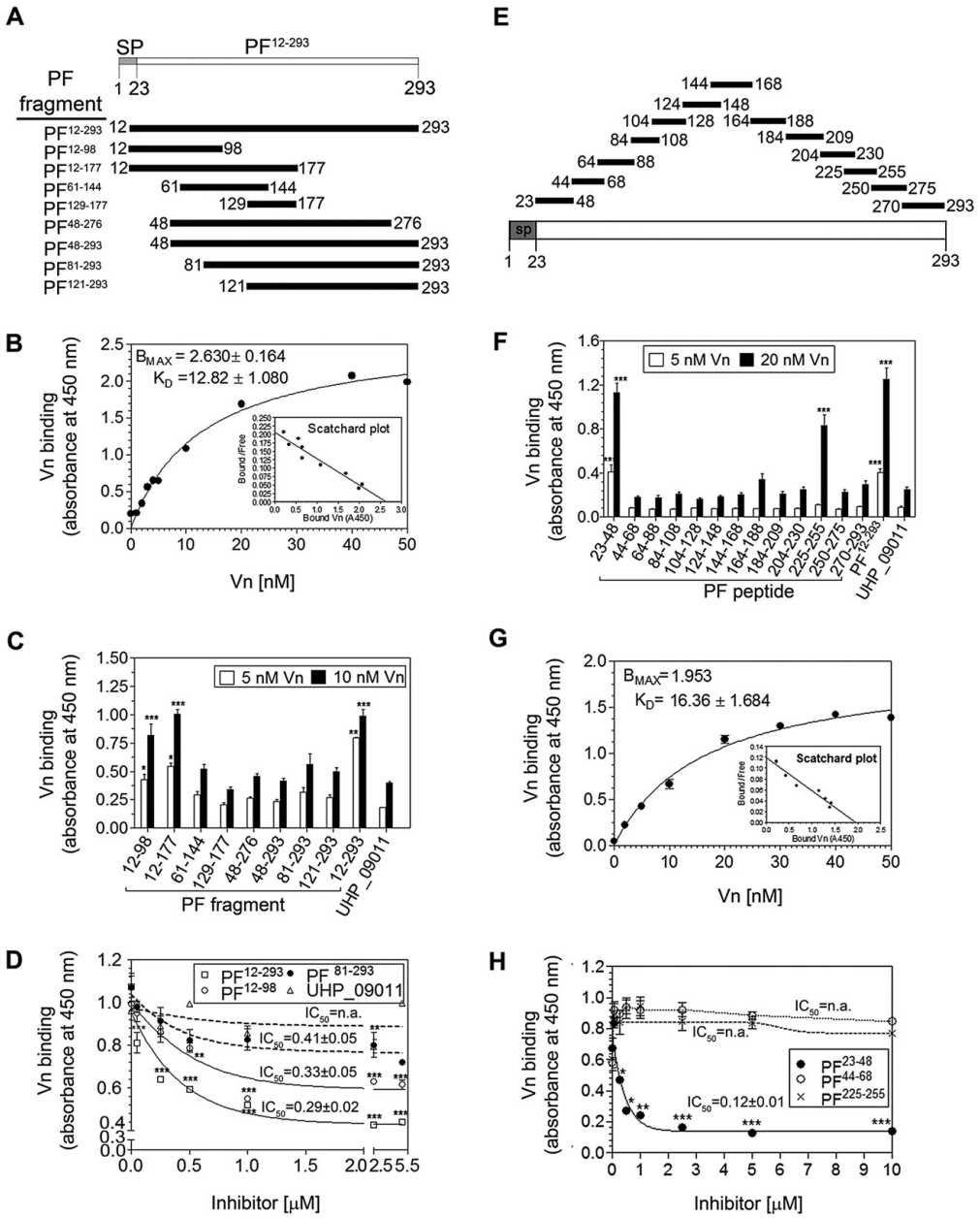
A
SP
PF12-293
PF fragment
1 23
293
PF12-293 12 293
PF12-98 12 98
PF12-177 12 177
PF61-144 61 144
PF129-177 129 177
PF48-276 48 276
PF48-293 48 293
PF81-293 81 293
PF121-293 121 293
E
144 168
124 148
104 128 164 188
84 108 184 209
64 88 204 230
44 68 225 255
23 48 250 275
270 293
sp
1 23 293
B
BMAX = 2.630± 0.164
KD =12.82 ± 1.080
Scatchard plot
Bound/Free
Bound Vn (A450)
Vn binding (absorbance at 450 nm)
Vn [nM]
F
5 nM Vn
20 nM Vn
Vn binding (absorbance at 450 nm)
23-48
44-68
64-88
84-108
104-128
124-148
144-168
164-188
184-209
204-230
225-255
250-275
270-293
PF12-293
UHP_09011
PF peptide
C
5 nM Vn
10 nM Vn
Vn binding (absorbance at 450 nm)
12-98
12-177
61-144
129-177
48-276
48-293
81-293
121-293
12-293
UHP_09011
PF fragment
G
BMAX= 1.953
KD= 16.36 ± 1.684
Scatchard plot
Bound/Free
Bound Vn (A450)
Vn binding (absorbance at 450 nm)
Vn [nM]
D
PF12-293
PF12-98
PF 81-293
UHP_09011
IC50=n.a.
IC50=0.41±0.05
IC50=0.33±0.05
IC50=0.29±0.02
Vn binding (absorbance at 450 nm)
Inhibitor [μM]
H
IC50=n.a.
IC50=n.a.
PF23-48
PF44-68
PF225-255
IC50=0.12±0.01
Vn binding (absorbance at 450 nm)
Inhibitor [μM]

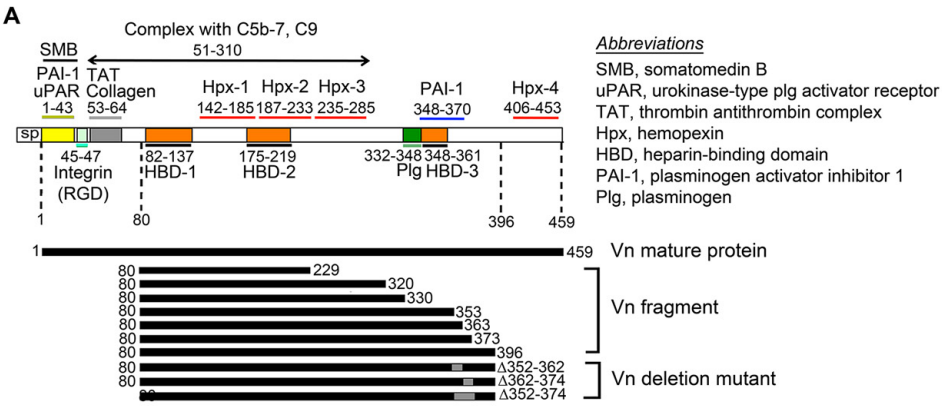
A
Complex with C5b-7, C9
51-310
SMB
PAI-1 TAT
uPAR Collagen
1-43 53-64
Hpx-1 Hpx-2 Hpx-3
142-185 187-233 235-285
PAI-1
348-370
Hpx-4
406-453
sp
45-47
Integrin
(RGD)
82-137
HBD-1
175-219
HBD-2
332-348 348-361
Plg HBD-3
1
80
396
459
Abbreviations
SMB, somatomedin B
uPAR, urokinase-type plg activator receptor
TAT, thrombin antithrombin complex
Hpx, hemopexin
HBD, heparin-binding domain
PAI-1, plasminogen activator inhibitor 1
Plg, plasminogen
Vn mature protein
Vn fragment
Vn deletion mutant
80-229
80-320
80-330
80-353
80-363
80-373
80-396
Δ352-362
Δ362-374
Δ352-374

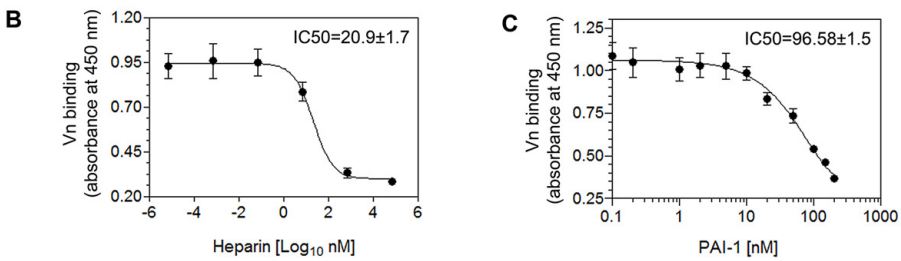
B
IC50=20.9±1.7
Vn binding (absorbance at 450 nm)
Heparin [Log10 nM]
C
IC50=96.58±1.5
Vn binding (absorbance at 450 nm)
PAI-1 [nM]

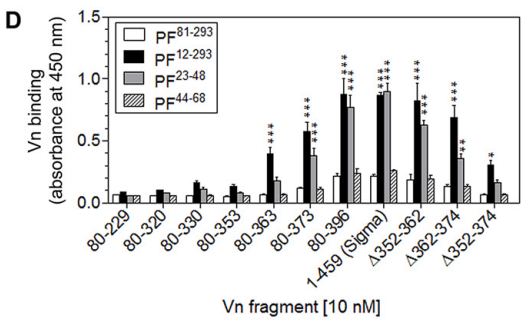
D
PF81-293
PF12-293
PF23-48
PF44-68
Vn binding (absorbance at 450 nm)
80-229
80-320
80-330
80-353
80-363
80-373
80-396
1-459 (Sigma)
Δ352-362
Δ362-374
Δ352-374
Vn fragment [10 nM]

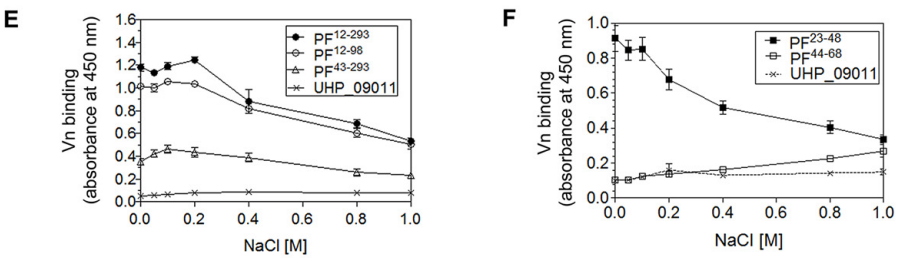
E
PF12-293
PF12-98
PF43-293
UHP_09011
Vn binding (absorbance at 450 nm)
NaCl [M]
F
PF23-48
PF44-68
UHP_09011
Vn binding (absorbance at 450 nm)
NaCl [M]

Fig. 6. Mapping of the PF binding site on the Vn molecule.
A. Schematic representation of the identified active ligand-binding domains of Vn. SP, signal peptide. Recombinant fragments of Vn are shown in black blocks and deleted regions in mutated variants are indicated in grey (Vn deletion mutants).
B and C. Inhibition of the Vn-PF interaction by heparin (6.7×10^{-6}–6.7×10^{4} nM) (B) and PAI-1 (0.1–200 nM) (C). Vn (10 nM) was pre-incubated with various concentrations of inhibitors. Reaction mixtures were thereafter incubated with $PF^{12–293}$ immobilized on microtitre plates. IC_{50}, the 50% inhibitory concentration of heparin or PAI-1.
D. Interaction of immobilized $PF^{12–293}$ and $PF^{23–48}$ to Vn variants (10 nM). The non-binding fragment ($PF^{81–293}$) and peptide ($PF^{44–68}$) were included as negative controls. An enhanced binding of truncated Vn fragments to the immobilized $PF^{12–293}$ and $PF^{23–48}$ was statistically significant as calculated by the two-way ANOVA when compared with the negative fragment and peptide respectively. $^{*}P \leq 0.05$; $^{**}P \leq 0.01$ and $^{***}P \leq 0.001$.
E and F. Characterization of the ionic interaction of PF protein fragments (E) and synthetic peptides (F) with Vn (10 nM) in the presence of various concentrations of NaCl (0.1–1.0 M). Vn-binding was measured in ELISA.
All data represent the mean of three independent experiments and error bars show the standard deviations.

heparin and PAI-1 inhibited binding of $PF^{12–293}$ to Vn in a dose-dependent manner (Fig. 6B and C) that indicated a potential overlapping Vn binding site. The results hence suggested that PF targets HBD-3 and the C-terminal PAI-1 binding site of the Vn molecule.

To support the observations outlined above, a series of truncated recombinant Vn fragments that were partially or completely devoid of HBD-3 and the C-terminal PAI-1 binding site were constructed and used to analyse binding to immobilized PF by ELISA (Fig. 6A). As can be seen in Fig. 6D, Vn fragments ($n = 4$) (comprising aa 80–229, 80–320, 80–330, and 80–353 respectively) did not interact with PF, whereas the other three Vn fragments comprising aa 80–363, 80–373, and 80–396 bound recombinant $PF^{12–293}$ and the synthetic peptide $PF^{23–48}$. Two PF constructs devoid of the Vn-binding regions ($PF^{81–293}$ and $PF^{44–68}$) were included as negative controls. These data indicated that aa spanning Vn 80–353 were not involved in interactions with PF, whereas the aa Vn 363–396 were crucial.

In order to further determine the PF binding region on the Vn molecule, we produced a series of Vn deletion mutants devoid of the specified C-terminal amino acid residues (VnΔ352–362, VnΔ362–374 and VnΔ352–374) (Fig. 6A; lower part). Both VnΔ352–362 and VnΔ362–374 bound recombinant PF in ELISA while extensive deletion of 20 amino acids between residues 352–374 (VnΔ352–374) caused a significantly reduced interaction with PF (Fig. 6D).

It is known that the interactions of heparin and PAI-1 at the polycationic C-terminus of Vn is sensitive to ionic strength (Gibson *et al.*, 1999; Schar *et al.*, 2008a,b). In parallel, we found that NaCl (titration 0.05–1.0 M) inhibited Vn binding to the immobilized recombinant fragments $PF^{12–293}$ and $PF^{12–98}$ (Fig. 6E) and the $PF^{23–48}$ peptide (Fig. 6F). A hyper-physiological concentration of salt (≥ 0.2 M) was required to disrupt and decrease the interaction between Vn and immobilized PF. In conclusion, PF (aa 23–48) directly interacts with the C-terminal part of Vn (aa 352–374) and the binding is based upon ionic interactions.

Protein F enhances bacterial serum resistance through the recruitment of Vn

Vn inhibits the formation of the MAC at the terminal lytic step of the complement cascade. Bacteria that recruit Vn would therefore be resistant against the bactericidal activity of NHS (Singh *et al.*, 2010a). Based upon our findings that PF has the ability to bind Vn, we subsequently investigated the role of PF in bacterial serum resistance. Deletion of PF resulted in a greater sensitivity to complement-mediated killing of NTHi 3655Δ*hpf* compared with the wild type NTHi 3655 (Fig. 7A). Importantly, trans-complementation of the isogenic mutant NTHi 3655Δ*hpf* with pKR7.2 containing the *hpf* gene restored the serum-resistant phenotype (Fig. 7B).

To reveal the direct role of PF in serum resistance in the absence of other NTHi proteins involved in subverting complement-mediated killing (Ho *et al.*, 2007; Hallström *et al.*, 2009; Clark *et al.*, 2012; Langereis *et al.*, 2012), PF-expressing *E. coli* was tested with 1% NHS. As shown in Fig. 7C, the presence of PF at the *E. coli* surface significantly promoted survival in NHS compared with control *E. coli* carrying the empty expression vector. Interestingly, we found that both the control *E. coli* and PF-expressing *E. coli* were equally susceptible to serum-mediated killing when Vn was depleted from the NHS (Fig. 7C; blue curves). In parallel, a similar increased bactericidal activity was observed with the NTHi wild type and the *hpf*-deleted mutant (Fig. 7A; blue curves). Importantly, when exogenous Vn (≥ 72 nM) was supplemented we managed to rescue PF-expressing *E. coli* and NTHi from serum-mediated killing (Figs 7D and S4A). This Vn concentration represented conversion of serum Vn in approximately 1% NHS (400 μg ml^{-1}; 5.3 μM). Heat inactivation of NHS (HIS) abolished the serum bactericidal activity in all experiments (Fig. 7A and C; red curves). In parallel with the data shown in Fig. 4C, blocking the Vn–PF interaction at the bacterial surface with anti-PF pAb further decreased the serum resistance in both *E. coli*-expressing PF and wild type NTHi (Fig. S4B and C). Taken together, we demonstrated that PF significantly

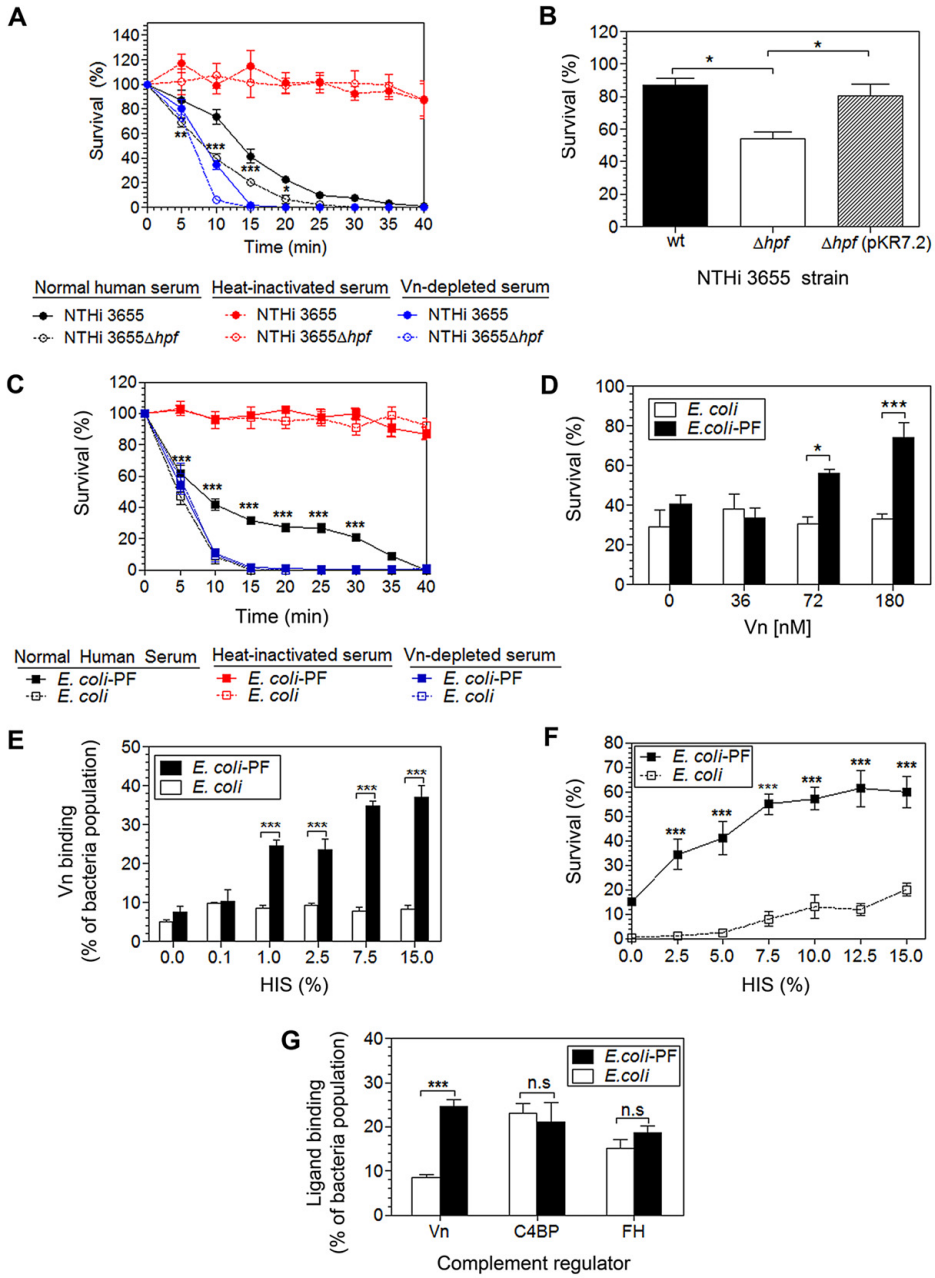
A
Survival (%)
Time (min)
Normal human serum
NTHi 3655
NTHi 3655Δhpf
Heat-inactivated serum
NTHi 3655
NTHi 3655Δhpf
Vn-depleted serum
NTHi 3655
NTHi 3655Δhpf
B
Survival (%)
wt
Δhpf
Δhpf (pKR7.2)
NTHi 3655 strain
C
Survival (%)
Time (min)
Normal Human Serum
E. coli-PF
E. coli
Heat-inactivated serum
E. coli-PF
E. coli
Vn-depleted serum
E. coli-PF
E. coli
D
E. coli
E.coli-PF
Survival (%)
Vn [nM]
E
Vn binding
(% of bacteria population)
E. coli-PF
E. coli
HIS (%)
F
E. coli-PF
E. coli
Survival (%)
HIS (%)
G
Ligand binding
(% of bacteria population)
E.coli-PF
E.coli
n.s
Vn
C4BP
FH
Complement regulator

Fig. 7. Enhanced serum resistance is exerted by PF-expressing bacteria.
A. Survival kinetics of NTHi in 5% normal (NHS), 5% Vn-depleted serum and HIS.
B. Restoration of the serum survival phenotype of the *hpf*-complemented mutant in 5% NHS for 10 min. wt, NTHi 3655 wild type; Δ*hpf*, mutant devoid of PF; Δ*hpf* (pKR7.2), *hpf* trans-complemented strain.
C. Survival kinetics of *E. coli* strains in 1% NHS, 1% Vn-depleted serum and 5% HIS.
D. Serum resistance of *E. coli* strains in 1% Vn-depleted serum that was supplemented with various concentrations (36–180 nM) of purified Vn. Bacterial survival was determined at 5 min.
E. The serum Vn-binding population as measured by flow cytometry.
F. Survival of *E. coli* in serum after pre-incubation with various concentrations of HIS (0.1–15%).
G. Deposition of serum Vn, C4BP and FH on *E. coli* strains following pre-incubation with 1% HIS.
All data represent the mean values of three independent experiments and error bars indicate the standard deviations. Statistical differences in serum resistance or in the ligand-binding population observed between the strains of NTHi 3655 or *E. coli* were calculated by the two-way ANOVA. $*P \leq 0.05$; $**P \leq 0.01$ and $***P \leq 0.001$, n.s.; not significant.

contributes to NTHi-dependent serum resistance via Vn binding.

To evaluate whether Vn was the primary complement inhibitor responsible for our observations, we pre-incubated *E. coli*-expressing PF and control *E. coli* with various concentrations of HIS to assess the bacterial recruitment of serum Vn in addition to other potential complement inhibitors. Heat treatment of serum does not abolish the inhibitory activities of the majority of soluble complement inhibitors, including Vn (Zhuang *et al*., 1996; Kask *et al*., 2004). We found that following pre-incubation with increasing concentrations of HIS, a dose-dependent Vn binding was observed with the PF-expressing *E. coli* population (Fig. 7E). This also reflected the increased concentration of serum Vn deposited at the surface of PF-expressing bacteria hence significantly improving the survival in NHS (Fig. 7F). Control *E. coli* did not exert any enhanced Vn binding or serum resistance.

We previously reported that the recruitment of C4BP, FH and Vn is required for NTHi-dependent serum resistance (Hallström *et al*., 2007; 2008; 2009). To avoid background binding by other NTHi-derived proteins, *E. coli*-expressing PF therefore was used to examine the direct interaction of PF with serum C4BP and FH. Recruitment of serum C4BP or FH derived from HIS was indistinguishable between *E. coli*-expressing PF and control *E. coli* as revealed by flow cytometry (Figs 7G and S5A) and ELISA (Fig. S5B), and did not correlate with the bacterial survival in serum. Collectively, our data proved that PF-dependent Vn binding at the bacterial surface thus contributes to bacterial serum resistance.

The vitronectin–PF complex inhibits MAC formation and delays deposition of C9 on bacteria

To ensure that the interaction of PF at the C-terminus of Vn would not interrupt or sterically alter the MAC inhibitory role of Vn, we performed a haemolytic assay with sheep erythrocytes and terminal complement proteins C5b-6, C7, C8 and C9. As shown in Fig. 8A, Vn that was pre-incubated with increasing concentrations of recombinant $PF^{12–293}$ (0.25–1 μM) remained active resulting in inhibition of the cytolytic activity executed by C5b-9. The data indicated an exclusive role of the PF–Vn complex in the inhibition of complement-mediated lysis that was not attributed to recombinant $PF^{12–293}$ alone.

We further characterized the effect of the PF–Vn complex on C9 deposition and polymerization at the bacterial surface. When NHS was incubated with the mutant NTHi 3655Δ*hpf* devoid of PF expression, an increased C9 polymer deposition (> 250 kDa) was observed after 40 min compared with the NTHi 3655 wild type (Fig. 8B). C9 deposition at the bacterial surface was quantified by flow cytometry and is shown in Fig. 8C. Moreover, we found that pre-incubation of whole bacteria with increasing concentrations of Vn prevented C9 deposition on NTHi 3655, but was unable to protect NTHi 3655Δ*hpf* (Fig. 8D and E). We therefore concluded that PF-dependent serum resistance requires Vn to delay C9 deposition.

Protein F and Protein E share homologous binding sites on vitronectin and are both important for NTHi serum resistance

PE is hitherto the only Vn-binding protein of NTHi reported and it is also known to contribute to serum resistance (Hallström *et al*., 2009; Singh *et al*., 2011). We therefore compared the relative Vn-binding affinity between *Haemophilus* PE and PF. As shown in Fig. 9A, purified recombinant PE interacted with Vn more effectively than recombinant PF ($P \leq 0.01$). The K_D value for the PE–Vn interaction as quantified by ELISA was calculated to 10.13 nM of Vn (Fig. S6), demonstrating a slightly higher affinity for Vn binding compared with PF (K_D = 12.82 nM). Pre-incubation of Vn with increasing concentrations (0.05–1.00 μM) of PE or PF resulted in the depletion of free Vn to immobilized PF or PE respectively (Fig. 9B). As PE was also reported to bind Vn at HBD-3 (Singh *et al*., 2011), our data thus demonstrated that PE and PF may share a common binding site on the Vn molecule.

We further investigated the relative Vn-binding role of PE and PF using whole bacteria. While NTHi 3655Δ*hpf* and NTHi 3655Δ*pe* individually exerted a low binding of Vn, we found that simultaneous mutation of both *pe* and

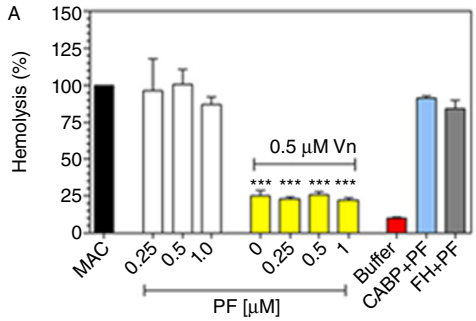

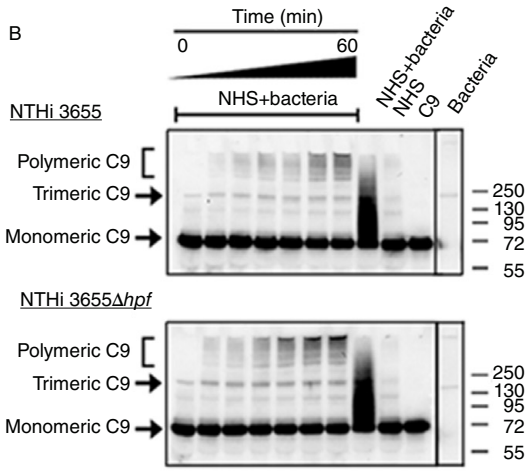

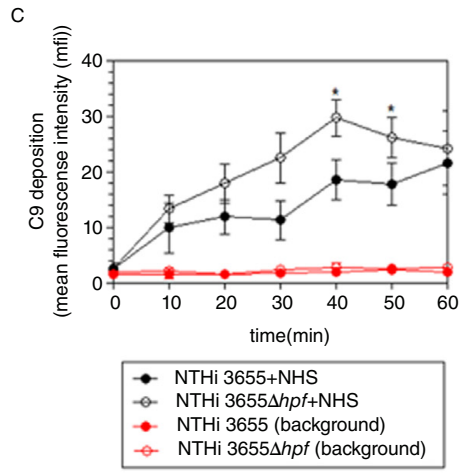

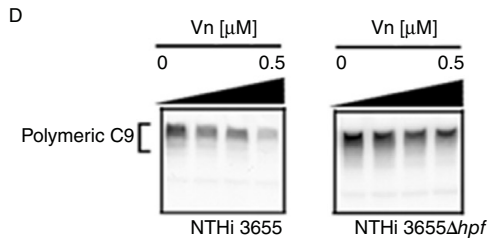

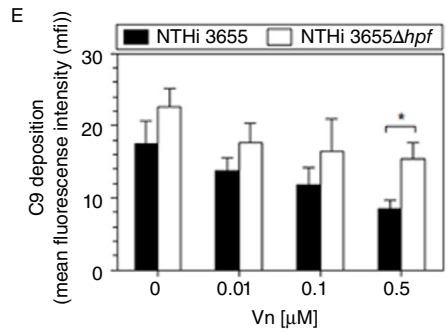

hpf further reduced the Vn binding by NTHi (Fig. 9C), albeit it was statistically insignificant. A slightly increased sensitivity to serum killing and C9 deposition was also observed with the double mutant (NTHi 3655Δ*pe/hpf*) compared with the single mutants (Fig. 9D and E). The data thus confirmed that both PE and PF are important for Vn binding and the consequent serum resistance of NTHi.

Fig. 8. The active inhibition of MAC formation and delayed C9 deposition by the Vn-PF complex.
A. The haemolytic inhibitory activity of Vn in the presence of recombinant $PF^{12–293}$ (0.25–1.0 μM). C4BP, FH, or buffer was included as negative controls. The difference in the haemolytic activity by MAC between the presence or absence of Vn was statistically significant as revealed by one-way ANOVA.
B. Western blotting analyses of C9 deposition on NTHi 3655 and NTHi 3655Δ*hpf* when incubated in 10% NHS at various time points. C9 was detected as high molecular weight polymers (> 250 kDa), trimers (~ 250 kDa) and monomers (~ 72 kDa). Activation of complement in NHS results in multimerization of C9 monomers into a trimeric and thereafter a polymeric form deposited on bacterial cells. However, only the polymeric C9 consequently makes up the cell-lytic MAC.
C. Quantification of the C9 polymer deposition as shown in (B) by flow cytometry. Bacteria incubated without NHS were included as a background control.
D. Effect on C9 deposition between strains of NTHi 3655 after pre-incubation (30 min at 37°C) with various concentrations of Vn (0.01–0.5 μM) prior to 30 min incubation with NHS. C9 polymer deposition was analysed by western blotting.
E. Quantification of the C9 polymer deposition as shown in (D) by flow cytometry.
For (C) and (E), data are presented as mean fluorescence intensities (mfi). All numerical data are the mean of three independent experiments and error bars represent the standard deviations. The difference of C9 polymer deposition observed between NTHi 3655 wild type and the PF mutant was statistically significant as determined by the two-way ANOVA. $*P \leq 0.05$ and $***P \leq 0.001$.

Protein F is a highly conserved Vn-binding protein in NTHi clinical isolates

We wanted to determine whether PF expression, and thus PF-mediated Vn binding, is conserved within the NTHi species. Flow cytometry analyses demonstrated that the majority of NTHi clinical isolates bound Vn (Fig. 10A). In addition, PF was ubiquitously expressed by all the isolates tested (Fig. 10B). Protein sequence alignment of PF from 18 different NTHi clinical isolates exerted 97.9–100% of sequence identity indicating that PF is a highly conserved protein. The sequence alignment is shown in Fig. S7. Importantly, we also found that knocking out *hpf* in the randomly selected NTHi isolates KR271, KR316, KR336 and KR385 (Fig. S8) resulted in a significantly reduced affinity for Vn (Fig. 10C), and consequently an increased sensitivity to the bactericidal effect of serum (Fig. 10D) when compared with the parental wild types. Taken together, PF is a highly conserved and ubiquitous surface protein mediating NTHi serum resistance.

Discussion

Inhibition of serum bactericidal activity by recruiting Vn is important for NTHi (Eberhard and Ullberg, 2002; Hallström *et al*., 2009; Ronander *et al*., 2009; Singh *et al*., 2011). In this paper we defined PF as a novel Vn-binding protein in addition to the well-characterized PE (Hallström *et al*., 2009; Singh *et al*., 2011). Acquisition of Vn by NTHi is thus depending on more than one OMP and represents an important survival strategy to evade complement-mediated killing. This multifaceted strategy has been reported to be essential for several serum-resistant pathogens, for example, Vn and FH binding in *Neisseria meningitidis* (Lewis *et al*., 2010; Sa *et al*., 2010; Griffiths *et al*., 2011) and C4BP recruitment in *Yersinia enterocolitica* (Kirjavainen *et al*., 2008).

Outer membrane vesicles are versatile cargo-containing vehicles that bud off from the outer membrane of Gram-negative bacteria. OMV released by NTHi contain mainly virulence-associated periplasmic and OMPs that are involved in the pathogenesis (Kahn *et al*., 1983; Wispelwey *et al*., 1989; Sharpe *et al*., 2011). Therefore, the use of OMV (instead of whole cell bacteria) for the global screening of NTHi Vn-binding OMPs was merited in this study. Furthermore, the use of OMV excludes potential problems associated with the cytoplasmic compartment of whole bacterial cells that could potentially result in background binding.

All microbial Vn receptors studied to date are surface-associated virulence factors (Singh *et al*., 2010a). Recognition of PF on NTHi and *E. coli*-expressing PF by anti-PF pAb revealed the surface localization in flow cytometry and TEM (Fig. 2). In parallel, a PF homologue of *H. parasuis* (GI: 219871287) (83.1% sequence similarity and 74.7% identity with NTHi PF) was also found at the bacterial surface and shown to be immunogenic in an animal model (Hong *et al*., 2011).

We presented significant evidence that PF is a Vn-binding factor at the surface of NTHi based upon analyses with NTHi *hpf* mutants (Fig. 3), surface expression of PF in *E. coli* (Fig. 4) and protein–protein interaction assays (Fig. 5). In addition, the capacity of PF-expressing bacteria to bind immobilized Vn implied a potential adhesive role for PF. By using Vn as a bridging molecule for attachment to integrins (e.g. $\alpha_v\beta_3$) on host cells, PF may potentially mediate NTHi colonization at the epithelium of the respiratory tract (Lopez-Gomez *et al*., 2012). This invasion strategy has also been demonstrated for other mucosal pathogens (Bergmann *et al*., 2009; Sa *et al*., 2010; Singh *et al*., 2010a).

In silico protein structure modelling of PF (Fig. S9) demonstrated that the Lys23-Glu48 region is exposed at the protein surface thus supporting the identification of the Vn-binding domain at the N-terminus of PF (Fig. 5). Here, we also revealed that PF targets the C-terminal region (Phe352-Ser374) of Vn containing the entire HBD-3 and C-terminal PAI-1 binding side (Fig. 6). This is in agree-

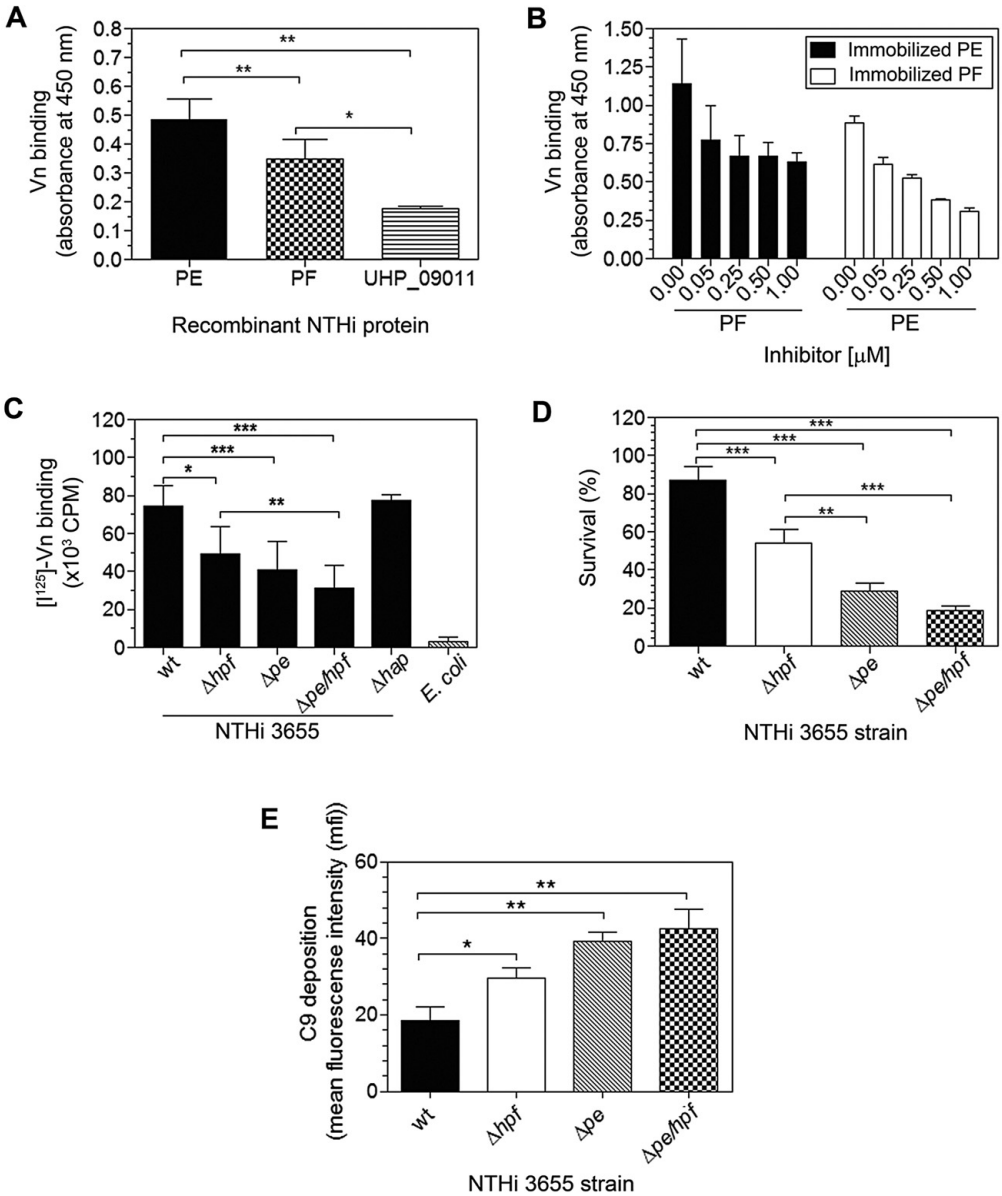

ment with previous work demonstrating that heparin inhibited the *H. influenzae* Vn binding (Eberhard and Ullberg, 2002). Interestingly, lung infection with NTHi triggers the upregulation of PAI-1 as a part of the host early immune defence by recruitment of polymorphonuclear neutrophils (Lim *et al.*, 2011). The role of an interaction between PAI-1 and Vn when bound to the NTHi surface remains, however, to be elucidated.

Antibody-depleted serum suggested that the classical pathway dominated the killing of the PF-knockout mutant

Fig. 9. Involvement of PE and PF in Vn-binding and the serum resistant phenotype of NTHi.
A. Comparison of Vn binding between recombinant PE and PF when measured by ELISA. Purified UHP_09011 was included as a negative control.
B. Inhibition assay of Vn binding to the immobilized PE and PF in the presence of increasing concentrations (0.05–1.00 μM) of PF or PE respectively.
C. Direct ligand binding assay with NTHi 3655 strains and radiolabellled [I^{125}]-Vn. Radioactivity (count per minute; CPM) represents the concentration of Vn bound to bacteria. The NTHi 3655Δ*hap* mutant and *E. coli* were included as negative controls. Hap is an autotransporter with adhesive properties that binds epithelial cells and laminin/collagen II but not Vn (Fink *et al.*, 2002).
D. Survival of NTHi 3655 strains in 5% NHS for 10 min.
E. C9 deposition on NTHi 3655 strains when incubated in 10% NHS for 40 min at 37°C. C9 deposition was quantified by flow cytometry.
In panels (C), (D) and (E): wt, NTHi 3655 wild type; Δ*hpf*, mutant devoid of PF; Δ*pe*, mutant devoid of PE; Δ*pe/hpf*, PE and PF double-knockout mutant; Δ*hap*, mutant devoid of Hap. All data represent mean values of three independent experiments and error bars indicate standard deviations. Differences between proteins or bacterial strains regarding Vn binding and serum survival were calculated by one-way ANOVA. $*P \leq 0.05$; $**P \leq 0.01$ and $***P \leq 0.001$ respectively.

(Fig. S4D). However, the relatively greater serum resistance observed in PF-expressing NTHi 3655 occurred via delayed C9 deposition during MAC formation at the terminal lytic step (Figs 7 and 8). Importantly, bacterial survival was related to PF-dependent recruitment of Vn. The serum resistance was restored after (i) introduction of the *hpf* gene in the PF-knockout mutant, and (ii) Vn addition to Vn-depleted serum. Active interaction of cell-associated PF with Vn in the fluid phase suggested a potential role of PF to scavenge Vn from either the blood stream during

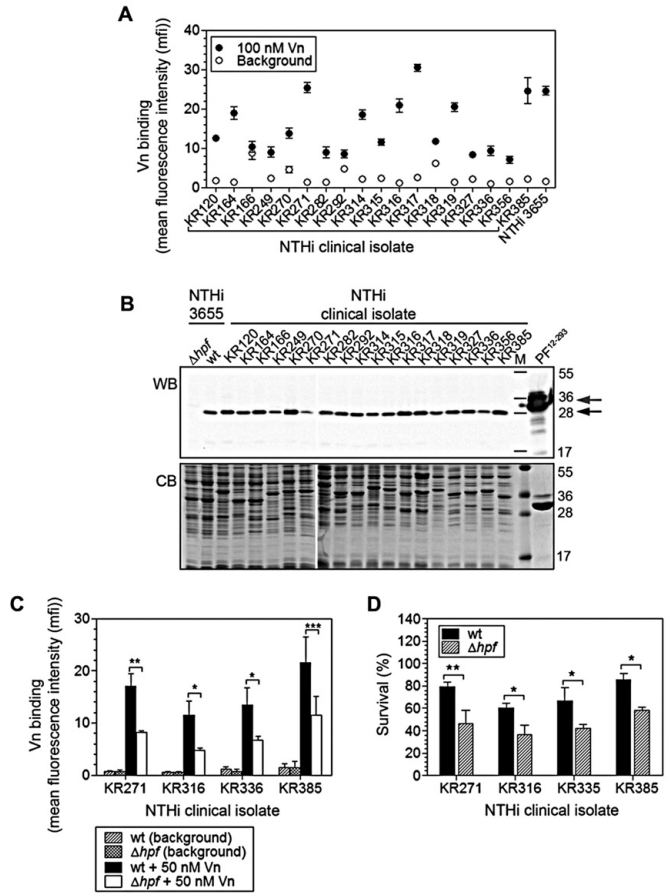

Fig. 10. PF is a conserved Vn-binding protein important for serum resistance in NTHi clinical isolates.
A. A series of NTHi clinical isolates ($n = 18$) were analysed for Vn binding. Binding (mfi) was measured by flow cytometry. Background binding represents experiments performed in the absence of Vn.
B. Detection of PF expression on NTHi clinical isolates by anti-PF pAb in western blotting. Grey and black arrows indicate purified recombinant and native PF respectively. CB, Coomassie blue stained SDS-PAGE; WB, western blotting. A representative gel image and blot of two independent experiments is shown.
C. Vn binding of PF-knockout mutants of NTHi KR271, KR316, KR335 and KR385 clinical isolates. Binding was measured by flow cytometry.
D. Survival of NTHi clinical isolates and their respective mutants devoid of PF in 5% NHS for 10 min.
In panel (C) and (D): wt, NTHi wild type; Δ*hpf*, PF mutant. For panel (A), (C) and (D) data represent mean values of three independent experiments and error bars indicate standard deviations. Differences in Vn-binding and serum survival between the NTHi wild types and PF mutants were calculated by a two-way ANOVA. $*P \leq 0.05$; $**P \leq 0.01$ and $***P \leq 0.001$.

invasive sepsis or from the pericellular ECM during respiratory tract infection. We found that PF binding did not interfere with the C5b-C9 inhibitory domain (Met51-Thr310) of Vn (Sheehan *et al.*, 1995) (Fig. 8). We therefore excluded the possibility of disruption of the MAC inhibition site or a conformational change of the Vn molecule after binding to PF. Delayed MAC formation on serum-resistant NTHi isolates can also be attributed to delayed deposition of antibodies or C3b and C4b (Figueira *et al.*, 2007; Ho *et al.*, 2007; Clark *et al.*, 2012; Langereis *et al.*, 2012), and host deficiencies in C3, C4 and C5 production (Toews *et al.*, 1985). We do not exclude the possibility that PF may also affect the activation or deposition of other components important in the classical complement pathway.

A functional similarity between PE and PF was observed regarding binding to the HBD-3 and C-terminal PAI-1 binding sites of Vn (Singh *et al.*, 2011). The Vn-binding domain derived from both PE (aa 84–108) (Hallström *et al.*, 2009; Singh *et al.*, 2011) and PF (aa 23–48) has, however, only 20.5% sequence similarity (Fig. S6), indicating that unique interactions are responsible for Vn binding. The relatively higher affinity for Vn by PE compared with PF implies an important role of PE in Vn-dependent serum resistance of NTHi, whereas PF may serve as an alternative/additional candidate. This is probably a back-up strategy for NTHi to consistently acquire Vn, and this dual Vn-binding strategy may have an impact on bacterial pathogenesis. NTHi 3655 devoid of either PF or PE resulted in decreased Vn-binding, serum resistance, and finally increased C9 deposition (Fig. 9C–E) when compared with the wild type. However, despite mutation of both the *hpf* and *pe* genes resulted in a decreased Vn binding it was not statistically significant compared with the *pe* single mutant. Thus, in our hands PE most likely plays a major role for vitronectin-mediated NTHi serum resistance.

We found that PF is a highly conserved Vn-binding protein in NTHi clinical isolates (Fig. 10). Since PF is also surface exposed and immunogenic, it may therefore serve as a potential vaccine candidate. Although immunization with PE has previously been proven to be protective in a mouse pulmonary clearance model (Ronander *et al.*, 2009), simultaneous targeting of both PE and PF, in addition to other conserved OMP (e.g. Omp6 and PD), may result in a more effective vaccine strategy (Pichichero *et al.*, 2010).

PF has also been designated as adhesin B (Lu *et al.*, 1998), HfeA (Harrison *et al.*, 2005) or YfeA-like protein (Whitby *et al.*, 2006), and belongs to the TroA superfamily with homology to YfeA from the *yfeABCD* operon of *Y. pestis* that is involved in Fe^{2+}, Mn^{2+} and Zn^{2+} uptake (Bearden and Perry, 1999). However, the role of PF in iron uptake has not yet been fully characterized. Importantly, PF expression was reported to be upregulated during iron/haem-restricted growth conditions, and in bacteria incubated with sputum derived from COPD patients (Whitby *et al.*, 2006; Qu *et al.*, 2010). *hpf* was also one of several NTHi genes shown to be essential for a delayed NTHi clearance in a pulmonary mouse model (Gawronski *et al.*, 2009). Moreover, PF orthologues are known virulence determinants in *Y. pestis* when causing bubonic plague (Bearden and Perry, 1999), in *Y. pseudotuberculosis* by mediating polymyxin B resistance and colonization (Arafah *et al.*, 2009), and also contribute to iron-uptake and consequently infection by *Shigella flexneri* (Runyen-Janecky *et al.*, 2003).

In summary, NTHi-dependent acquisition of Vn is multifactorial, and here we identified PF as a novel Vn-binding protein. The important role of PF in serum resistance and adhesion warrants further characterization for a full understanding of NTHi pathogenesis. Our findings may also be an impetus for development of a future vaccine against NTHi.

Experimental procedures

Bacterial strains

Clinical isolates ($n = 18$) (Table S1) and laboratory strains of NTHi 3655 (Table S2) were grown on chocolate agar or cultured in brain heart infusion (BHI) broth supplemented with NAD (Sigma-Aldrich, St Louis, MO) and hemin (Merck, Darmstadt, Germany) (each at 10 μg ml^{-1}) at 37°C in a humid atmosphere containing 5% CO_2. *E. coli* BL21(DE3) (Novagen, Darmstadt, Germany) and DH5α (Stratagene, Santa Clara, CA) were cultured in Luria–Bertani (LB) broth or on LB agar. Kanamycin (Km) and ampicillin (Amp) (Merck) were used at 50 μg ml^{-1} and 100 μg ml^{-1}, respectively, when indicated.

Construction of an NTHi hpf deletion mutant and trans-complementation of hpf

To delete the *hpf* gene in NTHi, the upstream (621 bp) and downstream (997 bp) flanking regions were amplified from NTHi 3655 genomic DNA with primers listed in *Supporting information* (Table S3). Primers used for the cloning of the flanking regions contained overhangs that are complementary to the chloramphenicol acetyltransferase gene (*cat*) (EMBL BAA78807). The *cat* gene was amplified from the plasmid pLYS (Novagen). A linear knockout vector fragment (2279 bp) was synthesized by using the two flanking regions containing *cat* overhang together with the *cat* amplicon as a template in an overlapping PCR reaction. The PF promoter was kept intact to obviate a possible polar effect caused by disruption of the PF operon by the *cat* promoter. The vector also included the *H. influenzae* uptake signal sequence (AAGTGCGGT). A schematic map for the *hpf* knockout is shown in Fig. S10. Competent NTHi was prepared and transformations were performed as previously described (Poje and Redfield, 2003). NTHi 3655 and NTHi 3655Δ*pe* were transformed with the vector resulting in the strains NTHi 3655Δ*hpf* and NTHi 3655Δ*pe/hpf* respectively. Transformants were selected on

chocolate agar plates containing chloramphenicol (Cm) (5 μg ml^{-1}) for NTHi 3655Δ*hpf* and combination of Cm and zeocine (Zeo) (15 μg ml^{-1}) for NTHi 3655Δ*pe/hpf*.

Trans-complementation of the *hpf* gene in NTHi 3655Δ*hpf* was achieved by genomic homologous recombination following a strategy described previously (Jones *et al*., 2002; Ünal *et al*., 2012). The pKR2 plasmid which contains the intergenic region from the locus CGSHi3655_06559 of NTHi3655 was used as starting material. A Km resistance cassette (*npt*I) amplified by PCR using the Primers Km_F and Km_R (Table S3) was inserted into the vector pKR2 using the restriction sites *Sph*I and *Sal*I leading to the vector pKR7.1. The *hpf* gene was amplified by PCR with primers PFprom_F and PF293_R from genomic DNA and cloned into pKR7.1 linearized by *EcoR*V and *Sal*I yielding the plasmid pKR7.2. The plasmids pKR7.1 and pKR7.2 contain either the promoter of *hpf* (pKR7.1) or *hpf* driven by its endogenous promoter (pKR7.2) followed by a Km resistance gene cloned in reverse direction (Fig. S10). Plasmids pKR7.1 and pKR7.2 were used as template for PCR amplification with the primers KS36 and KS37 to generate the constructs for transformation. The subproduct of pKR7.1 was used to transform NTHi3655Δ*hpf* in order to generate the control strain NTHi3655Δ*hpf* (pKR7.1). The PCR product derived from pKR7.2 was used to transform NTHi3655Δ*hpf* yielding the strain NTHi3655Δ*hpf* (pKR7.2) carrying *hpf* complemented *in trans*. Insertion of the elements in the CGSHi3655_06559 locus was confirmed by PCR using the primers PFprom_R and RecNTHi3655_F located upstream the insertion point of the construct transformed. Resulting NTHi 3655Δ*hpf* (pKR7.1) and NTHi 3655Δ*hpf* (pKR7.2) mutants were selected on a chocolate agar containing chloramphenicol (Cm) (Sigma) (5 μg ml^{-1}) and Km (15 μg ml^{-1}). All mutants were characterized and confirmed by DNA sequencing, growth curve analysis, SDS-PAGE, western blotting, and flow cytometry.

Sequence analysis of hpf in clinical isolates

For assessment of the *hpf* gene in clinical isolates, the gene was amplified from bacterial genomic DNA with primers For_PF_flank and Rev_PF_flank (Table S3) covering the upstream (CGHi3655_02304) and downstream flanking region (intergenic region, located at nucleotides 1034–1186). Purified PCR products were subjected to DNA sequencing. ORFs of PF variants were deduced from the sequenced DNA. Multiple sequence alignment was performed using Lasergene® MegAlign (DNAstar, Madison, WI).

Recombinant protein expression, peptides and antibodies

Full-length and truncated ORF of PF (GI: 145632610) were amplified from the genomic DNA of NTHi 3655 with site specific primers listed in *Supporting information* Table S4. The expression vector pET26b (Novagen) was used for cytoplasmic recombinant protein production, whereas pET16b (Novagen) was used for bacterial cell surface expression of the target protein. Resultant recombinant constructs were thereafter transformed into the chemically competent host *E. coli* DH5α. The authenticity of cloned DNA sequence was verified by DNA sequencing (MWG Eurofins, Ebersberg, Germany). Using the pET26b backbone constructs, recombinant proteins were produced in *E. coli* BL21(DE3) and harvested as previously described (Su *et al*., 2010). The polyhistidine-tagged recombinant proteins were purified from crude extracts using immobilized metal affinity chromatography-based Histrap™ FF Crude (GE Healthcare Biosciences, Uppsala, Sweden) according to the manufacturer's instructions. Protein concentrations were estimated at absorbance 280 nm with Nanodrop (Thermo Scientific) and analysed by SDS-PAGE. For expression of surface-bound PF, the *E. coli* expression culture was induced overnight, and used in a serum killing assay and flow cytometry analyses. A rabbit anti-PF pAb was prepared as previously described (Hallström *et al*., 2009). To increase the specificity, the rabbit anti-PF antiserum was subsequently affinity purified as previously described with PF$^{12–293}$ coupled to CNBr-activated Sepharose™ (GE Healthcare Biosciences).

A series of peptides (23–25 aa long) encompassing the entire PF protein sequence (excluding signal peptide aa 1–22) were also synthesized (Innovagen, Lund, Sweden).

Two-dimensional gel electrophoresis

Outer membrane vesicles of NTHi 3655 are enriched with periplasmic- and outer membrane-associated proteins (Schaar *et al*., 2011; Sharpe *et al*., 2011). In the following experiments, we thus used the OMV extract as the protein source of bacterial OMP in order to reduce contamination from the cytoplasmic compartment. The OMV of NTHi 3655 were prepared from overnight cultures and separated by 2D-gel electrophoresis as previously described with some modifications (Schaar *et al*., 2011). For the first dimension separation by isoelectric focusing (IEF), 125 μl of solubilized sample (100 μg) was removed and applied to a precast 7 cm pH 3–10 IPG gel strip (Immobiline Drystrips, GE Healthcare Biosciences) by in-gel sample rehydration method. Using IPGphor II electrophoresis unit (GE Healthcare Biosciences), IEF was performed with the following programme: 30 V for 0.30 hr (15 Vhr), 500 V for 0.30 hr (250 Vhr), 1000 V for 0.30 hr (500 Vhr), 2600 V for 0.15 hr (650 Vhr), 3500 V (875 Vhr) and 5000 V for 1.00 hr (5000 Vhr) yielding a total voltage of 7291 Vhr, with maximum current of 50 μA per strip. Thereafter, the strips were equilibrated as described elsewhere (Schaar *et al*., 2011) and run in a second dimension of gel electrophoresis on a 12% (v/v) SDS-polyacrylamide gel at 70 V for 15 min and 150 V for 40 min.

Protein spots on gels were visualized by silver staining (Bio-Rad) for image analysis and alternatively with Coomassie brilliant blue staining for protein sequence identification with mass spectrometry. Gels were scanned on a Chemi-Doc™ XRS+ System (Bio-Rad) and analysed with the Image Lab™ Software (Bio-Rad). Targeted Coomassie stained protein spots were manually excised and protein identification by Matrix-assisted laser desorption/ionisation-time of flight mass spectrometry (MALDI-TOF-MS) was performed by Protein Analysis Service available at Alphalyse (Odense, Denmark).

SDS-polyacrylamide gel electrophoresis

One-dimensional (1D) SDS-polyacrylamide gel electrophoresis (SDS-PAGE) was performed according to the Laemmli

method (Laemmli, 1970). Briefly, OMV (10 μg), purified protein (10 μg) or whole cell lysates [3×10^7 cfu (colony-forming units)] in PBS were heat-denatured at 95°C for 10 min in SDS-reducing sample buffer (50 mM Tris-Cl pH 6.8, 2% SDS, 6% Glycerol, 1% β-mercaptoethanol, 0.004% bromophenol blue). Thereafter, samples were resolved in 12% (v/v) SDS-polyacrylamide gel at 150 V for 60 min. Protein bands on gels were visualized by Coomassie blue staining and scanned as described above. For detection of Vn binding or PF expression, proteins on gels were subjected to western blotting.

Western blotting

Proteins separated in SDS-PAGE were transferred to a 0.45 μm Immobilon-P™ polyvinylidene fluoride (PVDF) membrane (Millipore) at 15 V for 16 hr. Membranes were blocked with blocking buffer [5% (w/v) skimmed milk in PBS] and washed with PBS containing 0.05% (v/v) Tween 20 (PBST). For detection of Vn-binding proteins, membranes were probed with human Vn (Sigma) (3 μg ml^{-1}) in blocking buffer for 1 hr at room temperature. Bound Vn was detected with a sheep anti-human Vn pAb (1:2000 dilution) (Abd Serotec, Oxford, UK) and horseradish peroxidase (HRP)-conjugated donkey anti-sheep pAb (1:4000 dilution) (AbD Serotec). For detection of PF, blots were incubated with rabbit anti-PF pAb (1:1500 dilution) followed by HRP-conjugated swine anti-rabbit pAb (1:1000 dilution) (Dako). Reactive antibodies were detected with enhanced chemiluminescence (ECL) western blotting substrate (Pierce, Rockford, IL). Chemiluminescence signals on membranes were visualized on a ChemiDoc™ XRS+ System.

Bacterial binding to Vn-coated glass slides

Glass slides (Menzel-Gläser, Thermo Scientific, Wilmington, DE) were incubated with 6 μg Vn (Sigma) for 1 hr at 37°C for immobilization. Bacteria were grown in broth until mid-log phase ($OD_{600} = 0.5$) and incubated on the Vn-coated glass slide for 1 hr at room temperature. Unbound bacteria were washed away with PBS, whereas bound bacteria were fixed by flaming and visualized by Gram-staining. Slides were prepared according to a standard protocol and analysed in an Olympus BX51 microscope at 400× amplification.

Transmission electron microscopy

Negative staining and TEM were used to visualize the localization of PF at the bacterial surface. NTHi 3655 and NTHi 3655 Δ*hpf* were incubated with a colloidal thiocyanate gold-labelled anti-PF pAb and visualized by a Jeol JEM 1230 electron microscope (JEOL, Tokyo, Japan) operated at 60 kV accelerating voltage was used. Images were recorded with a Gatan Multiscan 791 CCD camera (Gatan, Pleasanton, CA).

Serum bactericidal assay

NHS and Vn-depleted serum was prepared as previously described (Hallström *et al*., 2009). The NHS used in the present study was reactive against NTHi as revealed by western blotting (data not shown). Susceptibility of NTHi and *E. coli* BL21(DE3) to complement-mediated killing was tested as previously described (Yi and Murphy, 1997). The optimal concentration of serum used was as previously suggested (Hallström *et al*., 2009; 2010) and had been empirically determined for NTHi (5% NHS) and *E. coli* BL21(DE3) (1% NHS). Aliquots of 1.5×10^3 cfu in 150 μl of DVBS-BSA [2.5 mM Veronal buffer, pH 7.3, 1 mM $MgCl_2$, 2.5 mM $CaCl_2$, 2.5% (w/v) glucose and 10% (w/v) bovine serum albumin] were added with appropriate dilutions of serum and incubated at 37°C at the indicated times with gentle shaking. At 0 min (T_0 sample) and indicated times (T_t sample) aliquots of 10 μl of the reaction mixtures were plated on chocolate agar for NTHi or LB agar containing Amp for PF-expressing *E. coli* and incubated at 37°C. Percentage of bacterial killing was expressed as $(T_0 \text{ cfu} - T_t \text{ cfu})/T_0 \text{ cfu}) \times 100$. Three individual experiments, each performed in triplicates, were done. Control experiments were also performed as described above using heat-inactivated serum (HIS) (pretreated at 56°C for 30 min).

Expression of Vn fragments in HEK293 cell lines and protein purification

Vn fragments (spanning aa 80–396, 80–320, 80–229, 80–379, 80–373, 80–363, 80–353, 80–339, and 80–330) were expressed in HEK293T cells and purified as previously described (Singh *et al*., 2011). In addition, $Vn^{80–396}$ with internal deletions of amino acids 352–362, 362–374, and 352–374, were produced in the present study. The protein expression, purification and CD spectra analysis were performed as described elsewhere (Singh *et al*., 2011).

Direct protein binding assay

Human Vn (Sigma) was labelled with 0.05 M iodine (Amersham Biosciences, Buckinghamshire, UK) per mol protein using the chloramine-T method (Nordstrom *et al*., 2004). Bacterial colonies were resuspended in PBS to $OD_{600} = 0.5$, washed and resuspended in PBS-2% BSA. [I^{125}]-labelled-Vn (80 kcpm/sample) was added to bacterial suspensions containing 1×10^7 cfu and incubated for 1 hr at 37°C. After two washing steps with PBS-2% BSA, iodine-labelled protein bound to bacteria was measured in a gamma counter (Wallac, Espoo, Finland). *E. coli* Top10 was included as a negative control. All direct binding assays were performed in triplicates at three independent occasions.

Flow cytometry analyses

PF expression at the bacterial surface was detected using flow cytometry. NTHi from mid-log phase cultures or PF-expressing *E. coli* BL21(DE3) transformants induced overnight were resuspended in PBS containing 1% BSA (blocking buffer), and adjusted to 1×10^9 cfu ml^{-1}. Aliquots containing 5×10^7 cfu were incubated with anti-PF pAb for 1 hr, washed and pelleted by centrifugation. Thereafter, bacterial suspensions were incubated with FITC-conjugated swine anti-rabbit pAb (Dako) for 30 min.

For ligand binding at the bacterial surface, suspensions were incubated with increasing concentrations of Vn [1–400 nM for NTHi or 5–1×10^3 nM for *E. coli* BL21(DE3) expressing PF] for 1 hr at 37°C. After washing, bound ligands were detected using sheep anti-human Vn pAb (dilution 1:50),

followed by FITC-conjugated donkey anti-sheep pAb (dilution 1:150) (Abd Serotec). Serum C4BP and FH were detected with mouse anti-C4BP and anti-FH monoclonal antibodies (mAb) followed by FITC-rabbit anti-mouse pAb (Abd Serotec). For detection of C9 deposition at the bacterial surface, bacterial suspensions were incubated with 10% NHS as described in the C9 deposition assay as described below. Thereafter, cells were washed and surface-deposited C9 were detected using goat anti-C9 pAb (CompTech) (dilution 1:100) followed by FITC-conjugated donkey anti-goat pAb (Abd Serotec). Unspecific binding by secondary antibodies was assessed by omitting the primary antibodies, ligands or NHS. Bacteria were analysed in a flow cytometer (EPICS XL-MCL flow cytometer; Coulter, Hialeah, FL). Ten thousand events were examined for each sample. The positive population was gated at 5% of the background binding population in the control.

Enzyme-linked immunosorbent assay (ELISA)

The interaction of Vn with PF was analysed by ELISA. This assay was done by using PF recombinant proteins or synthetic peptides as indicated (Fig. 5A and E). Either the indicated PF synthetic peptides or recombinant PF proteins diluted at 50 nM in coating buffer (100 mM NaH_2CO_3, pH 8.6) were immobilized overnight on Polysorb microtitre plates. After washing, Vn fragments as outlined in Fig. 6A were added to each well at the indicated concentrations followed by incubation for 1 hr at room temperature. Thereafter, bound Vn was detected with sheep anti-human Vn pAb followed by HRP-donkey anti-sheep pAb. Signals of antigen–antibody complexes were developed with 20 mM tetramethylbenzidine and 0.1 M potassium citrate. Finally, the reactions were stopped with 1 M H_2SO_4. Signals developed were read at an absorbance of 450 nm. All experiments were performed in triplicates.

Haemolytic assay

The MAC inhibitory activity of PF-bound Vn was analysed in a haemolytic assay with sheep erythrocytes as previously described with some modifications (Hallström *et al.*, 2009). Briefly, sheep erythrocytes resuspended to 2×10^8 cells ml^{-1} in DVBS containing 0.1% gelatin (DGVB). Aliquots of 100 µl sheep erythrocytes were pre-incubated with 2 µg ml^{-1} C5b-6 (CompTech, Tyler, TX) for 30 min at 37°C. In a separate preparation, 0.5 µM Vn (Sigma) was pre-incubated with increasing concentrations of purified recombinant $PF^{12–293}$ (0.25–1.0 µM) for 15 min at 37°C in a final volume of 100 µl. Thereafter, the mixture was added with 2 µg ml^{-1} C7 (CompTech), 0.2 µg ml^{-1} C8 (CompTech) and 2 µg ml^{-1} C9 (CompTech), and further incubated for 30 min. After pre-incubation, the C5b-6 coated erythrocytes were added to the Vn–C7-9 mixture and incubated for 30 min at 37°C. Non-haemolysed erythrocytes were pelleted and the amount of haemoglobin representing the lysed erythrocytes was measured at 541 nm. The relative MAC inhibitory activity was presented in the percentage of total haemolysis.

C9 deposition assay

The effect of PF on MAC formation at the bacterial surface was assayed on the basis of C9 deposition on bacterial cells as previously described with some modifications (Singh *et al.*, 2011). Briefly, bacteria resuspended to $OD_{600} = 0.1$ in DGVB were pre-incubated with various concentrations of Vn. This was followed by incubation with 10% NHS in a final volume of 100 µl at 37°C at the indicated time points and mixtures were incubated on ice to stop the reactions. Thereafter, 10 µl aliquots were mixed with LDS sample buffer (Invitrogen, Carlsbad, CA) and boiled at 70°C for 10 min. Total bacterial cell proteins were separated on a 4–12% Bis-Tris gradient gel (Invitrogen) as described by the manufacturer. This was followed by western blotting with goat anti-C9 pAb and HRP-conjugated donkey anti-goat pAb (Abd Serotec). In parallel, C9 deposition at the bacterial surface was quantified by flow cytometry as described above.

Statistics

One- or two-way ANOVA tests were used to compare the difference between more than two experimental groups when indicated. Differences were considered statistically significant at $P \leq 0.05$. Statistical analyses were performed using GraphPad Prism® version 5.0 (GraphPad Software, La Jolla, CA).

Ethics statement

Normal human sera were obtained from healthy adult volunteers at Skane University Hospital, Malmo, Sweden, and prepared according to the general rules established by the Swedish Government (Svensk författningssamling 1988:534, Ändringsförfattning 2012:256; Riksdagen, Riksgatan 1, SE-111 28, Stockholm, Sweden). Ethical permit (M193-11) was obtained from Malmö/Lund District Court (Djurförsöksetiska nämnden, Tingsrätten, Byggmästaregatan 2, SE-222 37 Lund, Sweden). This body approved the protocol used in this study.

Acknowledgements

We thank Mrs Marta Brant for the flow cytometry analysis. We are also grateful to Drs Kalpana Singh, Can Ünal and Christophe Fleury for their excellent help with vector construction and trans-complementation. The Clinical Microbiology laboratory at Labmedicin Skåne is acknowledged for providing us with clinical isolates.

Funding

This work was supported by grants from the Alfred Österlund, the Anna and Edwin Berger, Greta and Johan Kock, the Gyllenstiernska Krapperup, Åke Wiberg, Hans Hierta, and the Marianne and Marcus Wallenberg Foundations, the Swedish Medical Research Council (Grant Number 521-2010-4221, http://www.vr.se), the Cancer Foundation at the University Hospital in Malmö, the Physiographical Society (Forssman's Foundation), and Skåne County Council's research and development foundation.

Conflict of interest

Conflict of interest between authors are not reported.

References

Arafah, S., Rosso, M.L., Rehaume, L., Hancock, R.E., Simonet, M., and Marceau, M. (2009) An iron-regulated LysR-type element mediates antimicrobial peptide resistance and virulence in *Yersinia pseudotuberculosis*. *Microbiology* **155:** 2168–2181.

Barthel, D., Singh, B., Riesbeck, K., and Zipfel, P.F. (2012) *Haemophilus influenzae* uses the surface protein E to acquire human plasminogen and to evade innate immunity. *J Immunol* **188:** 379–385.

Bearden, S.W., and Perry, R.D. (1999) The Yfe system of *Yersinia pestis* transports iron and manganese and is required for full virulence of plague. *Mol Microbiol* **32:** 403–414.

Bergmann, S., Lang, A., Rohde, M., Agarwal, V., Rennemeier, C., Grashoff, C., *et al.* (2009) Integrin-linked kinase is required for vitronectin-mediated internalization of *Streptococcus pneumoniae* by host cells. *J Cell Sci* **122:** 256–267.

Blom, A.M., Villoutreix, B.O., and Dahlback, B. (2004) Complement inhibitor C4b-binding protein-friend or foe in the innate immune system? *Mol Immunol* **40:** 1333–1346.

Clark, S.E., Snow, J., Li, J., Zola, T.A., and Weiser, J.N. (2012) Phosphorylcholine allows for evasion of bactericidal antibody by *Haemophilus influenzae*. *PLoS Pathog* **8:** e1002521.

Clemans, D.L., Bauer, R.J., Hanson, J.A., Hobbs, M.V., St Geme, 3rd, J.W., Marrs, C.F., and Gilsdorf, J.R. (2000) Induction of proinflammatory cytokines from human respiratory epithelial cells after stimulation by nontypeable *Haemophilus influenzae*. *Infect Immun* **68:** 4430–4440.

Eberhard, T., and Ullberg, M. (2002) Interaction of vitronectin with *Haemophilus influenzae*. *FEMS Immunol Med Microbiol* **34:** 215–219.

Ferreira, V.P., Pangburn, M.K., and Cortes, C. (2010) Complement control protein factor H: the good, the bad, and the inadequate. *Mol Immunol* **47:** 2187–2197.

Figueira, M.A., Ram, S., Goldstein, R., Hood, D.W., Moxon, E.R., and Pelton, S.I. (2007) Role of complement in defense of the middle ear revealed by restoring the virulence of nontypeable *Haemophilus influenzae sia*B mutants. *Infect Immun* **75:** 325–333.

Fink, D.L., Green, B.A., and St Geme, J.W., 3rd (2002) *The Haemophilus influenzae* Hap autotransporter binds to fibronectin, laminin, and collagen IV. *Infect Immun* **70:** 4902–4907.

Foxwell, A.R., Kyd, J.M., and Cripps, A.W. (1998) Nontypeable *Haemophilus influenzae*: pathogenesis and prevention. *Microbiol Mol Biol Rev* **62:** 294–308.

Gawronski, J.D., Wong, S.M., Giannoukos, G., Ward, D.V., and Akerley, B.J. (2009) Tracking insertion mutants within libraries by deep sequencing and a genome-wide screen for *Haemophilus* genes required in the lung. *Proc Natl Acad Sci USA* **106:** 16422–16427.

Gibson, A.D., Lamerdin, J.A., Zhuang, P., Baburaj, K., Serpersu, E.H., and Peterson, C.B. (1999) Orientation of heparin-binding sites in native vitronectin. Analyses of ligand binding to the primary glycosaminoglycan-binding site indicate that putative secondary sites are not functional. *J Biol Chem* **274:** 6432–6442.

Griffiths, N.J., Hill, D.J., Borodina, E., Sessions, R.B., Devos, N.I., Feron, C.M., *et al.* (2011) *Meningococcal* surface fibril (Msf) binds to activated vitronectin and inhibits the terminal complement pathway to increase serum resistance. *Mol Microbiol* **82:** 1129–1149.

Hallström, T., Trajkovska, E., Forsgren, A., and Riesbeck, K. (2006) *Haemophilus influenzae* surface fibrils contribute to serum resistance by interacting with vitronectin. *J Immunol* **177:** 430–436.

Hallström, T., Jarva, H., Riesbeck, K., and Blom, A.M. (2007) Interaction with C4b-binding protein contributes to nontypeable *Haemophilus influenzae* serum resistance. *J Immunol* **178:** 6359–6366.

Hallström, T., Zipfel, P.F., Blom, A.M., Lauer, N., Forsgren, A., and Riesbeck, K. (2008) *Haemophilus influenzae* interacts with the human complement inhibitor factor H. *J Immunol* **181:** 537–545.

Hallström, T., Blom, A.M., Zipfel, P.F., and Riesbeck, K. (2009) Nontypeable *Haemophilus influenzae* protein E binds vitronectin and is important for serum resistance. *J Immunol* **183:** 2593–2601.

Hallström, T., Resman, F., Ristovski, M., and Riesbeck, K. (2010) Binding of complement regulators to invasive nontypeable *Haemophilus influenzae* isolates is not increased compared to nasopharyngeal isolates, but serum resistance is linked to disease severity. *J Clin Microbiol* **48:** 921–927.

Harrison, A., Dyer, D.W., Gillaspy, A., Ray, W.C., Mungur, R., Carson, M.B., *et al.* (2005) Genomic sequence of an otitis media isolate of nontypeable *Haemophilus influenzae:* comparative study with *H. influenzae* serotype d, strain KW20. *J Bacteriol* **187:** 4627–4636.

Ho, D.K., Ram, S., Nelson, K.L., Bonthuis, P.J., and Smith, A.L. (2007) *lgt*C expression modulates resistance to C4b deposition on an invasive nontypeable *Haemophilus influenzae*. *J Immunol* **178:** 1002–1012.

Hogasen, K., Mollnes, T.E., and Harboe, M. (1992) Heparin-binding properties of vitronectin are linked to complex formation as illustrated by in vitro polymerization and binding to the terminal complement complex. *J Biol Chem* **267:** 23076–23082.

Hong, M., Ahn, J., Yoo, S., Hong, J., Lee, E., Yoon, I., *et al.* (2011) Identification of novel immunogenic proteins in pathogenic *Haemophilus parasuis* based on genome sequence analysis. *Vet Microbiol* **148:** 89–92.

Jones, P.A., Samuels, N.M., Phillips, N.J., Munson, R.S., Jr, Bozue, J.A., Arseneau, J.A., *et al.* (2002) *Haemophilus influenzae* type b strain A2 has multiple sialyltransferases involved in lipooligosaccharide sialylation. *J Biol Chem* **277:** 14598–14611.

Kahn, M.E., Barany, F., and Smith, H.O. (1983) Transformasomes: specialized membranous structures that protect DNA during *Haemophilus* transformation. *Proc Natl Acad Sci USA* **80:** 6927–6931.

Kask, L., Villoutreix, B.O., Steen, M., Ramesh, B., Dahlback, B., and Blom, A.M. (2004) Structural stability and heat-induced conformational change of two complement inhibitors: C4b-binding protein and factor H. *Protein Sci* **13:** 1356–1364.

Kirjavainen, V., Jarva, H., Biedzka-Sarek, M., Blom, A.M., Skurnik, M., and Meri, S. (2008) *Yersinia enterocolitica*

serum resistance proteins YadA and ail bind the complement regulator C4b-binding protein. *PLoS Pathog* **4:** e1000140.

Kost, C., Stuber, W., Ehrlich, H.J., Pannekoek, H., and Preissner, K.T. (1992) Mapping of binding sites for heparin, plasminogen activator inhibitor-1, and plasminogen to vitronectin's heparin-binding region reveals a novel vitronectin-dependent feedback mechanism for the control of plasmin formation. *J Biol Chem* **267:** 12098–12105.

Laemmli, U.K. (1970) Cleavage of structural proteins during the assembly of the head of bacteriophage T4. *Nature* **227:** 680–685.

Lane, D.A., Flynn, A.M., Pejler, G., Lindahl, U., Choay, J., and Preissner, K. (1987) Structural requirements for the neutralization of heparin-like saccharides by complement S protein/vitronectin. *J Biol Chem* **262:** 16343–16348.

Langereis, J.D., Stol, K., Schweda, E.K., Twelkmeyer, B., Bootsma, H.J., de Vries, S.P., *et al.* (2012) Modified lipooligosaccharide structure protects nontypeable *Haemophilus influenzae* from IgM-mediated complement killing in experimental otitis media. *mBio* **3:** doi:10.1128/mBio.00079-12

Lewis, L.A., Ngampasutadol, J., Wallace, R., Reid, J.E., Vogel, U., and Ram, S. (2010) The meningococcal vaccine candidate neisserial surface protein A (NspA) binds to factor H and enhances meningococcal resistance to complement. *PLoS Pathog* **6:** e1001027.

Liang, O.D., Rosenblatt, S., Chhatwal, G.S., and Preissner, K.T. (1997) Identification of novel heparin-binding domains of vitronectin. *FEBS Lett* **407:** 169–172.

Lim, J.H., Woo, C.H., and Li, J.D. (2011) Critical role of type 1 plasminogen activator inhibitor (PAI-1) in early host defense against nontypeable *Haemophilus influenzae* (NTHi) infection. *Biochem Biophys Res Commun* **414:** 67–72.

Link, A.J., Hays, L.G., Carmack, E.B., and Yates, J.R., 3rd (1997) Identifying the major proteome components of *Haemophilus influenzae* type-strain NCTC 8143. *Electrophoresis* **18:** 1314–1334.

Lopez-Gomez, A., Cano, V., Moranta, D., Morey, P., del Portillo, F.G., Bengoechea, J.A., and Garmendia, J. (2012) Host cell kinases, α5 and β1 integrins, and Rac1 signalling on the microtubule cytoskeleton are important for nontypable *Haemophilus influenzae* invasion of respiratory epithelial cells. *Microbiology* **158:** 2384–2398.

Lu, D., Boyd, B., and Lingwood, C.A. (1998) The expression and characterization of a putative adhesin B from *H. influenzae*. *FEMS Microbiol Lett* **165:** 129–137.

Marc, M.M., Korosec, P., Kosnik, M., Kern, I., Flezar, M., Suskovic, S., and Sorli, J. (2004) Complement factors c3a, c4a, and c5a in chronic obstructive pulmonary disease and asthma. *Am J Respir Cell Mol Biol* **31:** 216–219.

Mezei, G., Varga, L., Veres, A., Fust, G., and Cserhati, E. (2001) Complement activation in the nasal mucosa following nasal ragweed-allergen challenge. *Pediatr Allergy Immunol* **12:** 201–207.

Milis, L., Morris, C.A., Sheehan, M.C., Charlesworth, J.A., and Pussell, B.A. (1993) Vitronectin-mediated inhibition of complement: evidence for different binding sites for C5b-7 and C9. *Clin Exp Immunol* **92:** 114–119.

Morgan, B.P. (1999) Regulation of the complement membrane attack pathway. *Crit Rev Immunol* **19:** 173–198.

Nakamura, S., Shchepetov, M., Dalia, A.B., Clark, S.E., Murphy, T.F., Sethi, S., *et al.* (2011) Molecular basis of increased serum resistance among pulmonary isolates of non-typeable *Haemophilus influenzae*. *PLoS Pathog* **7:** e1001247.

Narkio-Makela, M., Jero, J., and Meri, S. (1999) Complement activation and expression of membrane regulators in the middle ear mucosa in otitis media with effusion. *Clin Exp Immunol* **116:** 401–409.

Narkio-Makela, M., Hellwage, J., Tahkokallio, O., and Meri, S. (2001) Complement-regulator factor H and related proteins in otitis media with effusion. *Clin Immunol* **100:** 118–126.

Nordstrom, T., Blom, A.M., Forsgren, A., and Riesbeck, K. (2004) The emerging pathogen *Moraxella catarrhalis* interacts with complement inhibitor C4b binding protein through ubiquitous surface proteins A1 and A2. *J Immunol* **173:** 4598–4606.

Persson, C.G., Erjefalt, J.S., Greiff, L., Andersson, M., Erjefalt, I., Godfrey, R.W., *et al.* (1998) Plasma-derived proteins in airway defence, disease and repair of epithelial injury. *Eur Respir J* **11:** 958–970.

Pichichero, M.E., Kaur, R., Casey, J.R., Sabirov, A., Khan, M.N., and Almudevar, A. (2010) Antibody response to *Haemophilus influenzae* outer membrane protein D, P6, and OMP26 after nasopharyngeal colonization and acute otitis media in children. *Vaccine* **28:** 7184–7192.

Podack, E.R., Preissner, K.T., and Muller-Eberhard, H.J. (1984) Inhibition of C9 polymerization within the SC5b-9 complex of complement by S-protein. *Acta Pathol Microbiol Immunol Scand Suppl* **284:** 89–96.

Poje, G., and Redfield, R.J. (2003) Transformation of *Haemophilus influenzae*. *Methods Mol Med* **71:** 57–70.

Qu, J., Lesse, A.J., Brauer, A.L., Cao, J., Gill, S.R., and Murphy, T.F. (2010) Proteomic expression profiling of *Haemophilus influenzae* grown in pooled human sputum from adults with chronic obstructive pulmonary disease reveal antioxidant and stress responses. *BMC Microbiol* **10:** 162.

Resman, F., Ristovski, M., Ahl, J., Forsgren, A., Gilsdorf, J.R., Jasir, A., *et al.* (2011) Invasive disease caused by *Haemophilus influenzae* in Sweden 1997-2009; evidence of increasing incidence and clinical burden of non-type b strains. *Clin Microbiol Infect* **17:** 1638–1645.

Ricklin, D., Hajishengallis, G., Yang, K., and Lambris, J.D. (2010) Complement: a key system for immune surveillance and homeostasis. *Nat Immunol* **11:** 785–797.

Ronander, E., Brant, M., Eriksson, E., Morgelin, M., Hallgren, O., Westergren-Thorsson, G., *et al.* (2009) Nontypeable *Haemophilus influenzae* adhesin protein E: characterization and biological activity. *J Infect Dis* **199:** 522–531.

Runyen-Janecky, L.J., Reeves, S.A., Gonzales, E.G., and Payne, S.M. (2003) Contribution of the *Shigella flexneri* Sit, Iuc, and Feo iron acquisition systems to iron acquisition in vitro and in cultured cells. *Infect Immun* **71:** 1919–1928.

Sa, E.C.C., Griffiths, N.J., and Virji, M. (2010) *Neisseria meningitidis* Opc invasin binds to the sulphated tyrosines of activated vitronectin to attach to and invade human brain endothelial cells. *PLoS Pathog* **6:** e1000911.

Schaar, V., de Vries, S.P., Perez Vidakovics, M.L., Bootsma, H.J., Larsson, L., Hermans, P.W., *et al.* (2011) Multicomponent *Moraxella catarrhalis* outer membrane vesicles induce

an inflammatory response and are internalized by human epithelial cells. *Cell Microbiol* **13:** 432–449.
Schar, C.R., Blouse, G.E., Minor, K.H., and Peterson, C.B. (2008a) A deletion mutant of vitronectin lacking the somatomedin B domain exhibits residual plasminogen activator inhibitor-1-binding activity. *J Biol Chem* **283:** 10297–10309.
Schar, C.R., Jensen, J.K., Christensen, A., Blouse, G.E., Andreasen, P.A., and Peterson, C.B. (2008b) Characterization of a site on PAI-1 that binds to vitronectin outside of the somatomedin B domain. *J Biol Chem* **283:** 28487–28496.
Schvartz, I., Seger, D., and andShaltiel, S. (1999) Vitronectin. *Int J Biochem Cell Biol* **31:** 539–544.
Sharpe, S.W., Kuehn, M.J., and Mason, K.M. (2011) Elicitation of epithelial cell-derived immune effectors by outer membrane vesicles of nontypeable *Haemophilus influenzae*. *Infect Immun* **79:** 4361–4369.
Sheehan, M., Morris, C.A., Pussell, B.A., and Charlesworth, J.A. (1995) Complement inhibition by human vitronectin involves non-heparin binding domains. *Clin Exp Immunol* **101:** 136–141.
Singh, B., Su, Y.C., and Riesbeck, K. (2010a) Vitronectin in bacterial pathogenesis: a host protein used in complement escape and cellular invasion. *Mol Microbiol* **78:** 545–560.
Singh, B., Blom, A.M., Ünal, C., Nilson, B., Morgelin, M., and Riesbeck, K. (2010b) Vitronectin binds to the head region of *Moraxella catarrhalis* ubiquitous surface protein A2 and confers complement-inhibitory activity. *Mol Microbiol* **75:** 1426–1444.
Singh, B., Jalalvand, F., Morgelin, M., Zipfel, P., Blom, A.M., and Riesbeck, K. (2011) *Haemophilus influenzae* protein E recognizes the C-terminal domain of vitronectin and modulates the membrane attack complex. *Mol Microbiol* **81:** 80–98.
Stenfors, L.E., and Raisanen, S. (1992) Opsonization of middle ear bacteria during chronic suppurative and secretory otitis media. *Acta Otolaryngol* **112:** 96–101.
Stockmann, A., Hess, S., Declerck, P., Timpl, R., and Preissner, K.T. (1993) Multimeric vitronectin. Identification and characterization of conformation-dependent self-association of the adhesive protein. *J Biol Chem* **268:** 22874–22882.
Su, H.R. (1996) S-protein/vitronectin interaction with the C5b and the C8 of the complement membrane attack complex. *Int Arch Allergy Immunol* **110:** 314–317.
Su, Y.C., Wan, K.L., Mohamed, R., and Nathan, S. (2010) Immunization with the recombinant *Burkholderia pseudomallei* outer membrane protein Omp85 induces protective immunity in mice. *Vaccine* **28:** 5005–5011.
Tan, T.T., Morgelin, M., Forsgren, A., and Riesbeck, K. (2007) *Haemophilus influenzae* survival during complement-mediated attacks is promoted by *Moraxella catarrhalis* outer membrane vesicles. *J Infect Dis* **195:** 1661–1670.
Thanavala, Y., and Lugade, A.A. (2011) Role of nontypeable *Haemophilus influenzae* in otitis media and chronic obstructive pulmonary disease. *Adv Otorhinolaryngol* **72:** 170–175.
Toews, G.B., Vial, W.C., and Hansen, E.J. (1985) Role of C5 and recruited neutrophils in early clearance of nontypable *Haemophilus influenzae* from murine lungs. *Infect Immun* **50:** 207–212.
Ünal, C., Singh, B., Fleury, C., Singh, K., Chavez de Paz, L., Svensater, G., and Riesbeck, K. (2012) QseC controls biofilm formation of non-typeable *Haemophilus influenzae* in addition tp an AI-2-dependent mechanism. *Int J Med Microbiol* **302:** 261–269.
Van Zele, T., Coppieters, F., Gevaert, P., Holtappels, G., Van Cauwenberge, P., and Bachert, C. (2009) Local complement activation in nasal polyposis. *Laryngoscope* **119:** 1753–1758.
Weiser, J.N., Pan, N., McGowan, K.L., Musher, D., Martin, A., and Richards, J. (1998) Phosphorylcholine on the lipopolysaccharide of *Haemophilus influenzae* contributes to persistence in the respiratory tract and sensitivity to serum killing mediated by C-reactive protein. *J Exp Med* **187:** 631–640.
Whitby, P.W., Vanwagoner, T.M., Seale, T.W., Morton, D.J., and Stull, T.L. (2006) Transcriptional profile of *Haemophilus influenzae*: effects of iron and heme. *J Bacteriol* **188:** 5640–5645.
Williams, B.J., Morlin, G., Valentine, N., and Smith, A.L. (2001) Serum resistance in an invasive, nontypeable *Haemophilus influenzae* strain. *Infect Immun* **69:** 695–705.
Wispelwey, B., Hansen, E.J., and Scheld, W.M. (1989) *Haemophilus influenzae* outer membrane vesicle-induced blood-brain barrier permeability during experimental meningitis. *Infect Immun* **57:** 2559–2562.
Yi, K., and Murphy, T.K. (1997) Importance of an immunodominant surface-exposed loop on outer membrane protein P2 of nontypeable *Haemophilus influenzae*. *Infect Immun* **65:** 150–155.
Zhuang, P., Blackburn, M.N., and Peterson, C.B. (1996) Characterization of the denaturation and renaturation of human plasma vitronectin. I. Biophysical characterization of protein unfolding and multimerization. *J Biol Chem* **271:** 14323–14332.
Zola, T.A., Lysenko, E.S., and Weiser, J.N. (2009) Natural antibody to conserved targets of *Haemophilus influenzae* limits colonization of the murine nasopharynx. *Infect Immun* **77:** 3458–3465.
Zwahlen, A., Winkelstein, J.A., and Moxon, E.R. (1983) Participation of complement in host defense against capsule-deficient *Haemophilus influenzae*. *Infect Immun* **42:** 708–715.

Supporting information

Additional supporting information may be found in the online version of this article at the publisher's web-site.

III

MAJOR ARTICLE

Haemophilus influenzae Protein F Mediates Binding to Laminin and Human Pulmonary Epithelial Cells

Farshid Jalalvand,[1] Yu-Ching Su,[1] Matthias Mörgelin,[2] Marta Brant,[1] Oskar Hallgren,[3] Gunilla Westergren-Thorsson,[3] Birendra Singh,[1] and Kristian Riesbeck[1]

[1]Medical Microbiology, Department of Laboratory Medicine Malmö, Skåne University Hospital, Malmö; [2]Section of Clinical and Experimental Infectious Medicine, Department of Clinical Sciences, and [3]Lung Biology Unit, Department of Experimental Medical Science, Lund University, Sweden

The mucosal pathogen nontypeable *Haemophilus influenzae* (NTHi) adheres to the respiratory epithelium or, in the case of epithelial damage, to the underlying basement membrane and extracellular matrix that, among other proteins, consists of laminin. We have recently identified protein F, an ABC transporter involved in NTHi immune evasion. Homology modeling of the protein F tertiary structure revealed a strong resemblance to the streptococcal laminin-binding proteins Lbp and Lmb. Here, we show that protein F promotes binding of NTHi to laminin and primary bronchial epithelial cells. Analyses with recombinant proteins and synthetic peptides revealed that the N-terminal part of protein F contains the host-interacting region. Moreover, protein F exists in all clinical isolates, and isogenic NTHi Δ*hpf* mutants display significantly reduced binding to laminin and epithelial cells. We thus suggest protein F to be an important and ubiquitous NTHi adhesin.

Keywords. ABC transporter; adhesion; laminin; nontypeable *Haemophilus influenzae*; protein F; pulmonary epithelial cells; respiratory tract infection; virulence.

Nontypeable *Haemophilus influenzae* (NTHi) is a gram-negative opportunistic pathogen that colonizes the nasopharynx of humans. It is one of the leading causes of bacterial respiratory tract infections, such as acute otitis media in children and bronchitis, as well as exacerbations in patients with chronic obstructive pulmonary disease (COPD) [1–3]. To prevent clearance by the ciliated respiratory tract mucosal epithelium an important initial step of bacterial colonization is adherence to host tissue [4]. In patients with disruption of the epithelial integrity caused by viral infections, mechanical damage, or chronic inflammation, the underlying basement membrane is exposed to the lumen and forms a viable attachment site for pathogens [5].

The heterotrimeric glycoprotein laminin (Ln; approximately 800 kDa) is one of the major constituents of the extracellular matrix (ECM) and the basement membrane. It is involved in an array of physiological functions, such as cellular proliferation, migration, and structural scaffolding in tissues [6–8]. During bacterial pathogenesis, Ln is frequently targeted for adherence by respiratory tract pathogens [9–16]. NTHi has previously been reported to bind Ln via the *Haemophilus* adhesion and penetration protein (Hap) and protein E (PE) [17, 18]. In parallel, Hap and PE interact with host epithelial cells [19, 20]. These interactions are thus multifactorial and involve several adhesins that mutually promote bacterial host-adhesion.

We recently identified a virulence factor in NTHi that we designated as protein F (PF; Su et al, unpublished data). PF (approximately 30 kDa) is annotated as a bacterial metal-binding receptor, belonging to the adenosine triphosphate–binding cassette (ABC) transporter family. During structural analysis of PF, we noticed a strong structural resemblance to the

Received 5 June 2012; accepted 3 October 2012; electronically published 10 December 2012.

Correspondence: Kristian Riesbeck, MD, Medical Microbiology, Department of Laboratory Medicine Malmö, Lund University, Skåne University Hospital, SE-205 02 Malmö, Sweden (kristian.riesbeck@med.lu.se).

The Journal of Infectious Diseases 2013;207:803–13

DOI: 10.1093/infdis/jis754

Ln-binding proteins of *Streptococcus pyogenes* (Lbp) and *Streptococcus agalactiae* (Lmb) [21, 22]. The structural similarity raised a hypothesis regarding the potential Ln-binding capacity of PF. In the present study, we show that PF is a novel surface-exposed Ln-binding protein that also promotes NTHi adherence to host epithelial cells. This is the first report that shows a direct interaction between a gram-negative ABC transporter protein and host components.

METHODS

Bacteria, Eukaryotic Cells, Culture Conditions, and Reagents

NTHi 3655 wild-type (wt), Δ*hap*, and Δ*pe* mutants, and clinical isolates KR217, KR314, KR315, KR336, KR385 obtained by nasopharyngeal swabbing from patients with upper respiratory tract infection, were cultured as described elsewhere [17]. Chloramphenicol (10 μg/mL) was used for selection of Δ*hpf* mutants. *Escherichia coli* BL21 (DE3; Novagen) and DH5α (Invitrogen) were cultured in Luria-Bertani broth and solid-phase medium supplemented with kanamycin (50 μg/mL) or ampicillin (100 μg/mL). The type II alveolar A549 (American Type Culture Collection [ATCC] CCL-185) and bronchial epithelial NCI H292 (ATCC CRL-1848) cell lines were cultured in F-12 and Roswell Park Memorial Institute medium (Gibco), respectively, with 10% fetal calf serum. Primary bronchial epithelial cells were obtained from a healthy adult donor with no history of lung disease. This protocol was approved by the Swedish Research Ethical Committee in Lund (FEK 413/2008), and written consent was obtained from the closest relatives. Cells were maintained in BEGM medium (Clonetics). All bacteria and human cells were cultured at 37°C with 5% CO_2. Anti-PF polyclonal antibodies (pAb) were raised in rabbits and affinity purified using recombinant PF (rPF) or PF peptides [23].

Structural Modeling and Bioinformatic Analyses

Modeling of PF was performed using the Swiss-Model automated server against homologous templates available in the Protein Data Bank (PDB; available at: http:/www.rcsb.org). Homologs were analyzed with BLAST (available at: http://www.ncbi.nlm.nih.gov/), and multiple alignment was performed using ClustalW (available at: http://www.ebi.ac.uk/). Three-dimensional models were prepared using PyMOL (available at: http://www.pymol.org/).

Construction of NTHi Δ*hpf* Mutants

Upstream (621 bp) and downstream (997 bp) flanking regions of the *hpf* gene (CGSHi3655_02309) from NTHi 3655 genomic DNA (GenBank accession number AAZF00000000) and *cat* (chloramphenicol acetyltransferase; BAA78807) from pLysS (Novagen) were amplified (Supplementary Table 1). Thereafter, we produced a linear knockout vector, inserting *cat* between the flanking regions, using an overlap extension polymerase chain reaction (Supplementary Figure 1). The *hpf* gene in NTHi 3655, clinical isolates, and the isogenic NTHi 3655 Δ*pe* was mutated as described elsewhere [24].

Recombinant Proteins and Peptides

We amplified full-length and truncated fragments of NTHi 3655 *hpf*, using specific primers (Supplementary Table 1). Restriction sites were introduced as indicated. pET26(b)+ (for purified recombinant proteins) or pET16b (Novagen; for surface expression of PF) were used and transformed into *E. coli* DH5α, followed by transformation into *E. coli* BL21 (DE3). Recombinant proteins were produced as described previously [25]. Peptides (approximately 25 amino acids long) spanning the entire mature PF and overlapping with neighboring peptides were from Innovagen. The radiolabeled peptide-binding assay was performed as described elsewhere [26].

Flow Cytometry and Transmission Electron Microscopy

For flow cytometry, stationary phase bacteria (10^9 colony forming units/mL) were washed and resuspended in phosphate buffered saline (PBS) containing 1% bovine serum albumin (BSA) followed by addition of Ln (Engelbreth-Holm-Swarm murine sarcoma basement membrane, Sigma-Aldrich). The samples were incubated at 37°C for 1.5 hours. Bacteria were thereafter washed in PBS plus 1% BSA and were incubated with rabbit anti-Ln pAb (Sigma-Aldrich). After washing, fluorescein isothiocyanate–conjugated swine anti-rabbit pAb (Dako) were added. Finally, bacteria were analyzed by flow cytometry (EPICS XL-MCL, Beckman Coulter). Ten thousand events were measured for each sample. Transmission electron microscopy (TEM) was performed as described previously [17].

Bacterial Adherence Assays

Adherence of NTHi to immobilized Ln was studied by bacterial probing over Ln-coated glass slides [17]. NTHi adherence to mammalian cell lines and primary cells was analyzed using [^{3}H]-thymidine-pulsed bacteria as described elsewhere [19]. Blocking was conducted with 20 μg of antibodies per well.

Enzyme-Linked Immunosorbent Assay (ELISA)

Laminin binding to rPF fragments was studied with an indirect ELISA as described previously [17]. Recombinant truncated PF fragments (50 nM) and synthetic PF peptides (1 μM) were immobilized on polysorp microtiter plates (Nunc). Blocking was done with PBS containing 5% milk for 1 hour at room temperature. For the binding-inhibition assay, Ln (10 nM) was preincubated with PF peptides (0–5 μM) at 37°C for 1.5 hours. The suspension was thereafter transferred to plates coated with rPF^{12-293}, and the binding was measured as described above. In the direct cell ELISA, cells were grown to confluency in 96-well plates (Nunc) and fixed with 2% formaldehyde for 30 minutes at room temperature. Thereafter, cells were incubated with PF and, subsequently, rabbit anti-PF

pAb. Horseradish peroxidase-conjugated anti-rabbit pAb (Dako) was used as the secondary layer for all ELISA.

Statistical Analyses

We used the Student *t* test and Mann–Whitney *U* test for statistical analyses of 2 parametrical sets of data and 2 nonparametric sets of data, respectively. Two-way analysis of variance was used for statistical analyses of several sets of data. Statistical analyses were performed using GraphPad Prism 5 (GraphPad Software). A *P* value of $\leq .05$ was considered statistically significant.

RESULTS

PF Is Surface Associated and Has a Tertiary Structure Similar to That of Streptococcal Laminin-Binding Proteins

We have recently identified PF, an NTHi protein involved in serum resistance (Su et al, unpublished data). The *hpf* gene encodes an uncharacterized 30-kDa iron-chelating protein and is one of 4 structural genes in an ABC transporter operon. The operon is present in all 20 available NTHi genomes in GenBank and is highly conserved (>98% identity; data not shown). To experimentally examine the subcellular localization of PF and determine whether it is exposed on the bacterial surface, we constructed an isogenic NTHi 3655 Δ*hpf* mutant (Supplementary Figure 1*A*). The physiological fitness of the mutant did not differ from the parental strain with regard to the whole cell protein profile, but a slightly slower growth was observed in soluble medium (data not shown). Transcription analysis showed that the other genes in the operon remained actively expressed in the isogenic mutant (data not shown). By use of TEM, gold-labeled anti-PF pAb recognized PF at the surface of NTHi 3655, but it did not recognize the PF-deficient mutant (Figure 1*A*). Since the affinity-purified anti-PF pAb were highly specific for PF (Supplementary Figure 1*B*), this experiment suggested that PF is a surface-exposed protein.

To elucidate the characteristics of the protein, we analyzed the tertiary structure of PF by using homology modeling. The manganese-binding protein MntC of cyanobacteria *Synechocystis* species (PDB code 1XVL) was found to be the closest structure-solved homolog with a 343-bit alignment score (52.1% identity/67.0% similarity) and was therefore used as the modeling template. The superimposition of PF with MntC is shown in Figure 1*B*. The structural model revealed that PF is constituted by distinct N- and C-terminal globular domains that are interlinked by a long helix backbone. A metal-binding active site is present between both lobes. Since the Ln-binding proteins Lbp, of *S. pyogenes* (PDB code 3GI1), and Lmb, of *S. agalactiae* (PDB code 3HJT), belong to the same bacterial ABC transporter family, we superimposed PF with their crystal structures. Interestingly, despite the weak primary sequence similarity (Lbp, 28.3% identity/46.9% similarity; Lmb, 28.0% identity/46.3% similarity), we observed a strong resemblance in the secondary structure and folding of PF and Lbp/Lmb (Figure 1*C*) [21].

PF Is a Ubiquitous Laminin-Binding Protein of *H. influenzae*

The structural resemblance between PF and Lbp/Lmb prompted us to investigate the potential Ln-binding capacity of PF. To study the PF-Ln interaction at the bacterial surface, we incubated NTHi 3655 wild-type and the PF-deficient NTHi 3655 Δ*hpf* with increasing concentrations of soluble Ln. The unbound Ln fraction was thereafter washed away, and bacterial Ln binding was analyzed by flow cytometry. Our data showed that the isogenic Δ*hpf* mutant bound significantly less Ln as compared to the NTHi 3655 wild-type ($P \leq .05$; Figure 2*A* and 2*C*).

To prove the Ln-binding property of PF at the bacterial surface, we introduced the *hpf* open reading frame into a heterologous *E. coli* host. After induction of *hpf* expression, we observed a Ln-binding phenotype in the PF-producing *E. coli*, compared with the control *E. coli* containing the empty plasmid (Figure 2*B* and 2*C*). Further analysis of the Ln interaction at the bacterial surface was conducted using TEM. The isogenic NTHi 3655 Δ*hpf* showed a marked reduction in Ln binding as compared to the parental strain (Figure 2*D*). Moreover, co-localization of gold-labeled Ln (10 nm) and PF (detected by gold-labeled anti-PF pAb; 5 nm) was observed at the surface of both PF-producing NTHi 3655 and *E. coli* (Figure 2*E*).

To study the functional bacterial binding to immobilized Ln, which is more representative of the in vivo basement membrane, Ln was coated on glass slides and incubated with various samples of NTHi and *E. coli* adjusted to the same cell density (optical density at 600 nm = 1.0). NTHi 3655 Δ*hpf* displayed a markedly weaker adherence to immobilized Ln as compared to the NTHi 3655 wild-type (Figure 2*F*). In parallel, PF-producing *E. coli* adhered to the Ln-coated glass slides, whereas the control *E. coli* did not. Taken together, the co-localization of PF and Ln at the surface of NTHi 3655, in addition to the PF-dependent Ln binding of heterologous host *E. coli,* suggest that PF is directly involved in Ln binding at the bacterial surface.

We further wanted to evaluate the Ln-interacting role of PF in a series of clinical NTHi isolates from patients with upper respiratory tract infection. PF-deficient mutants were produced in 5 clinical isolates, and Ln binding was assessed by flow cytometry (Figure 3*A*). A consistent decrease in Ln binding was observed in all strains in the absence of PF. The results indicate that PF is important for the NTHi-Ln interaction in several clinical isolates.

PF Contributes to the Multifactorial NTHi-Dependent Laminin Binding

Currently, there have been 2 reports regarding Ln-binding proteins in NTHi [17, 18]. To evaluate the relevance of PF in

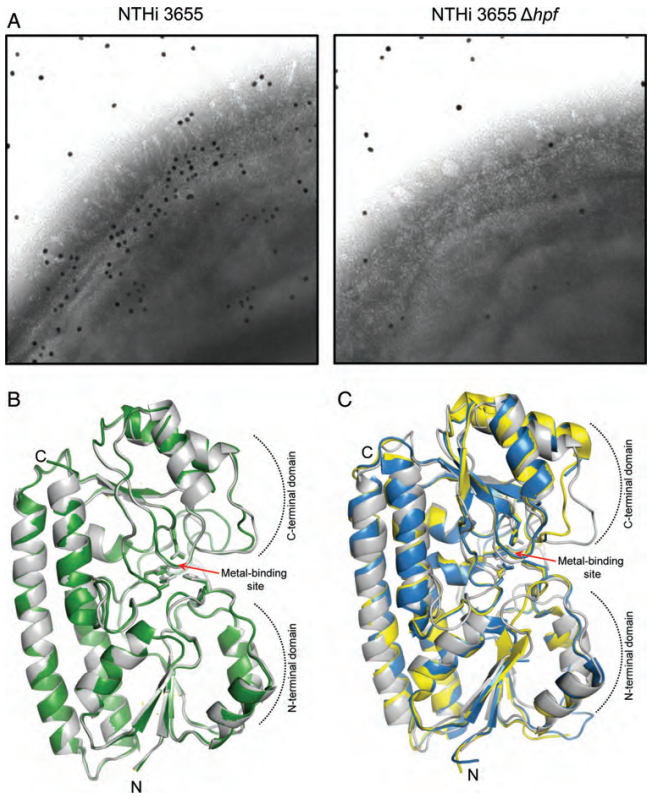

Figure 1. Subcellular localization of protein F (PF) and the structural model of the protein. *A*, Gold-labeled anti-PF polyclonal antibodies recognize PF at the nontypeable *Haemophilus influenzae* (NTHi) 3655 surface but not at the surface of the isogenic PF-deficient NTHi 3655 Δ*hpf* mutant, as revealed by transmission electron microscopy. *B*, Superimposed model of PF (grey) with the template MntC of *Synechocystis* species (Protein Data Bank code 1XVL) shown in green (52.1% identity and 67.0% similarity). *C*, Superimposition of PF (grey) with *Streptococcus pyogenes* laminin-binding protein (blue) and *Streptococcus agalactiae* laminin-binding protein (yellow). N- and C-terminal domains are indicated, with the metal ion-chelating active site residues shown in sticks, situated between both domains. Figures were prepared using PyMOL.

comparison to PE and Hap for the NTHi-Ln interaction, NTHi 3655 wild-type and knockout mutants were incubated with soluble Ln, and binding was measured with flow cytometry (Figure 3*B*). Our data demonstrated that all mutants had decreased Ln binding as compared to their wild-type counterparts, showing that PE, Hap, and PF contribute to the Ln interaction.

The N-terminal Region Lys23-Glu48 of PF Interacts With the C-terminus of the Laminin α-Chain

To study the PF-Ln interaction at the molecular level, a series of recombinant PF (rPF) fragments were produced (Figure 4*A* and Supplementary Table 2). The putative Ln-binding region of PF was determined by incubating immobilized truncated rPF fragments with increasing concentrations of Ln. Recombinant $PF^{12\text{-}293}$ and $rPF^{12\text{-}98}$ bound significantly better when compared to the nonbinding fragment $rPF^{61\text{-}144}$ ($P \leq .001$; Figure 4*B*). The N-terminal $rPF^{12\text{-}98}$ also exhibited saturable and dose-dependent Ln binding, whereas no binding to the negative control fragment $rPF^{129\text{-}177}$ was detected (Figure 4*C*).

The Ln-binding region of PF was further analyzed in detail by using 13 synthetic peptides that span the entire PF molecule (Figure 5*A*). $PF^{23\text{-}48}$ was identified as the major Ln-binding region ($P \leq .001$) in an indirect ELISA. Moreover, $PF^{23\text{-}48}$ exhibited saturable and dose-dependent binding to Ln, whereas the non–Ln-binding peptide $PF^{124\text{-}148}$ did not (Figure 5*B*). The specificity of the interaction with Ln was evaluated with a binding inhibition assay in which Ln was preincubated with various PF peptides prior to addition to

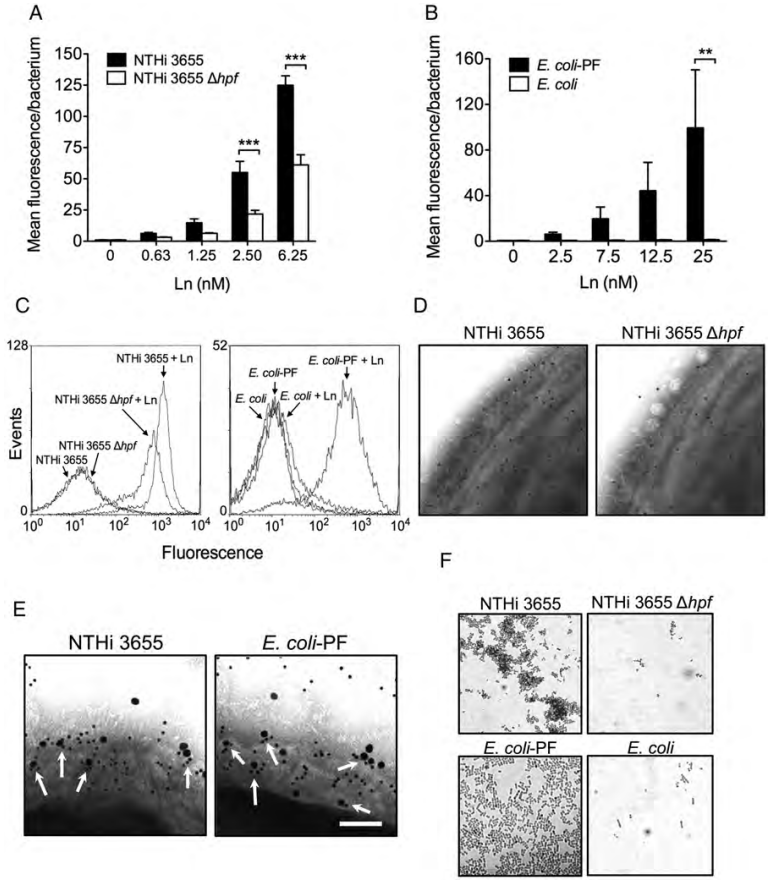

Figure 2. Protein F (PF) mediates laminin (Ln) binding at the surface of bacteria. *A* and *B*, Flow cytometry analysis shows significant differences in the Ln binding of nontypeable *Haemophilus influenzae* (NTHi) 3655 wild-type and NTHi 3655 Δ*hpf* (*A*) and PF-producing *Escherichia coli* (*B*) acquire previously nonexistent Ln binding, as measured by mean fluorescence intensity/bacterium. *E. coli* containing an empty plasmid was used as a control. The mean of 3 separate experiments is plotted, and error bars indicate the standard error of mean (*A* and *B*). Statistical analysis was performed using 2-way analysis of variance, and $P \leq .05$ was considered statistically significant. $^{**}P \leq .01$; $^{***}P \leq .001$. *C*, Histogram of a data set from *A* and *B*. *D*, Transmission electron microscopy shows a marked decrease of bound Ln (gold-labeled) at the surface of NTHi 3655 Δ*hpf* as compared to the parental wild-type strain. *E*, Arrows point to bound gold-labeled Ln (10 nm) that is colocalized with PF detected by gold-labeled anti-PF polyclonal antibodies (5 nm) at the bacterial surface. The bar indicates 100 nm. *F*, PF promotes NTHi 3655 and *E. coli*-PF adherence to immobilized Ln in a basement membrane-mimicking setting, whereas non–PF-producing bacteria are seen to exhibit markedly less binding to the Ln-coated surface.

microtiter plates coated with $rPF^{12\text{-}293}$ (Figure 5*C*). The peptide $PF^{23\text{-}48}$ inhibited Ln binding to $rPF^{12\text{-}293}$, proving that the $PF^{23\text{-}48}$-Ln interaction was specific. Although $PF^{184\text{-}209}$ bound Ln (Figure 5*A* and 5*B*), the peptide did not inhibit Ln binding to immobilized $rPF^{12\text{-}293}$ (Figure 5*C*). The N-terminal peptide $PF^{23\text{-}48}$ was thus identified as the main Ln-binding region.

To determine the PF-binding domain of the Ln molecule, TEM with Ln and gold-labeled $rPF^{12\text{-}293}$ was conducted. As seen in Figure 5*D*, PF consistently bound to the C-terminal part of the cruciform Ln molecule. When the length of the molecule was measured, PF appeared to bind to the C-terminal globular domains (LG1–5) of the Ln α-chain (Figure 5*D* and 5*E*). We conclude that the N-terminal region of PF interacts with the C-terminus of the Ln α-chain, as revealed by the peptide mapping approach and TEM.

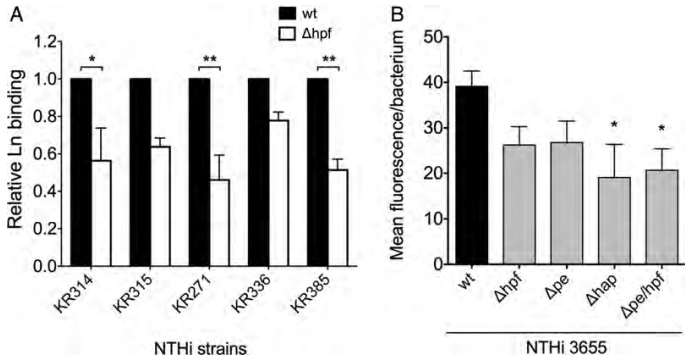

Figure 3. Protein F (PF) mediates laminin (Ln) binding in clinical isolates and contributes to the nontypeable *Haemophilus influenzae* (NTHi)–dependent Ln binding by an interaction analogous to that of PE and Hap. *A*, Flow cytometry analysis show that 5 clinical isolates display markedly decreased Ln-binding capacity when PF is knocked out, compared with the PF-producing parental wild-type (wt) strains. *B*, Comparison of PF-, PE-, and Hap-deficient mutants shows that the absence of all 3 proteins causes a decline in Ln binding (Ln concentration, 2.5 nM). The mean of 3 separate experiments is plotted in both graphs, error bars indicate the standard error of mean, and statistical differences are between wild-type and mutants. Statistical analysis was performed using analysis of variance, and $P \leq .05$ was considered statistically significant. $^{*}P \leq .05$; $^{**}P \leq .01$.

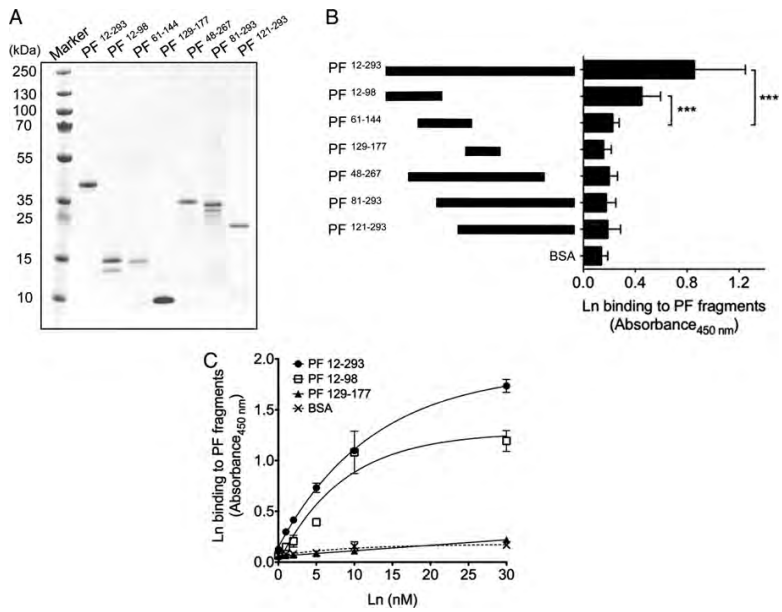

Figure 4. Recombinant protein F (rPF) binds laminin (Ln) via a region in $PF^{12\text{-}98}$. *A*, Results of Coomassie-stained sodium dodecyl sulfate polyacrylamide gel electrophoresis, showing the affinity purified recombinant truncated PF-fragments. *B* and *C*, $rPF^{12\text{-}98}$ contains the Ln-binding region and binds to Ln in a dose-dependent and saturable manner. Statistical analysis was performed using the Mann–Whitney *U* test. The mean of 3 separate experiments is plotted in *B*. In *C*, 1 set of data from 3 similar experiments is shown. Error bars indicate the standard error of mean in all experiments.

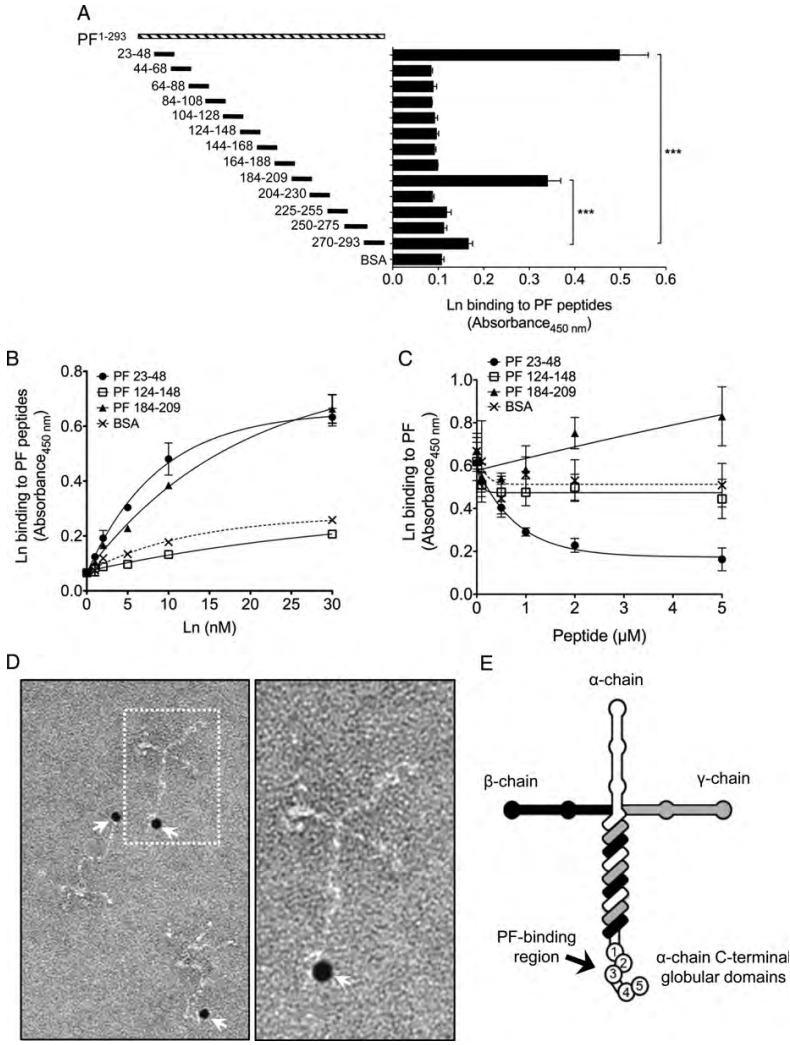

Figure 5. Protein F $(PF)^{23-48}$ interacts with the C-terminus of the cruciform laminin (Ln) macromolecule α-chain. *A*, To more precisely define the Ln-binding region of PF, a series of synthetic peptides spanning the entire PF molecule were produced. Two potential Ln-binding regions, PF^{23-48} (consistent with the data from the recombinant fragments) and $PF^{184-209}$, were identified using an indirect enzyme-linked immunosorbent assay. *B*, Ln binds to PF^{23-48} and, to a lesser degree, $PF^{184-209}$ in a dose-dependent and saturable manner. *C*, Only PF^{23-48} binds specifically to Ln and inhibits the interaction with recombinant PF (rPF^{12-293}). *D*, Electron microscopy showing gold-labeled rPF^{12-293} binding to the Ln α-chain C-terminus (as indicated by white arrows). *E*, Schematic representation of the Ln hetereotrimer, showing the α-, β-, and γ-chains that form the cruciform molecule. The PF-binding α-chain C-terminal globular domains are indicated by an arrow. Statistical analysis was performed using the Mann–Whitney *U* test, and error bars indicate the standard error of the mean for all experiments. The mean of 3 separate experiments are shown in *A* and *C*, whereas 3 separate experiments were performed with the same outcome for *B*, of which 1 set of data is shown. $P \leq .05$ was considered statistically significant. $^{***}P \leq .001$.

PF Mediates Adhesion of NTHi to Pulmonary Epithelial Cells via a Conserved N-Terminal Domain

Since several bacterial Ln-binding proteins, including the aforementioned PE, Hap, Lmb, and Lbp, have been reported to interact with epithelial cells [15, 19, 20, 27, 28], we analyzed the cell-adhesive capacity of PF. Epithelial cells were immobilized on a solid surface and incubated with increasing concentrations of rPF^{12-293} (Figure 6*A*). Recombinant PF bound to both NCI H292 and A549 cell lines in a dose-dependent and saturable manner. To evaluate the influence of PF on bacterial adhesion, NTHi 3655 wild-type and the PF-deficient Δ*hpf* mutant were pulsed with [^{3}H]-thymidine and incubated with pulmonary epithelial cells, and adhesion was measured after washing (Figure 6*B*). The adherence of NTHi 3655 Δ*hpf* to NCI H292 and A549 was reduced by 32.9% and 64%, respectively, compared with the PF-producing wild-type. Importantly, the isogenic mutant also showed a significant reduction (36.6%) in binding to primary bronchial epithelial cells obtained from a healthy adult donor ($P \leq .05$; Figure 6*B*).

To investigate the putative cell-adhesive region of PF, cell lines were probed with iodine-labeled synthetic PF peptides, followed by washes and measurement of binding (Figure 6*C*). Interestingly, the Ln-binding region PF^{23-48} (Figure 5*A*) also displayed the strongest binding to epithelial cells. Moreover, the bacterial-host cell interaction was significantly reduced ($P \leq .05$) when bacteria were preincubated with anti-PF^{23-48} pAb but not with the control anti-PF^{44-68} (Figure 6*D*). These results thus suggest that NTHi uses the same N-terminal PF region for both binding to Ln and attachment to epithelial cells.

Bioinformatic analyses and a detailed database search using BLAST showed that PF orthologs exist in a number of other pathogens. The partial alignment of PF^{23-48} with these is shown in Figure 7*A*. The orthologs present in several members of the family Pasteurellaceae and in other pathogens, such as *Eikenella corrodens* and *Yersinia pestis,* have highly similar N-termini (Figure 7*A*). In addition, *S. pyogenes* and *S. agalactiae* Lbp/Lmb N-terminal sequences display partial similarity to PF^{23-48} (Figure 7*B*). The 3D model of the cell- and Ln-binding region was analyzed in detail and revealed to comprise 2 β-sheets and 1 α-helix, connected by 3 loops (Figure 7*C*). Amino acid residues Lys23 and Lys25 in loop-1, Gln34, Asp35, Gln38, Asn39, and Asn43 in the α-helix, and Thr46 and Glu48 in β-sheet 2 are exposed on the protein surface, as predicted by the model (Figure 7*D* and 7*E*). Thus,

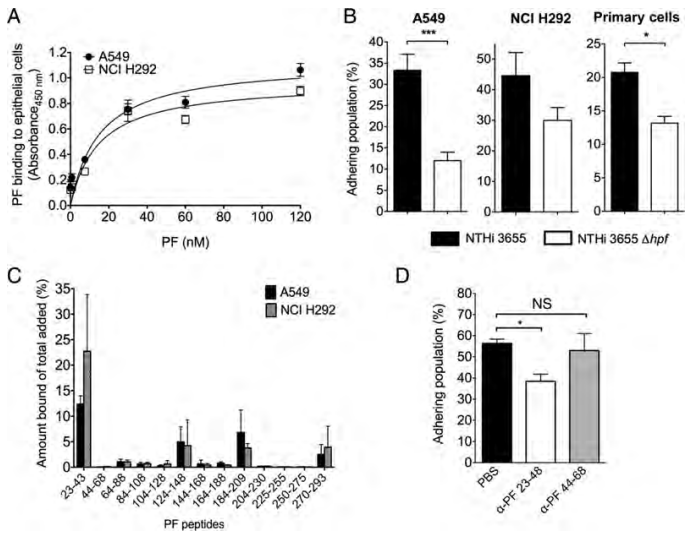

Figure 6. Protein F (PF) promotes nontypeable *Haemophilus influenzae* (NTHi) adherence to pulmonary epithelial cells via the N-terminus. *A,* A direct enzyme-linked immunosorbent assay shows that PF binds to fixed and immobilized NCI H292 and A549 in a saturable and dose-dependent manner. *B,* Deletion of *hpf* results in a marked decrease in the adhesion of NTHi to pulmonary epithelial cell lines, as well as to primary bronchial epithelial cells from a healthy adult donor. *C,* PF^{23-48} shows the strongest binding to both cell lines, as revealed by a radiolabeled peptide adherence assay. *D,* The NTHi interaction with A549 cells can be inhibited by epitope-specific anti-PF^{23-48} polyclonal antibodies but not with anti-PF^{44-68}. The mean of 3 separate experiments is used for all panels, and error bars indicate the standard error of the mean in all experiments. The Student *t* test was used for statistical analyses in panel *B* and for analysis of variance in panel *D*. $P \leq .05$ was considered statistically significant. $^*P \leq .05$; $^{***}P \leq .001$. Abbreviation: NS, not significant.

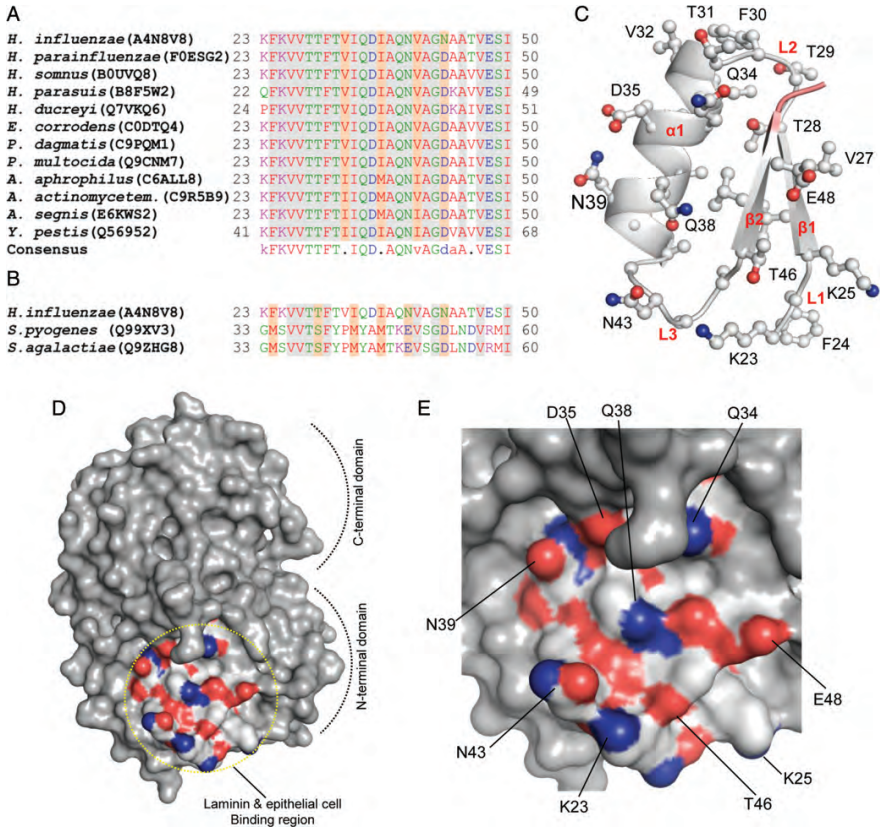

Figure 7. Bioinformatic analyses of protein F $(PF)^{23-48}$. *A*, PF homologs are present in other pathogens of the Pasteurellaceae family, including *Haemophilus parainfluenzae, Haemophilus somnus, Haemophilus parasuis, Haemophilus ducreyi, Pasteurella dagmatis, Pasteurella multocida, Aggregatibacter aphrophilus, Aggregatibacter segnis, Actinobacillus actinomycetemcomitans,* as well as *Yersinia pestis* and Eikenella corrodens belonging to other families. Partial alignment shows the highly conserved nature of the laminin (Ln)–binding region. *B*, Alignment of PF^{23-48} with Lbp and Lmb of *Streptococcus pyogenes* and *Streptococcus agalactiae*, respectively. *C*, A cartoon of PF^{23-48} with numbered β-sheets, α-helix, and loops with their side chains shown as a ball-and-stick model. *D*, The surface of the PF molecule. The Ln-binding region (encircled) is shown with colors indicating the charge distribution (blue represents positively charged and red negatively charged residues at the surface). E, The PF^{23-48} surface (encircled in C) is zoomed in. Figures were prepared using PyMOL.

the structural analysis shows that the experimentally defined host component-binding region Lys23-Glu48 contains several conserved and charged residues that are accessible for interaction with Ln and host epithelial cells.

DISCUSSION

NTHi has recently been reported to bind to ECM proteins such as Ln and vitronectin [17, 18, 29]. Here, we report that the NTHi ABC transporter protein PF to be a novel Ln- and cell-binding adhesin. ABC transporters constitute a large family of proteins that play important roles for bacterial pathogenesis [30]. Although previous reports have suggested similar proteins to be implicated in interactions between gram-negative bacteria and the host [31–35], this is the first study that shows a gram-negative ABC transporter protein directly mediating bacterial adherence to host components.

NTHi primarily colonizes the upper respiratory tract of humans and causes a range of airway infections. A significant rise in the occurrence of invasive NTHi infections has recently been observed, possibly due to a niche opening after the introduction of a capsule polysaccharide-conjugate vaccine against

H. influenzae serotype b [36, 37]. To disseminate from the primary site of infection, bacteria need to colonize and breach the basement membrane barrier. Pathogen interactions with ECM proteins are particularly important after epithelial disruption (such as that due to chronic inflammation and viral infections), which leaves the basement membrane exposed [5]. This is supported by the fact that NTHi infections are commonly identified in patients with COPD or during coinfections with viral pathogens [3, 38, 39]. Other respiratory tract pathogens, such as *S. pneumoniae, S. pyogenes, Moraxella catarrhalis,* and *Mycobacterium* species, have also been reported to interact with Ln and thereby augment their virulence [9–16]. Binding to ECM components such as Ln is thus most likely an important mechanism for bacterial pathogenesis.

In the present study, NTHi Δ*hpf* mutants were shown to lose a significant part of their Ln-binding capacity as compared to the parental PF-producing wild-type strains. Moreover, expression of *hpf* in the heterologous host *E. coli* verified the role of PF as a Ln-binding protein, and colocalization of PF and Ln could be observed at the surface of PF-producing bacteria. In addition, rPF was shown to bind to both alveolar and bronchial epithelial cell lines, and NTHi 3655 Δ*hpf* had a significant reduction in adherence to the cells as compared to the parental wild-type strain. Since NTHi 3655 Δ*hpf* also displayed a significant loss of binding to primary cells, our collective data indicate that PF may be clinically relevant for the course of infection by promoting bacterial adherence to the host epithelium and basement membrane during colonization.

The NTHi adhesins PE (a 16-kDa lipoprotein) and Hap (a 155-kDa autotransporter) have previously been shown to interact with Ln [17, 18]. These proteins share no structural or primary sequence similarity with PF or each other, demonstrating the multifariousness of the NTHi-Ln interaction. We show that PF contributes to NTHi Ln binding to approximately the same degree as PE and Hap (Figure 3*B*). Furthermore, our data show that PF interacts with the C-terminus of the Ln α-chain (Figure 5*D* and 5*E*), the same region that PE binds to [17]. Because PE and PF are not similar, these data could possibly hint at a general pathogen-specific binding region in the Ln molecule. The presence of additional Ln-binding factors in NTHi remains to be elucidated.

PF (also annotated as a *Y. pestis yfeA* homologue) has been identified among other *H. influenzae* proteins to be upregulated during physiological conditions [40, 41]. Culturing NTHi in sputum obtained from COPD patients resulted in a 3.9-fold increase in PF concentration. Moreover, during heme- and iron-restricted growth, *H. influenzae* Rd KW20 was reported to enhance the *hpf*-operon transcription up to 11.8-fold. As the iron-concentration is low in the epithelial mucosa [42], an iron-dependent upregulation of PF may enhance the adhesive capacity of NTHi during the initial colonization of the host. These data suggest that PF is important for NTHi in vivo, possibly mediating adherence and metal ion transport.

The 30-kDa PF shares a strong structural resemblance with streptococcal Ln-binding proteins Lbp and Lmb (Figure 1*B*), although the primary sequence similarities are relatively weak. Preliminary unpublished data from our laboratory indicate that PF chelates Zn^{2+} via an interaction analogous to that of Lbp/Lmb [21, 22]. Assuming that the proteins share the same Ln-binding mechanism, the interactions could either be mediated by several separate but conserved sites in the tertiary structure, or they could be confined to a small local region that is highly similar in both proteins. Concurrent Zn^{2+}-binding can be an additional mechanism, as has been suggested for *S. pyogenes* Lbp [21], since Ln is also known to bind Zn^{2+} [43]. However, we found that the PF-Ln interaction was unaffected by the divalent cation binding of PF (data not shown), suggesting that the mechanism behind the PF Ln binding is a protein-protein interaction.

In conclusion, PF is characterized as a novel NTHi adhesin that mediates binding to the basement membrane glycoprotein Ln, as well as to human pulmonary epithelial cells. Our data shed light on the host colonization strategies of the multifaceted and important respiratory tract pathogen NTHi and will be the impetus for further studies.

Supplementary Data

Supplementary materials are available at *The Journal of Infectious Diseases* online (http://jid.oxfordjournals.org/). Supplementary materials consist of data provided by the author that are published to benefit the reader. The posted materials are not copyedited. The contents of all supplementary data are the sole responsibility of the authors. Questions or messages regarding errors should be addressed to the author.

Notes

Financial support. This work was supported by the Alfred Österlund, the Anna and Edwin Berger, the Greta and Johan Kock, the Gyllenstiernska Krapperup, the Åke Wiberg, the Hans Hierta, and the Marianne and Marcus Wallenberg Foundations; the Swedish Medical Research Council (grant 521-2010-4221); the Cancer Foundation at the University Hospital in Malmö; the Physiographical Society (Forssman's Foundation); and Skåne County Council's research and development foundation.

Potential conflicts of interest. All authors: No reported conflicts.

All authors have submitted the ICMJE Form for Disclosure of Potential Conflicts of Interest. Conflicts that the editors consider relevant to the content of the manuscript have been disclosed.

References

1. Murphy TF, Faden H, Bakaletz LO, et al. Nontypeable *Haemophilus influenzae* as a pathogen in children. Pediatr Infect Dis J **2009**; 28:43–8.
2. Hallstrom T, Riesbeck K. *Haemophilus influenzae* and the complement system. Trends Microbiol **2010**; 18:258–65.
3. Moghaddam SJ, Ochoa CE, Sethi S, Dickey BF. Nontypeable *Haemophilus influenzae* in chronic obstructive pulmonary disease and lung cancer. Int J Chron Obstruct Pulmon Dis **2011**; 6:113–23.
4. Janson H, Carl n B, Cervin A, et al. Effects on the ciliated epithelium of protein D-producing and -nonproducing nontypeable *Haemophilus influenzae* in nasopharyngeal tissue cultures. J Infect Dis **1999**; 180: 737–46.

5. Strieter RM, Mehrad B. New mechanisms of pulmonary fibrosis. Chest **2009**; 136:1364–70.
6. Singh B, Fleury C, Jalalvand F, Riesbeck K. Human pathogens utilize host extracellular matrix proteins laminin and collagen for adhesion and invasion of the host. FEMS Microbiol Rev **2012**; 36:1122–80.
7. Durbeej M. Laminins. Cell Tissue Res **2010**; 339:259–68.
8. Yurchenco PD. Basement membranes: cell scaffoldings and signaling platforms. Cold Spring Harb Perspect Biol **2011**; 3: a004911.
9. Caswell CC, Oliver-Kozup H, Han R, Lukomska E, Lukomski S. Scl1, the multifunctional adhesin of group A *Streptococcus*, selectively binds cellular fibronectin and laminin, and mediates pathogen internalization by human cells. FEMS Microbiol Lett **2010**; 303:61–8.
10. Hytonen J, Haataja S, Gerlach D, Podbielski A, Finne J. The SpeB virulence factor of *Streptococcus pyogenes*, a multifunctional secreted and cell surface molecule with strepadhesin, laminin-binding and cysteine protease activity. Mol Microbiol **2001**; 39:512–9.
11. Tan TT, Forsgren A, Riesbeck K. The respiratory pathogen *Moraxella catarrhalis* binds to laminin via ubiquitous surface proteins A1 and A2. J Infect Dis **2006**; 194:493–7.
12. Hilleringmann M, Giusti F, Baudner BC, et al. Pneumococcal pili are composed of protofilaments exposing adhesive clusters of Rrg A. PLoS Pathog **2008**; 4:e1000026.
13. Alteri CJ, Xicohtencatl-Cortes J, Hess S, Caballero-Olin G, Giron JA, Friedman RL. *Mycobacterium tuberculosis* produces pili during human infection. Proc Natl Acad Sci U S A **2007**; 104:5145–50.
14. Pethe K, Bifani P, Drobecq H, et al. Mycobacterial heparin-binding hemagglutinin and laminin-binding protein share antigenic methyllysines that confer resistance to proteolysis. Proc Natl Acad Sci U S A **2002**; 99:10759–64.
15. Terao Y, Kawabata S, Kunitomo E, Nakagawa I, Hamada S. Novel laminin-binding protein of *Streptococcus pyogenes*, Lbp, is involved in adhesion to epithelial cells. Infect Immun **2002**; 70:993–7.
16. Ouattara M, Cunha EB, Li X, Huang YS, Dixon D, Eichenbaum Z. Shr of group A *streptococcus* is a new type of composite NEAT protein involved in sequestering haem from methaemoglobin. Mol Microbiol **2010**; 78:739–56.
17. Hallstrom T, Singh B, Resman F, Blom AM, Morgelin M, Riesbeck K. *Haemophilus influenzae* protein E binds to the extracellular matrix by concurrently interacting with laminin and vitronectin. J Infect Dis **2011**; 204:1065–74.
18. Fink DL, Green BA, St Geme JW 3rd. The *Haemophilus influenzae* Hap autotransporter binds to fibronectin, laminin, and collagen IV. Infect Immun **2002**; 70:4902–7.
19. Ronander E, Brant M, Janson H, Sheldon J, Forsgren A, Riesbeck K. Identification of a novel *Haemophilus influenzae* protein important for adhesion to epithelial cells. Microbes Infect **2008**; 10:87–96.
20. Hendrixson DR, St Geme JW 3rd. The *Haemophilus influenzae* Hap serine protease promotes adherence and microcolony formation, potentiated by a soluble host protein. Mol Cell **1998**; 2:841–50.
21. Linke C, Caradoc-Davies TT, Young PG, Proft T, Baker EN. The laminin-binding protein Lbp from *Streptococcus pyogenes* is a zinc receptor. J Bacteriol **2009**; 191:5814–23.
22. Ragunathan P, Spellerberg B, Ponnuraj K. Structure of laminin-binding adhesin (Lmb) from *Streptococcus agalactiae*. Acta Crystallogr D Biol Crystallogr **2009**; 65:1262–9.
23. Manolov T, Forsgren A, Riesbeck K. Purification of alpha1-antichymotrypsin from human plasma with recombinant *M. catarrhalis* ubiquitous surface protein A1. J Immunol Methods **2008**; 333: 180–5.
24. Poje G, Redfield RJ. Transformation of *Haemophilus influenzae*. Methods Mol Med **2003**; 71:57–70.
25. Singh B, Jalalvand F, Morgelin M, Zipfel P, Blom AM, Riesbeck K. *Haemophilus influenzae* protein E recognizes the C-terminal domain of vitronectin and modulates the membrane attack complex. Mol Microbiol **2011**; 81:80–98.
26. Ronander E, Brant M, Eriksson E, et al. Nontypeable *Haemophilus influenzae* adhesin protein E: characterization and biological activity. J Infect Dis **2009**; 199:522–31.
27. Tenenbaum T, Spellerberg B, Adam R, Vogel M, Kim KS, Schroten H. *Streptococcus agalactiae* invasion of human brain microvascular endothelial cells is promoted by the laminin-binding protein Lmb. Microbes Infect **2007**; 9:714–20.
28. Lafontaine ER, Cope LD, Aebi C, Latimer JL, McCracken GH Jr., Hansen EJ. The UspA1 protein and a second type of UspA2 protein mediate adherence of *Moraxella catarrhalis* to human epithelial cells in vitro. J Bacteriol **2000**; 182:1364–73.
29. Hallstrom T, Blom AM, Zipfel PF, Riesbeck K. Nontypeable *Haemophilus influenzae* protein E binds vitronectin and is important for serum resistance. J Immunol **2009**; 183:2593–601.
30. Garmory HS, Titball RW. ATP-binding cassette transporters are targets for the development of antibacterial vaccines and therapies. Infect Immun **2004**; 72:6757–63.
31. Gabbianelli R, Scotti R, Ammendola S, Petrarca P, Nicolini L, Battistoni A. Role of ZnuABC and ZinT in *Escherichia coli* O157:H7 zinc acquisition and interaction with epithelial cells. BMC Microbiol **2011**; 11:36.
32. Li MS, Chow NY, Sinha S, et al. A *Neisseria meningitidis* NMB1966 mutant is impaired for invasion of respiratory epithelial cells, survival in human blood and for virulence in vivo. Med Microbiol Immunol **2009**; 198:57–67.
33. Castaneda-Roldan EI, Ouahrani-Bettache S, Saldana Z, et al. Characterization of SP41, a surface protein of *Brucella* associated with adherence and invasion of host epithelial cells. Cell Microbiol **2006**; 8:1877–87.
34. Matthysse AG, Yarnall HA, Young N. Requirement for genes with homology to ABC transport systems for attachment and virulence of *Agrobacterium tumefaciens*. J Bacteriol **1996**; 178:5302–8.
35. Yang M, Johnson A, Murphy TF. Characterization and evaluation of the *Moraxella catarrhalis* oligopeptide permease A as a mucosal vaccine antigen. Infect Immun **2011**; 79:846–57.
36. Resman F, Ristovski M, Ahl J, et al. Invasive disease caused by *Haemophilus influenzae* in Sweden 1997–2009; evidence of increasing incidence and clinical burden of non-type b strains. Clin Microbiol Infect **2010**; 17:1638–45.
37. Brown VM, Madden S, Kelly L, Jamieson FB, Tsang RS, Ulanova M. Invasive *Haemophilus influenzae* disease caused by non-type b strains in Northwestern Ontario, Canada, 2002–2008. Clin Infect Dis **2009**; 49:1240–3.
38. De Schutter I, De Wachter E, Crokaert F, et al. Microbiology of bronchoalveolar lavage fluid in children with acute nonresponding or recurrent community-acquired pneumonia: identification of nontypeable *Haemophilus influenzae* as a major pathogen. Clin Infect Dis **2011**; 52:1437–44.
39. Murphy TF, Bakaletz LO, Smeesters PR. Microbial interactions in the respiratory tract. Pediatr Infect Dis J **2009**; 28:S121–6.
40. Whitby PW, Vanwagoner TM, Seale TW, Morton DJ, Stull TL. Transcriptional profile of *Haemophilus influenzae*: effects of iron and heme. J Bacteriol **2006**; 188:5640–5.
41. Qu J, Lesse AJ, Brauer AL, Cao J, Gill SR, Murphy TF. Proteomic expression profiling of *Haemophilus influenzae* grown in pooled human sputum from adults with chronic obstructive pulmonary disease reveal antioxidant and stress responses. BMC Microbiol **2010**; 10:162.
42. Ghio AJ. Disruption of iron homeostasis and lung disease. Biochim Biophys Acta **2009**; 1790:731–9.
43. Ancsin JB, Kisilevsky R. Laminin interactions important for basement membrane assembly are promoted by zinc and implicate laminin zinc finger-like sequences. J Biol Chem **1996**; 271:6845–51.

IV

Vaccine 32 (2014) 2261–2264

Contents lists available at ScienceDirect

Vaccine

journal homepage: www.elsevier.com/locate/vaccine

Brief report

Impact of immunization with Protein F on pulmonary clearance of nontypeable *Haemophilus influenzae*

Farshid Jalalvand, Nils Littorin, Yu-Ching Su, Kristian Riesbeck*

Medical Microbiology, Department of Laboratory Medicine Malmö, Lund University, Malmö, Sweden

ARTICLE INFO

Article history:
Received 6 November 2013
Received in revised form 24 January 2014
Accepted 25 February 2014
Available online 12 March 2014

Keywords:
ABC-transporter
Epitope mapping
Haemophilus influenzae
Immunization
Mouse
Opsonophagocytosis
Protein F
Pulmonary clearance

ABSTRACT

Nontypeable *Haemophilus influenzae* (NTHi) is one of the main aetiologies of childhood bacterial infections as well as exacerbations in COPD patients. Currently, no licensed NTHi vaccine exists. In the present study, we evaluated the potential of the conserved and ubiquitous surface protein *Haemophilus* Protein F (PF) as a vaccine candidate. Our results show that incubation of NTHi with anti-PF antibodies significantly increased the opsonophygocytosis of human promyelocytic leukemia cell line-derived granulocytes, leading to efficient killing of the bacteria ($P \leq 0.05$). The presence of anti-PF IgG titers in healthy adults ($n = 60$) was investigated, and we found that 26% of healthy blood donors carried antibodies with the main antigenic epitope being PF^{23-48}. Finally, mice immunized with PF^{23-48} attained a significantly increased capacity to clear NTHi as compared to a control group immunized with a peptide derived from *Moraxella catarrhalis* β-lactamase ($P \leq 0.05$). Taken together, our results indicate that PF is a potential NTHi-vaccine candidate.

1. Introduction

Nontypeable *Haemophilus influenzae* (NTHi) is a mucosal pathogen and a prevalent cause of exacerbations in patients with chronic obstructive pulmonary disease (COPD), the second most common cause of bacterial acute otitis media in children and occasionally disseminates from the respiratory tract to produce invasive disease [1,2]. Otitis media is one of the most common reasons for children seeking medical care, receiving antibiotic treatment and, in the case of reoccurrence, undergoing surgery [3]. While still remaining the foremost cause of recurrent otitis media, there are indications that NTHi is rising to also become the premier acute otitis media-causing pathogen following the introduction of pneumococcal vaccines [1,4,5]. There have been contradictory reports regarding the effect of the NTHi Protein D (PD)-conjugated pneumococcal vaccine on the carriage rates of NTHi in children, although NTHi-mediated acute otitis media was observed to decrease by approximately 30% [6–9]. The great socioeconomic burden of otitis media, in parallel with exacerbations in COPD patients, warrants the continued pursuit of a more potent NTHi vaccine.

We recently identified NTHi Protein F (PF), a surface-exposed and highly conserved protein mediating bacterial adhesion to host tissue and complement-evasion [10,11]. Protein F belongs to the ATP-binding cassette (ABC)-transporter superfamily, members of which have shown promise as potential vaccines candidates [12]. Indeed, a multiantigen-vaccine containing the *Staphylococcus aureus* ABC-transporter component MntC, a PF-homologue, is currently undergoing human clinical trials [13].

To study the potential of PF as a vaccine candidate, we tested the promotion of opsonophagocytosis of NTHi by raising rabbit anti-PF antibodies, investigating the presence of anti-PF antibodies in healthy adults and, finally, evaluating the prophylactic effect of PF-immunization *in vivo* in a murine pulmonary clearance model [14]. Our results indicate that PF may be a potential vaccine candidate against NTHi.

2. Material and methods

Bacterial strains, antibodies and recombinant constructs. NTHi3655 and KR403 were routinely cultured in brain heart infusion broth and chocolate agar plates as described [10,15]. A human promyelocytic leukemia cell line (HL60) was propagated in RPMI 1640 supplemented with 10% fetal bovine serum (Fetalclone

Abbreviations: Abs, antibodies; CFU, colony forming units; COPD, chronic obstructive pulmonary disease; NTHi, non-typeable *Haemophilus influenzae*; OPA, opsonophagocytic assay; PD, Protein D; PF, Protein F.

* Corresponding author. Tel.:+46 40 338494; fax: +46 40 336234.
E-mail address: kristian.riesbeck@med.lu.se (K. Riesbeck).

http://dx.doi.org/10.1016/j.vaccine.2014.02.082
0264-410X/

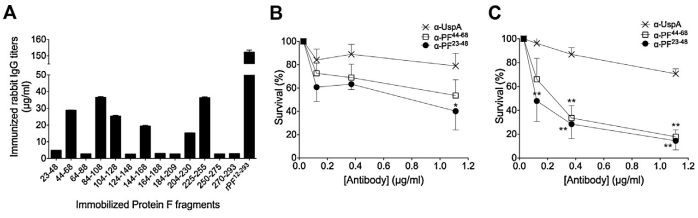

Fig. 1. Immunization of rabbits with Protein F elicits a humoral immune response against specific epitopes and the resulting Abs promote opsonophagocytosis of NTHi. (A) $PF^{44–68}$, $PF^{84–108}$, $PF^{104–128}$ and $PF^{225–255}$ contained the most immunogenic epitopes, whereas only low IgG titers could be detected against $PF^{23–48}$, a region that is responsible for interacting with the host components laminin and vitronectin. (B and C) Affinity-purified anti-PF Abs promoted HL 60-derived granulocyte-phagocytosis of NTHi more efficiently as compared to anti-UspA Abs that were included as a negative control. The NTHi strains 3655 (B) and KR403 (C) are shown. All experiments were repeated three times and results are presented as mean ± SEM. Statistical analyses were performed using two-way analysis of variance (ANOVA), and $P \leq 0.05$ was considered statistically significant compared to the negative control. * $P \leq 0.05$; ** $P \leq 0.01$.

I; HyClone, Logan, UT), 1% L-glutamine and penicillin/streptomycin (Invitrogen). Recombinant PF, PD and affinity-purified rabbit anti-PF and anti-*Moraxella catarrhalis* Ubiquitous Surface Protein A (UspA) antibodies (Abs) were raised as previously described [10,16,17].

Indirect enzyme-linked immunosorbent assay (*ELISA*). Synthetic peptides spanning the entire PF molecule (1 μM), recombinant full-length PF and PD and *Escherichia coli* BL21 lysate (100 ng/well) were immobilized on PolySorp (Nalge Nunc International, Rochester, NY) microtiter plates followed by ELISA as previously described [10]. Affinity-purified rabbit anti-PF polyclonal antibodies (pAbs) or sera obtained from healthy blood donors aged 18–65 years ($n = 60$) were used as primary Abs. Sera reacting with the *E. coli* BL21 lysate were excluded from analysis to prevent cross-reactivity with impurities in the recombinantly expressed proteins ($n = 10$). Titers were quantified as previously described [16].

Opsonophagocytic assay (*OPA*). A standardized OPA [18] was employed to determine the functionality of rabbit anti-PF Abs. Briefly, differentiation of HL60 cells into granulocytes was induced by suspending cells into culture medium containing 1.25% dimethyl sulfoxide for 5 days. Baby rabbit complement (Pel-freez Biologicals Rogers, AR) was used as a standardized source of complement. Bacteria were pre-incubated with various titers of affinity-purified Abs for 30 min at RT on a mini-orbital shaker. Subsequently, bacteria and HL60 cells were washed twice and diluted to 10^5 and 10^7 CFU/ml, respectively, and incubated together with baby rabbit complement for 45 min on a mini-orbital shaker at 37 °C, 5% CO_2. Fifty μl of the final reaction mixture was plated out and incubated overnight in 37 °C, 5% CO_2. Experiments with a nonspecific killing (in the absence of Abs) ≥30% were excluded.

Pulmonary clearance model. BALB/c mice ($n = 69$) at 8 weeks of age were subcutaneously immunized with 50 μg keyhole limpet hemocyanin (KLH)-conjugated $PF^{23–48}$ peptide or the KLH-conjugated control peptide *M. catarrhalis* β-lactamase$^{26–45}$. The first immunization was done with Freund's complete adjuvant. After four weeks, mice were immunized three more times at 7 day-intervals using alum as adjuvant (under the guidelines of the Ethical Committees on Animal Experiments, the Swedish Board of Agriculture, Freund's incomplete adjuvant is not allowed to be administered more frequently than once every fourth week. Alum, however, is allowed for administration once a week.). The animals were challenged with 10^6 CFU of NTHi3655 via the intranasal route seven days post-final immunization and bacterial load in the lungs were quantified as described previously [19]. As a mean of normalization, the highest ($n = 1$) and lowest ($n = 1$) values for each group were excluded. Mouse sera were collected and ELISA verified the presence of anti-PF Abs. Three animals that displayed weak/no humoral response to the antigen were excluded from the analysis.

Statistics. Student's *t* test and two-way analysis of variance (ANOVA) was used for statistical calculations of two and several sets of data, respectively. Statistical analyses were performed using GraphPad Prism 5 (GraphPad Software). A *P* value of ≤0.05 was considered statistically significant.

3. Results and discussion

We have previously shown that *Haemophilus* Protein F (PF) binds to the host extracellular matrix protein laminin, the complement-regulator vitronectin and to epithelial cells via an N-terminal region comprising amino acid residues Lys23-Glu48 ($PF^{23–48}$) [10,11]. To determine the immunodominant regions of PF, we raised and affinity-purified rabbit anti-PF pAbs using full-length recombinant protein. We analyzed the resulting IgG directed against synthetic peptides and identified $PF^{44–68}$, $PF^{84–108}$, $PF^{104–128}$ and $PF^{225–255}$ to contain the most immunodominant epitopes (Fig. 1A). Interestingly, we found only low titers of Abs directed towards $PF^{23–48}$, whereas the region ($PF^{44–68}$) adjacent to $PF^{23–48}$ was one of the most immunogenic.

To test the functionality of the anti-PF Abs, anti-$PF^{44–68}$ IgG directed against the N-terminal part of PF was affinity-purified from sera obtained from rabbits immunized with full-length PF. Moreover, we immunized rabbits with KLH-conjugated $PF^{23–48}$ to produce specific rabbit anti-$PF^{23–48}$ Abs that was also subsequently affinity-purified. The PF N-terminus is interesting from a host-interaction point of view since it targets epithelial cells and proteins derived from the extracellular matrix. Antibodies against this region would thus be effective in both blocking the host interaction as well as opsonizing the bacteria. As shown in Fig. 1B and C, both affinity-purified pAbs significantly promoted antibody-dependent opsonophagocytosis of NTHi3655 (Fig. 1B) and the heterologous strain KR403 isolated from the subepithelial compartment of a palatine tonsil [15] (Fig. 1C) as compared to affinity-purified anti-*M. catarrhalis* UspA IgG that was included as a negative control.

To investigate the presence of specific anti-PF IgG in a healthy adult population, sera obtained from healthy blood donors ($n = 60$) were analyzed. Since almost all humans are exposed to NTHi during childhood, we expected to observe the natural serological anti-PF IgG response in humans. Approximately 26% of the healthy blood donors were positive for anti-PF IgG (IgG concentration > highest concentration of IgG directed against the *E. coli* lysate control) (Fig. 2A), which corresponded to the anti-PD IgG levels (26% of donor sera) in our experimental set up. Surprisingly, no correlation between carriage of anti-PF and anti-PD IgG was found, indicating that humans may have different and individual serological responses to NTHi with regard to these antigens

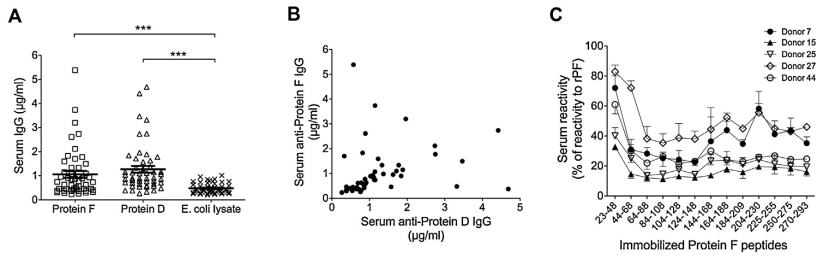

Fig. 2. Antibodies directed against Protein F exist in 26% of healthy blood donors, and primarily react against the epitope comprising $PF^{23–48}$. (A) Sera from healthy adult blood donors ($n = 60$) were tested for IgG reactivity against recombinant PF and PD at a dilution of 1:1,000. Those sera reactive to total cell lysate of *E. coli* BL21, which was the expression host of recombinant PF and PD, were excluded from the analysis to prevent a false positive bias ($n = 10$). (B) No correlation was found between high titers of anti-PF and anti-PD IgG ($R^2 = 0.0431$, two-tail Pearson's *r*). (C) Protein F-reactive sera ($n = 8$) were tested for epitope recognition. Three sera reacted only against full-length PF (data not shown). The remaining five sera had the highest IgG-titers against $PF^{23–48}$, which was unexpected since a low immunogenicity of this region was observed in rabbit. All experiments were repeated three times and the mean ± SEM is shown. In panel A, a statistical analysis was performed using two-tail Student's *t* test, and $P \leq 0.05$ was considered statistically significant. *** $P \leq 0.001$.

(Fig. 2B). Immunization with both proteins may thus complement each other, potentially in a multicomponent vaccine including other immunogenic proteins such as Protein E [19].

To delineate the immunodominant epitopes, donor sera with high concentrations of anti-PF Abs (defined as two-fold higher concentrations than to the *E. coli* lysate negative control) were selected ($n = 8$) for further analysis. Three of these sera reacted only against full-length PF, suggesting that the Abs recognized epitopes not encompassed by the shorter, presumably linear, peptides (data not shown). Surprisingly, however, we found that the most immunodominant epitope in the remaining five sera was $PF^{23–48}$ (Fig. 2C), which was in stark contrast to the epitope reactivity of the rabbit anti-serum (Fig. 1A). This confirmed that animals and humans do not have the same serological response to antigens with regard to epitope immunodominance [20]. The fact that NTHi is a human-specific pathogen may explain why humans, but not rabbits, develop Abs towards the PF N-terminus that interacts with host components.

Finally, we investigated the effect of PF immunization in a mouse pulmonary clearance model. $PF^{23–48}$ that binds to host components, and to which the highest IgG concentration was found in humans, was chosen as the antigen. Mice were subcutaneously immunized four times with KLH-conjugated $PF^{23–48}$ or the negative control peptide β-lactamase$^{26–45}$ derived from *M. catarrhalis* (Fig. 3). After 6 weeks, mice were challenged intranasally with NTHi3655 and clearance was monitored after 3 and 5 h. Our results revealed that mice immunized with the $PF^{23–48}$ peptide exhibited significantly better NTHi clearance at both tested time points as compared to the control group ($P \leq 0.05$).

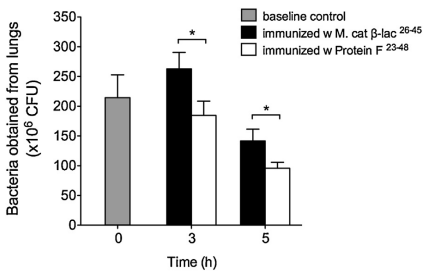

Fig. 3. Mice immunized with Protein F have a significantly increased clearance of NTHi. Mice immunized with $PF^{23–48}$ or the negative control peptide *M. catarrhalis* β-lactamase$^{26–45}$ were challenged intranasally with NTHi 3655 and bacterial loads in the lungs were quantified at 0 h (baseline control), 3 h and 5 h post-challenge. Statistical analysis was performed using one-tail Student's *t* test, and $P \leq 0.05$ was considered statistically significant. * $P \leq 0.05$.

4. Conclusions

The efficiency of anti-PF Abs in promoting opsonophagocytosis, in addition to an increased pulmonary clearance of NTHi in mice immunized with PF, suggests that this highly conserved and ubiquitous surface-protein would be a potential vaccine candidate against NTHi. Our results will thus be the impetus for further studies.

Conflict of interest statement

None.

Acknowledgements

This work was supported by grants from the Alfred Österlund, the Anna and Edwin Berger, Greta and Johan Kock, the Swedish Medical Research Council (grant number 521-2010-4221, www.vr.se), the Physiographical Society (Forssman's Foundation), and Skåne County Council's research and development foundation. We thank Mrs. Marta Brant for excellent technical assistance, and the Clinical Microbiology laboratory at Labmedicin Skåne for providing clinical isolates.

References

[1] Agrawal A, Murphy TF. *Haemophilus influenzae* infections in the *H. influenzae* type b conjugate vaccine era. J Clin Microbiol 2011;49:3728–32.
[2] Livorsi DJ, Macneil JR, Cohn AC, Bareta J, Zansky S, Petit S, et al. Invasive *Haemophilus influenzae* in the United States, 1999–2008: epidemiology and outcomes. J Infect 2012;65:496–504.
[3] Stol K, Verhaegh SJ, Graamans K, Engel JA, Sturm PD, Melchers WJ, et al. Microbial profiling does not differentiate between childhood recurrent acute otitis media and chronic otitis media with effusion. Int J Pediatr Otorhinolaryngol 2013;77:488–93.
[4] Sox C. Acute otitis media: antibiotics are moderately effective and mildly increase the risk of adverse effects; prevalence of different causative bacteria changed after introduction of the heptavalent pneumococcal conjugate vaccine. Evidence Based Med 2011;16:181–2.
[5] Wiertsema SP, Kirkham LA, Corscadden KJ, Mowe EN, Bowman JM, Jacoby P, et al. Predominance of nontypeable *Haemophilus influenzae* in children with otitis media following introduction of a 3 + 0 pneumococcal conjugate vaccine schedule. Vaccine 2011;29:5163–70.
[6] van den Bergh MR, Spijkerman J, Swinnen KM, Francois NA, Pascal TG, Borys D, et al. Effects of the 10-valent pneumococcal nontypeable *Haemophilus*

influenzae protein D-conjugate vaccine on nasopharyngeal bacterial colonization in young children: a randomized controlled trial. Clin Infect Dis 2013;56:e30–9.
[7] Prymula R, Kriz P, Kaliskova E, Pascal T, Poolman J, Schuerman L. Effect of vaccination with pneumococcal capsular polysaccharides conjugated to *Haemophilus influenzae*-derived protein D on nasopharyngeal carriage of *Streptococcus pneumoniae* and *H. influenzae* in children under 2 years of age. Vaccine 2009;28:71–8.
[8] Prymula R, Hanovcova I, Splino M, Kriz P, Motlova J, Lebedova V, et al. Impact of the 10-valent pneumococcal non-typeable *Haemophilus influenzae* Protein D conjugate vaccine (PHiD-CV) on bacterial nasopharyngeal carriage. Vaccine 2011;29:1959–67.
[9] Prymula R, Peeters P, Chrobok V, Kriz P, Novakova E, Kaliskova E, et al. Pneumococcal capsular polysaccharides conjugated to protein D for prevention of acute otitis media caused by both *Streptococcus pneumoniae* and non-typable *Haemophilus influenzae*: a randomised double-blind efficacy study. Lancet 2006;367:740–8.
[10] Jalalvand F, Su YC, Morgelin M, Brant M, Hallgren O, Westergren-Thorsson G, et al. *Haemophilus influenzae* protein F mediates binding to laminin and human pulmonary epithelial cells. J Infect Dis 2013;207:803–13.
[11] Su YC, Jalalvand F, Morgelin M, Blom AM, Singh B, Riesbeck K. *Haemophilus influenzae* acquires vitronectin via the ubiquitous Protein F to subvert host innate immunity. Mol Microbiol 2013;87:1245–66.
[12] Garmory HS, Titball RW. ATP-binding cassette transporters are targets for the development of antibacterial vaccines and therapies. Infect Immun 2004;72:6757–63.
[13] Gribenko A, Mosyak L, Ghosh S, Parris K, Svenson K, Moran J, et al. Three-dimensional structure and biophysical characterization of *Staphylococcus aureus* cell surface antigen-manganese transporter MntC. J Mol Biol 2013.
[14] Hansen EJ, Toews GB. Animal models for the study of noninvasive *Haemophilus influenzae* disease: pulmonary clearance systems. J Infect Dis 1992;165(Suppl 1):S185–7.
[15] Singh K, Nordstrom T, Morgelin M, Brant M, Cardell LO, Riesbeck K. *Haemophilus influenzae* resides in tonsils and uses immunoglobulin D binding as an evasion strategy. J Infect Dis 2013.
[16] Akkoyunlu M, Janson H, Ruan M, Forsgren A. Biological activity of serum antibodies to a nonacylated form of lipoprotein D of *Haemophilus influenzae*. Infect Immun 1996;64:4586–92.
[17] Manolov T, Forsgren A, Riesbeck K. Purification of alpha1-antichymotrypsin from human plasma with recombinant *M. catarrhalis* ubiquitous surface protein A1. J Immunol Methods 2008;333:180–5.
[18] Henckaerts I, Durant N, De Grave D, Schuerman L, Poolman J. Validation of a routine opsonophagocytosis assay to predict invasive pneumococcal disease efficacy of conjugate vaccine in children. Vaccine 2007;25:2518–27.
[19] Ronander E, Brant M, Eriksson E, Morgelin M, Hallgren O, Westergren-Thorsson G, et al. Nontypeable *Haemophilus influenzae* adhesin protein E: characterization and biological activity. J Infect Dis 2009;199:522–31.
[20] Bugelski PJ, Treacy G. Predictive power of preclinical studies in animals for the immunogenicity of recombinant therapeutic proteins in humans. Curr Opin Mol Ther 2004;6:10–6.